2006 NRL REVIEW

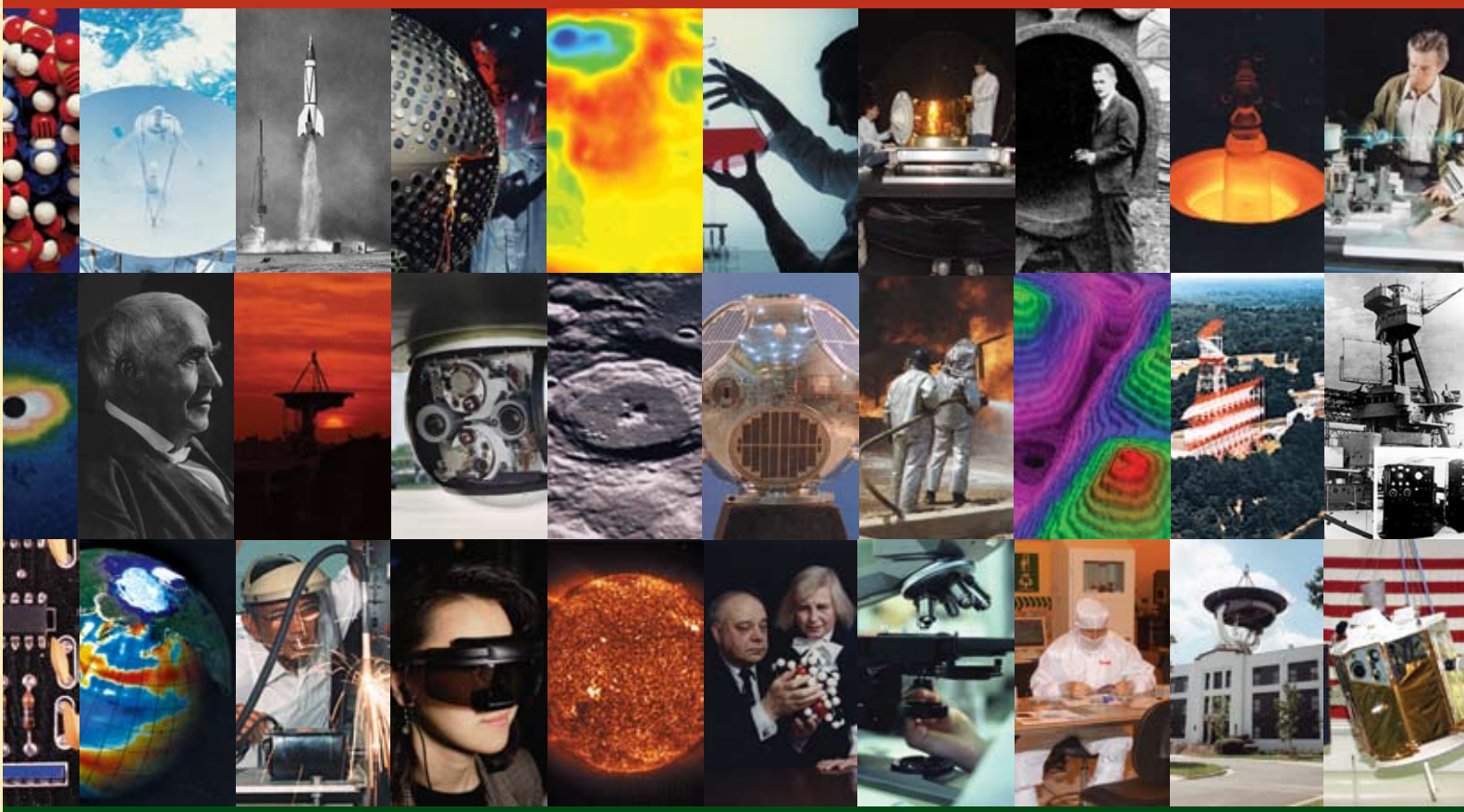

THE NAVY'S CORPORATE LABORATORY

NAVAL RESEARCH LABORATORY
Washington, DC 20375

Report Documentation Page

Form Approved
OMB No. 0704-0188

1. REPORT DATE	2. REPORT TYPE	3. DATES COVERED
2006		**00-00-2006 to 00-00-2006**

4. TITLE AND SUBTITLE	5a. CONTRACT NUMBER
2006 NRL Review	5b. GRANT NUMBER
	5c. PROGRAM ELEMENT NUMBER
6. AUTHOR(S)	5d. PROJECT NUMBER
	5e. TASK NUMBER
	5f. WORK UNIT NUMBER
7. PERFORMING ORGANIZATION NAME(S) AND ADDRESS(ES) **Naval Research Laboratory,Washington,DC,20375**	8. PERFORMING ORGANIZATION REPORT NUMBER
9. SPONSORING/MONITORING AGENCY NAME(S) AND ADDRESS(ES)	10. SPONSOR/MONITOR'S ACRONYM(S)
	11. SPONSOR/MONITOR'S REPORT NUMBER(S)

12. DISTRIBUTION/AVAILABILITY STATEMENT
Approved for public release; distribution unlimited

13. SUPPLEMENTARY NOTES

14. ABSTRACT

15. SUBJECT TERMS

16. SECURITY CLASSIFICATION OF:			17. LIMITATION OF ABSTRACT	18. NUMBER OF PAGES	19a. NAME OF RESPONSIBLE PERSON
a. REPORT	b. ABSTRACT	c. THIS PAGE			
unclassified	**unclassified**	**unclassified**	**Same as Report (SAR)**	**221**	

General information on the research described in this NRL Review can be obtained from the Public Affairs Office, Code 1030, (202) 767-2541. Information concerning Technology Transfer is available from the Technology Transfer Office, Code 1004, (202) 767-7230. Sources of information on the various educational programs at NRL are listed in the chapter entitled "Programs for Professional Development."

For additional information about NRL, the Fact Book lists the organizations and key personnel for each division. It contains information about Laboratory funding, programs, and field sites. The Fact Book can be obtained from the Technical Information Services Branch, Code 3430, (202) 404-4963. The web-based NRL Major Facilities publication, which describes each NRL facility in detail, can be accessed at http://www.nrl.navy.mil.

NRL REVIEW STAFF

SENIOR SCIENCE EDITOR
John D. Bultman

COORDINATOR
Jonna Atkinson

CONSULTANT
Kathy Parrish

DESIGN, LAYOUT, AND GRAPHIC SUPPORT
Jonna Atkinson and Donna Gloystein

EDITORIAL ASSISTANCE
Maureen Long, Saul Oresky, Kathy Parrish, Nancy Holly, and Claire Peachey

HISTORICAL UPDATE
John D. Bultman

PHOTOGRAPHIC PRODUCTION
Gayle Fullerton and Michael Savell

REVIEWED AND APPROVED
NRL/PU/3430--06-495
RN: 06-1226-2884
December 2006

Daniel R. Gahagan, Captain, USN
Commanding Officer

NRL's MISSION

To conduct a broadly based multidisciplinary program of scientific and advanced technological development directed toward maritime applications of new and improved materials, techniques, equipment, systems, and ocean, atmospheric, and space sciences and related technologies.

The Naval Research Laboratory provides primary in-house research for the physical, engineering, space, and environmental sciences; broadly based applied research and advanced technology development programs in response to identified and anticipated Navy and Marine Corps needs; broad multidisciplinary support to the Naval Warfare Centers; and space and space systems technology, development, and support.

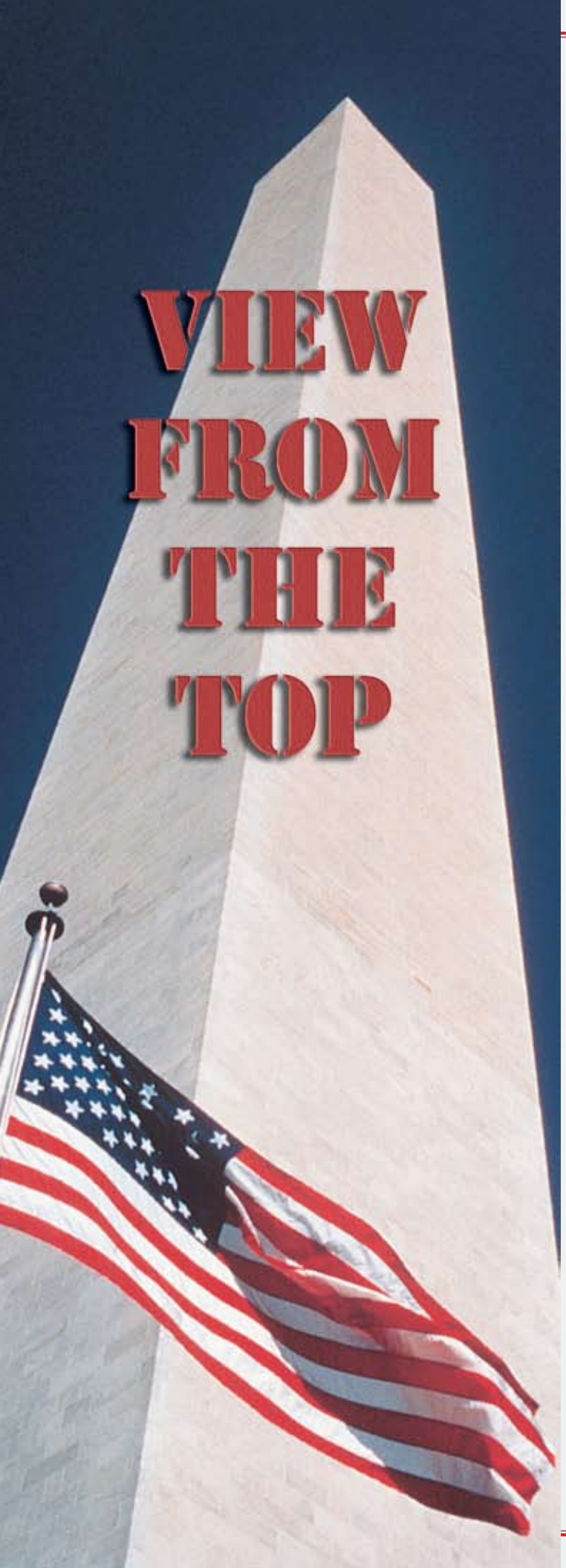

VIEW FROM THE TOP

Captain Daniel R. Gahagan
Commanding Officer

Dr. John A. Montgomery
Director of Research

In March 2006, the Naval Research Laboratory (NRL) was honored with the 2005 Roosevelts Gold Medal for Science. The Medal is presented annually by the New York Council of the Navy League of the United States "to an individual, institution or corporation for extraordinary scientific contributions to the security of America."

In receiving this prestigious award, NRL was cited as the "government's premier defense research laboratory" and was recognized by the League for its significant impact on both the U.S. Navy and the nation. The citation noted that

> *"NRL is responsible for a number of innovations that have revolutionized the capabilities of the United States Navy, and of the nation as a whole….NRL has made a profound difference, in times of war and in times of peace, through the creative work of scientists and engineers who serve the nation's interest."*

Another positive reflection of NRL's significance to the Department of Defense (DoD) was the outcome of the 2005 Base Realignment and Closure (BRAC) analyses, which gave high scores to the Laboratory in military value. Of the 617 technical activities evaluated (located at 282 military installations), NRL was ranked #1 in 6 of 13 Science & Technology (S&T) capability areas. The remaining seven areas included those in which NRL does not conduct significant effort, such as Ground Vehicles. NRL was the only DoD lab or center that was rated #1 in more than a single technical area.

The Laboratory's long and enviable record of success is no accident of history. At the most basic level, NRL's impact on science and national security is the result of hard work by talented scientists and engineers, using state-of-the-art equipment, in a mission environment. However, other laboratories, public and private, possess these factors as well. Therefore, it may be worthwhile to examine some other essential, but less obvious, reasons for NRL's sustained success.

The first is NRL's organizational position. In 1946, Public Law 79-588 created the Office of Naval Research (ONR) and placed it, along with NRL, in the Office of the Secretary of the Navy. That legislation was championed by a group of far-sighted Naval officers (the "Bird Dogs") who knew that the long-term needs of research and development do not fare well when in direct competition with short-term pressing operational requirements. The law ensured that NRL reported to the Chief of Naval Research, which is appropriate given the assigned Department-wide and national responsibilities of the Navy's Corporate Laboratory. More recently, the value and validity of NRL's unique organizational position and role were noted and reaffirmed by the 2005 BRAC Commission when it disapproved the proposal to merge NRL's installations-management functions with nearby operational installations.

A second important reason for NRL's success is the support it receives from ONR, its parent command. A 2002 report by the National Defense University underscored this fact by observing,

> *"The importance of a supportive ONR to an innovative NRL program cannot be overstated. With ONR's support, NRL's ability to pursue risky projects…fosters new, and at times revolutionary, military capabilities."*

A third reason is the dual funding processes of the Navy Working Capital Fund (NWCF) and the Laboratory-Directed S&T Program. The NWCF, also known as "industrial funding," is designed to produce world-class research results relevant to future Navy needs at the lowest possible cost. The system requires NRL's researchers to compete for their funding by satisfying sponsor needs. Sponsors have the choice of funding or not funding individual R&D projects on the basis of cost, scientific quality, and responsiveness to their needs. In effect, NRL is operated in a manner similar to private enterprise.

The Laboratory-Directed S&T Program, or "Base Program," drives an internal competition for funding that is intellectually vigorous and ensures both high quality and relevance; creates new technological capabilities that enable NRL to meet its assigned unique Navy-wide and national responsibilities; enhances the core strength and drives the scientific and technical vitality of the Laboratory; investigates rapidly changing fields of science and engineering to find materials, techniques, processes, and ideas that may prove to have some as yet undetermined military value, thereby avoiding "technological surprise;" and attracts and retains the most highly qualified scientists and engineers.

The effective balance NRL achieves through its dual-funding process was noted recently in a 2004 report by the Nuclear Energy Research Advisory Committee:

> *"A true world-class national laboratory develops a healthy balance between product focus and scholarship….Examples of this balance exist at the Naval Research Laboratory…"*

One more reason for NRL's sustained success is the multidisciplinary nature of its technical program, which includes, but is not limited to, physics, chemistry, computer science, acoustics, marine geosciences, materials science and technology, meteorology, oceanography, space science and technology, optical science and technology, and electronics. This broad range of scientific and engineering disciplines allows NRL to seek interdisciplinary solutions to difficult national problems.

The above factors–the obvious and the not-so-obvious–have together forged a record of success that the New York Chapter of the Navy League recognized as having "helped make the U.S. Fleet the most formidable naval fighting force in the world."

"government's premier defense research laboratory"

CONTENTS

2006 NRL REVIEW

LONG DISTANCE TRANSMISSION

27. In the light of the foregoing conclusions it is of interest to consider the character of the reception at various distances from the transmitter. No attempt to cover all details will be entered upon, but a few cases deserve remark. It is convenient to make the diagrams from the reflection theory; the conclusions from these will be the same as from a refraction theory. In Fig. 7 the curved line AL is the surface

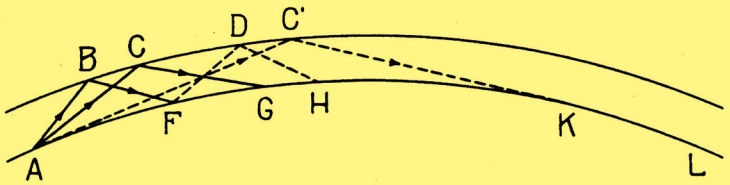

Fig. 7. Paths taken by radio rays in traveling around the earth.

of the earth and BC' the Kennelly-Heaviside layer at a height of 150 miles. Suppose that the radio rays from the transmitter A are confined to the space BAC. The upper limiting ray AB descends to F,

Radio Propagation and the "Skip-Distance" Effect

Achievement: In 1925, NRL discovered the principles governing the "skip-distance" effect, which could not at the time be explained by the prevailing wave-propagation theory. The effect refers to radio signals that disappear after the "ground wave" dissipates but reappear at a considerable distance, varying with frequency, time of day, and season. Building upon the work of Sir Joseph Larmor, NRL's A. Hoyt Taylor and E.O. Hulburt jointly published in 1926 a modification of the theory that adequately explained the high-frequency (HF) "skip-distance" effect and that agreed with the experimental data. In connection with this high-frequency-propagation work, NRL was the first to determine the frequency above which radio waves would penetrate the Earth's atmosphere and propagate through outer space, making radio communication in space possible. NRL would later develop the world's first satellite communication system using the Moon as a relay.

NRL's work in this area further demonstrated that around-the-world HF transmissions could be obtained through successive reflections from the Earth's ionosphere with the proper choice of frequency, time of day, and season. Encirclement of the globe as many as three times in the same transmission and in both directions was observed in 1926. At the same time, reflections of the pulsed HF transmissions from Earth surface prominences, currently called "backscatter," were first observed. These HF "backscatter" observations generated the first concept of detecting and ranging on targets over very long distances. This concept led to the later development of over-the-horizon radar by NRL.

Impact: NRL's seminal work in the field of radio propagation laid the foundation for modern HF wave-propagation theory, led to the Navy's acceptance of HF radio frequencies which had a profound effect upon naval communications for the next 50 to 60 years, led to NRL's development of the world's first satellite communication system, and led to the Laboratory's development of over-the-horizon radar.

NRL Awarded the Roosevelts Gold Medal for Science

The Roosevelts Gold Medal was conceived by the New York Council, Navy League of the United States, and designed by Tiffany, in 1986. It is awarded "to an individual, institution, or corporation for extraordinary scientific contributions to the security of America."

The Gold Medal for Science carries the profiles of Franklin and Theodore Roosevelt, both assistant Secretaries of the Navy on their way to the White House, and both keen supporters of "Strength Through Science" – a lesson both Roosevelt and Eisenhower learned from Churchill in World War II. For over 100 years, the traditional objective of both the Navy and the Navy League has been "Peace Through Strength – Strength Through Science."

–The New York Council of the Navy League of the United States

This year's recipient is the government's premier defense research laboratory, the U.S. Naval Research Laboatory (NRL). Over the last 80 years, NRL has been responsible for a number of innovations that have revolutionized the capabilities of the United States Navy, and of the nation as a whole. Among these innovations are radar, the first intelligence satellite, and key ideas for the Global Positioning System (GPS).

THE COMMISSIONING OF

USS NEW YORK *(LPD 21)*

The USS *New York* (LPD 21) is now under construction in Louisiana. This ship will be special not just because it will bear the name of a great state and city but because the name for this ship was selected in order to honor the heroes and victims of the September 11, 2001, attacks on the World Trade Center. The commissioning of this ship will take place in New York harbor in early 2008.

LPD 21 will be the ninth Navy ship to bear the name *New York*. However, she may be the first ship to be named after both the state and the city.

The Predecessors

The first *New York*, a gondola, was launched just as the United States was beginning in the summer of 1776. She was built by General Benedict Arnold's troops to counter the British forces on Lake Champlain. She fought at the Battle of Valcour Island on October 11, 1776, and then again two days later near Crown Point. She was badly damaged and run aground and burnt. While these battles were tactical defeats for the Americans, they were strategic victories.

The next *New York* was commissioned in 1800 and was one of five frigates built by the states for the federal government. She mounted 36 guns and fought in the undeclared war with France and in the Barbary Coast War. Some 11 years later, the British burned the *New York* at the Washington Navy Yard where she had been placed in reserve.

In 1816, Congress authorized a 74-gun ship of the the line and she was laid down at Norfolk Navy Yard in 1820. Work did not proceed apace on this ship, and by the time the Civil War broke out, she still had not been completed. To prevent her from falling into enemy hands, Federal troops burnt the ship before Confederate forces seized the Navy Yard.

In 1863, work began on a screw frigate to be named *Ontario* at the New York Navy Yard. However, work was suspended on this ship shortly after the end of the Civil War. She was renamed *New York* but she remained unfinished and was sold while still on the stocks in 1888.

The next *New York* had a hull number ACR 2 and is considered the first U.S. Navy armored cruiser. The 8,200-ton *New York* was faster than more powerful ships and capable of overtaking 95% of the world's merchant fleet and thus was well-suited to be a commerce raider. She saw action in the Spanish American War. ACR 2 was renamed *Saratoga* in 1911 and in 1917 was renamed *Rochester*.

The ship that prompted the first name change of ACR 2 was the battleship *New York* (BB 34). Commissioned in 1914, *New York* served as the flagship of the American battleship squadron that was attached to the British Grand Fleet following America's entry into the First World War. Between the wars, the Navy's first operational shipboard radar, the XAF, was installed aboard the *New York*. Built by NRL, the radar was able to detect ships at 12 miles and aircraft at 85 miles. During WWII, *New York* did convoy duty and provided gunfire support for the invasions of North Africa, Iwo Jima, and Okinawa.

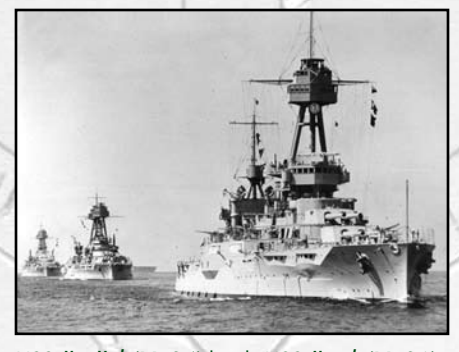

USS ***New York*** (BB 34) leads USS ***Nevada*** (BB 36), USS ***Oklahoma*** (BB 37), and USS ***Langley*** (CV 1) during maneuvers in 1932. (U.S. Navy photo - NH 48138)

The Idea

With the smoke clouds still hanging over the World Trade Center site following the September 11, 2001, attacks, Governor of New York George E. Pataki wrote a letter to then-Secretary of the Navy Gordon England requesting that the Navy bestow the name "USS *New York*" on a surface warship involved in the War on Terror in honor of September 11's victims.

The decision to name a ship after both the state and the city was announced on September 11, 2002, at a ceremony at the Intrepid Sea-Air-Space Museum. Secretary England said: "When our Sailors and Marines set out to sea on the USS *New York*, this ship will serve as a worldwide deployable symbol of the spirit of all heroes, past and present, living and fallen, who have blessed this great city and great state. . . The citizens of America will never forget what happened in New York on September 11, will never forget the sacrifices of the brave citizens of this city and state, and the Navy and Marine Corps will never forget."

On September 10, 2003, more than twenty tons of steel salvaged from the World Trade Center were melted and poured into the mold for the bow stem of the *New York* at Amite Foundry and Machine, Inc., in Louisiana. "A piece of our city will travel the world in democracy and freedom," former New York City Mayor Rudolph Giuliani wrote in a letter read at the ceremony. Dotty England, wife of the former Secretary and sponsor of the *New York*, said as the steel was poured into the mold: "For all who will serve on USS *New York*, and for all who suffered from the attacks of 9-11, let us never forget." "Never forget" will be the motto of the ship. An additional 21,000 pounds of World Trade Center steel was put aside and will be made into anchor-handling castings.

Workers from the Amite Louisiana foundry pour molten steel recycled from the World Trade Center into the mold of the bow stem of the Amphibious Transport Dock ship USS ***New York*** (LPD 21). About 24 tons of steel was salvaged from the World Trade Center, which was destroyed in the terrorist attacks of September 11, 2001. (U.S. Navy photo)

Hurricane Katrina
and the Navy's Relief Efforts

NRL InfraLynx Deployed to the Gulf Coast

Two InfraLynx vans parked in Memphis, Tennessee, a safe-range for the vehicles between Hurricanes Katrina and Rita. A training session is underway in the light-colored van with the deployed antenna. Clouds banding the sky are an early sign that Rita is advancing.

The InfraLynx SUV, which provides support for the vans, outside the Superdome in New Orleans, where it was stationed following Hurricane Katrina.

Setting up the InfraLynx van outside the emergency operations center (EOC) in Jasper, Texas. Nearly 100 miles inland from Hurricane Rita, Jasper sustained winds of 100 to 120 miles per hour for nine hours as the city's trees toppled homes and power lines.

Hurricane Katrina was the eleventh named tropical storm, fifth hurricane, third major hurricane, and first Category 5 hurricane of the 2005 Atlantic hurricane season. It was the third most powerful storm of the season, and the sixth-strongest Atlantic hurricane ever recorded. Katrina formed over the Bahamas on August 23, 2005, and crossed southern Florida at Category 1 intensity before strengthening rapidly in the Gulf of Mexico, becoming the strongest hurricane ever recorded at that time in the Gulf. (Hurricane Rita broke this record later in the season.) The storm weakened considerably before making its second landfall as an extremely large Category 3 storm on the morning of August 29 along the Central Gulf Coast near Buras-Triumph, Louisiana.

The storm surge from Katrina caused catastrophic damage along the coastlines of Louisiana, Mississippi, and Alabama. Levees separating Lake Pontchartrain from New Orleans were breached by the surge, ultimately flooding about 80% of the city. Wind damage was reported well inland, impeding relief efforts. Katrina is estimated to be responsible for $75 billion in damages, making it the costliest hurricane in United States history; the storm has killed 1,418 people, becoming the deadliest U.S. hurricane since the 1928 Okeechobee Hurricane. (http://en.wikipedia.org/wiki/Hurricane_Katrina)

At the request of RADM Christopher Weaver, Commander, Navy Installations Command, NRL deployed two InfraLynx communications vans to the Gulf Coast area devastated by Hurricane Katrina. The InfraLynx team departed the Laboratory on September 6, 2005, enroute to the New Orleans area.

While assigned to Joint Task Force Katrina, the NRL team used the InfraLynx vans to provide network, non-secure phone connections, and commercial television capabilities for the Eighth Coast Guard District, headquartered in New Orleans. InfraLynx allowed the Eighth District office to reestablish its presence in the city, following Katrina. The group also provided services to the Army National Guard's 35th Infantry Division, which was coordinating 2,000 troops from several states. Navy reservists served as liaisons between the NRL technical team and Department of Defense and Department of Homeland Security activities in New Orleans.

Technical assistance was also given by NRL to the U.S. Northern Command, which had deployed its own NRL-designed InfraLynx vehicle to the distressed area, the Joint Force Maritime Component Commander, and the Army's 82nd Airborne Division.

NRL's mission assistance was completed shortly before the arrival of Hurricane Rita, after which, at the request of the Department of Justice, the team was relocated to Jasper, Texas. After arriving in Jasper, the InfraLynx provided Internet and non-secure telephone connections to the Jasper County Sheriff's Emergency Operations Center (EOC). All communications, in both Texas and Louisiana, were linked via satellite to NRL's ground entry point in Washington, D.C.

InfraLynx

VXS-1 Takes Part in History

Plane commander and the lead project officer,
.

It's been roughly 30 years since the United States Navy deliberately operated an aircraft within the hurricane environment to collect meteorological information. This past summer, the VXS-1 Warlocks of Scientific Development Squadron One completed a project for NCAR (National Center for Atmospheric Research) and NOAA (National Oceanic and Atmospheric Administration), by conducting airborne hurricane research in a uniquely configured P-3 Orion. The NSF (National Science Foundation) also played a key part by providing three million dollars to fund the project. The project, called RAINEX (Hurricane Rainband and Intensity Change Experiment), focused on the relationship between the outer rainband and the inner eye of the hurricane to influence storm intensity. Operating mainly out of MacDill AFB in Tampa, Florida, VXS-1 took part in the project from August 15th to September 30th. During this time period, VXS-1 was instrumental in supplying research data for hurricanes Katrina, Ophelia, and Rita by taking measurements from inside the storms with a unique Doppler radar.

The project took several years of research and planning before it all came together for this busy hurricane season. The P-3B was outfitted with the most sophisticated three-dimensional Doppler radar in the world, capable of gathering storm data by making in-situ measurements. The aircraft also carried GPS dropsondes that were used to measure the wind speed and direction, temperature, humidity, and atmospheric pressure by being dropped from altitude while near major convection. The crew consisted of seven USN operators and eight civilian scientists. The research followed the hurricanes from tropical storm strength all the way to their landfall as hurricanes with most of the measurements occurring in Category 3 hurricanes or stronger. Using a two-dimensional aircraft nose weather radar and guidance from the scientists and base stations, the aircrew methodically worked to maneuver the aircraft in a safe position to conduct the research while inside the tropical storm environment. Thanks to this teamwork, vital data was recorded documenting the rainbands and their interaction with the storm during normal hurricane activity and eye wall replacement cycles. The overall project was a resounding success and gathered a dataset never before attained.

Hurricane Katrina's Devastation

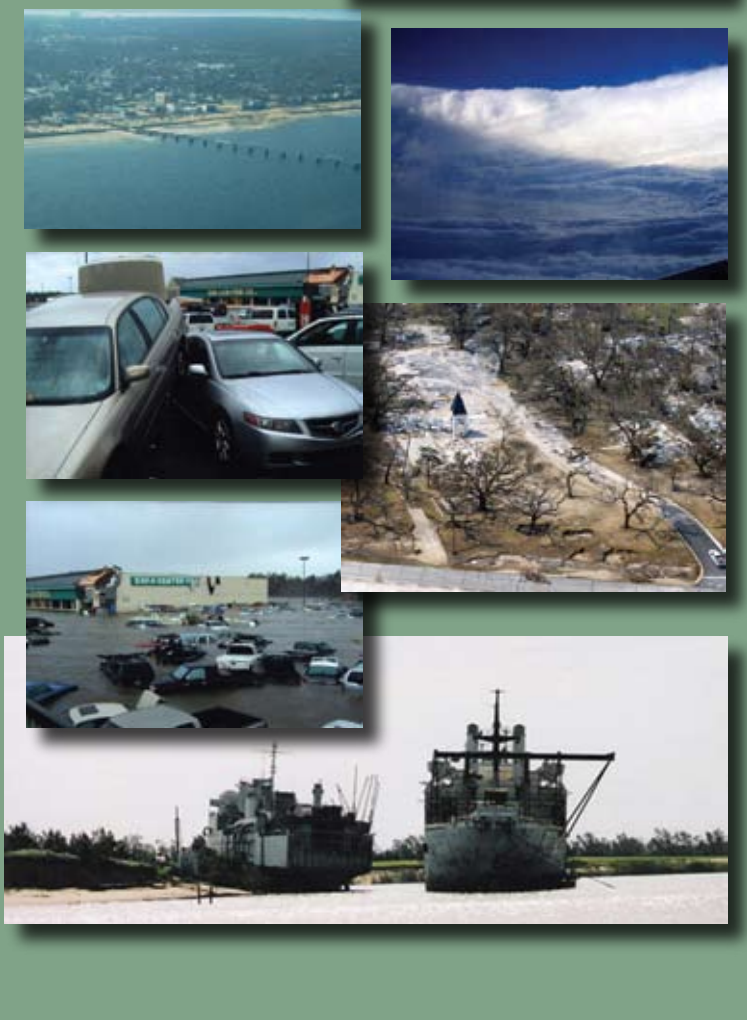

NRL-SSC Hurricane Relief

A great number of NRLers reached out to their colleagues at Stennis Space Center during their struggle with the aftermath of Hurricane Katrina. Many of the NRL Stennis employees, military, and contractors lost all of their possessions and homes. The VXS-1 NP-3 delivered 3,400 pounds of much needed donations. In total, more than 8,000 pounds of donated food, clothing, and personal hygiene items helped sustain NRL Stennis employees and their families.

Invention of U.S. Radar

Achievement: Prior to the development of radar, Navy ships could track other ships or aircraft only by using optical techniques, sound ranging, or primitive radio direction finding. New methods of detection and ranging were necessary. In 1922, while working on radio direction finders for aircraft, A.H. Taylor and L.C. Young noted a distortion of "phase shift" in radio signals reflected from a steamer on the Potomac River. In short, NRL had detected a moving ship by radio waves and had, as a result, discovered the radar principle. Eight years after the initial discovery of the radar principle, NRL scientists observed that reflections of radio waves from an airplane could also be detected.

From 1930 to 1940, NRL explored the use of radio for detection and ranging. In 1933, the use of a pulse technique to detect aircraft and ships was proposed by Young. R.M. Page made major advances over the next few years in the area of transmitters and receivers, eventually developing the highly important "duplexer" in 1936. The duplexer permitted the use of the same antenna for both transmitting and receiving. The pulse technique combined with the duplexer did away with the separate receiving and transmitting antennas that most of the other early radar developers employed. Page and Young received the patents for the duplexer, an invention that dramatically changed the nature of radar in the U.S. and abroad.

Impact: NRL invented, developed, and installed the first operational U.S. radar, the XAF, on the battleship USS *New York* in 1939. It was rapidly transferred to industry for production. By the time of the attack on Pearl Harbor, 20 radar units were in operation. Radar of this type contributed to the victories of the Coral Sea, Midway, and Guadalcanal.

The invention of radar and the developments that flowed from it (e.g., monopulse radar and over-the-horizon radar) are among the foundations of modern military power. And as a sensor for navigation and surveillance, radar plays a major role in the operation of civilian transportation systems, weather forecasting, astronomy, and automation, among other uses.

NRL — OUR HERITAGE

Today, when government and science seem inextricably linked, when virtually no one questions the dependence of national defense on the excellence of national technical capabilities, it is noteworthy that in-house defense research is relatively new in our Nation's history. The Naval Research Laboratory (NRL), the first modern research institution created within the United States Navy, began operations in 1923.

Thomas Edison's Vision: The first step came in May 1915, a time when Americans were deeply worried about the great European war. Thomas Edison, when asked by a *New York Times* correspondent to comment on the conflict, argued that the Nation should look to science. "The Government," he proposed in a published interview, "should maintain a great research laboratory....In this could be developed...all the technique of military and naval progression without any vast expense." Secretary of the Navy Josephus Daniels seized the opportunity created by Edison's public comments to enlist Edison's support. He agreed to serve as the head of a new body of civilian experts—the Naval Consulting Board—to advise the Navy on science and technology. The Board's most ambitious plan was the creation of a modern research facility for the Navy. Congress allocated $1.5 million for the institution in 1916, but wartime delays and disagreements within the Naval Consulting Board postponed construction until 1920.

The Laboratory's two original divisions—Radio and Sound—pioneered in the fields of high-frequency radio and underwater sound propagation. They produced communications equipment, direction-finding devices, sonar sets, and perhaps most significant of all, the first practical radar equipment built in this country. They also performed basic research, participating, for example, in the discovery and early exploration of the ionosphere. Moreover, the Laboratory was able to work gradually toward its goal of becoming a broadly based research facility. By the beginning of World War II, five new divisions had been added: Physical Optics, Chemistry, Metallurgy, Mechanics and Electricity, and Internal Communications.

The War Years and Growth: Total employment at the Laboratory jumped from 396 in 1941 to 4400 in 1946, expenditures from $1.7 million to $13.7 million, the number of buildings from 23 to 67, and the number of projects from 200 to about 900. During WWII, scientific activities necessarily were concentrated almost entirely on applied research. New electronics equipment—radio, radar, sonar—was developed. Countermeasures were devised. New lubricants were produced, as were antifouling paints, luminous identification tapes, and a sea marker to help save survivors of disasters at sea. A thermal diffusion process was conceived and used to supply some of the ^{235}U isotope needed for one of the first atomic bombs. Also, many new devices that developed from booming wartime industry were type tested and then certified as reliable for the Fleet.

NRL Reorganizes for Peace: Because of the major scientific accomplishments of the war years, the United States emerged into the postwar era determined to consolidate its wartime gains in science and technology and to preserve the working relationship between its armed forces and the scientific community. While the Navy was establishing its Office of Naval Research (ONR) as a liaison with and supporter of basic and applied scientific research, it was also encouraging NRL to broaden its scope and become, in effect, its corporate research laboratory. There was a transfer of NRL to the administrative oversight of ONR and a parallel shift of the Laboratory's research emphasis to one of long-range basic and applied investigation in a broad range of the physical sciences.

However, rapid expansion during the war had left NRL improperly structured to address long-term Navy requirements. One major task—neither easily nor rapidly accomplished—was that of reshaping and coordinating research. This was achieved by transforming a group of largely autonomous scientific divisions into a unified institution with a clear mission and a fully coordinated research program. The first attempt at reorganization vested power in an executive committee composed of all the division superintendents. This committee was impracticably large, so in 1949, a civilian director of research was named and given full authority over the program. Positions for associate directors were added in 1954.

The Breadth of NRL: During the years since the war, the areas of study at the Laboratory have included basic research concerning the Navy's environments of Earth, sea, sky, and space. Investigations have ranged

widely—from monitoring the Sun's behavior, to analyzing marine atmospheric conditions, to measuring parameters of the deep oceans. Detection and communication capabilities have benefitted by research that has exploited new portions of the electromagnetic spectrum, extended ranges to outer space, and provided a means of transferring information reliably and securely, even through massive jamming. Submarine habitability, lubricants, shipbuilding materials, firefighting, and the study of sound in the sea have remained steadfast concerns, to which have been added recent explorations within the fields of virtual reality, superconductivity, and biomolecular science and engineering.

The Laboratory has pioneered naval research into space—from atmospheric probes with captured V-2 rockets, through direction of the Vanguard project (America's first satellite program), to inventing and developing the first satellite prototypes of the Global Positioning System. Today, NRL is the Navy's lead laboratory in space systems research, fire research, tactical electronic warfare, microelectronic devices, and artificial intelligence.

The consolidation in 1992 of NRL and the Naval Oceanographic and Atmospheric Research Laboratory, with centers at Bay St. Louis, Mississippi, and Monterey, California, added critical new strengths to the Laboratory. NRL now is additionally the lead Navy center for research in ocean and atmospheric sciences, with special strengths in physical oceanography, marine geosciences, ocean acoustics, marine meteorology, and remote oceanic and atmospheric sensing. The expanded Laboratory is focusing its research efforts on new Navy strategic interests and needs in the post-Cold War world. Although not abandoning its interests in blue-water operations and research, the Navy is also focusing on defending American interests in the world's littoral regions. NRL scientists and engineers are working to give the Navy the special knowledge and capabilities it needs to operate in these waters.

2005 IN REVIEW

In the year just past, the scientific community at NRL has conducted innovative research across a wide spectrum of technical areas in addition to that reported elsewhere in this *NRL Review*, and part of this scientific effort is reflected in the following material.

AMRFC: The growing number of topside antennas appearing on Navy Ships is presenting several operational problems: increased antenna blockage, difficulty with hull-related electromagnetic interference, and an increased radar cross-section. In addition, few of these systems are integrated, thus each requiring its own set of spare parts, maintenance personnel, and operators. Consequently, the Advanced Multifunction Radio Frequency Concept (AMRFC) Testbed Program was launched to design, build, and test a proof-of-principle system that would integrate many sorts of shipboard radio frequency functions by utilizing a common set of broadband array antennas, signal and data processing, signal generation, and display hardware. In the early fall of 2005, testbed development at NRL's Chesapeake Bay Detachment was completed with all major goals accomplished, thereby *simultaneously* integrating under real-world conditions in a relative environment, several different classes of RF functions into a common set of antennas, RF and processing equipment, and real-time control software.

LAEMAR: There is a need for a method and apparatus for producing specialized audio signals for military personnel wearing helmets. The goal of this research, Localized Audio Environment for Mobile Augmented Reality, is sponsored by the Office of Naval Research to investigate methods of delivering informational sound and conversations to soldiers. A key feature was to investigate the use of spatialized audio: sound that gives the listener the impression of a sound source within a three-dimensional environment. However, spatialized sound typically requires headphones to deliver two distinct channels (i.e., stereo). Their use occludes the ears, thereby attenuating the environment and conversations. Thus, military ground personnel using only one headphone negate the advantage of the natural ability to monitor two conversations or hear the direction from which a sound originates. A system was developed that combines previously known technology for generating spatial sound with a new way of positioning the speakers to solve some of the known limitations of headphone-based sound. This system provides a way, without occluding the wearer's ears, to use sound to deliver multiple radio channels to a ground combatant wearing a helmet so that spatialized sound as well as ambient sound and conversation can be heard. This development has application for military communication systems to and between soldiers wearing helmets.

UAVs: Electrically propelled unmanned aerial vehicles have an advantage over those UAVs using internal combustion propulsion; however, as an energy source, batteries have lower endurance capability than those UAVs using internal combustion power because

batteries have a lower specific energy than hydrocarbon fuels. Military UAVs currently in operation (Dragon Eye, Raven, Sentry Owl) are limited to 1 or 2 hours of flight. A fuel cell power system would enable an electrically powered UAV to use a higher specific energy fuel as its energy source. To this end, the Chemistry and Tactical Electronic Warfare Divisions of NRL have jointly developed a proton exchange membrane (PEM) fuel cell using commercially available components that combines stored hydrogen electrochemically with atmospheric oxygen to produce water and electrical power. This energy source was used to power a 5.6 pound experimental, remotely controlled UAV (Spider Lion) for 103 minutes (an unofficial world record) using a fuel load of 10 grams of hydrogen gas. Significant project goals achieved include demonstration of the feasibility of a PEM fuel cell to power a UAV; extension of the flight time available with batteries; and experience gained with all of the ramifications of fuel cell operation. It is envisioned that efficient, fuel cell-powered UAVs will achieve 8 to 10 hours of flight during persistent surveillance missions.

Towed Decoy Progress: Towed decoys are used to protect military fighter and transport aircraft against radar-guided air-to-air or surface-to-air missiles. Deception transmitters placed in decoys in a towline can render a missile's proximity fuse harmless by misguiding its monopulse radars. However, the sheathing of towlines subjected to a fighter jet's afterburner plume can be thermo-oxidatively degraded, causing a subsequent breakdown of the conducting and communication components. To address this weakness, a joint Navy/Air Force program has been established to develop advanced towline systems by incorporating and evaluating high temperature thermo-oxidatively stable inorganic/organic hybrid materials, such as diacetylene-containing poly(carbor-anylenesiloxanes) developed at NRL, to provide thermo-oxidative protection of the high performance organic (Zylon or carbon) fibers and conducting materials used in towlines. Adequate thermal protection for the structural member of the towline can provide for storing longer, thinner towlines in the deployment canister. This will provide for a greater tow distance between the canister and the military aircraft and provide greater protection from missiles.

Preventing launch-related damage: Launch-related damage to shuttles is a fairly common occurrence, and there is an urgent requirement for the development of a capability to make on-orbit repair to critical components damaged during launch or while in orbit. Some shuttle surfaces are composed of silicon carbide-coated carbon-carbon composite (RCC) material, while other surfaces are covered with lower temperature insulating tiles, both of which are subject to damage by launch debris. Nearly all repair techniques extant require heating the repair material to moderate or high temperature to ensure survival of the repair during entry. This requirement places a severe strain on the modest energy source available for such repair. At the behest of NASA, NRL has developed a microwave system providing an S-band (2.45 GHz) microwave source that can effectively heat-repair RCC and other types of lower temperature insulation surfaces to the required cure temperature. This microwave system is superior to extant methods for effecting repair curing. Microwaves are suitable for such repairs because of their ability to localize energy deposition spatially and deposit energy in depth. The curing of repairs to RCC material can be performed with about 10% of the power and energy required for the next best technique (heating blankets). The feasibility of developing a portable battery-powered repair system to be used by an astronaut working outside the shuttle was demonstrated.

Doping nanocrystals: Nanocrystals are tiny semiconductor particles that exhibit unique electronic, optical, and magnetic properties utilized in many technologies, and chemical methods have been optimized to synthesize pure nanocrystals. However, to tailor these crystals to make them useful for specific applications, they have to have selected impurities controllably incorporated into them. The mystery: why some nanocrystals can't be doped successfully. It was found that successful doping is resident in the crystal's surface. If an impurity atom absorbs on the crystal surface strongly enough it can eventually be incorporated into the nanocrystal as it grows. If the impurity binds to the crystal too weakly, or if the strong binding surfaces are only a small fraction of the total, then doping will be difficult. This new understanding of the mechanism of doping announced by NRL and the University of Minnesota should enable a variety of new technologies such as high-efficiency solar cells, lasers, and ultra-sensitive biodetection devices. It also overturns a previous view that nanocrystals are intrinsically difficult to dope because they "self purify" by expelling impurities from their interiors so that the same mechanisms that made it possible to grow pure nanocrystals also made it extremely difficult to dope them.

Easier imaging: Transmission imaging of electronic and defect properties of wide bandgap semiconductors has been achieved using optical scanning. This allows for the characterization of defects in wide bandgap semiconductors using commercially available optical scanners equipped with transparency or negative scanning capability. A semiconductor wafer is placed between crossed polarizers or between a linear

polarizer and a circular polarizer. Scanner exposure is adjusted so regions without a wafer are considered 100% transmission; regions completely blocked are considered 0% transmission. The resulting scan reveals nothing for a perfect wafer; for imperfect wafers, defects are revealed as regions of varying brightness. Detailed information about wafer imperfections is obtained with high spatial resolution, approximately 6 microns. When wafers are scanned without the use of polarizers, it is possible to obtain optical transmission maps containing information about doping density and thickness variations. There is a darkening of the wafer when doping density is high. This technique has simplified the approach of using optical transmission to obtain information about the quality of SiC wafers. In a cross-polarized mode, defect information is obtained; when using unpolarized light, doping density and total thickness variations can be obtained.

BUG: Nearly all oceanographic instrumentation relies on batteries for power. Since batteries are depletable, this greatly limits deployment duration and requires costly resource-intensive instrument retrieval and battery replacement. To alleviate this problem, a two-electrode fuel cell-like power generator, Benthic Unattended Generator (BUG), has been developed consisting of an anode embedded in marine sediment connected by an external circuit to a cathode positioned in overlying water. The generator is an energy producer that can generate electric power indefinitely on the surface of marine sediment by oxidation of sediment organic matter with oxygen in the water. The anode, configured as an array of trapezoidal parallel plates vertically attached to a sled–like carriage, is embedded in the sediment by application of horizontal tension to the deployment line.

Noninterferometric Fiber-optic Microphone: Conventional capacitive microphones typically require large expensive preamps at the sensor head. Such microphones also lead to large levels of 1/f noise that limit the use of such devices at low frequency levels and prevent their use in pseudostatic applications. In addition, these electrical devices are problematic in high EMI and explosive environments. Also, there has been a long-term general need for non-electrical microphone technology capable of monitoring low acoustic levels. A new NRL-designed noninterferometric fiber-optic microphone combines a slender fiber-optic probe with a micro-machined silicone diaphragm. The microphone is small, inexpensive, has a very low threshold detectability, and is very broadband, with an almost flat internal noise power spectrum. And being based on optical intensity measurements, it does not require the sophisticated, complex, and costly demodulation designs and associated components required by interferometric fiber-optic sensors. This technology represents accomplishments in design, fabrication, and integration of thin micro-machined diaphragms, the fiber optic probe itself, and the adaptability to fiber-optic microphones.

Simulating Ocean Acoustics: Shallow water solitons are one example of how an ocean feature can disturb the nominal acoustic field propagating in shallow water. While smaller magnitude oceanographic changes affect the acoustic field less dramatically than do solitons, the cumulative effects on long-range acoustic propagation can be significant. At one end of the spectrum of nonlinear wave phenomenon are the solitons. These extremely stable solitary waveforms, whose stability is due to a balance between nonlinear and dispersive effects, are best known for their remarkable ability to interact like particles. At the other end of the spectrum are propagating singular surfaces, in particular *acceleration* and *shock waves*. Under certain conditions, the amplitude of acceleration waves can develop a singularity in finite-time and a shock wave is formed. In particular types of dissipative media, shock waves can be focused in this way by controlling the amplitude and/or frequency of the input signal. Completion of this work would couple analytically oceanography to ocean acoustics via each primitive parameter in the oceanographic equations that affects the ocean acoustic field, thus allowing simulation studies of shallow water effects of small scale changes on the acoustic field.

Milky Way as Teacher: At 25,000 light years (2.5×10^{20} m), the center of our galaxy, the Milky Way, provides the foundation for understanding phenomena in other galaxies. The central black hole and regions of intense star formation in its vicinity can be probed at 100 times the resolution of even the nearest galaxies. However, its magnetic field, which has the potential to transform, store, and explosively release energy, to transport angular momentum, and to confine high-energy plasmas into powerful jet flows, remains poorly understood. Magnetic fields are found throughout the Milky Way. Measurements suggest that the magnetic field in the spiral disk of our galaxy has two components, one globally ordered and the other random, with approximately equal strengths of ~0.3 nT; the globally ordered component generally follows the spiral arms of the galaxy. Recent observations at radio and submillimeter wavelengths have revealed that the magnetic filaments are more widespread than previously thought. They also exhibit a geometric complexity inconsistent with the prevailing notion of a strong, space-filling magnetic field in the region that is not accounted for in current models of the magnetic environment at the galactic center.

ORGANIZATION AND ADMINISTRATION

The Naval Research Laboratory is a field command under the Chief of Naval Research, who reports to the Secretary of the Navy via the Assistant Secretary of the Navy for Research, Development and Acquisition.

Heading the Laboratory with joint responsibilities are CAPT Daniel R. Gahagan, USN, Commanding Officer, and Dr. John A. Montgomery, Director of Research. Line authority passes from the Commanding Officer and the Director of Research to three Associate Directors of Research, the Director of the Naval Center for Space Technology, and the Associate Director for Business Operations. Research divisions are organized under the following functional directorates:

- Systems
- Materials Science and Component Technology
- Ocean and Atmospheric Science and Technology
- Naval Center for Space Technology.

NRL operates as a Navy Working Capital Fund (NWCF). All costs, including overhead, are charged to various research projects. Funding in FY05 came from the Chief of Naval Research, the Naval Systems Commands, and other Navy sources; government agencies, such as the U.S. Air Force, the Defense Advanced Research Projects Agency, the Department of Energy, and the National Aeronautics and Space Administration; and several nongovernment activities.

PERSONNEL DEVELOPMENT

At the end of FY05, NRL employed 2752 persons—35 officers, 88 enlisted, and 2629 civilians. In the research staff, there are 813 employees with doctorate degrees, 337 with masters degrees, and 460 with bachelors degrees. The support staff assists the research staff by providing administrative, computer-aided design, machining, fabrication, electronic construction, publication and imaging, personnel development, information retrieval, large mainframe computer support, and contracting and supply management services.

Opportunities for higher education and other professional training for NRL employees are available through several programs offered by the Employee Relations Branch. These programs provide for graduate work leading to advanced degrees, advanced training, college course work, short courses, continuing education, and career counseling. Graduate students, in certain cases, may use their NRL research for thesis material.

In a change of command ceremony held at NRL on October 7, 2005 CAPT David Schubert (center) retired from naval service and handed over command of NRL to CAPT Daniel Gahagan (right). RADM Jay Cohen (left) looks on during the ceremony.

For non-NRL employees, several postdoctoral research programs exist. There are also agreements with several universities for student opportunities under the Student Career Experience Program (formerly known as Cooperative Education), as well as summer and part-time employment programs. Summer and interchange programs for college faculty members, professional consultants, and employees of other government agencies are also available.

For more information, see the *NRL Review* chapter, "Programs for Professional Development."

NRL has active chapters of Women in Science and Engineering, Sigma Xi, Toastmasters International, and the Federal Executive and Professional Association. Three computer clubs meet regularly—NRL Microcomputer User's Group, NeXT, and Sun NRL Users Group. An amateur radio club, a drama group (the Showboaters), and several sports clubs are also active. NRL has a Recreation Club that provides sports leagues and swim, whirlpool bath, gymnasium, and weight-room facilities. The Recreation Club offers classes in martial arts, aerobics, swimming, and water walking.

The award winning Community Outreach Program directed by the Public Affairs Office, traditionally has used its extensive resources to foster programs that provide benefits to students and other community citizens. Volunteer employees assist with and judge science fairs, give lectures, and serve as tutors, mentors, coaches, and classroom resource teachers. The program sponsors African American History Month art and essay contests for local schools, student tours of NRL, an annual holiday party for neighborhood children in December, and a book donation program for both students and teachers. Through the Community Outreach

Program, NRL has active partnerships with four District of Columbia public schools.

NRL has an active, growing credit union. Since its creation in 1946, NRL Federal Credit Union (NRLFCU) has grown to about $360 million in assets and serves about 22,000 NRL employees, contractors, select employee groups, and their families. With the addition of their newest branch in Waldorf, Maryland, NRLFCU remains a leader in providing innovative financial services such as a dynamic home page and online access (Internet home banking) with free bill payer. Focusing on its mission of Trusted Partners for Life, NRLFCU offers a wide array of no-fee services plus financial education and assistance. NRLFCU is a full-service financial institution offering various savings programs, creative lending services, and mortage programs. NRLFCU also offers full-service investment and brokerage services. For information about membership or any financial services, call (301) 839-8400 or click on www.nrlfcu.org.

Public transportation to NRL is provided by Metrobus. Metrorail service is three miles away.

SCIENTIFIC FACILITIES

In addition to its Washington, D.C., campus of about 130 acres and 85 main buildings, NRL maintains 11 other research sites, including a vessel for fire research and a Flight Support Detachment. The many diverse scientific and technological research and support facilities are described in the following paragraphs.

RESEARCH FACILITIES

Institute for Nanoscience

The revolutionary opportunities available in nanoscience/nanotechnology have led to a National Nanotechnology Initiative. NRL has been a major contributor to the science of nanostructures and is making a commitment to expand that effort. The NRL Institute for Nanoscience has been established with a $10 million annual budget in core research funds. The mission of the Institute for Nanoscience is to conduct highly innovative, interdisciplinary research at the intersections of the fields of materials, electronics, and biology in the nanometer-size domain. The Institute will exploit the broad multidisciplinary character of the Naval Research Laboratory to bring together scientists with disparate training and backgrounds to pursue common goals at the intersection of their respective fields at this length scale. The objective of the Institute's programs is to provide the Navy and DoD with scientific leadership in this complex, emerging area and to identify opportunities for advances in future Defense technology.

Official ribbon cutting ceremony at the grand opening of the new NRLFCU Waldorf branch.

Its current research program emphasizes multidisciplinary, cross-division efforts in nanomaterials, nanoelectronics, and nanosensors/devices.

Radar

NRL has gained worldwide renown as the "birthplace of radar" and, for a half-century, has maintained its reputation as a leading center for radar-related research and development. A number of facilities managed by NRL's Radar Division continue to contribute to this reputation.

A widely used major facility is the Compact Antenna Range (operated jointly with the Space Systems Development Department) for antenna design and development, as well as radar cross-section measurements. The range is capable of simulating far-field conditions from 1 to 110 GHz, with a quiet zone of approximately 7 ft in diameter and 8 ft in length. Instrumentation covers from 1 to 95 GHz. Another strong division capability is in the Computational Electromagnetics (CEM) Facility, which has capabilities for complex electromagnetic modeling, including radar target and antenna structures. The Radar Signature Calculation Facility within this group produces detailed computations of radar cross sections of various targets, primarily ships. The CEM facility includes multiple-CPU supercomputers that are also used to design phased array radar antennas. The tremendous synergism between the CEM group and the Compact Range Facility provides the ability to design in the CEM environment, to test in the compact range, and to have immediate feedback between the theoretical and experimental aspects to shorten the development cycle for new designs.

In connection with airborne radar, the division operates a supercomputer-based Radar Imaging Facil-

ity and an inverse synthetic aperture radar (ISAR) deployed either in the air, on the ground, or aboard ship for radar-imaging data collection. A P-3 aircraft equipped with the AN/APS 145 radar and cooperative engagement capability is also available for mounting experiments.

In connection with ship-based radar, the division operates the Radar Test-Bed Facility at the Chesapeake Bay Detachment (CBD), Randle Cliffs, Maryland. The site has radars for long-range air search and surface search functions and features the newly developed W-band Advanced Radar for Low Observable Control (WARLOC), a fully operational high-power coherent millimeter wave radar operating at 94 GHz. The WARLOC transmitter is capable of producing 10 kW of average power with a variety of waveforms suitable for precision tracking and imaging of targets at long range. Waveforms with a bandwidth of 600 MHz can be transmitted at full power. A 6-ft cassegrain antenna is mounted on a precision pedestal and achieves 62 dB of gain.

The Advanced Multifunction RF Concept (AMRFC) test bed is a new installation at CBD, operated by the Radar Division, but with joint participation of several other NRL divisions as well. The goal of the AMRFC program is to demonstrate the integration of many sorts of shipboard RF functions, including radar, electronic warfare (EW), and communications by utilizing a common set of broadband array antennas, signal and data processing, signal generation, and display hardware. The test bed consists of separate active transmit and receive arrays that operate over the 6- to 18-GHz band (nominally). Current functionality of the testbed includes a multimode navigation/surface surveillance Doppler radar, multiple communication links (line-of-sight and satellite), and passive and active EW capabilities. Test-bed electronics are housed in seven converted 20-ft shipping containers and trailers. The arrays are mounted on a 15° tilt-back in the ends of two of the trailers overlooking the Chesapeake Bay, emulating a possible shipboard installation.

The AMRFC testbed, located at NRL's CBD, was developed as a proof of principle demonstration system that is capable of simultaneously transmitting and receiving multiple beams from common transmit and receive array antennas for radar, electronic warfare, and communications. These RF functions are controlled by common resource allocation manager (RAM) software over a real-time control network. New RF functionality may be readily added to the testbed as required for further demonstrations.

The division also has access to other radar systems: the Microwave Microscope (MWM); the Navy's relocatable over-the-horizon radar (AN/TPS-71); and an experimental Cooperative Aircraft Identification system. The internally developed MWM has a high-resolution (2-cm) ultrawideband capability that is used to investigate backscatter from surface and volumetric clutter, has through-wall detection capability, and characterizes the impulse responses of scattering objects. With respect to the AN/TPS-71, the division provides direct technical support and has direct access to data. The Cooperative Aircraft Identification system is used to explore system concepts and engineering developments in connection with target identification.

Information Technology

The Information Technology Division (ITD) is at the forefront of DoD research and development in artificial intelligence, telecommunications, net-centric distributed computing, human-computer interaction, information security and assurance, parallel supercomputing, and computer science.

The division maintains local-area computer networks to support its research, and it hosts testbeds for advanced high performance optical network research. These networks make hundreds of high performance computers across DoD available to local and remote users. The ITD research networks connect internal NRL networks via high-speed links to the NASA Science Internet (NSI); to OC-12c (622 Mbps) on DREN/S-DREN; to OC48c on DREN and S-DREN to HPCMP sites; and to OC192c and all optical wavelengths across ATDnet and BoSSNET to form the DoD's Global Information Grid Evaluation Facility (GIG-EF) internetworking facility. GIG-EF provides wavelengths for DoD end-to-end demonstration, system engineering, and experimentation. GIG-EF provides a coalition of early adopters the key test validation infrastructure for transforming the DoD to network-centric IPv6/MPLS convergence for future use by the services, NASA, and Intelligence and Coalition partners.

The ATDnet and BoSSNET also provide the core of an extended all-optical network that supports advanced signaling, routing, and switching research with transparent wavelengths. Major collaborators include the National Security Agency, the Defense Information Systems Agency, the Defense Advanced Research Projects Agency, the Defense Intelligence Agency, the National Aeronautics and Space Administration, the

The 256-processor Silicon Graphics Altix 3000 with 1 terabyte of RAM (the first production unit in the world with this capability). It was brought online in the third quarter FY04.

Mid-Atlantic Crossroads (MAX), and the Massachusetts Institute of Technology/Lincoln Laboratory. Optical research includes introduction and testing of new network protocols that emphasize low latency and wave-division multiplexing, greatly increased network capacity for both aggregate and single flows, and the evolution of all-optical networks with direct switching and tuning at the optical layer.

Research of high-end computational assets and networks results in close association with ONR/Naval S&T applications' communities that demand these leading-edge capabilities. This has allowed ITD to achieve significant results in a number of areas. Current efforts include raising the state-of-the-art in motion imagery with progressive scan high-definition sensors and displays where 1 to 10 Gbps data streams are used to handle raw output to disk-based archives. The Motion Imagery Laboratory (MIL) continues exploitation of imagery to provide a flexible, immersive visualization environment for experiments in the convergence of progressive motion imagery; high performance distributed computing; large distributed, federated, scalable petabyte datasets; and dynamic wavelength networking that allow the end user to be enveloped in the data presentation immersively, with a capability for real-time manipulation and fusion.

The Defense Research and Engineering Network (DREN) is a high-speed Continental U.S. (CONUS) network that connects the four High Performance Computing Modernization Program (HPCMP) Major Shared Resource Centers (MSRCs), and the 16 Distributed Centers (DCs), as well as a number of service user organizations that use HPCMP resources.

As one of the HPCMP DC sites, ITD's Center for Computational Science (CCS) supports a range of shared resources, including large memory parallel supercomputers, SAN archives, and high performance networks. Current systems include an SGI Altix 3000 Scalable Linux Supercomputer with Intel Itanium 2 processors (384 Madison) and 1.25 terabytes of shared memory, an SGI Onyx 3400 IR4, a Cray XD1 with dual core AMD Opteron processors (576), and an Onyx4 visualization capability. The Altix supercomputer extends NRL-SGI's first successful attempt to pioneer the use of Linux as the basis of a single scalable shared memory (SHMEM) image supercomputer. The Cray XD1 was new in late 2005 and, like the Altix, is a LINUX-based machine. The Cray XD1 brings a new capability to the Center with the integration of 144 Field Programmable Gate Arrays (FPGA) closely coupled in the machine's architecture. The CCS has approximately 30 terabytes of nearline shared rotating disk and robotic storage for fileserving and archiving that holds 500 terabytes and is capable of multipetabyte scale. The Center manages the NRL local area NICEnet, a fully switched infrastructure based on ATM and gigabit ethernet backbones. The goal of the Center is to provide digital transparency of information resources with security across the information assured infrastructure from globally available archives, to computational engines, to autonomous networks that bring resources together at 10 Gbps directly to desktops of the most demanding researchers. NICEnet provides external connections to other Federal networks and to the Internet.

Division facilities include an Information Security Engineering Laboratory, a Robotics Laboratory, an Immersive Simulation Laboratory, an Audio Laboratory, a Warfighter Human-System Integration Laboratory, and a high-data-rate multimedia satellite transmission facility.

The Integrated Communications Technology (ICT) Test Lab provides a rapidly reconfigurable means to perform testing and evaluation of advanced networking technologies in support of multiple DoD programs such as Joint Tactical Radio System (JTRS), Fleet Battle Experiments, Joint Forces Command Modeling & Simulation, Joint Experimentation, JTF WARNET, and Dragon Warrior. It provides connectivity to both classified (SIPRNet) and unclassified (NIPRNet) networks through high-speed Ethernet and ATM interfaces with connections to the Defense Research and Engineer-

ing Network (DREN) to facilitate collaborative efforts with other DoD facilities. It is an integral part of the Global Information Grid End-to-End Evaluation Facilities (GIG-EF), and is also a component of the JTRS Joint Virtual Lab (JVL). The ICT Test Lab houses a large base of networking equipment and test gear such as network traffic generators and analyzers, signal generators, and spectrum analyzers, which allow real-time injection and monitoring of wired and wireless traffic flows from simulated and "real world" data sources. Lab computers running NRL-developed software test programs tailored to meet specific test requirements can assess the performance of military and commercial off-the-shelf (COTS) equipment such as network radios, routers, and communications security (COMSEC) devices. This facility is instrumental in providing the kind of simulation and test environment required to support the research and development of advanced dynamic networking protocols, wireless mobile ad-hoc routing techniques, and bandwidth, power, and quality of service (QoS) management for the Navy's current and future communication networking needs.

The Mobile and Dynamic Network Laboratory facility supports development and evaluation of next-generation communication technologies for mobile and dynamic data networks. This includes wireless and other challenging communication environments relevant to military systems. The laboratory provides for large-scale network simulation, real-time network emulation, and tools to support live field tests of wireless, mobile networks. The facility has provided support for a variety of ongoing NRL-, ONR-, and DARPA-sponsored projects including cooperative international research in support of coalition networks.

The General Electronics Environmental Test Facility includes automated electronic test equipment and instrumentation, a phase noise measurement system, a noise figure measurement system, precision spectrum analyzers, wide-band signal generators, a 40-cubic-foot environmental chamber, and an EMI test chamber located off-site. A variety of additional test equipment including signal generators, signal analysis, electrical and optical stimulation and response measurement equipment are employed in the performance validation of electronic and fiber-optic equipment. This facility provides resources for testing the performance and function of electronic and fiber-optic equipment under conditions that represent the environment that the equipment could experience during the deployment to and installation in a Naval ship or Marine Corps tactical environment. Several laboratories are available to test electronic and fiber-optic equipment to validate the performance under the conditions described in MIL-PRF-28800F. The test conditions defined in MIL-PRF-28800F are designed to replicate the variety of environmental conditions that test equipment could experience when deployed to the Fleet.

The Naval Cryptographic Technology Laboratory provides a secure environment to perform research and develop prototype programmable cryptographic technologies for Navy and DoD applications. The Laboratory also allows for development of certifiable Communications Security (COMSEC)/Information Security (INFOSEC) products, including programmable cryptographic devices, cryptographic applications, and high assurance cross-domain solutions.

The Naval Key Management Laboratory provides a secure environment to conduct research and develop advanced electronic key management and networked key distribution technologies for the Navy and DoD. This Laboratory, in conjunction with ITD's Naval Cryptographic Technology Laboratory, serves as a testbed for testing new key management components and key delivery protocols developed for the Electronic Key Management System (EKMS) and the modernized Key Management Infrastructure (KMI).

The Fleet Information Systems Security Technology Laboratory (FISSTL) provides unique facilities for NRL research into Navy and DoD information technology network security. FISSTL provides direct support in the areas of Computer Network Defense, Cross-Domain Solutions, Reverse Code Analysis and Support, and Global Information Grid Evaluation Facilities. From architectural design, review, and prototyping, to component evaluation and integration, the FISSTL ensures secure capability and availability of DoD and Navy network-centric information operations.

The 3-D Mixed and Virtual Environments Laboratory (3DMVEL) is exploring the means by which 3-D computer graphics can be used to aid in the collection, interpretation, and dissemination of information for both operational and training purposes. Mixed Reality is a continuum from virtual reality (in which a user is immersed in a completely generated world) to augmented reality (in which the user sees the real world, which has been annotated using computer graphics). The 3DMVEL has a comprehensive range of hardware to support experiments across the entire continuum. Virtual reality (VR) equipment includes desktop VR systems (conventional PCs with graphics accelerated hardware), head-mounted displays (HMDs), the Responsive Workbench, and the surround-screen immersive room. The Responsive Workbench is an interactive 3-D tabletop environment that displays computer-generated stereographics on the workbench surface for use in battlespace situation awareness, simulation-based design, and other applications. The surround-screen Immersive Room is a multiuser, high-resolution, 3-D visual, and audio environment that projects computer-generated images onto three walls

Nanochannel glass draw towers housed in a Class 100 clean room. Inset — Preform to be drawn into a photonic crystal fiber.

and the floor, creating an immersive, large-scale, shared virtual environment. Augmented reality equipment includes wearable computers, optical and video see-through head mounted displays, vision and non-vision-based tracking hardware, global positioning systems, and inertial systems.

ITD has the facilities to support a range of motion-based research on human performance. A one-person, three-degrees-of-freedom platform is available for vestibular research. A ship motion simulator, owned and operated by NRL since 1943, is available to evaluate the impact of pitch and roll on task performance.

Optical Sciences

The Optical Sciences Division has a broad program of basic and applied research in optics and electro-optics. Areas of concentration include fiber optics, integrated optical devices, signal processing, fiber-optic and infrared sensors, optical information processing, panchromatic and hyperspectral imaging for surveillance and reconnaissance, and laser development.

The division occupies some of the most modern optical facilities in the country. This includes several fiber-optic facilities including preform fabrication, draw towers, optical fiber coaters, fiber splicers, and fiber-optic sensor testing stations such as an acoustic test cell and a three-axis magnetic sensor test cell. There is also an Ultralow-loss, Infrared (IR) Fiber-Optic Waveguide Facility using high-temperature IR glass technology. The Focal-Plane Evaluation Facility allows measurement of the optical and electrical characteristics of infrared focal-plane arrays being developed for advanced Navy sensors. The IR Missile-Seeker Evaluation Facility performs open-loop measurements of the susceptibilities of IR tracking sensors to optical countermeasures. The Large-Optic, High-Precision Tracker system is used for atmospheric transmission and target signature measurements. The Infrared Test Chamber is an ultradry test chamber used to measure the IR signatures of new surface treatments, scale models, and components used for signature control on ships, aircraft, and missiles. A UHV multichamber deposition apparatus for fabrication of electro-optical devices is interfaced to a surface analysis chamber equipped with UPS, XPS, AFM, and STM. Other scanning probe facilities are equipped with Atomic Force and Magnetic Force Microscopes. An extensive set of laboratories exist to develop and test new laser and nonlinear frequency conversion concepts and to evaluate nondestructive test and evaluation techniques.

Electronic Warfare

The scope of the Tactical Electronic Warfare (TEW) Division's program for electronic warfare (EW) research and development covers the entire electromagnetic spectrum. The program includes basic technology research and advanced developments and their applica-

HMMWV installation of the Gunfire Detection and Location System that includes an IR detection sensor that automatically slews a day-night sensor suite to the position of hostile gunfire. The warfighter observes the scene and takes appropriate actions.

bility to producing EW products. The range of ongoing activities includes components, techniques, and subsystems development as well as system conceptualization, design, and effectiveness evaluation. The focus of the research activities extends across the entire breadth of the battlespace. These activities emphasize providing the methods and means to counter enemy hostile actions—from the beginning, when enemy forces are being mobilized for an attack, through to the final stages of the engagement. In conducting this program, the TEW Division has an extensive array of special research and development laboratories, anechoic chambers, and modern computer systems for modeling and simulation work. Dedicated field sites and an NP-3D EW flying laboratory allow for the conduct of field experiments and operational trials. This assembly of scientists, engineers, and specialized facilities also supports the innovative use of all Fleet defensive and offensive EW resources now available to operational forces through the Naval Fleet/Force Technology Innovation Office.

Laboratory for Structure of Matter

This laboratory investigates the atomic arrangements in materials to improve them or facilitate the development of new substances. Various diffraction methodologies are used to make these investigations. Subjects of interest include the structural and functional aspects of energy conversion, ion transport, device materials, and physiologically active substances such as drugs, antibiotics, and antiviral agents. Theoretical chemistry calculations are used to complement the structural research. A real-time graphics system aids in modeling and molecular dynamics studies. The facilities include three X-ray diffraction units, two being state-of-the-art facilities, and an atomic force microscope.

Chemistry

NRL has been a major center for chemical research in support of naval operational requirements since the late 1920s. The Chemistry Division continues this tradition. It is pursuing a broad spectrum of basic and applied research programs focusing on controlled energy release (fuels, fire, combustion, countermeasure decoys, explosives), surface chemistry (corrosion, adhesion, tribology, adsorbents, film growth/etch), advanced materials (high-strength/low-weight structures, drag reduction, damping, polymers, thin films, nanostructures), and advanced detection techniques (environment, chemical/biological, surveillance). Facilities for research include the following:

Chemical Analysis Facilities, with a wide range of modern photonic/electronic, magnetic- and ionic-based spectroscopic/microscope techniques for bulk and surface analysis;

Synchrotron Radiation Facility, with intense, monochromatic X-ray photon beams tunable from 10 eV to 12 KeV available from four beam lines developed by NRL at the National Synchrotron Light Source at the Brookhaven National Laboratory. Environmental target chambers span a pressure range from 10^{-12} to 10^{5} atm and temperatures from 10 to 1500 K;

Nanometer Measurement/Manipulation Facility, which includes fabrication and characterization capability based on scanning tunneling microscopy/spectroscopy, atomic force microscopy, and related techniques;

Materials Synthesis/Property Measurement Facility, with special emphasis on polymers, surface-film processing, and directed self assembly;

Fire Research Facilities, ranging from laboratory combustion chemistry to a 10^{4} ft^{3} fire-research chamber (Fire I) and the 475-ft ex-USS *Shadwell* (LSD-15) advanced fire research ship;

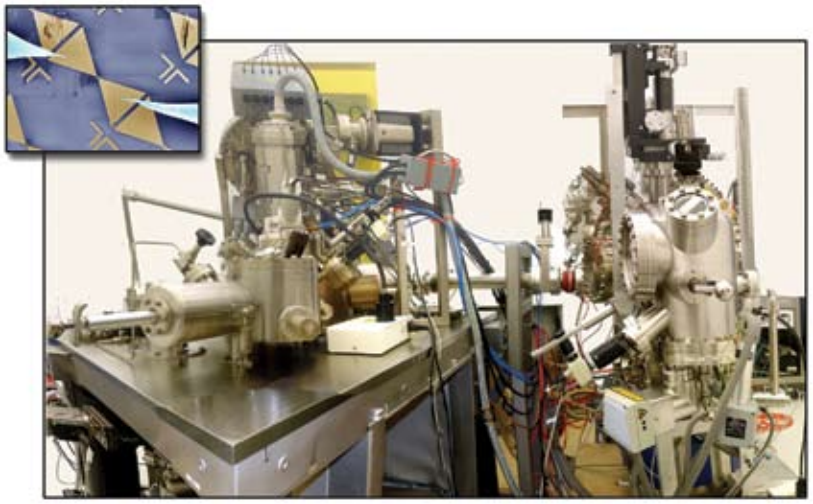

The Nanomanipulation and Characterization Facility, unique in the world, integrates a high-resolution scanning electron microscope (SEM) capable of nanoscale chemical analysis with a four-tip scanning probe system. The adjoining ultra-high vacuum surface analysis chamber (on the right) houses a combination scanning tunneling/atomic force microscope. Inset — A false-color SEM image showing two tips contacting gold microstructures.

Commensurate support has been devoted to survivorability of the new classes of ships, DDX, LUN21, LPD17, and LHA(R); and

Marine Corrosion Test Facility, located on Fleming Key at Key West, Florida, offers an ocean-air environment and clean, unpolluted, flowing seawater for studies of environmental effects on materials. Equipment is available for experiments involving weathering, general corrosion, fouling, and electrochemical phenomena as well as coatings, cathodic protection devices, and other means to combat environmental degradation.

Materials Science and Technology

The Materials Science and Technology Division at NRL conducts materials research using seven major division facilities.

The *Magnetoelectronics Fabrication Facility* consists of a Class 1000 clean room facility equipped with tools for lithographic construction of magnetoelectronic and spintronic devices. It provides pattern definition, metallization, dielectric layer deposition, and both reactive and Ar^+ ion etching of wafers and small pieces.

The *Electrical, Magnetic, and Optical Measurement Facility* is comprised of several complementary instruments that allow for the magnetic, electrical, optical and heat capacity characterization of materials and devices. SQUID and vibrating sample magnetometry are used to determine important properties of superconducting, paramagnetic, diamagnetic, and ferromagnetic materials. The transport properties of materials, namely the temperature and magnetic field-dependent resistivity combined with heat-capacity measurements, allow for a fundamental physical understanding of electronic properties.

The *Materials Processing Facility* includes apparatuses for powder production by fluid atomization, thermal evaporation, arc erosion, and a physical vapor deposition system designed to produce and coat submicron powders, in situ. Facilities to process powder into bulk specimens by hot and cold isostatic pressing permit a variety of consolidation possibilities. Isothermal heat treatment facility and quenching dilatometer permit alloy synthesis and single crystal growth. Bulk alloys can be prepared by induction melting, while rapid solidified metals of thin cross section can be made by splat quenching and melt spinning. Ceramic and ceramic-matrix composites processing facilities include a wide variety of conventional, controlled atmospheric furnaces, hot presses, ball milling apparatus and particle size determination, and sol-gel and organometallic coating processing capabilities.

The *Mechanical Characterization Facility* consists of various testing systems, many with automated computer control and data acquisition, for determining the mechanical response of materials under controlled loading/deformation and environmental conditions. Basic capabilities include quasistatic tensile and fracture testing, dynamic storage and loss moduli as a function of frequency and temperature, cyclic fatigue crack growth and corrosion fatigue testing, and stress-corrosion cracking testing.

The *Thin-Film Materials Synthesis and Processing Facility* provides users a wide variety of techniques for growth and processing of thin films (thickness 1 μm or less). Sputter deposition offers a versatile method of depositing metallic and dielectric films and is a primary tool of this facility. Thermal evaporation of metals is implemented in both high-vacuum and ultrahigh vacuum systems. Pulsed laser deposition (PLD) with temperature-variable stage temperature

The Magnetoelectronics Fabrication Facility consists of a Class 1000 clean room facility equipped with tools for lithographic construction of magneto-electronic and spintronic devices.

and controlled atmosphere allows growth of oxides. Electrolytic deposition offers efficient growth of gold and silver films. Laser direct write—both ablation and deposition—provide unique methods for imposing CAD-defined features via ablation of a substrate film and ablative mass transfer to a substrate.

The *3-MV Tandem Pelletron Accelerator Facility* uses two "pelletron" charging chains to produce a terminal voltage up to 3 MV in the accelerator. Negative ions are injected at 10 to 70 keV, accelerated up to the terminal where they undergo collisions with a stripper gas or a carbon stripper foil and lose electrons, then are accelerated as positive ions back to ground potential. Protons can be accelerated up to 6 MeV, He up to 9 MeV, and highly stripped Au (+12) up to 39 MeV. The lower limit of beam energy is about 400 keV. On the analysis beam line, the sample of interest is located at the end of the beam line, and a signal generated by scattering of incident high-energy ions indicates the composition of the sample. Incident high-energy ions can also be used to damage the surface of a sample of interest, or to introduce a dopant.

The *Micro-Nano Structure Characterization Facility* is capable of performing transmission electron microscopy, scanning transmission electron microscopy, ARTEM, electron energy loss spectroscopy, Z-contrast imaging, and spectral imaging through the use of a JEOL 2010F Transmission Electron Microscope, a Phillips CM30 Transmission Electron Microscope, and a Leo Scanning Electron Microscope. Other standard microstructure characterization instruments are also available.

Laboratory for Computational Physics and Fluid Dynamics

The Laboratory for Computational Physics and Fluid Dynamics (LCP&FD) maintains a very powerful collection of computer systems applied to a broad collection of work. There is currently a total of 120 parallel SGI processors, 512 clustered x86 processors, and several other support systems. In addition, there are over 50 Macintoshes in the group, most of which are capable of large calculations both indendently and in parallel ad hoc clusters.

The SGI computer systems comprise a 64 processor Itanium 2 processor SGI Altix, a 12 Itanium 2 processor SGI Altix, a 28 R12K processor Origin 3800, an 8 processor R14K processor Origin, and an 8 R12K processor Origin 2000. There are two 256 x86 processor clusters well coupled with Myrinet high-speed switched interconnect.

Each system has on the order of 200 gigabytes of disk space for storage during a simulation, and at least 512 megabytes of memory per processor. All unclassified systems share a common disk space for home directories as well as almost 250 gigabytes of AFS space, which can be used from any AFS-capable system throughout the allowed Internet.

The Micro-Nano Structure Characterization Facility is capable of performing TEM, STEM, ARTEM, EELS, and Z-contrast imaging and spectral imaging.

The AFS capability also allows access to other storage systems including NRL's multiresident AFS (MRAFS) system, which automatically handles archival to a multi-terabyte tape archival system.

Plasma Physics

The Plasma Physics Division is the major center for in-house Navy and DoD plasma physics research. The division conducts a broad experimental and theoretical program in basic and applied research in plasma physics, which includes laboratory and space plasmas, pulsed-power sources, plasma discharges, intense electron and ion beams and photon sources, atomic physics, laser physics, advanced spectral diagnostics, plasma processing, nonlinear dynamics and chaos, and numerical simulations. The facilities include an extremely high-power laser—Pharos III—for the laboratory simulation of space plasmas and nuclear weapons effects studies and two short-pulse high-intensity lasers—the Table-Top Terawatt (T^3) laser and the new Ti:Sapphire Femtosecond Laser (TFL)—to study intense laser-plasma, laser-electron beam, and laser-matter interactions. The division also has an 11-m^3 space chamber capable of reproducing the near-Earth space plasma environment and a Large Area Plasma Processing System (LAPPS) facility to study material modification such as surface polymerization or ion implantation. The division has developed a variety of pulsed-power sources to generate intense electron and ion beams, powerful discharges, and various types of radiation. The two largest of these pulsers—GAMBLE II and MERCURY—are used to study the production of terawatt electron and ion beams and to produce very hot, high-density plasmas. Other generators are used to

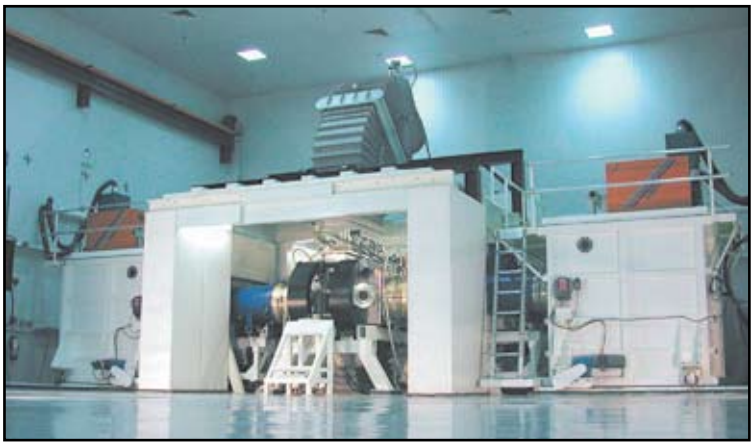

The NRL Electra system is used to develop high-energy high-repetition-rate KrF laser technology. The Electra 30-cm aperture electron-beam-pumped amplifier is shown in the photograph. A portion of the recirculating system that cools the laser gas can be seen at the top. This amplifier is capable of a 5 Hz repetition rate and has produced up to 700 J of laser light per pulse.

produce particle beams that are injected into magnetic fields and/or cavities to generate intense microwave pulses. A large array of high-frequency microwave sources (2.45, 35, and 83 GHz) are available to conduct research on microwave processing of advanced ceramic materials. In particular, the division added a 20-kW, continuous wave, 83 GHz gyrotron to its facility for research on high-frequency microwave processing of materials. The Russian-made gyrotron produces a focused, high-intensity millimeter-wave beam (10^3 – 10^5 W/cm^2) that has unique capabilities for rapid, selective heating of a wide range of nonmetallic materials.

A major 3 kJ KrF laser facility (Nike) opened in June 1995. This facility is made up of 56 laser beams and is single-pulsed (4-ns pulse). This facility provides intense radiation for studying inertial confinement fusion (ICF) target heating at short wavelengths (0.25 μm) and high-pressure physics. A second major inertial fusion system, Electra, is used to develop high-energy, high-repetition rate KrF technology. The amplifier is capable of a 5 Hz repetition rate and has produced up to 700 J of laser light in extended operation.

Electronics Science and Technology

The Electronics Science and Technology Division conducts a multidisciplinary basic and applied research program to exploit the creation/discovery/invention of new enabling materials, components, and techniques in electronics. In-house efforts include research and development in solid-state electronics; electronic materials including growth, theory, and characterization of semiconductors, heterostructures, and superconductors; surface and interface science; microwave and millimeter-wave components and techniques; microelectronic device research and fabrication; nanoelectronics science and technologies; vacuum electronics; power electronics; device and process modeling and simulation; and cryoelectronics.

In addition to specific equipment and facilities to support individual science and technology programs, the division operates the Compound Semiconductor Processing Facility (CSPF), the Laboratory for Advanced Materials Synthesis (LAMS), the Epicenter, the Vacuum Electronics Fabrication Facility (VEFF), the Ultrafast Laser Facility (ULF), the Wafer Bonding Facility (WBF), and the Space Solar Cell Characterization Facility (SSCCF).

The CSPF is dedicated to processing compound semiconductor devices and circuits, to providing micro- and nanofabrication processing support, and to selectively serving the hands-on fabrication needs of individual division and NRL scientists. The LAMS uses metallorganic chemical vapor deposition to synthesize a wide range of thin films, particularly wide bandgap semiconductors such as GaN and related alloys. The Epicenter (a joint activity of the Electronics Science and Technology, Materials Science and Technology, Optical Sciences, and Chemistry Divisions) is dedicated to the growth of multilayer nanostructures by molecular beam epitaxy (MBE). Current research involves the growth and etching of conventional III-V semiconductors, ferromagnetic semiconductor materials, 6.1 Å

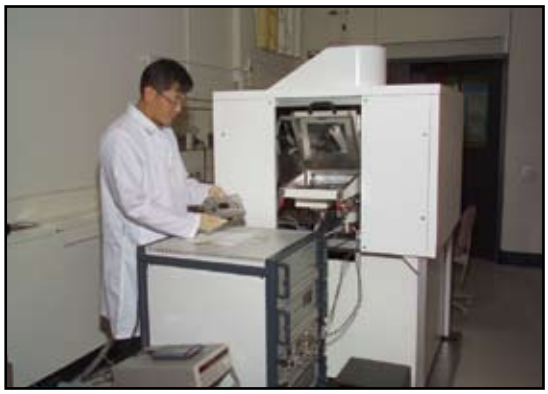

Electronics Science and Technology Division's ultrahigh-resolution electron beam lithography and metrology system.

III-V semiconductors, magnetic materials, and II-VI semiconductors. The structures grown in this facility are analyzed via in situ scanning tunneling microscopy and angle-resolved electron spectroscopy. The Ultrafast Laser Laboratory is optimized for the characterization of photophysical and photochemical processes in materials on a timescale of tens of femtoseconds. It includes a synchronously pumped dye laser system for simulating the effects of charge deposited in semiconductors characteristic of space radiation. The Wafer Bonding Facility is a Class 100 clean room facility for conducting research on the fabrication of high-voltage wafer-bonded power devices and the development of novel high-performance wafer-bonded substrates for epitaxial growth of both narrow bandgap and wide bandgap material layers. The Power Device Characterization Facility characterizes the performance and reliability of silicon and SiC power devices. The SSCCF studies the effect of particle irradiation on new and emerging solar cell technologies for space applications. The VEFF provides electrical and mechanical design, fabrication, assembly, modification, and repair, as well as processing services for vacuum electronic devices.

Bio/Molecular Science and Engineering

The Center for Bio/Molecular Science and Engineering conducts research and development using biotechnological approaches to support the Navy, DoD, and the nation at large. Studies are currently underway to investigate biomaterial development (for electronic and structural applications), environmental quality (including pollution cleanup and control), and chemical/biological warfare defense. Other program areas of interest include optical biosensors, nanoscale manipulations, genomics and proteomics, controlled sustained release, bio/molecular and cellular arrays, surface modification and patterning, energy harvesting, viral particles as scaffolds, advanced materials from self-assembly, and liquid-crystal-based electro-optic materials.

The staff of the Center is an interdisciplinary team with expertise in bio- and surface chemistry, biophysics, genetic engineering, cell biology, advanced organic synthesis, solid-state and theoretical physics, and electronics and materials engineering. In addition, the Center has collaborations throughout the Laboratory, with other government laboratories, at universities, and in industry.

The Center occupies laboratories and offices in Buildings 30 and 42. These modern facilities include general laboratories for research in chemistry, biochemistry, molecular biology, and physics. Specialized areas include a 600-ft^2 Class-1000 clean room, an advanced electron microscope facility, and a scanning probe microscope laboratory. Instrument rooms provide access to a variety of spectrophotometers and other equipment used in biochemical or physical analyses of biomaterials. Additional laboratories accommodate an X-ray diffraction instrument, a liquid crystal fabrication facility, and equipment for advanced electronics, microarrays, and biosensor programs. The Center has

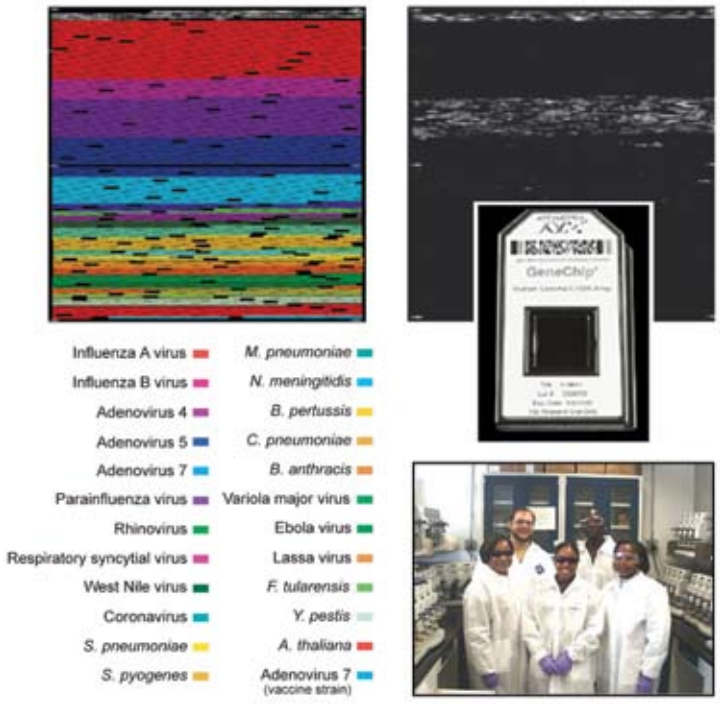

Resequencing Microarray System. The Respiratory Pathogen Microarray (key to this technique) is pictured with images of the processed chip (results) on the top right and left. On the bottom right is a photograph of the staff (two NRL employees, two Air Force personnel, one contractor) with multiple Affymetrix fluidic stations.

added a plastic microfabrication facility, which enables fabrication of microfluidic and micro-optical systems in polymers, and a state-of-the-art LC-MS for molecular characterization.

The Center's facilities were used to demonstrate the capabilities of a microarray system developed at NRL for analyzing thousands of samples in a high throughput production process. The previous figure illustrates the infectious and bioterrorism agents that could be detected. This successful demonstration used the Center's laboratory facilities with staffing from NRL, Air Force medical personnel, and contractors. At the completion of that program, a smaller scale version of the microarray system remained at the Center to continue research in the area of multiplex genomics-based molecular diagnostic arrays.

Acoustics

The Acoustics Division has three integrated structural acoustic facilities—two pools (including one with a sandy bottom) and a large in-air, semi-anechoic laboratory—that support research in submarine target characteristics for antisubmarine warfare, submarine acoustic design and quieting, sensors for hull-mounted sonars, mine detection and identification, torpedo quieting, and interior noise control in air platforms and submarines. Scaled submarine structures, real mines, sensors on hull simulators, underwater buried objects, torpedoes, aircraft fuselages, and space payload launch fairings and containers can all be examined with advanced nearfield holographic and scanning 3-D laser vibrometer systems to measure nearfield, farfield, and interior sound fields as well as the physics of the sound-structure-fluid interactions.

The division operates state-of-the-art laboratories equipped to study the structural dynamics and performance of high-Q oscillators and other micro-mechanical systems. A number of laser Doppler vibrometers, including a super-resolution nearfield scanning optical microscope (NSOM), permit spatial mapping of the complex vibratory motion down to resolutions of 100 nm. The laboratories include the ability to measure the mechanical and electrical properties of the micro-oscillators, and of thin films applied to them, down to 370 mK.

The division operates a portable, ocean-deployable synthetic aperture acoustic measurement system. The primary elements are sources and receivers attached to a robotic carriage that can be positioned precisely at any point along a 100-meter rail using an encoder feedback system. A separate source tower enables bistatic scattering data collection. Bidirectional control and data transfers are made over a dedicated RF link to a surface platform. This facility supports the collection of high quality, scattering cross sections of mines, and the associated clutter necessary for the implementation of new broadband MCM technologies on UUVs.

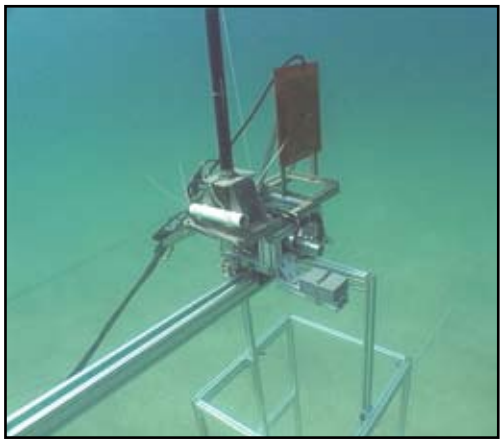

The 100-meter underwater rail-based synthetic aperture acoustic measurement system. Sources and receivers can be attached to a robotic carrier (shown here at one end of the rail). The carriage is shown in a monostatic configuration with integrated broadband projector (rectangle) and vertical receiver array (black cylinder).

The Acoustics Division Salt Water Tank Facility is designed to provide a controlled environment for studying a variety of complex ocean processes under saline conditions, especially the study of the acoustics of bubbly media. Instrumentation includes acoustic sources, amplifiers, hydrophones, environmental sensors, a digital holographic imaging system, high-speed digital cameras, and a LabVIEW-based data acquisition system.

The division operates several sound sources for the generation and reception of sound in at-sea experiments. Sound sources include three XF-4 units, one ITC 2077 source that can be operated while being towed by a ship, two battery-operated organ-pipe sources that can project single tones from offboard moorings, and a towable, directional source array for active sonar studies consisting of 10 individually controllable elements, at frequencies 2.5 to 5 kHz. In addition, the division has several battery-operated rubidium-clock-controlled, programmable sound source moorings that can transmit sounds having arbitrary waveforms.

The division has a 64-channel broadband source-receiver array with time-reversal mirror functionality. Projects involving scanning focused acoustic fields and phase conjugation for multistatic sonar will utilize the new array to test and study time reversal methods. The transducers for the array are 6-in. spheres that operate from 500 to 3500 Hz.

The Acoustics Division performs research to relate acoustic array gain variability to fluid dynamic variability and bottom-heterogeneity in the littorals. The measurements are made with an autonomous acoustic

data acquisition suite. Three independent autonomous 32-channel vertical arrays and a 465-m 96-channel horizontal array receive and store 24-bit data at a 4 kHz sample rate for 22 days. The acoustic sources operate at 300 and 500 Hz center band with ±10% bandwidth and generate programmable waveforms at 50% duty cycle for 22 days. As presently configured, the systems will operate to water depths of 500 m. The division also has unique, self-recording digital acquisition buoy systems (DABS) that are used to obtain multichannel (up to 128) acoustic data in the 10 Hz to 5 kHz regime. These systems provide up to 250 gigabytes of data on a single 15-in. reel of 1-in. tape.

The Acoustics Division has a radio-controlled buoy system with underwater receive arrays to collect acoustic and oceanic data, unattended, for periods of up to one month. The system can currently handle 64 channels of acoustic data (distributed on one or two arrays), and can implement onboard signal processing prior to data transmission. The system contains a high-speed line-of-sight data link utilizing a GPS-linked directional antenna. A low-speed command and control link is available to remotely control buoy functions and array settings.

The division conducts research addressing the channel capacity of multinode underwater acoustic communications networks. The research is conducted in the 2 to 5 kHz, 6 to 14 kHz, and 10 to 24 kHz frequency bands using three 8-channel acoustic communications data acquisition systems or modems, which can be moored or towed. The 8-element vertical arrays are configured in a 2-m or 20-m aperture and remotely controlled using a wireless LAN.

Narrow beam 200 and 350 kHz acoustic backscattering (flow visualization) systems are used to study fine structure, internal wave, and larger scale fluid dynamic perturbation of the density and sound speed field in the ocean. A deck-mounted towing assembly consists of transducers, power amplifiers, and a real-time display and digital data acquisition system. A 25 kW radar system is used in conjunction with the flow visualization system to record the surface expression of internal waves.

The surface unit in the photo is part of the Acoustic Communications Data Storage (ACDS) system.

The division operates high-frequency (up to 600 kHz) acoustic measurement systems to obtain scattering, target strength, and propagation data using bottom-moored instrumentation towers and a remotely operated vehicle. These data are used to simulate the performance of weapons and mine countermeasure sonars.

Remote Sensing

The Remote Sensing Division conducts a program of basic research, science, and applications to develop new concepts for sensors and imaging systems for objects and targets on Earth, in the near-Earth environment, and in deep space. The research, both theoretical and experimental, leads to discovery and understanding of the basic physical principles and mechanisms that give rise to background environmental emissions and targets of interest and to absorption and emission mechanisms of the intervening medium. Accomplishing this research requires the development of sensor systems technology. The developmental effort includes active and passive sensor systems used for study and analysis of the physical characteristics of phenomena that evolve from naturally occurring background radiation, such as that caused by the Earth's atmosphere and oceans, and man-made or induced phenomena, such as ship/submarine hydrodynamic effects. The research includes theory, laboratory, and field experiments leading to ground-based, airborne, or space systems for use in remote sensing, astrometry, astrophysics, surveillance, nonacoustic ASW, meteorological/oceanographic support systems for the operational Navy, and the environmental/global climate change initiatives. Special emphasis is given to developing space-based platforms and exploiting existing space systems. Specific projects include:

Maritime Hyperspectral Imaging (HSI) Program: The Remote Sensing Division conducts airborne hyperspectral data collections for characterization of the environment. Hyperspectral data are series of pictures, taken simultaneously, of a scene at many different wavelengths (colors). The sensors are built and calibrated in-house, although they rely heavily on commercial off-the-shelf elements. Our current operational sensor is the airborne Portable Hyperspectral Imager for Low-light Spectroscopy (PHILLS) system, which

was specifically designed for use over maritime areas. It covers the 400- to 1000-nm wavelength range with 128 different wavelengths (channels). PHILLS consists of a standard video camera lens, a grating spectrograph, and a 1024 × 1024 pixel charge-coupled device (CCD). The system is designed for maximum sensitivity in the blue end of the spectrum in order to optimize water-penetrating measurements. This makes possible the retrieval of in-water geophysical parameters such as the ocean bottom type (coral, sea grass, sand, rock, etc.) to water depths of as much as 20 m (in clear water), and the identification of material in the water column (phytoplankton, sediments, colored dissolved organic matter, etc.). PHILLS is very compact and can be flown at heights of 8000 to 10,000 ft.

Proper interpretation of the hyperspectral data requires calibration of the sensor; this means both radiometric and spectral calibration. The latter plays a critical role in the successful correction of the data for atmospheric effects. The Remote Sensing Division operates an Optical Calibration Facility to perform these calibrations, which includes a NIST-traceable integrating sphere, and a set of gas emission standards for wavelength calibration. As a result, the complete process of data collection through data analysis can be handled in-house.

To validate the results of airborne hyperspectral sensing, and to support interpretation of the physical processes they reveal, the Remote Sensing Division has developed a Profiling Optics Package. This system measures the inherent optical properties of water (absorption, attenuation, and scattering) in the 400 to 700-nm range, and collects water samples for various laboratory measurements. The package has a maximum depth rating of 300 m, although it is usually operated in coastal waters of less than 50 m.

Hydrodynamics: The Remote Sensing Division conducts a wide range of numerical and analytical research dealing with the physics of the ocean's free surface. Direct numerical simulations (DNS) of turbulence are made in which the free surface is treated as either flat, or as a fully nonlinear, deformable surface with waves. The presence of surfactants and their influence on the dynamics and heat transfer properties may be simulated as well. To test and validate the numerical results and analytical theories, extensive experiments are conducted in the Free-Surface Hydrodynamics Laboratory. This laboratory is used to study interactions of turbulence with the free-surface, wave-generation phenomena, jet flows, vorticity dynamics, and free-surface/surfactant interactions. Emphasis is placed on those processes that determine the fluxes of heat, mass, and momentum across the air-sea interface. State-of-the-art diagnostic tools are available, such as a Langmuir film balance to measure the properties of surface films, hot-wire and laser-Doppler anemometry, and the new quantitative flow techniques of laser speckle, particle tracking, and particle image velocimetry. The laboratory is also equipped with an IR camera with a 0.02 °K resolution. These experimental diagnostic techniques use high-powered lasers, high-tolerance optical lenses, and extensive ultra-high-resolution video-imaging hardware and PC-based computerized systems. Further computational assets consist of powerful graphical computer work stations, the NRL Connection Machine, and other off-site Cray supercomputer systems.

Astronomy: The Navy Prototype Optical Interferometer (NPOI), a major facility of the Remote Sensing Division, is actually two collocated instruments for making high-angular-resolution optical measurements of stars. Light from widely separated individual siderostats is combined simultaneously to synthesize the angular resolution of a telescope tens to hundreds of meters in diameter. Four siderostats are placed in an array with extremely accurate metrology to enable very-high-precision measurements of stellar positions (wide-angle astrometry). These measurements are used by the U.S. Naval Observatory to refine the celestial reference frame, determine Earth rotation parameters, and thus satisfy Navy requirements for precise time and navigation data. They also provide determinations of basic astrophysical parameters, such as stellar masses and diameters. Additional relocatable siderostats can be placed out to distances of up to (when complete) 250 m from the array center, and used to construct very-high-resolution images of stars. These images provide fundamental astrophysical information on stellar structure and activity. When complete, the NPOI will be the most advanced high-resolution imaging optical interferometer in the world.

The Remote Sensing Division also has a strong program in radio astronomy, with emphasis on low-frequency (< 100 MHz) observations. As part of this program, the Division has developed and installed 74 MHz receivers on the National Radio Astronomy Observatory's Very Large Array (VLA), thereby producing the world's highest angular resolution and most sensitive astronomical interferometric array operating below 150 MHz. In contrast to the VLA's maximum baseline of 35 km, all previous astronomical interferometers operating below 150 MHz had baselines less than 5 km because ionospheric structure had been thought to impose phase variations that would corrupt the interferometric imaging. Work in the Remote Sensing Division has shown that radio astronomical techniques can now remove the ionospheric phase variations and extend interferometer baselines to arbitrary lengths. The NRL/NRAO 74 MHz system has been used for a variety of innovative observations with encouraging initial results in solar system, Galactic,

WindSat payload in the thermal/vacuum chamber. The cold sky reflector has been removed in this picture.

The Navy Prototype Optical Interferometer (NPOI) is used for both operational astrometry and for development of distributed aperture imaging techniques.

and extragalactic astrophysics. The success of the NRL/NRAO 74 MHz system indicates that it is possible to open a new high-resolution, high-sensitivity astronomical window by going to an even larger, more sensitive system. Several such large interferometric systems are now in various stages of planning and development. This includes the Long-Wavelength Array (LWA), which is a joint collaboration between the University of New Mexico, University of Texas, Los Alamos National Laboratory, and the NRL Remote Sensing Division.

Remote Sensing of the Atmosphere and Ocean Surface: The NRL Polar Ozone and Aerosol Measurement (POAM) instrument is a space-based 9-channel UV-Vis solar photometer for measuring ozone and other important constituents of the stratosphere using the solar occultation technique. The POAM program consists of two missions: POAM II was launched in October 1993 on the French SPOT 3 satellite, and operated until contact with the host satellite was lost in November 1996; POAM III was launched in March 1998 on the SPOT 4 satellite, and is still operational. POAM is an important part of the national ozone monitoring effort because it is currently (and has been for most of the mission life) the only instrument that makes high-vertical-resolution (1 km) measurements of ozone in the polar regions of both hemispheres on a continuous basis, including unprecedented space-based coverage of the Antarctic ozone hole. As such, POAM contributes data on a major policy issue: global ozone depletion. Because of the importance of this issue, international protocols have been implemented to phase out chlorofluorocarbons (CFCs), which are known to destroy the ozone. The economic impact of the protocols on the military (as well as the private sector), in terms of phase out and the search for replacement compounds, has been substantial. POAM's orbit is ideal for monitoring the effect of the CFC restrictions, and the effect of replacement chemicals, because ozone depletions are most severe in the polar regions during the late winter/early spring season in each hemisphere.

WindSat, developed and built by NRL and launched in January 2003, is the first spaceborne polarimetric microwave radiometer. Its primary mission is to demonstrate the capability to remotely sense the ocean surface wind speed and direction (wind vector) with a passive system. WindSat, the primary payload on the DoD Space Test Program Coriolis mission, provides major risk reduction for the National Polar-orbiting Operational Environmental Satellite System (NPOESS) Conical Microwave Imager and Sounder. WindSat has successfully demonstrated the capability to measure the ocean surface wind vector. Although WindSat wind vector retrieval algorithm development is still an important R&D effort in the Remote Sensing Division, the current algorithm is run operationally at the Navy Fleet Numerical Meteorology and Oceanography Center (FNMOC). Wind vectors are available in real time, and are included in the NRL Monterey satellite cyclone Web site. In addition, the Remote Sensing Division is exploiting WindSat's unique data set to develop retrievals for other environmental parameters such as sea surface temperature, soil moisture, and sea ice concentration.

The Airborne Polarimetric Microwave Imaging Radiometer (APMIR) is a state-of-the-art multichannel microwave radiometer system designed and built by the Remote Sensing Division. APMIR was built primarily to provide extensive airborne calibration and validation of spaceborne remote sensing assets: the NRL WindSat mission, the Defense Meteorology Space Program (DMSP) Special Sensor Microwave Imager/Sounder (SSMIS) mission, and the future Conical Scanning Microwave Imager/Sounder (CMIS) to fly on the converged National Polar-orbiting Operational Environmental Satellite System (NPOESS). APMIR covers five frequency bands from 5 to 37 GHz, and the 10.7, 18.7, and 37 GHz measurement bands are fully polarimetric. Frequency agility allows for frequency matching to each of the spaceborne systems of interest. In addition to validation, APMIR is an important science tool, providing measurements of the ocean surface wind vector, sea surface temperature, atmospheric water vapor and cloud parameters below the airplane, soil moisture, and ice/snow properties. The APMIR system is deployed on the NRL P-3 aircraft (mounted in the bomb bay), and flown at altitudes ranging from 500 to 25,000 ft over the ocean.

Oceanography

The Oceanography Division is the major center for in-house Navy research and development in oceanography. It is known nationally and internationally for its unique combination of theoretical, numerical, experimental, and remotely sensed approaches to oceanographic problems. The division modeling focus is on a truly integrated global-to-coastal modeling strategy, from deep water up to the coast including straits, harbors, bays, and inlets. This requires emphasis on both ocean circulation and wave/surf prediction, with additional emphasis on coupling the ocean models to biological, optical, and sediment models. This modeling is conducted on the Navy's and DoD's most powerful vector and parallel-processing machines. To study the results of this intense modeling effort, the division operates a number of highly sophisticated graphic systems to visualize ocean and coastal dynamic processes. The seagoing experimental programs of the division range worldwide. Unique measurement systems include a wave measurement system to acquire

SEPTR is the prototype of a trawl-resistant, bottom-mounted ADCP system that includes a pop-up profiling float for real-time observation and reporting. After a successful test in the Adriatic Sea in May 2003, SEPTR is being winched aboard NURC's research vessel *Alliance*. NRL and NURC continue a cooperative agreement for engineering development of SEPTR and for deployment of several in a real-time environmental assessment system.

in-situ spatial properties of water waves; a salinity mapper that acquires images of spatial and temporal sea surface salinity variabilities in littoral regions; an integrated absorption cavity, optical profiler system, and towed optical hyperspectral array for studying ocean optical characteristics; self-contained bottom-mounted upward-looking acoustic Doppler current profilers for measuring ocean variability, and an in-situ volume scattering function measurement system to support remote sensing and in-water optical programs. Specifically, NRL is working jointly with NATO Undersea Research Center (NURC) for development and deployment of the SEPTR instrument. This is a trawl-resistant, bottom-mounted ADCP system that includes a pop-up profiling float for real-time observation and reporting. The Division is in the process of acquiring four oceanographic gliders with optical sensors for autonomous measurement of in-situ ocean properties.

In the laboratory, the Division operates an environmental scanning electron microscope for detailed studies of biocorrosion in naval materials. The Division's remote sensing capabilities include the ability to analyze and process multi/hyperspectral, IR, SAR, and other satellite data sources. The Division is a national leader in the development and analysis of MODIS ocean color data for oceanographic processes and naval applications in littoral areas.

Marine Geosciences

The Marine Geosciences Division is the major Navy in-house center for research and development in marine geology, geophysics, geodesy, geoacoustics, geotechnology, and geospatial information and systems. The division has unique suites of instrumentation and facilities to support laboratory and field experimental programs.

The instrumentation used in the field experiments is deployable from ships, remotely operated and unmanned vehicles, and airborne platforms and by divers. Instrumentation includes an integrated airborne geophysical sensor suite with gravity, magnetic, and sea/ice/land topographic profiling sensors, all based on cm-level KGPS aircraft positioning. Seafloor and subseafloor measurements use the Deep-Towed Acoustic Geophysical System (DTAGS—220 to 1000 Hz); chirp sub-bottom profiler; high-resolution sidescan sonars (100 and 500 kHz); the Acoustic Seafloor Characterization System (ASCS-15, 30, and 50 kHz); an optically pumped marine magnetometer; several gravimeters; the In Situ Sediment Acoustic Measurement System (ISSAMS); underwater stereo photography; and nearshore video imaging systems. ISSAMS has specialized probes that measure acoustic compressional and shearwave velocities and attenuation, sediment shear strength, and electrical conductivity in surficial marine sediments.

Five instrumented, 8-ft-long, 2220-lb, minelike cylinders are used to gather impact burial data (one system) and scour and sand wave burial data (four systems) for validation of mine burial prediction models.

Laboratory facilities include sediment physical, geotechnical, and geoacoustic properties and sediment core laboratories. The Electron Microscopy Facility is the focal point for research in microscale biological, chemical, and geological processes. The key instrumentation includes a 300 kVa transmission electron microscope with environmental cell. The environmental cell allows hydrated and gaseous experiments.

A high-resolution industrial CT scanner is a recent addition to the laboratory. It will be used for investigating volumetric heterogeneity of sediments.

The Moving Map Composer Facility is used to design and write mission-specific map coverages for F/A-18 and AV-8B tactical aircraft onto militarized optical disks. The National Geospatial-Intelligence Agency also uses this state-of-the-art computer facility

to update the compressed aeronautical chart library on CD for distribution. The Geospatial Information Data Base (GIDB) capability provides Internet access to the Digital Nautical Chart data, mapping data, imagery, and other data types such as video and pictures. This development tool can be used for planning, training, and operations.

Marine Meteorology

The Marine Meteorology Division is located in Monterey, California. NRL-Monterey (NRL-MRY) serves the Navy's needs for basic and applied research in atmospheric sciences and develops meteorological analysis and prediction systems and other products to support global and tactical operations.

NRL-MRY is collocated with Fleet Numerical Meteorology and Oceanography Center (FNMOC), the Navy's operational center of expertise in numerical weather prediction (NWP) and satellite data products. NRL-MRY's Atmospheric Prediction System Development Laboratory has connectivity to the FNMOC internal network, which provides NRL-MRY with efficient access to a variety of classified and unclassified computer resources and databases to support development and transition of operational analysis and prediction systems. In addition, interfaces to the Defense Research and Engineering Network provide access to the DoD High Performance Computing resources, which can be accessed directly from any office in the Atmospheric Research Laboratory via a recently upgraded network that offers gigabit/second speed to the office capability. NWP and aerosol prediction system development is further supported by the in-house Daley Supercomputer Resource Center, which currently includes an SGI Origin 2000 128-processor supercomputer and a 44-processor LINUX cluster. These computers are supported by a 28-terabyte Storage Area Network, which enables the division to save observational and model output data to support research in atmospheric processes and development of improved numerical prediction systems for Fleet operations around the globe.

A state-of-the-art Satellite Data Processing Laboratory allows local collection of real-time NOAA geostationary data (imagery and sounder data from GOES-E and GOES-W) and supports real-time data feeds via FNMOC and the Air Force Weather Agency for the remaining three geostationary satellites and a number of polar orbiting satellites (3 from NOAA, 4 from the Defense Meteorological Satellite Program, and 5 from NASA—Tera, Aqua, TRMM, SEAWifs, and QuikScat). All together, NRL-MRY processes data from 22 low-earth orbiting sensors and uses these data along with geostationary satellite data to conduct research and develop multisensor, multiplatform products for a variety of DoD operations, from monitoring and analyzing tropical cyclone intensity in support of the Joint Typhoon Warning Center to providing dust enhancement imagery in support of strike warfare operations in Southwest Asia. These products are typically transitioned to FNMOC or to one of the Navy's regional METOC centers, which use their local FMQ-17 to process satellite data using algorithms developed by NRL for data display on the TeraScan system. The Satellite Data Processing Laboratory is supported by the 24-terabyte Bergen Data Center, which has a hierarchical storage management capability to provide archival and easy retrieval or research data sets. The Bergen Data Center also provides support for the data that is archived as part of the Master Environmental Library.

NRL-MRY's Classified Satellite/Radar Data Processing Facility, consistent with the FORCEnet vision, hosts classified computer systems for receiving, processing, and storing classified and unclassified satellite, radar, and observational data and development of applications using those data. This facility has a 22-processors LINUX cluster for high performance computing, two LINUX workstations for data processing, a LINUX database workstation and two desktop computers, along with a 128 Kb SIPRNET connection in a shielded workspace. This facility provides the environment for the classified high-resolution data integration and fusion technology development using through-the-sensor data collected from shipboard weather radars and direct broadcast low-earth orbiting meteorological satellite sensors to generate products for direct dissemination to the tactical decision-makers.

To support the division's growing program in aerosol research and aerosol prediction system development, NRL-MRY has designed and built the Mobile Atmospheric Aerosol and Radiation Characterization Observatory (MAARCO). MAARCO is a modified 20-ft × 8-ft climate controlled container that contains an integrated suite of meteorological, aerosol, gas, and radiation instruments, with space maintained for guest instrumentation. MAARCO can be easily deployed in areas with limited facilities, thereby enabling research on atmospheric aerosols, gases, and radiation in areas of key interest, including remote areas, overseas locales, and onboard ships. The radiation suite includes an AERONET Sun Photometer, solar and IR radiometers, a Total Sky Imager, and a Micro-pulse Lidar. A 3-wavelength Nephelometer; Aerodynamic Particle Size, total suspended particulates (TSP) filter sampler; tapered-element oscillating microbalance (TEOM) sampler; SO2 and Ozone monitors; and a Micro-Orifice Uniform Deposit Impactor (MOUDI) sampler complete the aerosol and gas suite. Meteorological data are provided by a weather station and a Rawinsonde system. MAARCO was successfully deployed in the UAE in late summer of 2004 to collect aerosol, chemistry, radia-

The Mobile Atmospheric Aerosol and Radiation Characterization Observatory (MAARCO) on deployment near Abu Dhabi, UAE, in August through October 2004, to gather data to support research on atmospheric aerosols, gases, and radiation. An instrumented Aerocommander is conducting an overflight.

tion, and weather data during the United Arab Emirates United Aerosol Experiment (UAE^2). The collected data will be used in investigations of boundary layer meteorology, aerosol microphysics, and electro-optical propagation.

In addition to computational and instrumented facilities, NRL-MRY's research program is supported by an on-site library, which maintains current and past copies of most of the U.S. and many of the international journals dedicated to the atmospheric, oceanographic, and computational sciences, as well as a number of reference books and hundreds of scientific texts in the mathematical, physical, and earth sciences. The library also serves as a repository for technical publications from a number of national and international institutions engaged in atmospheric and oceanographic research, including technical reports from the laboratories that preceded NRL at the Monterey site. The Monterey library also maintains historical and current copies of the graduate theses and dissertations written by students in meteorology and oceanography at the Naval Postgraduate School.

Space Science

The Space Science Division conducts and supports a number of space experiments in the areas of upper atmospheric, solar, and astronomical research aboard NASA, DoD, and other government agency space platforms. Division scientists are involved in major research thrusts that include remote sensing of the upper and middle atmospheres, studies of the solar atmosphere, and astronomical radiation ranging from the ultraviolet through gamma rays and high-energy particles. In support of this work, the division maintains facilities to design, construct, assemble, and calibrate space experiments. A network of computers, workstations, image-processing hardware, and special processors is used to analyze and interpret space data. The division's space science data acquisition and analysis efforts include: observation of the Sun's interaction with the Earth's upper atmosphere through the Solar Ultraviolet Spectral Irradiance Monitor (SUSIM) experiment in support of NASA's Upper Atmosphere Research Satellite (UARS); observation and analysis of solar flares using the Bragg Crystal Spectrometer (BCS) on the Japanese Yohkoh space mission; and observation and analysis of the evolution and structure of the solar corona from the disk to 0.14 AU. This latter effort involves acquiring and analyzing data from the Large-Angle Spectrometric Coronagraph (LASCO) and the Extreme Ultraviolet Imaging Telescope (EIT) on the Solar Heliospheric Observatory satellite. In each of these missions, NRL maintains a complete database of spacecraft observations and control over acquisition of data from new observations. These data are available to qualified investigators at DoD and civilian agencies. In addition, the division has a sounding rocket program that affords the possibility of obtaining specific data of high interest and of testing new instrument concepts. These include the general area of high-resolution solar and stellar spectroscopy, extreme ultraviolet imagery of the Sun, and high-resolution, ultraviolet spectral-imaging of the Sun.

Division scientists have developed and maintain physical models in support of their research, including Mass Spectrometer and Incoherent Scatter Radar (MSIS), the standard model for the density of the upper atmosphere; Global Assimilation of Ionospheric Measurement (GAIM), a physics-based model of the ionosphere; Navy Operational Global Atmospheric Prediction System–Advanced Level Physics High Altitude (NOGAPS-ALPHA), a model to extend weather modeling into the upper atmosphere; Cosmic Ray Effects on Micro Electronics (CREME), the standard model of the effect of energetic solar particles and cosmic rays; and GAIM, a physics-based model of the ionosphere that is gaining acceptance as the standard ionospheric model.

The division is currently developing a number of new space instruments, including: Sun Earth Connection Coronal and Heliospheric Investigation (SECCHI), the coronagraph and solar disk imagers for NASA's STEREO mission; Extreme Ultraviolet Imaging Spectrometer (EIS), the extreme ultraviolet imaging spectrometer for Japan's SOLAR-B mission; Gamma Ray Large Area Space Telescope (GLAST), a high energy gamma ray detector for NASA; Spatial Heterodyne Imager for Mesopheric Radicals (SHIMMER), a Michelson interferometer for upper atmospheric research for a DoD mission; and Tether Physics and Survivability Experiment (TiPS), ultraviolet spectrometers for upper atmospheric research for Taiwan's COSMIC program.

Optical calibration facilities, including clean rooms, are maintained to support these activities. These calibration facilities are routinely used by outside groups to support their own calibration requirements.

Space Technology

In its role as a center of excellence for space systems research, the Naval Center for Space Technology (NCST) designs, builds, analyzes, tests, and operates spacecraft and identifies and conducts promising research to improve spacecraft and their support systems. NCST facilities that support this work include large and small anechoic radio frequency chambers, clean rooms, shock and vibration facilities, an acoustic reverberation chamber, large and small thermal/vacuum test chambers, heat pipe integration and test facility, a spacecraft robotics engineering and control system interaction laboratory, satellite command and control ground stations, a fuels test facility, and modal analysis test facilities. Also, the Center maintains and operates a number of electrical and electronic development laboratories and fabrication facilities for radio frequency equipment, spacecraft power systems, telemetry, and command and control systems, and includes an electromagnetic interference-electromagnetic compatibility test chamber. NCST has a facility for long-term testing of satellite clock time/frequency standards under thermal/vacuum conditions linked to the Naval Observatory; a 5-m optical bench laser laboratory; and an electro-optical communication research laboratory to conduct research in support of the development of space systems.

RESEARCH SUPPORT FACILITIES

Exhibits Office/Marketing Services

This office designs and develops full-sized and portable displays and posters for technical conferences and symposia, briefings on Capitol Hill, at DoD installations, Laboratory special events, and public events. The NRL booth at trade shows and technical conferences provides a platform for scientists and engineers to market research projects and also enhances NRL's technology transfer efforts.

The Exhibits Office also designs and develops static displays for buildings, i.e., wall arrangements, division research highlights, and award panels and cases. The static displays found in Buildings 72, 43, 226, 28, 222, and Quarters A are maintained by the Exhibits Office. Other available services to the researcher and Lab management are: assistance in presentation development including research, writing, layout, design, photo/video

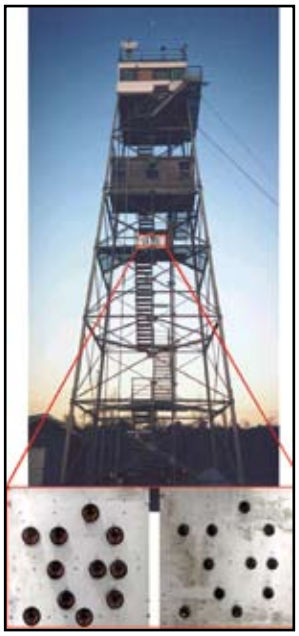

Retro-reflectors on NRL's Tilghman Island tower on the eastern shore of the Chesapeake Bay. These retro-reflectors and a transceiver at NRL's Chesapeake Bay Detachment are used to test long-range free-space laser communication links in a maritime environment. Laser communication links at data rates up to 2.5 Gbps have been successfully demonstrated over this 32-km test range.

archival searches, and finalized vugraph/computer presentation products; and acting as a translator between the researcher and the artist to assist researchers in developing the artist's concept that visually explains their research concept.

The Exhibits Office produces, directs, and develops multimedia products (CD-ROMs, videos, and films) to enhance exhibits at trade shows and to directly support Laboratory presentation capabilities needed for briefings to existing sponsors, potential sponsors, Congressional representatives, and for recruitment and special events. The most recent "A Tour of NRL" has won four international awards: the Crystal, the Gold Aurora, and two Bronze Tellys.

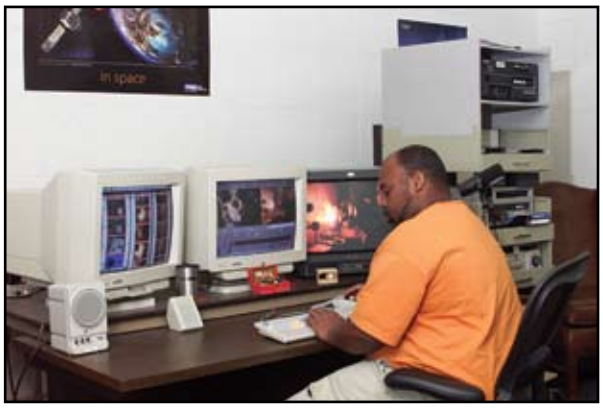

Videographer editing promotional information with the AVID, digital nonlinear video editing system, which provides professional quality videos and DVDs.

Technical Information Services

The Technical Information Services Branch combines publications, graphics, photographic, multimedia, and video services into an integrated organization. Publication services include writing, editing, composition, publications consultation and production, and printing management. Quick turnaround digital black-and-white and color copying/printing services are provided. The primary focus is to use digital publishing technology to produce scientific and technical reports that can be used for either print or Web. Graphic support includes technical and scientific illustrations, computer graphics, design services, photographic composites, display panels, sign making, and framing. The NovaJet Pro 600e and HP Designjet 5500ps printers offer exceptional color print quality up to 600 dpi. They produce large-format indoor posters and signs with 56 inches being the limitation on one side. Lamination and mounting are available. Photographic services include digital still camera coverage for data documentation, both at NRL and in the field. Photographic images are captured with state-of-the-art digital cameras and can be printed on a variety of digital media. Photofinishing services provide automatic and custom printing from digital files on a new digital minilab. Quick-service color prints are also available. Video services include producing video reports of scientific and technical programs. Digital video editing equipment is available to support video production and produce QuickTime movies.

Administrative Services

The Administrative Services Branch is responsible for collecting and preserving the documents that comprise NRL's corporate memory. Archival documents include personal papers and correspondence, laboratory notebooks, and work project files—documents that are appraised for their historical or informational value and considered to be permanently valuable. The Branch provides records management services, training, and support for the maintenance of active records, including electronic records, as an important informa-

Mail clerks using Folder/Inserter machine to tri-fold brochures to be distributed.

tion resource. The Branch is responsible for processing NRL's incoming and outgoing correspondence and provides training and support on correct correspondence formats and practices. The Branch is responsible for NRL's Forms and Reports Management Programs (including designing electronic forms and maintaining a website for Lab-wide use of electronic forms), compiles and publishes the NRL Code Directory and Organizational Index, and is responsible for providing NRL postal mail services for first class and accountable mail and for mail pickup and delivery throughout NRL. The Branch also provides NRL Locator Service.

Ruth H. Hooker Research Library

The NRL Ruth H. Hooker Research Library offers a full range of traditional and digital library services to enhance and support the research program of the Naval Research Laboratory. Traditional library services include an extensive technical report, book, and journal collection dating back to the 1800s housed within a physical facility configured for study and research, staffed with subject specialists and information professionals. To enhance traditional services, the NRL Research Library has developed and is continuing to enhance the NRL Digital Library. The Digital Library currently provides desktop access to thousands of journals, books, and reference sources at NRL-DC, NRL-Stennis, NRL-Monterey, and the Office of Naval Research.

The NRL Research Library collections are focused to specifically support the research areas at NRL, including physics, chemistry, oceanography, meteorology, and space sciences. The collections include 150,000 books and journal volumes, 3,000 current journal subscriptions, and nearly 2 million technical reports in paper, microfiche, or digital format (Classified and Unclassified). Services include reference assistance in using the collections and locating information from external sources; mediated literature searches of several hundred online databases, including classified databases, to produce on-demand subject bibliographies; circulation of materials from the collection including classified literature up to the SECRET level; interlibrary loan to obtain needed items from other scientific and research libraries or from commercial document providers; ordering all journals for office retention; and user education and outreach to help researchers improve productivity through effective use of the physical library and the rapidly growing Digital Library resources available through InfoWeb, TORPEDO *Ultra*, and the World Wide Web. The "portal" to the NRL Digital Library is located at http://library.nrl.navy.mil, and provides desktop access to all of the online resources licensed through the NRL library. A key Digital Library service is TORPEDO *Ultra*, which serves as a digital archive for thousands of licensed journals and technical reports with over 5.5 million items currently available.

FIELD STATIONS

NRL has acquired or made arrangements over the years to use a number of major sites and facilities for research. The largest facility is located at the Stennis Space Center (NRL-SSC), in Bay St. Louis, Mississippi.

TORPEDO *Ultra*, one of the Web-based services available through the NRL Research Library.

Others include a facility at the Naval Postgraduate School in Monterey, California (NRL-MRY), and the Chesapeake Bay Detachment (CBD) in Maryland. Additional sites are located in Maryland, Virginia, Alabama, and Florida.

Scientific Development Squadron One (VXS-1)

On February 18, 2005, the Flight Support Detachment (NRL FSD) located at Naval Air Station Patuxent River, Lexington Park, Maryland, was established as a Navy Squadron and renamed, Scientific Development Squadron One (VXS-1). Manned by approximately 13 officers, 70 enlisted personnel, and 8 civilians, VXS-1 is currently responsible for the maintenance and security of three, uniquely configured NP-3D Orion research aircrafts and one C-12 Beech KingAir research aircraft acquired at the beginning of FY06. The squadron conducts numerous single-aircraft detachments around the world in support of a wide range of scientific research projects.

In FY05, VXS-1 provided flight support for diverse research programs including, Cooperative Engagement Capability (CEC), an airborne suite to test USN Aegis Cruiser systems; RAINEX, a joint project with NOAA studying hurricane intensity change, specifically for Hurricanes Katrina and Rita; and The Antarctic Sea Ice Mission, a joint project with NASA, which was based out of Argentina and studied the movements of sea ice. VXS-1's flight safety record spans over 40 years and includes over 63,000 mishap-free flight hours.

Chesapeake Bay Detachment (CBD)

CBD occupies a 168-acre site at Randall Cliffs, Maryland, and provides facilities and support services for research in radar, electronic warfare, optical devices, materials, communications, and fire research. A ship-motion simulator (SMS) is used to test and evaluate radar, satellite communications, and line-of-sight RF communications systems under dynamic conditions (various sea states). The SMS can handle up to 12,000 lb of electronic systems. A roll motion of up to 30 deg (15 deg to port and 15 deg to starboard) can be applied to this axis. The pitch axis has a fixed motion of 10 deg (5 deg to stern and 5 deg to bow). Periods along both axes, pitch and roll, are variable—from a slow 32-s to a brisk 4-s rate. Variable azimuth motion can also be added to the pitch and roll action. Synchronized positioning information (×1 and ×36) is available for each of the three axes of the SMS.

Because of its location high above the western shore of the Chesapeake Bay, unique experiments can be performed in conjunction with the Tilghman Island site, 16 km across the bay from CBD. Some of these experiments include low clutter and generally low-background radar measurements. By using CBD's support vessels, experiments are performed that involve dispensing chaff over water and radar target characterizations of aircraft and ships. Basic research is also conducted in radar antenna properties, testing of radar remote-sensing concepts, use of radar to sense ocean waves, and laser propagation. CBD also hosts facilities of the Navy Technology Center for Safety and Survivability, which conducts fire research on simulated carrier, surface, and submarine platforms.

Stennis Space Center (NRL-SSC)

The NRL Detachment at Stennis Space Center, Mississippi (NRL-SSC) consists of NRL's Oceanography Division and portions of the Acoustics and Marine Geosciences Divisions. NRL-SSC, a tenant activity at NASA's John C. Stennis Space Center (SSC), is located in the southwest corner of Mississippi, about 50 miles northeast of New Orleans, Louisiana, and 20 miles from the Mississippi Gulf Coast. Other Navy tenants at SSC include the Naval Meteorology and Oceanography Command, the Naval Oceanographic Office, the Navy Small Craft Instruction and Training Center, the Special Boat Team-Twenty-two, and the Human Resources Service Center South East. Other Federal and State agencies at SSC involved in marine-related science and technology are the National Coastal Data Development Center, the National Data Buoy Center, the U.S. Geological Survey, the Environmental Protection Agency's Gulf of Mexico Program and Environmental Chemistry Laboratory, the Center for Higher Learning, University of Southern Mississippi, and Mississippi State University.

The Naval Meteorology and Oceanography Command and the Naval Oceanographic Office are major operational users of the oceanographic, acoustic, and geosciences technology developed by NRL researchers. The Naval Oceanographic Office operates the Major Shared Resource Center (MSRC), one of the nation's High Performance Computing Centers, which provides operational support to the warfighter and access to NRL for ocean and atmospheric science and technology.

The Acoustics, Marine Geosciences, and Oceanography Divisions occupy more than 175,000 ft^2 of research, computation, laboratory, administrative, and warehouse space. Facilities include the dual-use analysis center, sediment core laboratory, transmission electron microscope, moving-map composer facility, underwater navigation control laboratory, computed tomography scanning laboratory, visualization laboratory, ocean color data receipt and processing facility, environmental microscopy facility, maintenance and

calibration systems, environmental modeling and simulation high-speed network, and numerous laboratories for acoustic geosciences and oceanographic computation, instrumentation, analysis, and testing. Special areas are available for constructing, staging, refurbishing, and storing sea-going equipment.

Marine Meteorology Division (NRL-MRY)

NRL's Marine Meteorology Division (NRL-MRY) is located in Monterey, California, on the grounds of the Naval Postgraduate School (NPS) Annex, which is about a mile from the NPS main campus. The NRL facility is collocated with the Navy's operational Fleet Numerical Meteorology and Oceanography Center (FNMOC) and with a NOAA National Weather Service Forecast Office (NWSFO). The NPS Annex campus, which covers approximately five acres, comprises four primary buildings—one occupied exclusively by NOAA, one that houses both the NRL and FNMOC supercomputer/operational facilities, and two large buildings containing office space, computer laboratories, and conference facilities that are shared by FNMOC and NRL-MRY personnel. The site also provides two modular office buildings, warehouse space, and recreational facilities. NRL-MRY occupies approximately 30,000 ft^2 in shared buildings. This includes not only office and meeting space, but also a small library, the Daley Supercomputer Resource Center, the Bergen Data Center, the Satellite/Radar Processing Facility, and space for the hardware supporting the Navy Integrated Tactical Environmental System (NITES), the Coupled Ocean/Atmosphere Mesoscale Prediction System-On Scene (COAMPS-OS®), the Master Environmental Laboratory, and the Division's SIPRNET connection.

NRL-MRY is dedicated to advancing fundamental scientific understanding of the atmosphere, including the air-sea interface, and to applying those scientific discoveries in the development of innovative objective weather prediction systems. FNMOC is the Navy's central facility for the production and distribution of numerical weather prediction and satellite products in support of Navy operations around the globe, as well as to other defense-related activities. Fleet Numerical and the Navy's regional METOC Centers are the primary customers for the numerical weather prediction and satellite product systems that are developed by NRL-MRY. This collocation of the scientific developer with the operational customer offers advantages for the successful implementation of new systems and system upgrades, and for the rapid infusion of new research results from the community at large. NRL-MRY has direct access to FNMOC's large classified supercomputers and other systems. This allows advanced development to take place using the real-time on-site global atmospheric and oceanographic databases. Collocation also offers the opportunity for FNMOC scientists to team with NRL-MRY scientists during the transition and implementation process, and NRL-MRY scientists remain readily available for consultation on any future problems that arise.

NRL-MRY benefits from the opportunities provided by NPS for continuing education and collaborative research with the Meteorology and Oceanography Departments, while NPS utilizes the expertise of NRL scientists as guest lecturers and thesis committee members. NRL-MRY also maintains collaborative relationships with a number of the 25 local organizations that make up the Monterey Bay Crescent Ocean Research Consortium, which coordinates and promotes research, education, and outreach activities using the Monterey Bay as a natural laboratory.

Midway Research Center

The Midway Research Center (MRC) is located on a 162-acre site in Stafford County, Virginia. Located adjacent to the Quantico Marine Corps' Combat Development Command, the MRC has 16,000 ft^2 of operations and administration area. Instruments include three precision 18.5-m-diameter parabolic antennas housed in 100-ft radomes, a fast-tracking 1-m telescope currently used for satellite laser ranging, and a transportable 16-in. telescope capable of passive optical tracking and laser communications. The MRC, under the auspices of the Naval Center for Space Technology, provides NRL with state-of-the-art facilities dedicated solely to space-related applications in naval communications, navigation, and basic research.

Research Platforms

Mobile research platforms contribute greatly to NRL's research. These include six P-3 Orion turboprop aircraft and one ship, the ex-USS *Shadwell* (LSD-15), berthed in Mobile Bay, Alabama. The ex-USS *Shadwell* is used for research on aboard-ship fire-suppression techniques.

LOOKING AHEAD

To conduct preeminent research for tomorrow's Navy, NRL must maintain and upgrade its scientific and technological equipment and provide modern research facilities. The physical plant to house this equipment must also be state of the art. NRL has embarked on a Corporate Facilities Plan to accomplish these goals. This plan and future facility plans are described below.

THE CORPORATE FACILITIES INVESTMENT PLAN (CFIP)

The CFIP is a capital investment plan that uses both Congressionally approved military construction (MILCON) and Laboratory overhead funds to provide modern, up-to-date laboratory facilities for NRL. Past MILCON projects have included the Electro-Optics Building at NRL-DC, the Ocean Acoustics Research Laboratory at NRL-SSC, and the Nanoscience Research Laboratory at NRL-DC. Future MILCON projects include an Autonomous Vehicles Research Building in the FY09 time frame.

To complement these efforts, overhead funds have been used to renovate and upgrade laboratory and support areas in several existing buildings. Modern laboratory facilities have recently been provided for the Center for Bio/Molecular Science and Engineering, the Materials Science and Technology Division, the Remote Sensing Division, the Acoustics Division, the Information Technology Division, the Radar Division, and the Naval Center for Space Technology.

In parallel with efforts to upgrade laboratory buildings to the most modern standards, those buildings that were built during World War II and do not lend themselves to renovation are being demolished. This will provide space for the construction of future MILCON buildings, and it will also reduce the Laboratory's overhead costs.

Institute for Nanoscience

The manipulation and measurement of materials with nanometer dimensions is very difficult. One must be able to reliably and precisely locate structures of nanometer dimensions in much larger areas. Furthermore, the measurement of nanostructure properties is difficult simply because not many atoms/molecules are present. Vibrations and thermal/humidity/pressure fluctuations in the environment can cause major problems in positioning a tool. Good signal-to-noise ratios require electromagnetic and acoustic interference-free environments. Airborne contamination can readily cover a nanostructure. A new Nanoscience Research building has been constructed that controls these sources of "noise"; it became available for use in January 2004. There are 5000 ft^2 of Class 100 clean room for device fabrication; 4000 ft^2 of "quiet" space with temperature controlled to 0.5 °C, acoustic isolation at the NC35 standard (35 dB at 1 kHz), floor vibration isolation to <150 µm/s rms 10 to 100 Hz and <0.3 mOe magnetic noise at 60 Hz. There are also 1000 ft^2 of "ultra-quiet" space with temperature controlled to 0.1 °C and acoustic isolation at the NC25 standard (25 dB at 1 kHz).

Ruth H. Hooker Research Library

The Ruth H. Hooker Research Library has encouraged "Innovation for Research" for many years, exemplified by the first-of-its-kind systems such as InfoNet, InfoWeb, and TORPEDO *Ultra*. These custom systems, combined with the licensing of online resources for all NRL sites, have dramatically increased the resources available at the desktop and changed the research process. Over the next several years, the NRL Research Library plans to continue to expand desktop access to include all current and historical journals and conference proceedings that are relevant to NRL research. The NRL Research Library is also capturing a complete record of research results (journal articles, conference proceedings, books, etc.) of all Laboratory researchers, both a bibliographic citation and a copy of the physical artifact, for use with annual reviews and higher level summaries of productivity. Finally, the NRL Research Library is evolving all services to a more reliable and intuitive infrastructure that is focused on the needs of NRL researchers and engineers.

Information Technology

The Information Technology Division's Center for Computational Science (CCS) operates scalable, massively parallel Global Shared Memory (GSM) computer systems, including a 384-processor SGI Altix with cache-coherent Non-Uniform Memory Access (ccNUMA) architecture. Other major resources include a 576 processor Cray XD1 computer. Altix is particularly interesting as it is the first HPC machine to run a single system image across more than 128 processors using a commercially available LINUX operating system (Red Hat). These systems comprise the Distributed Center (DC) at NRL whose hardware is funded by the DoD High Performance Computing Modernization Program (HPCMP). The systems are used in the innovative exploration and evaluation of massively parallel processing (MPP) technology for solving significant

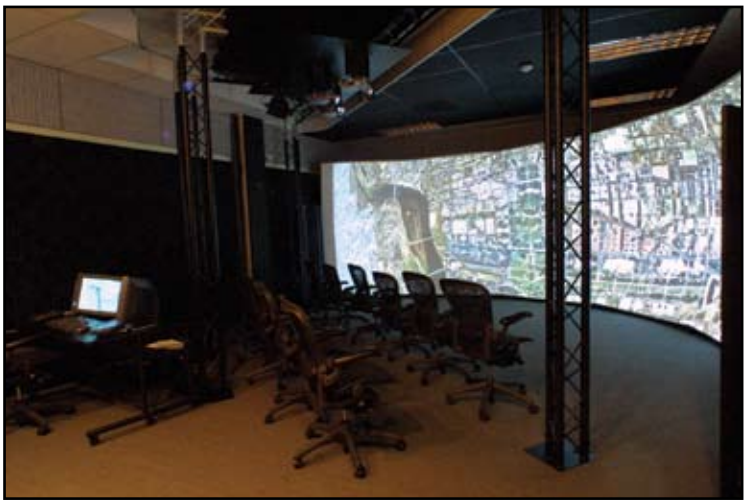

The Motion Imagery Lab in the Center for Computational Science. This resource brings together extremely high resolution global images in progressive scan combined with high performance distributed databases, computing, and networking support of decision-making tools for the warfighter.

militarily relevant problems relating to computational and information science. The systems allow leading-edge research in support of heterogeneous parallel processing applications by the Navy and DoD science and technology communities.

Chemistry

Force Protection/Homeland Defense (FP/HD) has been a focus of the Chemistry Division since September 11, 2001, especially in the development of improved detection techniques for chemical, biological, and explosive threats. In conjunction with technologies contributed by other divisions, the Chemistry Division staff is a major contributor to the definition and development of new technology systems. In a parallel and complementary multidivisional program, the Chemistry Division is a major contributor to the NRL Nanoscience Research Institute. Nanoscience complements FP/HD in that nanoscience is expected to provide dramatic improvements to chemical/biological detection, protection, and neutralization. Chemistry will approach the nanoscale from the bottom-up—building smaller atoms and molecules into nanostructures with new properties and developing the directed assembly of nanostructures into hierarchical systems. The NRL Nanoscience building is linked directly into the Chemistry building to provide both controlled access and auxiliary space for work not requiring a "low noise" environment.

Plasma Physics

The Plasma Physics Division has established a new Electromagnetic Gun Laboratory to study barrel materials science issues associated with an electric gun for a future all-electric warship. The laboratory will house a 6-m-long railgun, a 10 to 16 MJ capacitive energy storage bank, and solid-state switching hardware capable of driving up to 2 MA current in a barrel. The interface between the sliding projectile and the rails will be studied by a multidivision research team in an effort to design a high performance and long-lived electric gun barrel.

Electronics Science and Technology

The Electronics Science and Technology Division has expanded the capabilities of the Ultrafast Laser Facility (ULF) to include (1) a tunable source of mid-IR to UV high-power light pulses and (2) an infrared imaging system and high-precision positioning system. The imaging system produces sub-micron resolution images of single event effects in microelectronic circuits. Single event effects can compromise the reliability of electronic circuits. The described ULF expanded capabilities should be ready in time to impact the 2006 research program. The Silicon Carbide Processing Laboratory (SCPL) and the Advanced Silicon Carbide Epitaxy Laboratory (ASCEL) are nearing completion to establish full functionality in early 2006. These silicon carbide laboratories serve the Division's thrust into the area of power electronics materials and devices.

Acoustics

NRL's Salt Water Tank Facility is designed to provide a controlled environment for studying complex bubble-related processes found in the ocean. It is an experimental pool facility for studies of underwater

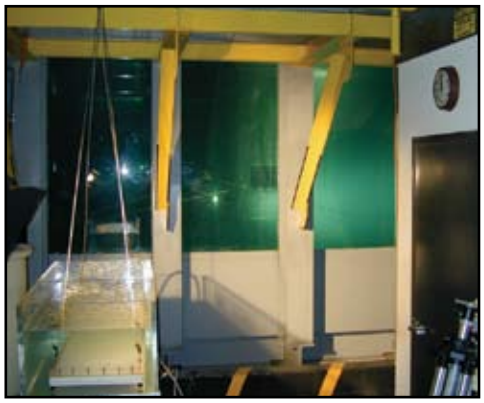

The Acoustic Division's Salt Water Tank Facility is designed for studying underwater acoustics in controlled, saline environments. Currently, this facility is being used to make measurements of sound propagation through bubble clouds.

acoustics, fluid dynamics, and air-sea interface environmental topics under saline conditions. This facility is currently being used to study the acoustics of bubbly media, including bubble entrainment and ambient noise generation, scattering from bubbly structures, and propagation through bubbly media. Future studies include the interaction of bubbles with turbulent fluid flows, bubble coalescence and dissolution, effects of surfactants and contaminants, and bubble-related gas exchange across the air-sea interface.

The Geoacoustic Model Fabrication Laboratory allows researchers to fabricate rough topographical surfaces in various materials (usually plastics) for acoustic scattering and propagation measurements in water-tank facilities. The facility consists of a three-axis computer-controlled milling machine equipped with vacuum holddown and capable of cutting with 100-μm accuracy over a 1.37- × 1.27-m region.

The Division operates state-of-the-art laboratories now resident in NRL's new Nanoscience Building. These new capabilities, dedicated to the study of the behavior of electromechanical systems confined to the near atomic scale (< 100 nm), are referred to as the "Nanomechanics Laboratory" and the "Low Temperature Near-field Scanning Optical Microscopy (NSOM) Laboratory." These laboratories allow temperature/size scaling experiments involving the broadband (~3 GHz) linear and non-linear dynamics of individual Nanoelectromechanical Systems (NEMS) devices and artificial crystal arrays formed from nanomechanical unit cells.

Remote Sensing

The Long Wavelength Array (LWA), to be constructed in the State of New Mexico as a collaboration between The University of New Mexico, University of Texas, Los Alamos National Laboratory (LANL), and NRL, will open a new, high-resolution window on the electromagnetic spectrum from 23 to 80 MHz (corresponding to wavelengths of 13 to 4 m). This region has been poorly explored because ionospheric microstructure had prevented conventional interferometry on baselines longer than approximately 5 km, limiting imaging to coarse angular resolution and sensitivity. Development of ionospheric phase-compensation techniques on the NRL-NRAO 74 MHz VLA receiving system now make it possible to explore this region at unprecedented angular resolution by extending maximum baselines to as much as 400 km.

The LWA will be a powerful instrument for delineating the interaction between nonthermal emitting plasmas and thermal absorbing gas, for differentiating between self-absorption processes, and for exploring the universe for coherent emission processes. For solar, planetary, Galactic, and extragalactic work, it will provide unique information on the distributions of ionized gas, relativistic particles, and magnetic fields. The distribution and spectrum of the cosmic-ray electron gas, high-redshift radio galaxies and quasars, shocks driven by infalling matter in clusters of galaxies, pulsars in the Milky Way and in external galaxies, and radio emission from extrasolar planets are all steep-spectrum processes, which could be especially well studied.

It will provide high-spatial and temporal sampling of the ionosphere for characterizing ionospheric phenomenology, and probing ionospheric microstructure and physics.

It is also the ideal receiver for proposed solar radar systems which can be used to image Earthward bound coronal mass ejections for geomagnetic storm prediction.

Development of a prototype station for the LWA is underway. Contingent upon funding levels, the LWA will be constructed in phases with the last phase scheduled for completion in 2011.

The Remote Sensing Division's experience in developing and deploying the PHILLS airborne hyperspectral systems, and developing algorithms to retrieve coastal ocean bathymetry, water clarity, and other information valuable to the Navy, form the basis for the next step of maritime hyperspectral imaging from space. An orbiting platform will provide long-term, repeat access to coastal areas worldwide, which is not feasible using aircraft. The hyperspectral data will be used to develop seasonal models of selected coastal areas, including areas to which access is otherwise denied. The Remote Sensing Division is beginning a two-phase program for maritime hyperspectral imaging from space. The first phase, now under way, is to develop a PHILLS airborne imager for use in space. This rapid-development program will provide an initial, limited data stream to set up and validate data processing algorithms, and

develop channels to disseminate the data products. The second phase will be to build and launch the fully space-qualified Coastal Ocean Imaging Spectrometer (COIS), with significantly improved performance, and the capability to image 20 coastal regions per day.

Ocean Research Laboratory

NRL's Ocean Research Laboratory is a 52,000 ft^2 building that houses the Oceanography Division of the Ocean and Atmospheric Science and Technology Directorate. The building contains office space, oceanographic laboratories, staging areas, a small machine shop, electronic and secure laboratories, and visualization and computing facilities for research and development in ocean science and remote sensing.

Marine Geosciences

The Marine Geosciences Division has greatly enhanced the capabilities and quality of seafloor sediment fabric analyses through completion of installation and staff training for its High-Resolution Industrial CT Scanner. The CT Scanner is a powerful tool for investigating volumetric heterogeneity of materials. By using X rays at energies from 10 to 225 kV and 0-1 mA, the scanner can image single- or multi-phase media with resolving power as fine as 10-µm voxel size with the microfocus system. The system is capable of rendering and storing real-time radiographic images, reconstructing the images in three dimensions, and processing the images to fit a wide range of project applications.

Vacuum Ultraviolet Space Instrument Test Facility

The Space Science Division facilities include an ultraclean solar instrument test facility in Building A-13 on the main NRL campus. The facility is designed to satisfy the rigorous contamination requirements of state-of-the-art solar spaceflight instruments. The facility has a 400-ft^2 Class 10 clean room and a large Solar Coronagraph Optical Test Chamber (SCOTCH). This completely dry-pumped, 550-ft^3 vacuum chamber is maintained at synchrotron levels of cleanliness. Solar instrumentation up to 1 m in diameter and 5 m in length can be physically accommodated in the chamber. The instrument's optical performance is probed and calibrated with a variety of visible and XUV sources mounted on the chamber's 11-m beamline. The optical testing and characterization of the Large-Angle Spectrometric Coronagraph (LASCO) instrument for the European Space Agency's Solar Heliospheric Observatory satellite were conducted in this chamber. Coronagraph stray-light characterization was carried out by mounting a set of baffles in the main beamline, illuminating the instrument with a simulated solar beam, and measuring the residual radiation. A stray light background measurement of 10^{-12} was successfully measured in the LASCO C3 channel. Coronagraph calibration was carried out by installing back-illuminated calibrated opals in front of the instrument entrance aperture. Instrument polarization properties were analyzed by using a variety of polarizers installed in a wheel located between the opal and the instrument. The wheel was remotely controlled from outside the chamber. Instrument Mueller matrices were verified with a 12-in. diameter, two-plate partial polarizer. Calibration and focus of XUV solar instrumentation are accomplished by exposing the instrument to an XUV windowless collimator at the end of the tank. The facility also has a small thermal bake/vacuum test chamber used for vacuum conditioning and thermal testing of spaceflight components and subassemblies. Both the SCOTCH and the small test chamber are instrumented with temperature-controlled quartz-crystal monitors and residual gas analyzers for real-time, quantitative measurements of volatile contamination.

REHABILITATION OF SCIENTIFIC FACILITIES

Specialized facilities are being installed or upgraded in several of the research and support divisions.

Scientific Development Squadron One (VXS-1)

VXS-1 has continued to improve both capabilities and diversity among its aircraft platforms. Most recently VXS-1 has acquired a C-12 Beech KingAir, a small twin-engine aircraft with a ceiling of 30,000 ft. This new platform will enable VXS-1 to cater to even the smallest project while research customers can align their Science & Technology projects to the most economical platform. This new addition to our aviation fleet will ensure that NRL will continue to have the finest and most diversified airborne research capabilities well into this century.

An example of VXS-1's newly acquired C-12 Beech KingAir, which will enable smaller research projects to be flown more economically.

Information Technology

The Information Technology Division continues to transition stable technology from high performance network testbed activities into the NRL local area network. This effort includes support of ATM technology at stream rates of 2.5 Gbps (OC48) across the enterprise with demonstrations and technology integration to allow first use of 10 Gbps single streams and higher. The current computing architectures and the SGI Altix and Cray XD1 are continuously undergoing upgrade and evaluation of both hardware and software. The NRL Center for Computational Science (CCS) works closely with the DoD HPC community and the HPC vendors to provide insight, balance, and value-added capabilities within the massively parallel processing (MPP) testbed infrastructure.

Personnel who work in the Integrated Communications Technology (ICT) Test Lab have extensive knowledge of multiprotocol network interactions and are poised to support future Navy and DoD network research, evaluation, and integration efforts. The ICT Test Lab will be involved in future networking efforts to provide a transition between high-performance fiber-optic technologies and wireless tactical networking.

The Advanced Information Technology (AIT) Branch is currently developing an Intent/Deception (ID) Laboratory for testing various sensor suites, algorithms, and processes associated with behavioral indicators of deception. Sensors include computer vision cameras, pupil trackers, thermographic IR cameras, and high-end audio collection equipment. The ID Lab will serve as an integration facility for the various sensors and an evaluation center for the algorithms needed to automate the process of determining deception.

Plasma Physics

A single-shot, short-pulse (400 fs), high-intensity Table-Top Terawatt (T^3) laser has been recently upgraded for operation with two independently timed beams, one with up to 15 TW and 3×10^{19} W/cm^2, and the other up to 2 TW for intense laser-matter interaction studies, including particle acceleration. A new 10 Hz ultrashort-pulse (40 fs), Ti:Sapphire Femtosecond Laser (TFL) system is now operational at 10 TW. These lasers comprise a facility to do fundamental physics experiments in intense laser-plasma interactions, intense laser-electron beam interactions, and intense laser-matter interactions.

The division has built two large electron-beam-pumped krypton-fluoride (KrF) laser systems that have applications to both fusion energy and defense. Nike is a large 5 kJ system used for studies of laser-target interaction, while the Electra system is developing the next-generation efficient and reliable technologies needed to progress from the laboratory to commercial laser-fusion energy. Electra has a goal of a laser output of 700 J at 5 Hz. Larger KrF systems that would be needed for a fusion driver are being designed based on experience with these systems.

The new Mercury pulsed-power generator became operational in 2004. The facility is located in renovated space in Building 256. Mercury is an inductively isolated, voltage-adder device that is capable of producing a 6-MV, 360-kA, 50-ns electrical power pulse for driving electron beam and ion beam diodes. The new facility will support ongoing radiographic source development for the Department of Energy and nuclear weapons effects simulation for the Defense Threat Reduction Agency.

Electronics Science and Technology

The Electronics Science and Technology Division has rehabilitated four laboratory modules in Building 208 to provide a new home for the Ultrafast Laser Facility (ULF), which was recently moved from Building 75. This new space will also house the expanded capabilities of a new infrared imaging system and a new tunable high-power light source, which were added in 2005. To address the Division's needs in power electronics research, four laboratory modules in Building 208 were rehabilitated in 2005 to establish the Advanced Silicon Carbide Epitaxy Laboratory (ASCEL). The ASCEL will house a new silicon carbide epitaxial reactor and a variety of supporting equipment necessary to meet operational and safety standards. Two additional adjacent modules are being rehabilitated to provide space for silicon carbide materials inspection and characterization.

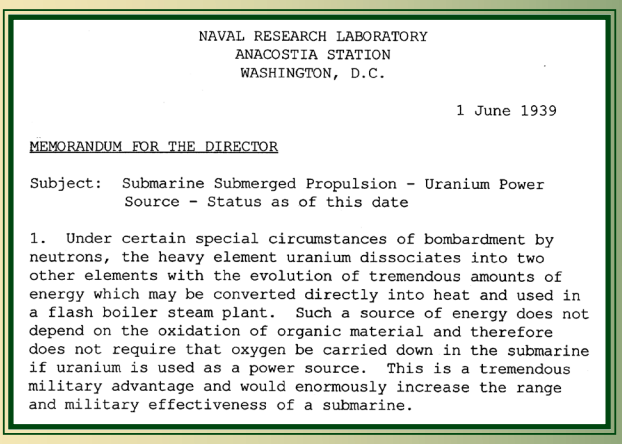

NAVAL RESEARCH LABORATORY
ANACOSTIA STATION
WASHINGTON, D.C.

1 June 1939

MEMORANDUM FOR THE DIRECTOR

Subject: Submarine Submerged Propulsion - Uranium Power Source - Status as of this date

1. Under certain special circumstances of bombardment by neutrons, the heavy element uranium dissociates into two other elements with the evolution of tremendous amounts of energy which may be converted directly into heat and used in a flash boiler steam plant. Such a source of energy does not depend on the oxidation of organic material and therefore does not require that oxygen be carried down in the submarine if uranium is used as a power source. This is a tremendous military advantage and would enormously increase the range and military effectiveness of a submarine.

First Proposal of a Nuclear Submarine

Achievement: The use of nuclear power to propel submarines under water was first proposed by an NRL physicist, R. Gunn, soon after fission was discovered in 1939. In March 1939, Navy officials, one of which was Gunn, met with several civilian scientists who felt the military should be made aware of the vast possibilities of nuclear fission. Among the civilian scientists was Enrico Fermi. While most of the Navy personnel present at the meeting concentrated their attention on a nuclear weapon, Gunn was conceiving the idea of using nuclear power to drive the world's first nuclear submarine.

Within a few days after this historic meeting, Gunn had requested and received $2,000 for preliminary work on the possibility of developing nuclear power for ship propulsion. Later, in June 1939, in a memo to the NRL Director, Gunn stated:

> "Under certain special circumstances of bombardment by neutrons, the heavy element uranium dissociates into two other elements with the evolution of tremendous amounts of energy which may be converted directly into heat and used in a flash boiler steam plant. Such a source of energy does not depend on the oxidation of organic material and therefore does not require that oxygen be carried down in the submarine if uranium is used as a power source. This is a tremendous military advantage and would enormously increase the range and military effectiveness of a submarine."

In April 1946, NRL forwarded a report to the Bureau of Ships entitled "The Atomic Energy Submarine," which concluded that it was considered feasible to construct atomic power plants of a size and output suitable for ship propulsion. This report also marks the first interest in liquid metal coolants for reactors.

Impact: NRL was first to conceive, propose, and investigate the use of nuclear power in submarine propulsion, and through subsequent efforts the Laboratory contributed to the planning and development of the world's first atomic-powered submarine, the USS *Nautilus*. The nuclear submarine is one of the most formidable weapons systems ever developed.

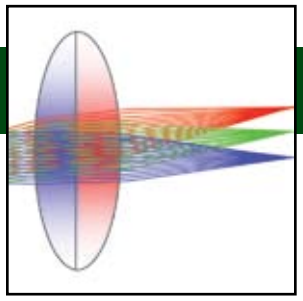

Biomimetic Gradient Index (GRIN) Lenses

J.S. Shirk,[1] M. Sandrock,[2] D. Scribner,[1] E. Fleet,[1] R. Stroman,[3] E. Baer,[4] and A. Hiltner[4]
[1]*Optical Sciences Division*
[2]*SFA, Inc.*
[3]*Chemistry Division*
[4]*Case Western Reserve University*

A new class of hierarchically structured polymer optical materials possessing an internal refractive index gradient that mimics biological optical materials is described. The new materials permit the fabrication of gradient refractive index (GRIN) lenses with an unprecedented variety of index gradients. Gradients with different functional forms in both the radial and axial directions have been fabricated. Materials with gradients with a $\Delta n \sim 0.17$ have been made, and larger index ranges are possible. Flat GRIN lenses and shaped lenses with specified internal index gradients have been fabricated from the new materials. The new polymer materials show promise for use in optical systems that have fewer, lighter lenses than traditional lens systems. They encourage the exploration of new paradigms for bio-inspired optical designs that could not be implemented by using homogeneous lens materials.

The fabrication of practical GRIN polymer optical materials involved a series of advances. The first was the recognition that a transparent polymer film with a specified refractive index could be fabricated using nanolayer polymer extrusion technology. The nanolayered films are stacked to create a material with an index gradient defined by the order in which the different nanolayered films are stacked. The stacking order, and thus the gradient, can be defined as desired. These materials are then molded into the GRIN lenses. To take advantage of the ability to construct a specific index gradient in a shaped lens, an optimum index gradient for such lenses had to be designed.

These new materials facilitate the application of GRIN optics to a variety of optical systems and devices. They support the development of bio-inspired lenses and optical systems. The wide range of lens shapes and index profiles that can be fabricated gives an optical designer substantial control over the focal properties of each lens.

INTRODUCTION

Optical systems capture light and use it to produce images with information about the environment. In nature, each set of optics is tailored to fit the specific needs of its owner. Optics inspired by nature's designs have an enormous potential for transforming the process of image collection.[1] A DARPA program, Bio-Optic Synthetic Systems, has the goal of demonstrating the power of such bio-inspired optical concepts.

Eyes for different species are adapted for seeing in the day or night, short or long distances, or with wide or narrow fields of view. Nature tends to optimize these systems to provide the optics required for survival. Eagles have acuity at long distances and the ability to maintain a focus during a rapid descent. The eyes of the prey monitor a wide field of view and permit it to detect an attacker early enough to allow an escape. Human eyes can produce quite high-resolution, relatively aberration-free images with only two optical components, the cornea and the crystalline lens. We perform this imaging feat both close up and at long distances, providing the lenses in question are not over about 40 years old.

Natural optical systems have a feature not usually found in man-made imaging technologies. Bio-optical materials are formed by hierarchical layered protein structures. These give rise to index gradients that can enhance focusing power, correct aberrations, and reduce the number of components needed for an effective optical system. We have developed a new class of nanostructured polymer optical materials that can mimic the layered protein structures found in biological materials. These materials enable the fabrication of a new class of polymer GRIN lenses, lenses that possess a variation in the refractive index within the material.

The new materials enable us to incorporate this important feature of biological vision systems into man-made optical systems. The first examples of the new polymer GRIN optics include single lenses inspired by cephalopod (octopus) eyes and a three-lens, wide field of view, optical system for a surveillance sensor.

GRADIENT REFRACTIVE INDEX OPTICS

Traditional optical materials are homogeneous; the refractive index is uniform throughout the material. In such a lens, a light ray is refracted at the lens surface where there is an abrupt change of the refractive index from air. The imaging properties are determined by the surface shape. GRIN optical materials possess a variation or gradient in the refractive index within the material. The variation of the refractive index within the material causes light rays to be bent within the lens. With a GRIN lens, focusing and imaging depends on how the refractive index varies within the lens material (Fig. 1). GRIN lenses can also be shaped like traditional lenses. Then the focal properties depend both on the surface shape of the lens and on the index gradient within the material.

The theory of gradient index optics is well known.[2] R.W. Wood described a flat radial GRIN lens in 1905.[3] It has been long recognized that GRIN elements add considerable power and flexibility to the design of optical systems. Because GRIN lenses can have flat surfaces, they are useful in optical systems where this geometry allows the simplified assembly of systems of lenses. Varying the thickness of the lens can vary the focal length and working distance. The image plane can be made to lie directly on the exit surface of the lens. Unlike conventional lenses, GRIN lenses can maintain their focusing ability under water.

A traditional lens designer can vary the curvatures, the thickness, and the refractive index of the material. In addition, a GRIN lens designer can also use index gradients to simplify or enhance the optical system. For example, axial gradients, where the index of refraction varies along the optical axis can perform the same functions as an aspheric surface in a traditional lens. A traditional lens design that requires an aspheric surface can be replaced with a spherical surface that is substantially easier to form and polish if an axial gradient is introduced. Even more useful are radial gradient lenses, where the index of refraction is a function of the distance from the center of the lens. Radial gradients can add focusing power and control specific aberrations.

NANOLAYER POLYMER GRIN MATERIALS

Despite the appeal of GRIN optics, actual applications have been limited to fiber optics and small lens systems. This is primarily because the fabrication of materials with a sufficient and controllable refractive index gradient over a 1- to 2-cm diameter lens has not been very practical. In earlier GRIN materials, the index gradient was typically formed by a diffusion process or a copolymerization process in a polymer. The index gradient that can be achieved with such processes is determined by diffusion and is often quite small.

The initial step in the development of the new GRIN materials was the recognition that a transparent polymer film with a specified refractive index could be fabricated using microlayer polymer coextrusion technology. The process, described in the sidebar, has been known for more than 35 years.[4,5] Beginning in 1969, a series of patents and publications describe a coextrusion process using layer-multiplying dies that can produce large sheets of layered polymer materials with hundreds of layers. The process was further developed by Baer and coworkers at Case Western Reserve University.[6] Their recent advances enable the facile production of nanolayer polymer materials with tens of thousands of layers and layer thicknesses as small as 5 nm.[7] This continuous process produces layered polymer materials in the form of flexible sheets and films with large surface areas.

The utility of coextrusion to produce optical materials arises from the variety of polymers and polymer dopants that can be used to make nanolayered polymer materials. Practically, the polymer components are limited to those that mutually adhere and have compatible processing properties. Even with these restrictions, however, it is possible to choose polymer pairs so that the materials in the alternating layers have substantial differences in the index of refraction (n). The resulting layered materials possess a modulation in the index with a period corresponding to the layer thickness.

The layered polymer materials are of particular interest for optics when the layer thickness and thus the period of the modulation in the index is either (A)

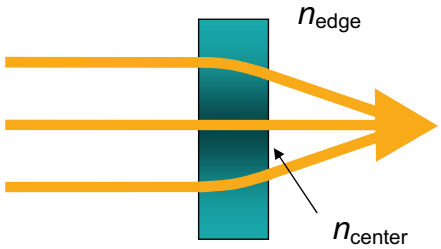

FIGURE 1
Focusing by an index gradient alone.

Microlayer Polymer Processing

The basic ideas of the nanolayer processing are shown in Fig. S1. The two-component coextrusion system consists of two single-screw extruders, each connected by a melt pump to a coextrusion feed block. The feed block combines polymer A and polymer B as two parallel layers. By adjusting the melt pump speed, the relative layer thickness, that is, the ratio of A to B, can be varied. From the feed block, the melt goes through a series of multiplying elements. The multiplying die (Fig. S2) first slices the AB structure vertically, then subsequently spreads the melt horizontally. The illustration shows how the flowing streams recombine, doubling the number of layers. An assembly of n multiplier elements produces an extrudate with the layer sequence $(AB)x$ where x is equal to $(2)^n$. Nanolayered structures with up to 4096 layers have been successfully processed, and more are possible. By altering the relative flow rates or the number of layers while keeping the film or sheet thickness constant, individual layer thickness can be controlled. Nanolayered film or sheet with overall thickness ranging from 0.5 to 60 mils has been processed, and samples with individual layer thickness less than 5 nm have been produced.

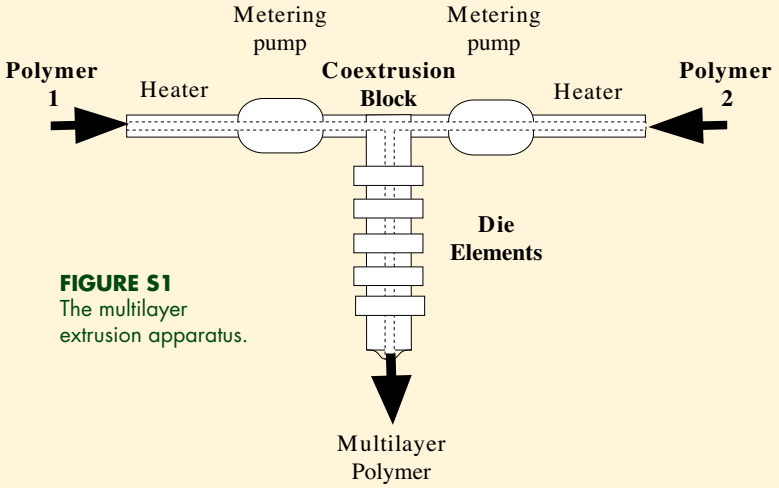

FIGURE S1
The multilayer extrusion apparatus.

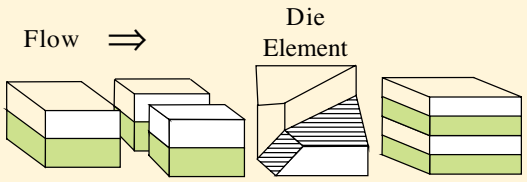

FIGURE S2
Details of a die.

on the order of the wavelength of light or (B) shorter than the wavelength of light of interest. The two cases are illustrated in Fig. 2. In the first case, when the modulation period and layer thickness are $\lambda/4n$, the materials show a high reflectivity at the wavelength λ. They are effective dielectric reflectors or 1-dimensional photonic crystal materials. The reflected wavelength can be selected by varying the layer thickness. In the second case, where the layer thickness is less than $\lambda/4n$, the optical properties are that of an effective medium composite.[8] The refractive index and transmission are an average of those of the component materials.

In case A, when the layer thickness is $\lambda/4$, this technology has been commercialized to make a variety of polymer dielectric reflectors and filters with specific transmission properties and passbands.[9] The extrusion process is well-suited to making large-area reflectors that are difficult to make by using traditional techniques. Layered birefringent polymers yield polarization-selective reflectors that are commonly used to enhance the brightness of laptop computer displays. They also can be used to produce dielectric mirrors that maintain reflectivity over a broad band of incident angles[10] and are useful as light pipes. These layered polymers have also been used to create an iridescent Christmas tinsel.[11]

To fabricate the materials of interest for gradient refractive index materials, the layer thickness is

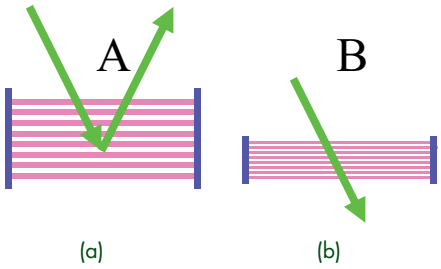

FIGURE 2
Optical function of layered polymer materials. (a) Layer thickness equal to $\lambda/4n$: dielectric filters and mirrors; (b) Layer thickness much less than $\lambda/4n$: effective medium composite.

chosen to be 50 nm or less so that the films do not reflect visible light. In this thickness range, the material properties are described by effective medium theory. The refractive index of the layered film corresponds approximately to a thickness-weighted average of the indices of the component polymers. Figure 3 shows the refractive index of a set of 101 films fabricated by layering polycarbonate (PC) (n = 1.58) and polymethyl methacrylate (PMMA) (n = 1.49) as components. The films were about 50 µm thick overall and had 2048 layers, so that the thickness of an individual layer in the material with equal amounts of PC and PMMA, for example, is about 25 nm. The composition of the polymer film can be varied by adjusting the relative thickness of the different polymer layers. Figure 3 shows that the observed index varies linearly with the composition (relative layer thickness), demonstrating that it is possible to make a polymer film with a refractive index selected to be any value between the indices of the component polymers. The index difference between any two sequential films is small; in this case, the smallest index difference is 0.0009. Such nanolayered composites can be made to be quite transparent; transmissions between 85% and 90% are common. To our knowledge this is the most practical way to fabricate layered composite polymer films with layers thin enough that the material behaves as a transparent effective medium.

A polymer with an index profile is made by stacking a set of such nanolayered polymeric films. The films are stacked in the order that gives the desired index gradient. Figure 4 shows the steps in the process. For example, by sequentially stacking a single film of each of the 101 compositions starting with a pure PMMA film, then one with a 99/1 ratio of PMMA to PC, then a 98/2 ratio, to the 101st layer that is pure PC, a polymer with a linear refractive index gradient varying from 1.49 to 1.58 was made. Notice that this material has a hierarchical structure. It is an ordered array of 50-µm thick composite films; on a finer scale, each of these composite films is made up of 2048 layers of alternating PC and PMMA with a layer thickness of a few nanometers.

More complex index gradients can be made by changing the order in which the nanolayered films are stacked. The final GRIN material typically contains more than 200,000 nanolayers, a number comparable to the number of protein layers found in the biological lenses. The sets of stacked polymer films are consolidated to produce a transparent thick sheet of material with the desired index gradient.

As illustrated in Fig. 4, the gradient is normal to the surface in the consolidated material. Observed from the side, a linear gradient gives a GRIN prism and a parabolic gradient gives a GRIN cylindrical lens. A lens machined from this polymer will have a refractive index gradient in the axial direction. A radial variation in index can be introduced by the molding process illustrated in Fig. 4. A plano-convex lens with both radial and axial gradients can be made by shaping the appropriate preform to the desired curvature, then cutting and polishing the shaped lens.

DESIGNING POLYMER GRIN LENSES

To take advantage of our ability to construct a shaped lens with a specific index gradient, it was necessary to design the lens shape and index gradient. The initial example was a lens designed to demonstrate that a nanolayer polymer GRIN lens, with a proper gradient, can provide both focusing and aberration correction within a single lens. Figure 5 illustrates this strategy.

The starting index profile for the optimization was inspired by that found in many biological eyes, for example an octopus eye. The octopus lives in water, where the refractive index is close to that of the protein on the surface of the eye (Fig. 6). The curvature of a lens is less effective at focusing under water than in air. The octopus solves the problem with an eye that has thousands of layers of protein with different refractive indices. The index gradient gives the octopus the focusing capability and aberration correction needed.

In the octopus, the index gradient was optimized by natural selection. The Navy is not so patient, so an appropriate gradient was designed using the optical ray-tracing program, ZEMAX. The index profile in the first model lenses was designed to provide aberration correction but not underwater operation. As we develop polymer sets with a larger index contrast, it may be possible to extend this design to underwater lenses.

In one lens design, different gradients were used for each half of the lens. The index gradients are shown in Fig. 7. The rationale for the optimized gradient is easy to understand. Spherical aberration is reduced

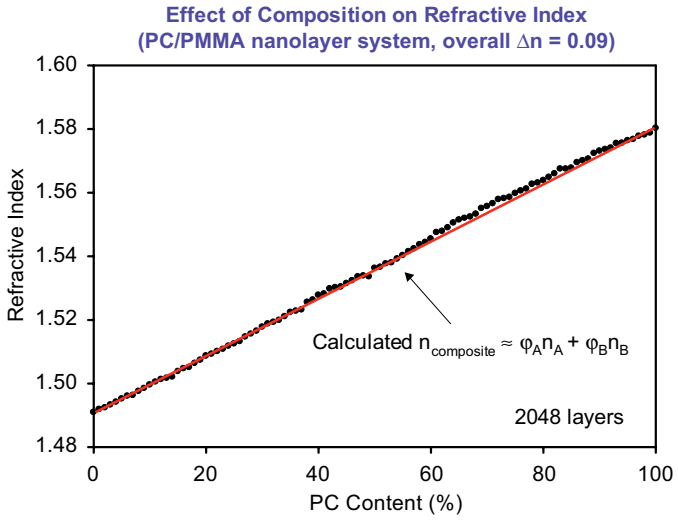

FIGURE 3
Refractive index of a set of films made of layered polycarbonate (PC) poly methylmethacrylate (PMMA) as a function of relative layer thickness/composition.

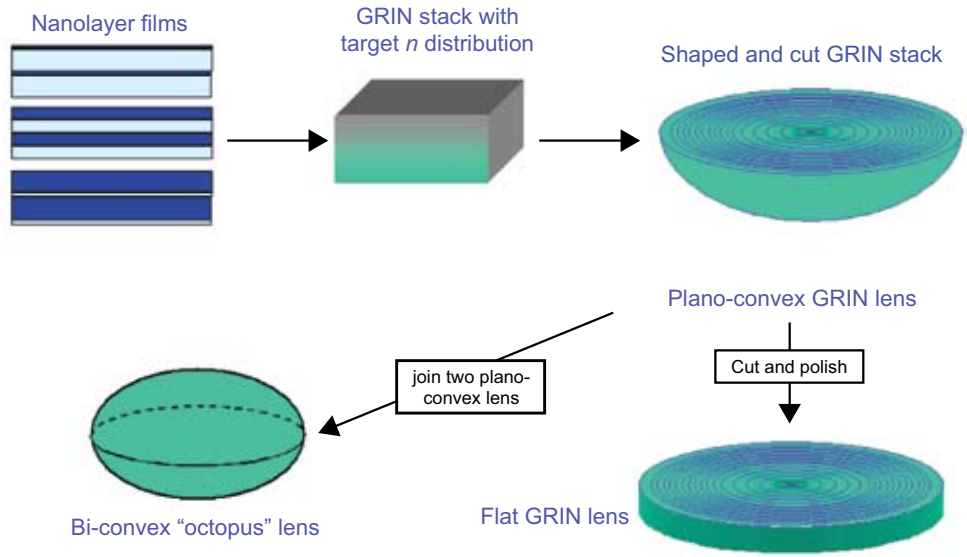

FIGURE 4
Steps to fabricate a polymer GRIN lens.

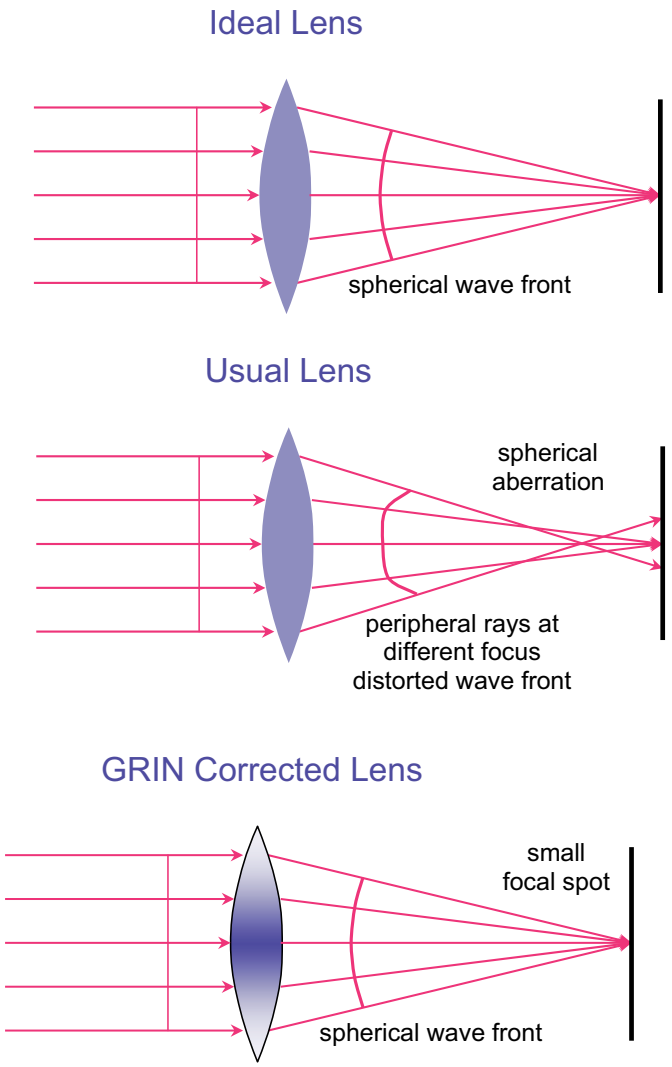

FIGURE 5
Strategy for spherical aberration correction in a convex lens.

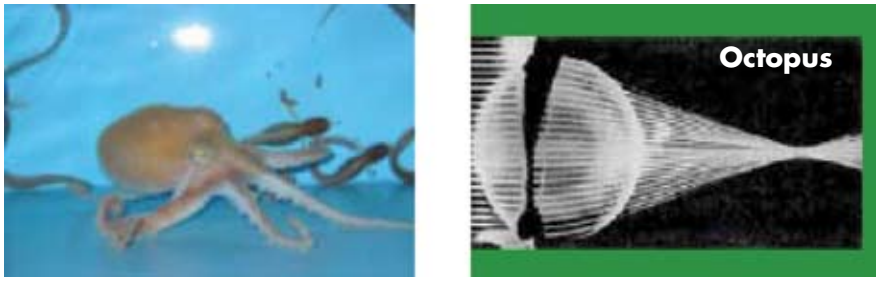

FIGURE 6
Octopus lens with minimal spherical aberrations.

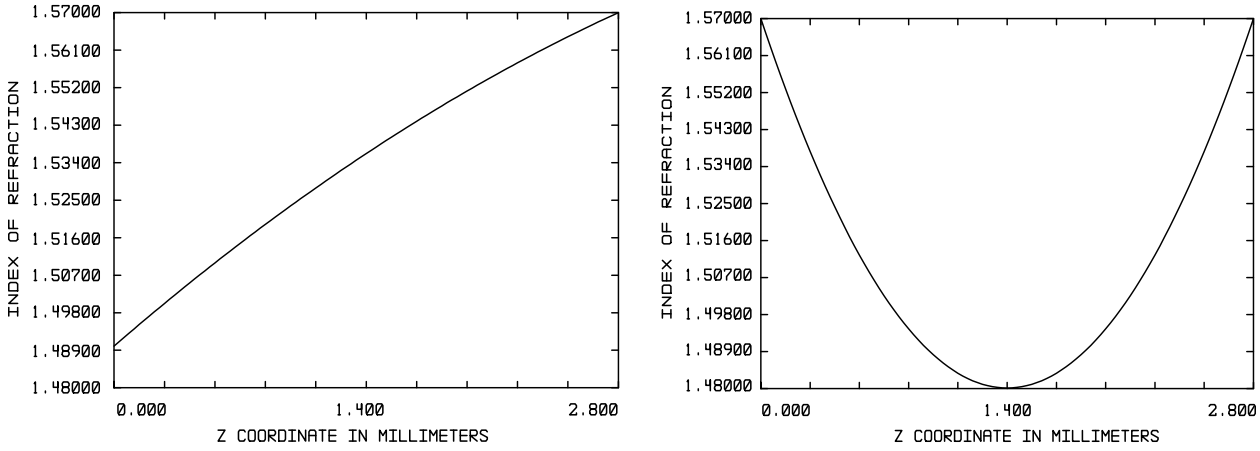

(a) First half (b) Second half

FIGURE 7
Optimized index profiles to correct for spherical aberration in a double convex lens.

with a lower index and hence a shorter optical path near the edges of the lens. The index gradient performs a function similar to that of an aspheric (Schmidt) corrector plate that is sometimes added to telescope designs with homogeneous lenses.

GRIN lenses were produced using the fabrication techniques described above. A Shack-Hartmann wave front analyzer measured the shape of the propagating wave front after the lens. The Zernike polynomial representation of the wave front showed substantially lower spherical aberration in the GRIN lens compared to a similar homogeneous lens. Although the GRIN lens was not free of aberrations, we demonstrated an ability to design and fabricate a GRIN lens with a substantial reduction in a specific aberration.

GRIN OPTICAL SYSTEMS

To explore the potential applications to Navy optical devices, we have begun to design small, lightweight, robust, optical systems that use the polymer GRIN lenses to reduce the complexity and weight of multielement imaging devices. Ray tracing techniques are used to design such systems. Figure 8 shows the initial design of a three-lens system to provide a large field of view for a short wave infrared (SWIR) sensor array.

The optical system was constructed using lenses that were designed with appropriate index gradients. Figure 9 shows an image taken with this lens set imaging onto a SWIR camera. Details are easily resolvable with the polymer lens.

This lens system was installed on an *Evolution* unmanned aerial vehicle (UAV) with a visible sensor, flown to altitudes of up to 1000 ft and used to record video images. The camera provided good image resolution and contrast in the flight test, indicated by the readily identifiable ground vehicles in the images. The flight tests illustrated the ability of this new GRIN lens technology to be transitioned to a lightweight, robust, optical system. We are now extending this technology to develop a small, lightweight zoom lens that uses variable focal length lenses inspired by the structure of the human eye.

SUMMARY

We have introduced a new class of hierarchically structured polymer optical materials where the refractive index can vary in a controllable way within the material. The new GRIN materials permit the fabrication of gradient refractive index lenses with a variety of index gradients. A wide range of lens shapes and index profiles are feasible, giving an optical designer substantial control over the focal properties of these lenses.

The development of these GRIN polymer optical materials began with the recognition that we could make transparent layered composite polymer films with a specified refractive index via a well-known nanolayer polymer extrusion technique. By stacking a set of these films with very small differences in index, we created a polymer with an internal index gradient. The index gradient is defined by the order in which the films are stacked. Molding this material gives a shaped GRIN lens with the desired gradient. Ray tracing techniques allowed us to optimize the index gradients for specific lenses and optical systems. A biconvex lens corrected for spherical aberration and a small, lightweight, robust, multielement lens for a SWIR camera were designed, fabricated, and characterized. The latter lens system was installed in an NRL *Evolution* UAV and used to record video images at a height of up to 1000 ft.

The index gradients in the polymer materials emulate an important feature of optical systems found

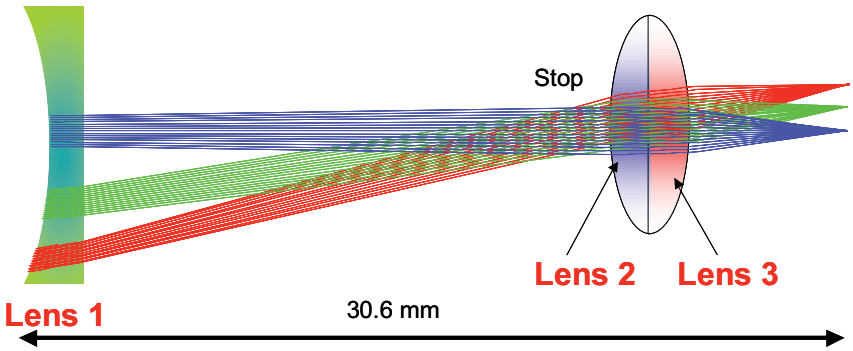

FIGURE 8
Camera lens system designed with a 60° field of view composed of three GRIN lenses with complex refractive index profiles. All the GRIN lenses were made from nanolayered SAN17/PMMA films.

FIGURE 9
Infrared image obtained using the GRIN lens system in Fig. 8 coupled to a SWIR camera.

in nature. The index gradients that enhance focusing power and correct aberrations in nature can perform the same function in man-made optics. An optical designer can look to the intriguing array of optical systems found in nature for inspiration in developing new optical systems using these materials. Such bio-inspired optical systems can be simpler, lighter, and less complicated than traditional glass lens systems.

ACKNOWLEDGMENTS

This was a collaborative project between groups at NRL and Case Western Reserve University. Michael J. Wiggins, who worked at both NRL and Case, was responsible for some of the early optical characterization. Yi Jin and Huwen Tai at Case were responsible for coextruding the nanolayered sheets and fabricating the GRIN lenses.

We also acknowledge useful and stimulating discussions with Dr. Leonard J. Buckley.

[Sponsored by DARPA]

References

[1] G. Zuccarello, D. Scribner, R. Sands, and L. Buckley, "Materials for Bio-inspired Optics," *Adv. Mats.* **14**, 1261-1264 (2002).
[2] D.T. Moore, "Gradient-Index Optics — A Review," *Appl. Optics* **19**, 1035-1038 (1980).
[3] R.W. Wood, *Physical Optics* (Macmillin, New York) pp 86-91 (cited in Ref. 1).
[4] T. Alfrey, E.F. Gurnee, and W.J. Schrenk, "Physical Optics of Iridescent Multilayered Plastic Films," *Poly. Eng. Sci.* **9**, 400-404 (1969).
[5] W.J. Schrenk and T. Alfrey, "Some Physical Properties of Multilayered Films," *Poly. Eng. Sci.* **9**, 393-399 (1969).

[6] E. Baer, "Micro and Nanolayered Polymers," *Macromol. Symp.* **104**, 31 (1996).
[7] R.Y.F. Liu, T.E. Bernal-Lara, A. Hiltner, and E. Baer, "Polymer Interphase Materials by Forced Assembly," *Macromol.* **38**, 4819-4827 (2005).
[8] R.J. Gehr and R.W. Boyd, "Optical Properties of Nanostructured Optical Materials," *Chem. Mat.* **8**, 1807-1819 (1996).
[9] W.J. Schrenk, J.A. Wheatley, R.A. Lewis, and C.B. Arends, "Nanolayer Polymeric Optical Films," *Tappi J.* **75**, 169-174 (1992).
[10] M.F. Weber, C.A. Stover, L.R. Gilbert, T.J. Nevitt, and A.J. Ouderkirk, "Giant Birefringent Optics in Multilayer Polymer Mirrors," *Science* **287**, 2451-2456 (2000).
[11] W.J. Shrenk, "Method of Making Christmas Tinsel," U.S. Patent #3,480,502, issued November 25, 1969. ★

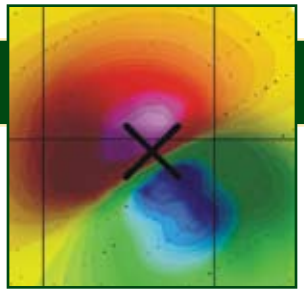

Airborne Magnetometry Surveys for Detection of Unexploded Ordnance

H.H. Nelson[1] and J.R. McDonald[2]
[1]*Chemistry Division*
[2]*AETC, Inc.*

Unexploded ordnance (UXO) contamination is a high-priority problem for the Department of Defense (DoD). As used here, UXO refers to explosive, propellant, or chemical-containing munitions that are armed, fired, and remain unexploded because of malfunction. Approximately 1,400 DoD sites, comprising about 10 million acres, are known to or are suspected of containing UXO. A typical site is thousands of acres; many exceed 10,000 acres, a few are several hundred thousand acres. Most of these sites are Formerly Used Defense Sites (FUDS) for which the DoD retains liability for ordnance. Remediation of such large areas would cost tens of billions of dollars. However, according to some estimates, no more than 20 percent of those 10 million suspected acres are actually contaminated with UXO. Thus, identifying a technology or combination of technologies to accurately delineate the contaminated areas on each site would significantly reduce the actual area that would require a site investigation and response. This would allow limited cleanup resources to be used more effectively.

INTRODUCTION

The Defense Science Board (DSB) Task Force on Unexploded Ordnance issued a series of recommendations about this problem in their December 2003 report.[1] Recommendation 1 was "Institute a national area assessment of the identified 10 million acres [of land involved]." They elaborate on this recommendation, saying "The Task Force envisions an intensive five-year campaign to assess all 10 million acres with the goal of delineating where the UXO *are* and where they *are not*. This campaign would use the full range of techniques and instruments including the helicopter-borne sensor where applicable."

One of the helicopter-borne sensors to which they refer is the Naval Research Laboratory's airborne magnetometer array whose development was supported by the Environmental Security Technology Certification Program (ESTCP). This airborne system was developed as an adjunct to the vehicular Multi-sensor Towed Array Detection System (MTADS) and is often referred to as airborne MTADS.

TECHNOLOGY DESCRIPTION

Sensors

The airborne array (Fig. 1) comprises seven magnetometers spaced at 1.5 m in a 9-m boom mounted just forward of the blade tips of a Bell LongRanger helicopter.[2] The sensors are cesium-vapor total-field magnetometers that measure localized perturbations to Earth's magnetic field caused by ferrous metal, in this case UXO. The magnetometer signals are sampled at 100 Hz that, combined with a typical survey speed of 10 m/s, results in a down-track measurement spacing of ~10 cm.

Sensor positions are determined by using two GPS antennas configured as a master/slave pair. The master receiver receives corrections from a fixed-base station; it reports real-time kinematic (RTK) positions at 20 Hz with an accuracy of ~5 cm and the vector to the slave at 10 Hz with similar accuracy. To obtain height-above-ground measurements, which are useful for the data analyst, a laser altimeter is mounted under the body of the helicopter, and acoustic altimeters are mounted alongside the laser altimeter and under the two GPS antennas. Altitude readings are recorded at 10 Hz. All sensor readings are time-stamped with a time that can be related to the UTC time reported in the GPS position string.

All sensor outputs are sent to a data acquisition computer that is mounted in the rear starboard seat of the helicopter. During testing and initial surveys, an operator in the rear port seat monitored the survey progress. In later production demonstrations, the data were recorded on the data acquisition computer and sensor health and status information was telemetered to a ground observer. This minimized the number of personnel in the aircraft for safety considerations.

Survey Data Acquisition

The helicopter flies preplanned survey lines by monitoring a sunlight-readable navigation guidance display developed specifically for this program. The

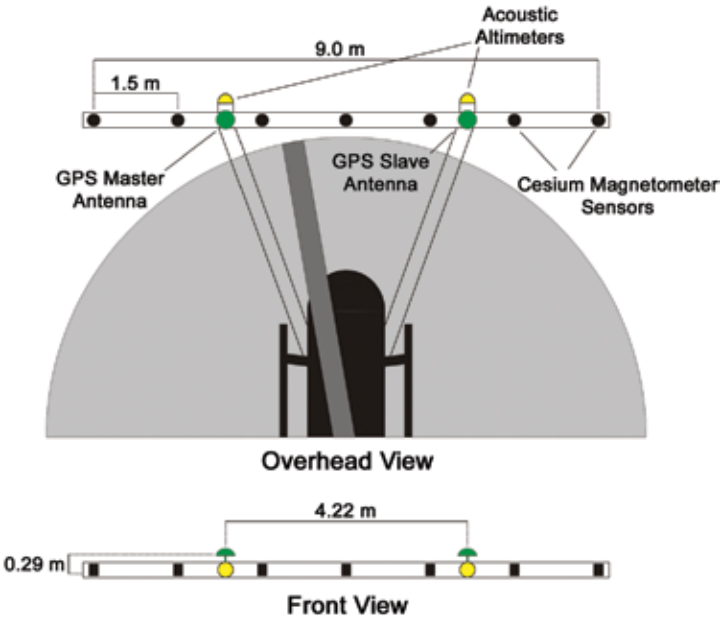

FIGURE 1
Major system components of the airborne magnetometer array. The seven total-field magnetometers are mounted just forward of the blade tips and are spaced at 1.5 m across track. Sensor positions are derived from a pair of GPS antennas and height above ground is derived from acoustic altimeters mounted under the GPS antennas and under the body of the aircraft and a laser altimeter mounted under the aircraft.

display is mounted to the right of the instrument panel. It is in the field of view of the pilot but does not interfere with the pilot's ability to see the entire forward boom and the ground immediately ahead of the aircraft.

The navigation guidance display (Fig. 2), provides the pilot left-right indicators, an altitude indicator, an automatic line number increment, a color-coded flight swath overlay, and the ability to zoom the map scale in or out as desired. The survey course-over-ground is plotted in real time on the display using information from the GPS receivers. This allows the pilot to respond rapidly to both visual cues on the ground and to the navigation guidance.

Survey lines typically have a spacing of 7 m. This allows for a significant overlap of adjacent survey passes of the 9-m sensor boom and ensures that there are no gaps in survey coverage, even in moderately windy conditions. Since the amplitude of the anomaly signal measured by the magnetometers falls off as the third power of the target-to-sensor distance; it is important to keep the sensors as close to the ground as possible. Our nominal survey altitude is 1.5 m, although this can be relaxed somewhat when searching only for large targets. Figure 3 shows the system conducting a survey at the Badlands Bombing Range Impact Area in southwestern South Dakota.

The cost of chartering the helicopter is one of the largest expenses in a survey. For this reason, we make every effort to minimize the time that the aircraft is flying without data being collected. Because the survey ranges are former military test and training ranges, a typical survey site is many miles from the nearest town. We normally place the aircraft at the nearest community airport, often 10 to 20 miles from the survey site. To avoid having to fly this round trip for each refueling (2 to 2½ hours) we base a jet fuel tank on the survey site itself. Thus, at each refueling interval, the pilot can take a rest break while the aircraft is being refueled and no flight time is lost. On a typical operational day we can survey 400 acres. By employing two pilots and extra support crew, we have achieved survey coverage of 800 to 900 acres a day.

Data Preprocessing

All survey data are transferred using removable media to a field computer for inspection and processing. The analyst initially inspects the files for completeness and data quality. Typically, a low-pass filter is applied to the magnetometer data. This removes the effects of platform-induced directional errors and large-scale geologic interferences.

The primary platform-induced interference is that associated with the rotor hub of the aircraft. The hub assemblies are magnafluxed during overhauls to inspect for stress and fatigue cracks and often are not completely demagnetized following the overhaul. The primary noise appears at 6.5 Hz (corresponding to the 390 rpm fixed rotation rate of the blades) and at 13 Hz. There is also a significant noise spike at 25 Hz, which we believe is associated with a standing-wave vibration of the forward boom assembly. All of these frequencies are significantly above the frequencies associated with UXO targets; therefore we remove them by applying a series of narrow notch filters.

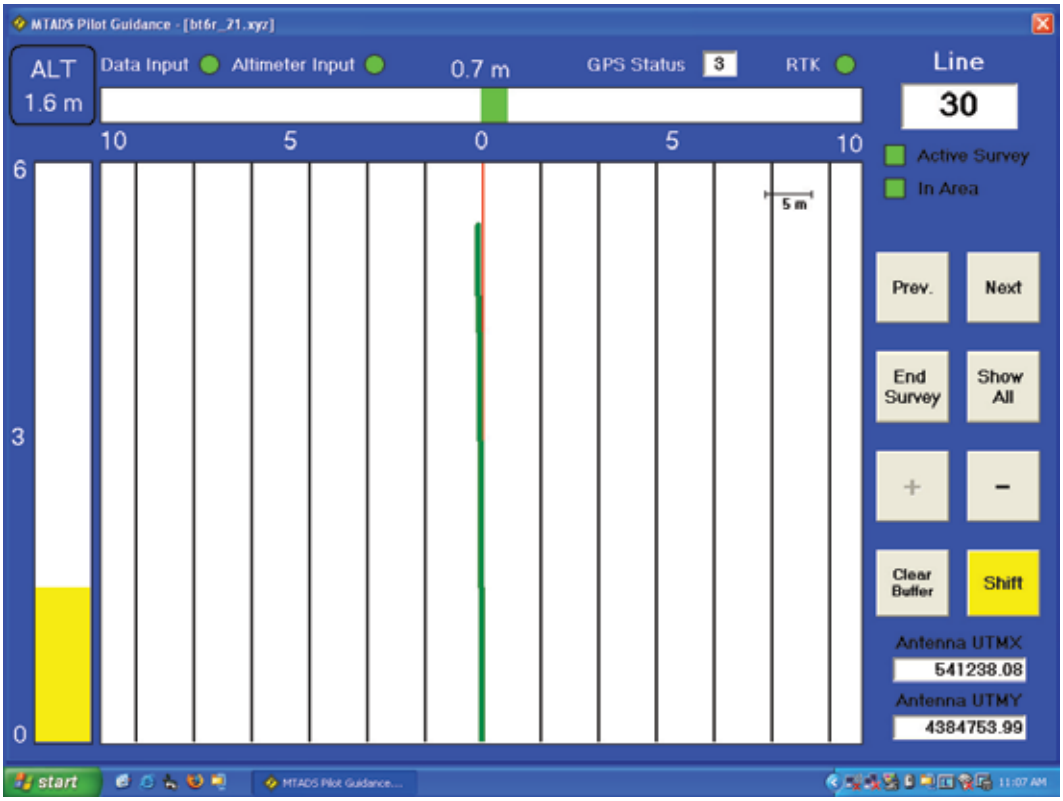

FIGURE 2
Detail of the pilot-guidance display showing the pilot flying up line 30 (highlighted in red) of the preplanned survey. The actual position of the aircraft is plotted in green on the survey grid and an indication of left-right position is shown by the color bar above the map. Altitude (1.6 m, in this case) is indicated by the color bar on the left.

FIGURE 3
Airborne magnetometer array mounted on a Bell LongRanger helicopter performing a geophysical survey.

The final step in data preprocessing is assigning a position to each magnetometer sensor reading. We accomplish this directly by using the measured boom position and orientation. The altitudes derived by this method are relative to the ellipsoid, not the Earth's surface. This has proven inconvenient for two reasons. The analyst needs an estimate of target depth below the surface to assist in classifying detected targets as UXO (which are typically buried) and fins and fragments (which are often at or near the surface). In addition, remediation crews are much more efficient if they have an accurate depth estimate to guide their removal digs, e.g., should they use a shovel or a backhoe to uncover the object. To connect the height-above-ellipsoid values to height-above-ground, we construct a Digital Elevation Model (DEM) using the altimeter readings.

Figure 4 illustrates the main components used to derive a DEM. Two adjacent passes of the array are shown, each at a slightly different elevation and orientation. For each pass, altitude data are collected from the laser altimeter and the three acoustic altimeters (the third is collocated with the laser altimeter under the body of the aircraft). These data allow us to derive a digital elevation model referenced to the ellipsoid and then to reference the estimated target locations in the earth to this ground surface model.

Data Analysis

The preprocessed mapped data files, displayed as a magnetic anomaly image, are given to an analyst for target selection and analysis. Working systematically through the survey data, the analyst visually identifies anomalies that are consistent with compact ferrous objects (i.e., UXO), boxes an appropriate subset of the data, and submits the selected data to a seven-parameter model match routine for estimating magnetic dipole parameters. From the amplitude of the anomaly signal and the spatial extent of the anomaly, an estimate of target depth and size is derived.

An example of this is shown in Fig. 5, which plots an anomaly selected from a survey of the Browns Island Range at Camp Lejeune, North Carolina. The measured survey data are plotted as an interpolated image on the left-hand side of the figure; actual measurement locations are indicated by the dots. We typically collect 50 to a few hundred measurements over each anomaly. These measurements are submitted to the model-match routine, and the results are plotted on the right-hand side of the figure. As can be seen, the agreement is excellent. The modeled data correspond to a target roughly the size of a 500-lb bomb buried 90 cm below the surface. The expected targets on this range are 105-mm projectiles and 500-lb bombs.

DEMONSTRATION RESULTS

Individual Ordnance Detection

The airborne magnetometer system has been tested and demonstrated at a number of prepared and live ranges. Reference 2 provides a complete list of areas surveyed and individual discussions of the findings. The primary objectives of a UXO survey system are:

- detect all UXO;
- predict accurate sizes, locations, and depths to maximize the efficiency of recovery (remove less dirt from each hole) and allow for leaving small, shallow fragments in the field; and
- collect data of sufficient quality to support classification (UXO vs not-UXO) of the detected targets.

For ranges with reasonably low levels of geologic interference containing ordnance larger than a 2.75-in. rocket warhead, the airborne system can meet these objectives. We have demonstrated probabilities of detection (P_D) of 95% or greater for these targets.

Figure 6 shows an example of the target location accuracy of the system. These are data from a survey of Target S1 on the Isleta Pueblo just south of Albuquerque, New Mexico. This was a target used for training high-speed bomber pilots during World War II. The airborne system surveyed ~1,500 acres centered on the bombing target, and the vehicular system covered the center 150 acres for validation purposes. Two areas away from the target were selected for remediation and more than 300 targets were dug in each area. Data from the central area are shown in Fig. 6. The left-hand panel shows the difference between the predicted position and the actual, measured position of the target plotted on a polar plot. Most of the targets were located within 0.5 m, and there is no obvious directional bias of the predicted position. The miss distance is quantified in the right-hand panel as a histogram. The mean miss distance was just under 50 cm, and 90% of the targets were within 90 cm of the prediction. The Isleta site provided more challenging geology than typical, and P_Ds were in the range of 65%.

Wide Area Detection

When used in the Wide Area Detection role envisioned by the DSB task force, the goal is locating targets on a large range and, by extension, areas that are free of UXO contamination; detecting individual anomalies is less important. In this case, we are looking for concentrations of anomalies with enough resolution to accurately determine the extent of UXO-contaminated

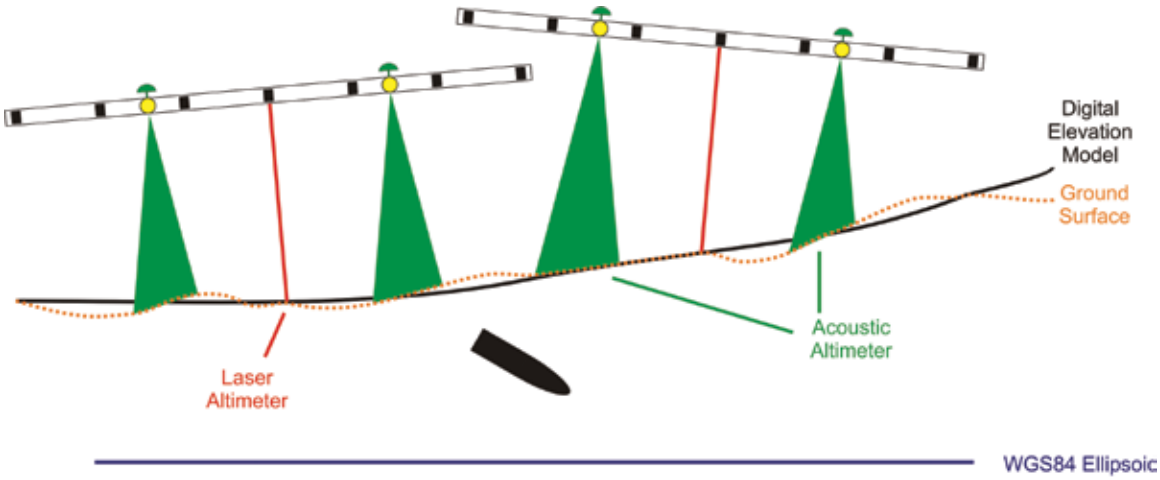

FIGURE 4
Schematic showing the process of deriving a Digital Elevation Model (DEM). The GPS-derived sensor positions are referenced to the Ellipsoid. This is all that is required to locate the UXO, but it has proven difficult for the analyst to judge the reliability of the model match without reference to ground level. Two adjacent passes of the array at slightly different elevations and orientations are shown. The primary altitude measurement is the laser altimeter (red line) but these data are relatively sparse. We supplement these with the acoustic altimeter data to derive the DGM.

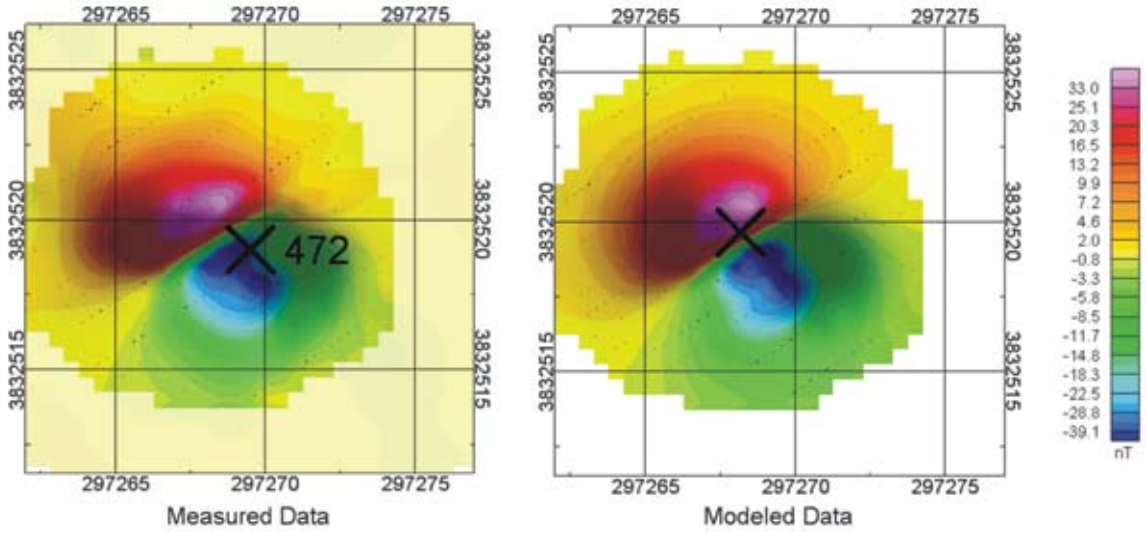

FIGURE 5
Example of measured anomaly data and resulting model-match results. Measured data are on the left and modeled data are on the right. On both plots, the actual measurement locations are indicated by individual dots.

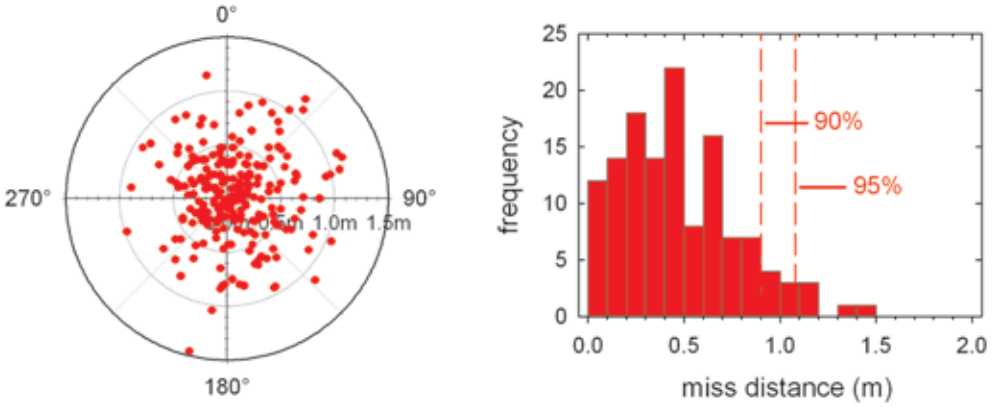

FIGURE 6
Location performance of the airborne system for remediated targets from a survey of Target S1 on Isleta Pueblo, New Mexico. The left-hand plot shows the difference between predicted target positions and actual position plotted on a polar plot. There is no obvious directional bias to the predictions. The right-hand plot is a histogram of miss distance for the 338 targets dug in this demonstration. The mean miss distance is 49 cm; 90% of the predictions are within 90 cm.

areas so that they can be delimited from UXO-free areas.

In the summer of 2005, the Environmental Security Technology Certification Program, with direction from the Congress, conducted a Wide Area Assessment Pilot Program. Demonstrations were conducted at three sites, Pueblo Precision Bombing Range 2 near La Junta, Colorado; former Kirtland Precision Bombing Ranges N1, N3, N4, and New Demolitions in Albuquerque, New Mexico, and Victorville Precision Bombing Range Y near Palm Springs, California. The NRL airborne array was flown by Sky Research, Inc., of Ashland, Oregon as one component of these demonstrations.

Each demonstration site was roughly 5,000 acres. Figure 7 shows data collected on the northern portion of the Kirtland site. Historical records on this site discuss the existence of two practice bombings targets and one target for high-explosive bombs. These targets can be seen in the upper left and lower right corners of the area presented.

Historical records also mention a Simulated Oil Field Target, but the location was not known. Survey data reveal a concentration of anomalies in the middle of the area shown in Fig. 7. The inset is a 15-acre blowup of this area. Hundreds of individual magnetic anomalies are in this area, indicating that this is likely the position of the unlocated target. Intrusive investigations carried out in the spring of 2006 confirmed this assignment.

A close analysis of the data in Fig. 7 reveals additional detail. The target in the northwest corner of the site is obviously composed of a primary, central target with several smaller target areas surrounding the central region. This is an example of the resolution required to precisely bound the edges of targets and return as much land as possible to productive use.

SUMMARY

We have designed, constructed, and demonstrated a helicopter-borne magnetometer array for the detecting buried UXO. The system has proven to be useful for both detecting and accurately locating individual UXO items the size of 2.75-in. warheads and larger and for detecting and bounding target areas on large ranges. This highly successful system will be an integral part of any national assessment of UXO contamination on Closed, Transferred, and Transferring Ranges.

ACKNOWLEDGMENTS

The authors thank Mr. David Wright and Dr. Nagi Khadr of AETC, Inc., for assistance in the design of the hardware and analysis routines, respectively.

[Sponsored by ESTCP]

References

[1] Office of the Under Secretary of Defense for Acquisition, Technology, and Logistics, Washington, D.C. 20301-3140, "Report of the Defense Science Board Task Force on Unexploded Ordnance," December 2003, http://www.acq.osd.mil/dsb/uxo.pdf.

[2] H.H. Nelson, J.R. McDonald, and D. Wright, "Airborne UXO Surveys Using the MTADS," NRL/MR/6110--05-8874, April 5, 2005.

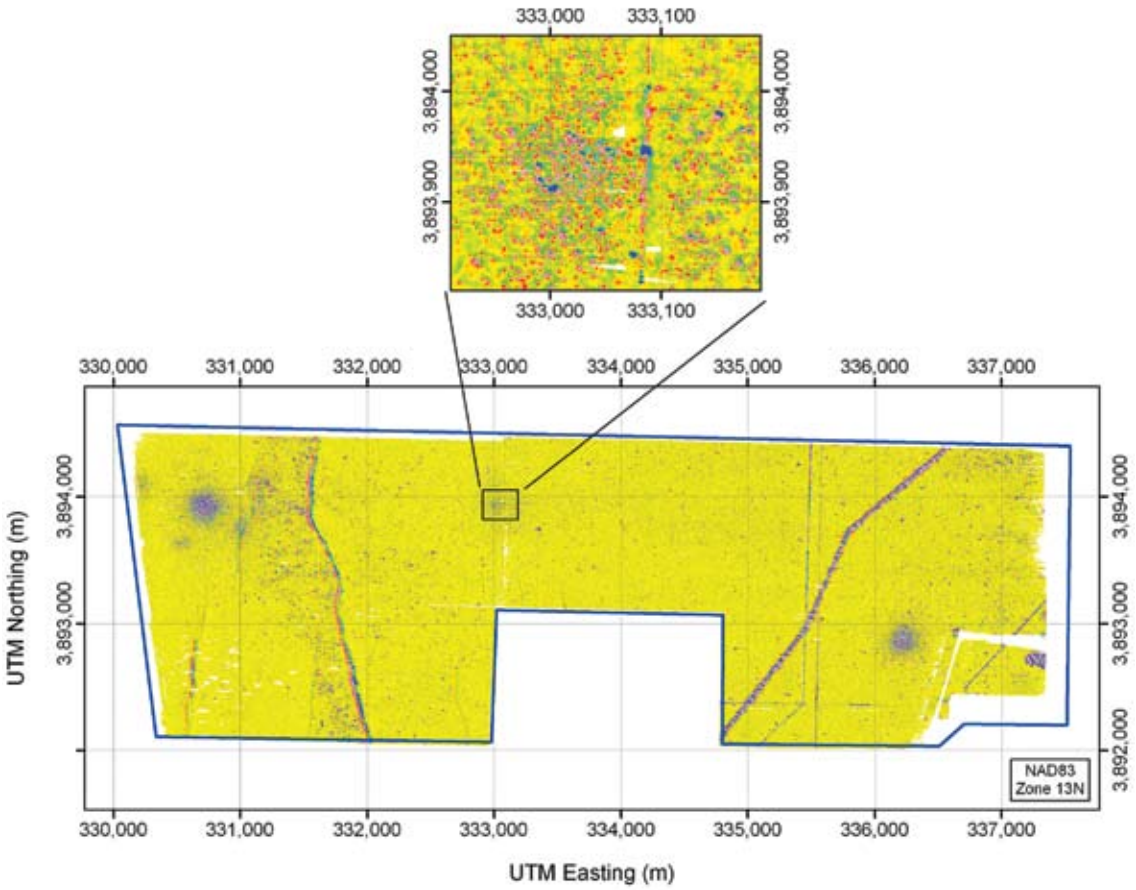

FIGURE 7
Survey results from the northern section of former Kirtland Targets N1, N3, N4, and New Demolitions Area. The historical documents for this site discussed a Simulated Oil Field Target but the position was not known. The inset is a blow-up of a 15-acre portion of the site and shows the large number of UXO targets discovered. This established the location of the Simulated Oil Field Target.

QuadGard Arm and Leg Protection Against IED's

P. Matic,[1] G.K. Hubler,[1] J.A. Sprague,[1] K.E. Simmonds,[1] N.L. Rupert,[2] R.S. Bruno,[2] J.J. Frost,[3] D.H. Branson,[4] C. Farr,[4] and S. Peksoz[4]
[1]*Materials Science and Technology Division*
[2]*Army Research Laboratory*
[3]*FS Technology, LLC*
[4]*Oklahoma State University*

The Naval Research Laboratory (NRL) led a government-university-industry team that developed the "QuadGard" arm and leg body armor from initial concept to industrial production over a period of 17 months. QuadGard provides extremity protection against fragments from conventional munitions and improvised explosive devices (IED's) in an innovative flexible design, based on combat casualty trends. Weighing only 10 lb, it achieved a high level of acceptance during test and evaluation by warfighters for its flexibility and comfort. The first three design phases were performed under an Office of Naval Research program, from April to December 2004. The final design phase and preparation for production was performed for the Marine Corps Systems Command (MCSC) in the spring of 2005. More than 4800 sets of QuadGard were then procured by MCSC for use by 50-caliber turret gunners and shipped forward for operations in Iraq between October 2005 and January 2006. An additional 300 sets were purchased by the Joint IED Defeat Task Force. These were delivered in November and December 2005 for test, evaluation, and operational use in Iraq by additional Marine Corps, Army, and Air Force units. Finally, 100 sets were purchased by the Naval Facilities Expeditionary Logistics Center in January 2006 for the Navy's Seabees in Iraq.

INTRODUCTION

Improvised explosive devices (IED's), such as those in Iraq, are a challenging threat to U.S. military forces. These blast weapons, often rigged to detonate conventional munitions such as artillery shells, have caused fatalities and severe injuries to Marines and soldiers. The introduction of the outer tactical vest (OTV) with soft armor to protect the upper torso against fragments, along with the ceramic small arms protective insert (SAPI) plates, has shifted the injury patterns sustained by Marines and soldiers. The superb effectiveness of this armor protects soldiers who would otherwise have received fatal wounds to the chest, but produces significant numbers of casualties with arm and leg injuries. Now, as a result of this trend, one quarter of all injuries incurred affect the arms and one third affect the legs. Limb amputation rates have been more than twice as common as in previous conflicts. New lightweight and flexible limb protection options were needed for the Marines and soldiers.

After visiting amputees at Walter Reed Army Medical Center in late 2003, Secretary of the Navy Gordon England asked the Office of Naval Research (ONR) to assess the situation and develop new protective equipment options for the Marines in Iraq. The assignment was handed to the Naval Research Laboratory's Materials Science and Component Technology Directorate (Code 6000) in early 2004. NRL applied its expertise in materials and the biomechanics of blast injuries to understand the unique aspects of the IED problem. By April 2004, it had formulated a strategy for a rapid response program to develop extremity armor. A multidisciplinary team was organized that consisted of NRL as program lead, the U.S. Army Research Laboratory (ARL) Weapons and Materials Research Directorate, the ARL Human Research and Engineering Directorate, FS Technology, LLC (FST), and the Oklahoma State University (OSU) Design, Housing and Merchandising Department. ARL was particularly helpful in identifying team members who possessed world-class expertise. Each team member had primary responsibilities, listed in Table 1, while at the same time contributing to and supporting each task.

The QuadGard team was then funded by ONR to design, prototype, and test the system. Follow-on funding from the Marine Corps turned the prototypes into production items that were shipped to Iraq. The time from initial design to initial shipments for operational use in Iraq covered a period of 17 months. This article describes the development of the QuadGard extremity armor system.

TABLE 1 — Major Tasks and Primary Responsibilities of the QuadGard Multidisciplinary Development Team

Expertise	Institute
Program coordination	NRL
Medical assessment	NRL
Threat assessment	NRL, ARL
Ballistic materials performance	ARL, FST
Extremity armor objectives	NRL
Extremity armor design	OSU, FST
Prototype design and fabrication	OSU, FST
Human factors assessment	ARL
Warfighter feedback	ARL, NRL
Transition to production	FST, OSU

DESIGN PHILOSOPHY

Arm and leg armor in the form of gauntlets for the arms and greaves for the lower legs has been used for thousands of years to protect against low velocity penetrating and blunt trauma. These were constructed from wood, leather, and bronze, culminating in the use of iron and steel by Asian and European armies in the Middle Ages. Body armor disappeared at the end of the Renaissance when rifles and artillery were introduced to the battlefield.[1]

Perhaps the first practical reappearance and use of modern body armor against higher velocity fragments was the "flak jacket" issued to aircraft crews during World War II. The use of fragment protection vests was extended to Marines and soldiers on the ground in Korea and Vietnam. The current OTV was issued in large numbers during the late 1990s, and its first widespread use in combat has been in Afghanistan and Iraq. The OTV is made of Kevlar and it provides blast fragment protection to the upper torso. The OTV with the addition of front and back ceramic SAPI plates provide protection against small arms fire using full metal jacket ammunition, such as used in the AK-47 rifle.

The convergence of the IED blast weapon threat, modern materials technology, and modern military medicine on today's battlefield has effectively reopened the possibility, for the first time in 400 years, of a full body armor ensemble to protect the torso, arms, and legs of today's warfighter.

The Challenge of Minimizing Added Weight

The IED threat is ever-present for the Marines and soldiers conducting ground operations, and it can come from any direction. Therefore, 360-deg protection for the extremities is highly desirable. A Marine is also already burdened with the weight of his body armor, helmet, weapon, ammunition clips, grenades, water, first-aid kit, pistol, knife, radio, extra batteries, and more, depending on the mission and function of his unit. This often amounts to a minimum load of 45 lb, although it can often increase to between 75 and 100 lb. Therefore, any armor for the arms and legs must be very lightweight. From preliminary estimates of weight, level of protection, and flexibility from available ballistic protection materials technologies, 10 lb of additional weight for arm and leg armor appeared to be acceptable and was adopted as a design goal.

Determining the Area of Coverage

To assess the relative vulnerability of different areas on the arms and legs, medical personnel were consulted from Walter Reed Army Medical Center in Washington, DC, the National Naval Medical Center in Bethesda, Maryland, and the Naval Medical Center in Portsmouth, Virginia. Together, their combat casualty care experience ranged from initial stabilization of casualties on the front lines in Iraq, to hospitals in Kuwait and Germany, and to long-term hospital treatment and rehabilitation back in the United States. They provided an early and unique perspective on the emerging casualty trends that was invaluable in the QuadGard design process.

In addition to these in-depth discussions, all available data on combat casualties from Operation Iraqi Freedom (OIF) and from Operation Enduring Freedom (OEF) in Afghanistan were reviewed for trends relevant to the armor design. Information was also obtained from the Naval Health Research Center, ONR-Human Systems Science and Technology Department; the United States Army Institute for Surgical Research; the Armed Forces Institute of Pathology; the Army Research Laboratory, Aberdeen Test Center (ATC); and others.

As might be anticipated, injuries to the extremities tracks quite well with the projected area of the extremities and constitute 60 to 65% of the debilitating injuries. Contained within the details of these gross percentages, however, were a number of valuable lessons learned from both the combat casualty care communities and the data analyses. The following design guidelines were generated from these lessons: protection against smaller fragments is both possible and valuable; protect the vulnerable areas where nerve and vascular bundles are concentrated and near the surface (i.e., behind the knee, inside the elbow, around the shoulder, under the arm); protect joints where prognosis for full recovery from injury is poor (i.e., knees, elbows, hips); protect the sciatic nerve in the lower back and buttocks (which is essential for leg function); protect the femoral arteries in the lower abdomen; and use "shadowing" by the armor on exterior surfaces to shield interior surfaces left uncovered

for flexibility and comfort (such as inside surfaces of the upper arm, the torso under the upper arm, and the upper leg to facilitate major sweat gland ventilation and comfort).

Selecting a Level of Ballistic Protection

Determining the level of ballistic protection is the most challenging part of limb armor design. There is no definitive model to predict the injury level or severity caused by a fragment of a given size and strike velocity. There also is no definitive model that predicts the ballistic performance of soft armor, where the problem is complicated by the lack of high shear rate mechanical property data, fabric denier effects, and fiber-to-fiber interactions that are difficult to model. Therefore, quantitative methods to predict the effect of arm and leg body armor on blast injury severity from the IED threat do not currently exist.

Information on the blast-weapon and IED threat was assessed from background information provided by ARL, ATC, the Navy explosive ordnance disposal community, National Ground Intelligence Center, and OIF and OEF briefs. Many types of devices and methods are used against the Marines and soldiers in OIF and OEF, and no "typical" IED exists.

The general consensus from these sources was that IED's were based on conventional munitions such as artillery shells. These were generally devices of varying explosive yield deployed in nonoptimal fashion (e.g., buried in the ground or positioned above the ground in nonoptimal orientations). The IED designs evolve over time to use available materials and current operational tactics employed by the insurgent forces. The lethal radius of these devices for persons without armor is estimated to be from 10's to 100's of feet.

Although IED's can generate larger fragments, smaller fragments often dominate the fragment yield. Conventional artillery munitions produced by NATO or Warsaw Pact sources generate large numbers of 100 to 250-mg engineered fragments. IED's are often augmented with nails, washers, and bolts. Grenades and antipersonnel mortars also generate relatively small fragments. Gravel and sand are also entrained by blast weapons, and become part of the fragment yield. These smaller fragments are aerodynamically inefficient, meaning their velocity drops rapidly over a shorter distance from the blast and they are less effective as penetrators of body armor.

Consistent with the recommendations from combat casualty care communities and practical concerns about added weight, the QuadGard design focused on stopping the smaller fragments with soft armor at a level of protection slightly below that of the soft OTV. Standards developed by the National Institute of Justice (NIJ)[3] were used to quantify the level of protection during the materials selection process, prior to testing using Marine Corps production testing standards. This level of protection is both medically relevant, meets the 10-lb weight limit, and allows full coverage of all limbs and joints. Design options at higher levels of protection were also examined to match 100% of the OTV level of protection, with the same area of coverage. This was done for comparative purposes and future options, with a projected total weight of under 15 lb.

Designing for Human Factors and Warfighter Acceptance

In addition to considerations of coverage, ballistic protection level, and weight, the "human factors" that govern warfighter acceptance and use are just as important as physical performance of the armor. Armor is not useful if a Marine or soldier does not wear it. Conversely, a high rate of acceptance maximizes the potential range of uses in the field. By paying special attention to flexibility, mobility, heat management, appearance, and overall comfort, the QuadGard design has tried to maximize acceptance and use by Marines and soldiers. Table 2 summarizes key design objectives and solutions.

Based on the above considerations, the QuadGard design that evolved covers most of the arms and shoulders, while the pants cover the entire lower torso beneath the OTV, the hips, the buttocks, and the legs. The decision was made to design QuadGard to be compatible with the groin protector currently issued to all Marines and soldiers as part of their OTV ensemble.

Figure 1 shows features of the QuadGard arms. The arms are attached to the OTV by using three straps, one of which connects the arms together across the back. The arm length is adjustable up and down to ensure that the flexible elbow joint is aligned properly with the wearer's elbow. The arms are open along the inside of the upper arm for ventilation and do not impede arm motion in any way, while maintaining 360-deg armor protection around the elbow. Velcro straps at the cuff allow expansion of the sleeve circumference for donning and for increased ventilation when needed. Shoulder pads protect the shoulder joints. The lower arm portion resembles ancient Roman gauntlets.

The QuadGard legs are actually pants held up by suspenders that cover most of the lower torso, buttocks, hips, and legs (Fig. 2). The unique knee design covers the back of the knee, with a hinged flap of the armor material attached to the pants above and below the knee joint. In the standing position, the flap covers a small area behind the knee designed without armor to make the knee joint flexible. When the knee flexes, the flap folds, slides down the calf, and allows a

TABLE 2 — The QuadGard Design was Based on a Set of Key Objectives and Solution Strategies that Balanced Weight, Ballistic Protection, Flexibility, and Comfort

Functional Parameters	Design Strategy
Area of coverage	Cover medically vulnerable areas
Level of protection	Small fragments at moderate velocity
Thermal management	Segmented and vented design
Weight	10 lb maximum (<OTV with SAPI plates)
Comfort	OTV attachments and suspenders
Flexibility	Innovative elbow and knee joints
Mobility	Consistent with dismounted activities
Appearance	Consistent with warfighter image
Compatability	Helmet, OTV, weapon, equipment
Environmental durability	Comparable to OTV
Cost	Comparable to OTV w/SAPI plate

(a) Front view (b) Back view

FIGURE 1
QuadGard arms attached to the Outer Tactical Vest.

(a) Front view (b) Back view

FIGURE 2
QuadGard pants.

complete crouch by the wearer. Nonballistic kneepads protect the knee from bumps.

Zippers along the outside of the legs open from either the top or bottom for ventilation and as an aid in donning and doffing the pants. Flaps at each hip can be folded open for maximum ventilation or fastened down with Velcro straps for maximum protection. The design of the flaps allows ready access to the Marine's side pockets on his combat utilities worn under the QuadGard pants. A carry strap was included at belt level on the rear of the pants for rescue and evaluation. The QuadGard armor is shipped with wicking undershirts that have been proven to increase the comfort of the OTV in hot weather.

Operational Benefits and Uses

In operational terms, the QuadGard extremity body armor provides ballistic protection that can increase nonlethal and safe operating areas around an IED by reducing these minimum standoff distances from the warfighter to the device. An associated reduction in injury severity can mean quicker return to duty for relatively minor injuries (e.g., hours or days instead of weeks), reduced time need for intensive medical treatment and rehabilitation for severe injuries (e.g., weeks instead of months), or the difference between injuries producing or not producing fatalities, amputation, or disability.

Potential operational uses of QuadGard were gleaned from discussions and feedback with warfighter communities in the Marine Corps, Army, and Navy. These include

- vehicle occupants/convoy crews,
- sentry and checkpoint duty,
- security and support operations,
- roadside patrols,
- explosive ordnance reconnaissance,
- forward-deployed medical personnel,
- military operations in urban terrain,
- combat engineers, and
- aircraft crews and passengers.

Although ballistic protection was the primary goal, additional secondary benefits of QuadGard were identified as protection against blunt trauma from direct exposure to blast pressure waves, and protection against flash burns beyond that provided by the blouse and trousers of the standard combat utility uniform.

BALLISTIC MATERIALS TESTING AND PERFORMANCE

The selection of a lightweight, soft ballistic material system to provide fragment protection was based on the ballistic testing of a series of candidate material systems. Candidate systems were chosen from experience with the newer commercially available products having the best potential for increased performance, on a unit weight basis, over the ballistic materials currently used in protective equipment. Sixteen different ballistic material combinations, including both homogenous and hybrid systems, were tested at ATC according to Marine Corps production standards. The monolithic materials were found to perform better than the hybrid systems. The material systems are tested using standard 18 × 18-in. square shoot packs, freely suspended on the ballistic test range, subjected to multiple impacts in a specified geometric pattern. Steel right circular cylinders of 2-, 4-, 16- and 64-grain weights, and 9-mm 124-grain full metal jacket (FMJ) ammunition were used to evaluate candidate armor material performance. V_{50} testing is used to determine level of ballistic performance where V_{50} is defined as the velocity at which 50% of the projectiles are stopped and 50% penetrate the armor. The specification requires that the statistics of the measured spread in V_{50} velocities not exceed a specified small value for the test to be valid.

The ballistic material system found to provide the best desired ballistic performance, by weight, was unidirectional DSM Dyneema in a cross-ply lay-up. Dyneema is a relatively new product that consists of high molecular weight polyethylene fibers in a flexible fabric. It has demonstrated 20% improvement in ballistic performance by weight compared to Kevlar, a fact that is very useful for body armor applications. It is also more environmentally stable than Kevlar, resistant to environmental factors such as water, chemicals, and ultraviolet radiation.

PROTOTYPE TESTING AND EVALUATION

Using the protection, material, and weight guidelines previously discussed, the design team produced a series of prototypes in four phases through an iterative design cycle. Funding from ONR was received in mid-April 2004 to support a three-phase design effort. In one month, five sets of the Phase I concept design prototypes were produced to demonstrate the essential features of coverage and flexibility.

By the end of July 2004, 20 sets of Phase II prototypes were fabricated and feedback was being obtained from Marines, Army, and Navy warfighter communities who provided feedback on wearability, flexibility, and comfort. ARL also conducted static exercises to assess range of motion, ease of movement, and overall compatibility with the basic fighting load ensemble including the OTV (with groin and neck protectors), helmet, and rifle while wearing the QuadGard system. The static exercises included arm and leg movements, various standard rifle firing postures, climbing, and a

short distance run. No major problems were identified related to the QuadGard system. A number of recommendations for functional refinements and improvements were noted and implemented during the next design iteration.

By December 2004, 20 sets of Phase III prototypes were completed and ready for ARL evaluations using static exercises; the 500-m "known distance" mobility/portability obstacle, also known as the KD-range; and the small arms firing range, also known as M-range, both at ATC. Figure 3 is a collage of photographs showing QuadGard undergoing testing on the ATC ranges.

The KD-range consists of an open course interrupted by a series of obstacles designed to measure essential physical performance skills associated with a combat environment. The course consists of 20 individual obstacles spread over a twisting course of about 500 m. The course requires the participants to perform maneuvers that test their running, jumping, climbing, crawling, and balancing skills, and their ability to negotiate buildings, stairs, and windows. Incompatabilities between new equipment and existing equipment or weapons will be most evident during obstacle course runs. The time to run the course was measured. When weight and bulk is worn or carried, especially by the lower extremities, course completion time increases and performance degrades. When QuadGard is added to the base system of the OTV, helmet, and rifle, the time to complete the course increased by 34%. This performance falls in the range expected for the added weight according to data taken for many studies of various types of equipment on the KD-range.

The M-range is a fully instrumented and automated facility to assess individual marksmanship performance. Participants fired a commonly zeroed M4 carbine and M240 machine gun, with and without the QuadGard limb protection system, while wearing the OTV and helmet. Eighteen targets appeared in a random sequence, at ranges from 50 to 300 m, to the participant who fired in semiautomatic mode. Participants used the foxhole supported, basic prone unsupported, kneeling unsupported, and standing firing positions. The participants said they were comfortable wearing the QuadGard system while firing their weapons, and no compatibility issues were identified. Target scoring with QuadGard was consistent or slightly better than without QuadGard. One expert marksman noted that the QuadGard system provided more support and was more comfortable than his personal shooting jacket.

Questionnaires were filled out by the participants to solicit their ratings, comments, and suggestions on QuadGard features and their ability to perform while wearing the system. The quantitative portion of the questionnaire requested ratings on a numerical scale of 5 = Excellent, 4 = Good, 3 = Acceptable, 2 = Poor, and 1 = Unsatisfactory. An example of results for a group of 17 participants shows that the majority regarded the system fit, task performance, system features, movement, fasteners, and closures as "Acceptable to Good." Figure 4 shows an overall "Good" rating regarding one's ability to move while wearing the system. Figure 5 shows that while concerns about additional heat and bulk of QuadGard were noted by the participants, which were comparable to historical concerns about the OTV and other comparable equipment, the armor is still viewed as comfortable and compatible. Overall, the ratings were exemplary considering the historical trend for body armor evaluations.

The Phase III testing at ARL was instrumental in showing that the QuadGard concept was meeting the design goals and maturing as a system. This generated new interest and support at the Marine Corps Warfighting Laboratory (MCWL), which evaluates new concepts and equipment, and at the Marine Corps Systems Command (MCSC), which develops and procures equipment for the Corps. In early 2005, MCSC initiated support of QuadGard Phase IV development with the goal of a production-ready system. Phase IV incorporated more than 20 improvements and refinements over Phase III that were suggested by the results of testing at ARL. Twenty sets of QuadGard Phase IV were delivered in April 2005. Final testing on the KD-range and M-range began at ARL, with assistance of personnel from the Army's 16th Ordnance Battalion and the Marine Corps Detachment at Aberdeen Test Center.

In early 2005, in parallel to the development effort being conducted for the Marine Corps, the Joint IED Defeat Task Force became interested in evaluating QuadGard along with other arm and leg protection systems. Twenty sets of QuadGard prototypes were provided to the Rapid Equipping Force, who conducted wearability and warfighter acceptance testing for the Task Force between July 2005 and January 2006, with the Army's 14th Engineers at Fort Lewis in Yakima, Washington; with the Marines at the Marine Corps Air/Ground Combat Center in Twentynine Palms, California; and the Air Force 820th Security Forces Group at Moody Air Force Base in Georgia. Figure 6 shows QuadGard Phase IV being worn during training exercises at Twentynine Palms.

In these exercises, QuadGard was evaluated against two other arm and leg protection systems. This testing was consistent with the results of the ARL human factors testing. Participants deemed QuadGard more desirable than two other competing systems. In late 2005, 300 sets of QuadGard were purchased by the Task Force for evaluation and use in Iraq by Army, Marine Corps, and Air Force units.

FIGURE 3
QuadGard testing by Army Research Laboratory at Aberdeen Test Center obstacle course and marksmanship range demonstrates the flexibility of the design and its compatability with existing body armor and infantry equipment.

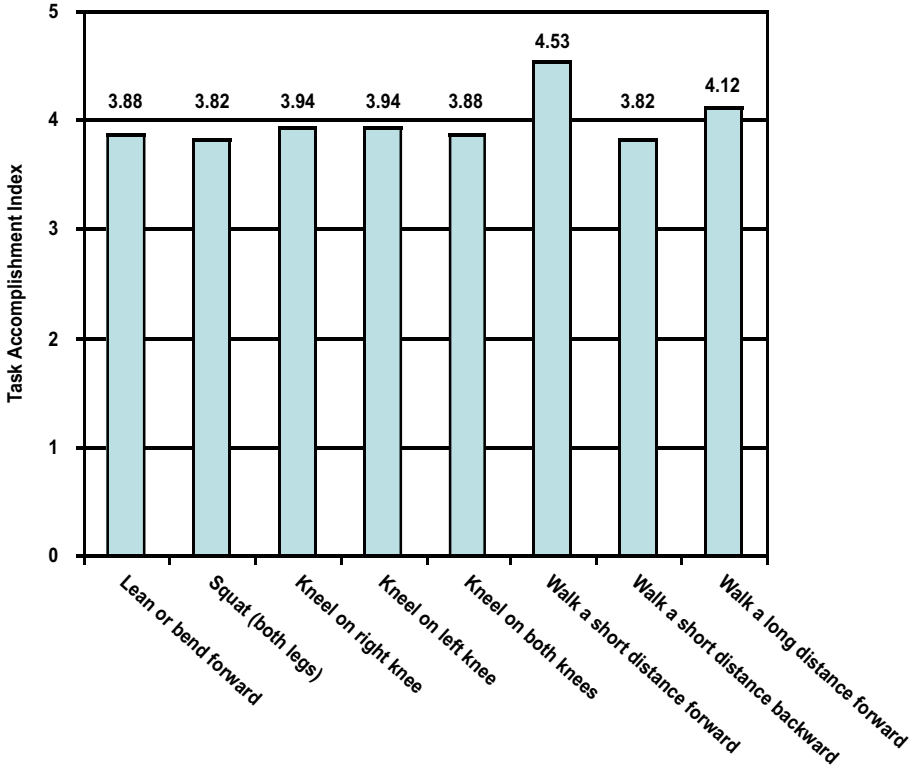

FIGURE 4
QuadGard task accomplishment data, obtained from warfighter testing and evaluation. High scores reflect the flexibility of the QuadGard design and compatability with the OTV, helmet, and rifle.

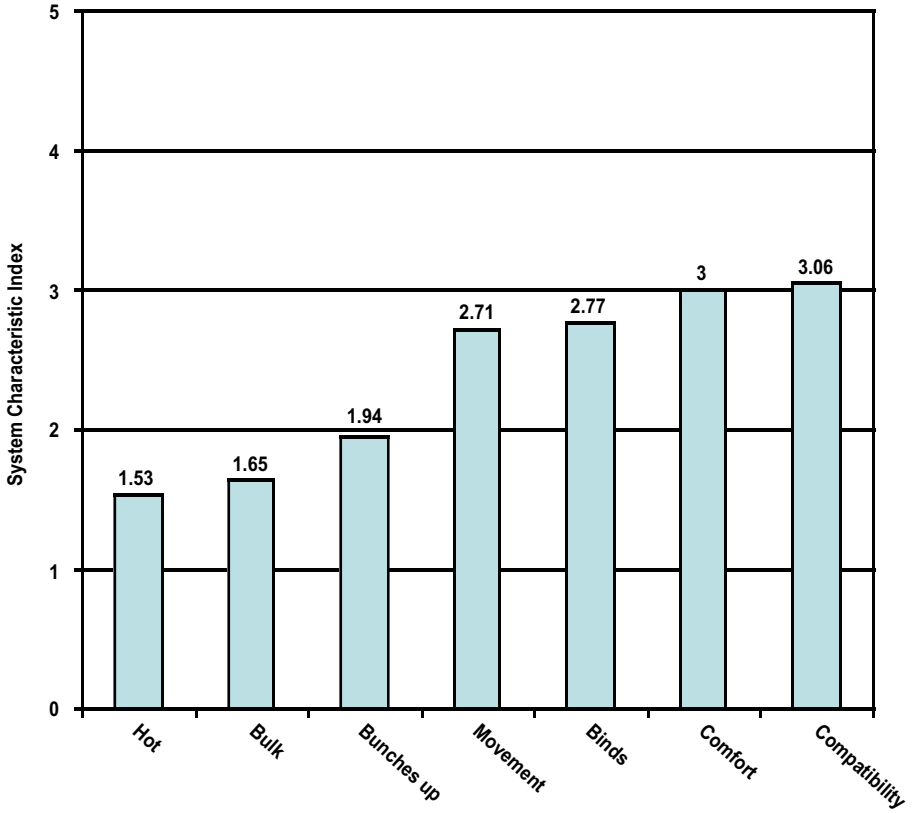

FIGURE 5
QuadGard system characteristics data while under movement, obtained from warfighter testing and evaluation. QuadGard scores are excellent compared to historical values for new body armor. The values show some heat and bulk concerns, but overall satisfaction including comfort and compatability.

FIGURE 6
Testing and evaluation of QuadGard during training exercises by the Marine Corps at the Air/Ground Combat Center in Twentynine Palms, California.

QUADGARD TO IRAQ

In July 2005, the Marine Corps Systems Command received an urgent Universal Needs Statement (UNS) from Iraq for protection for 50-caliber turret gunners. MCSC ran a standard set of more extensive preproduction ballistic tests of the Dyneema material system to certify the level of protection against fragments. MCSC also had independent analyses performed to predict the effect of QuadGard's armor materials and area of coverage on casualties and fatalities. This analysis was conducted using the Casualty Reduction (CASRED) simulation program with a standard set of ballistic fragment characteristics and data closest to the IED threat. The results of the CASRED analysis predict a 35% reduction in casualties and 10% reduction in fatalities. Based on these results, MCSC immediately ordered 4,800 sets of QuadGard for deployment in response to the UNS. The first sets of QuadGard were delivered to the Marines Corps in early October 2005. The order was completed in January 2006.

In August 2005, the Joint IED Defeat Task Force ordered 300 sets of QuadGard Phase IV for use in Iraq by the Army, Marine Corps, and Air Force units. This order was met from production in November and December 2005.

Finally, in December 2005, the Navy Facilities Logistics Center made inquiries about the QuadGard system for Seabee units deployed to Iraq. They purchased 100 sets, which were delivered in January 2006.

SUMMARY

The development effort and progress to date on the QuadGard arm and leg armor for Marines and soldiers covers an integrated effort involving the synthesis of combat casualty trends, blast weapon threats, soft ballistic armor materials, equipment design, human factors, and warfighter feedback into fully functional and accepted equipment. The armor design is lightweight, flexible, compatible with the OTV and other infantry equipment, and provides the needed protection against blast fragments.

The effort went from initial concept to the first delivery, for operations in Iraq, in 17 months. Production runs over the following four months met requests for a total of more than 5,000 sets of QuadGard from the Marine Corps Systems Command, Joint IED Defeat Task Force, and the Naval Facilities Expeditionary Logistics Center. QuadGard is presently manufactured by CoverCraft Industries at their production facilities in Pauls Valley, Oklahoma, and Wichita Falls, Texas. Following the initial costs of transitioning the design to production, the cost of QuadGard is presently $1,520 per set. It is listed under a National Stock Number.

MCSC has funded the QuadGard team for development for a Phase V version that offers added features including modular area of coverage with detachable lower arm and leg segments, removable soft armor packs allowing laundering of the carrier garment, options for increased protection level options in the soft armor packs, and design for quick doffing. Prototypes of QuadGard V have been produced for human factors testing and warfighter feedback in preparation for production.

ACKNOWLEDGMENTS

The authors thank the military participants from the Army Research Laboratory, the Army 16th Ordnance Battalion, and the ARL Marine Corps Detachment for their support in evaluating the QuadGard system as documented in this paper. The authors acknowledge the support received from RADM Jay Cohen of the Office of Naval Research and from Major Wendell Leimbach and Capt. John Gutierrez of the Marine Corps Systems Command.

[Sponsored by MSCS]

References

[1] R.C. Woosnam-Savage and A. Hall, *Brassey's Book of Body Armor* (Brassey's, Dulles, VA, 2001).

[2] Casualty Reduction (CASRED) is a deterministic model that calculates lethal areas for fragmentation weapons engaging personnel targets. For more information see http://www.msrr.army.mil/index.cfm?top_level=ORG_A_1000023&taxonomy=ORG.

[3] The National Institute of Justice (NIJ) Ballistic Standard 0101.04 for testing of ballistic protection materials and vests uses a 124-grain 9-mm bullet. This standard is found at www.ojp.usdoj.gov/nij/welcome.html. The Army and Marine Corps test procedures to determine the V_{50} performance of soft ballistic materials and vests use 2-, 4-, 16-, and 64-grain right circular steel cylinder fragment simulators. ★

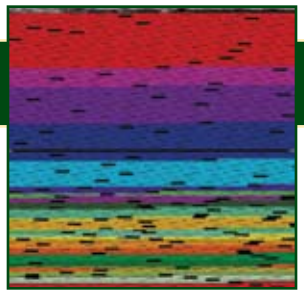

The Silent Guardian Demonstration

F.S. Ligler, J.M. Schnur, A.W. Kusterbeck, C.R. Taitt, L.C. Shriver-Lake, B. Lin, and D.A. Stenger
Center for Bio/Molecular Science and Engineering

From October 2004 through March 2005, the Naval Research Laboratory (NRL) transformed a research protocol for gene-based pathogen identification into a demonstration project called Silent Guardian. Silent Guardian executed a bio-surveillance operation in the Washington, DC, region during the weeks surrounding the 2005 Presidential inauguration. To perform this bio-surveillance, nasal wash specimens were collected from patients presenting with flu-like symptoms at six military clinics in the Military District Washington and taken to NRL for testing. Simultaneous analysis for both common respiratory pathogens and bioterrorism agents was performed 24 hours a day for two months.

The Silent Guardian Demonstration achieved four major objectives:

- Pathogens were unequivocally identified from a general urban population within 24 hours;
- The ability to sequence genes from more than 20 pathogen species was demonstrated in a production mode;
- The capability of moving cutting edge technology from research to production within a six-week period was demonstrated by combined military/civilian teams; and
- A clear path was identified that could lead to an automated, portable, user friendly system.

This is the first documented application of DNA microarray technology to operational, broad-spectrum strain-level pathogen identification in an urban population.

INTRODUCTION

During the winter months, runny noses, fevers, and other flu-like symptoms are common among the general population. After September 11th, 2001, concerns increased over the use of bioterrorist agents, which present clinically with similar symptoms. One approach to surveillance for a bioattack is to monitor for unusual outbreaks of flu-like symptoms. Identification of the causative agent could be subsequently determined by traditional reference methods (usually culture, requiring days to weeks, or a DNA-based identification method known as a polymerase chain reaction or PCR). In the latter, the DNA target or cDNA (DNA copied from RNA targets) is amplified with specific primer pairs. Recently, real-time PCR (using fluorescent signals for real-time monitoring of PCR products) has shown great potential for more rapid pathogen detection. Up to four different targets can be detected simultaneously in one solution by using fluorescent labels of different colors with appropriately configured optical detectors. However, the number of targets that can be measured simultaneously is limited by the number of colors that can be measured simultaneously.

Microarrays provide a means to discriminate among a much higher number of amplified DNA products. In this method, multiple DNA "capture" probes are separated in a geometrically defined manner and capture the different "target" sequences of complementary DNA in a sample. The most commonly used form of microarrays, known as spotted arrays, however, are subject to false positives resulting from cross talk between spots, and they do not provide specific sequence information that leads to strain identification. NRL has designed a "resequencing array" that uses a high density of micron-sized squares with 25-base DNA capture probes (25-mers). The 25-mers represent consecutive regions in 200-500 base-long gene sequences that are characteristic of particular pathogens. By measuring the binding to the capture probes, the sequence of the genes present can be determined and the pathogen and strain identified.

One requirement for using microarrays is that targets must be amplified prior to hybridizing the target DNA to the immobilized capture probes. The methods for amplification include (1) specific PCR and (2) random amplification. In specific PCR, DNA primers with sequences exactly complementary to the ends of the target DNA are used to start the amplification. The reaction is fast, sensitive, and specific. However, the number of specific primers that can be multiplexed may be limited, and specific PCR may not amplify rapidly evolving species because of changes in the gene sequences. Potential complications caused by cross-reactions in the PCR, possibly affecting sensitivity and specificity for all targets, must be examined for each added primer pair in multiplexed assays. This is not a problem in random amplification since *all* DNA molecules in the complex mixture are amplified.

However, with random amplification, each individual target is usually amplified fewer times than would be the case if a specific primer were used. When a random amplification and a microarray are combined, a large amount of "noise" can also appear on the array. NRL invented a bioinformatics analysis method to distinguish the sequence and prevent the background noise from producing spurious sequence reads.[1] However, the noise can still interfere with the ability of small amounts of pathogen target to produce a hybridization pattern that is visible above the background, thereby reducing the sensitivity of the assay. Therefore, random amplification is particularly valuable for identifying rapidly evolving species, while specific amplification excels for detecting previously identified species—even at vanishingly low concentrations.

The Respiratory Pathogen Microarray (RPM v.1) used in this project is a custom designed resequencing microarray. It was designed by the Naval Research Laboratory and manufactured by Affymetrix (Santa Clara, California). The RPM v.1 was intended for the detection of common respiratory pathogens (especially Adenovirus, Influenza A/B viruses, and *Streptococcus pyogenes*) encountered in the military training populations (Fig. 1). In addition, the RPM v.1 chips have regions specific for several Centers for Disease Control Category A biothreat pathogens: *B. anthracis* (three regions), Variola major virus (two regions), Ebola virus (one region), Lassa fever virus (one region), *F. tularensis* (two regions), and *Y. pestis* (two regions).

SILENT GUARDIAN DEMONSTRATION

The Silent Guardian Demonstration Project was initiated in October 2004 according to instructions from the Assistant to the Secretary of Defense Dale Klein and Deputy Assistant to the Secretary of Defense Klaus O. Schafer. The demonstration required NRL to transition the bench-top laboratory protocol for individual clinical samples into an "assembly-line process suitable for implementation." The goal was for the laboratory to have minimal capability within three weeks of receiving initial funds and to be at full operational capability within 10 weeks, including all reagents and equipment needed to process 10,000 samples on site. An entire laboratory infrastructure with supporting Laboratory Information Management System (LIMS), Quality Control/Quality Assurance (QA/QC) measures, biosafety issues addressed for Biosafety Level 2, and a biothreat contingency protocol (in the event of a positive assay) were rapidly designed and implemented to enable this schedule. Implementation involved recruitment of skilled Department of Defense management and technical personnel, facility modification, protocol development, and training of all staff. After these tasks were completed, patient specimens provided by six military treatment facilities (MTFs) located throughout the Military District of Washington were transferred to NRL for analysis and the results reported to the Air Force Medical Service COHORT electronic surveillance system, a database developed and maintained by the Air Force Surgeon General's Office. NRL hosted more than 40 active duty Air Force and Navy personnel and provided technical support to implement and operate a central laboratory capable of processing more than 300 clinical specimens per day with laboratory practices consistent with those prescribed by the College of American Pathologists. Meeting these objectives imposed major new requirements for biochemical processing of clinical samples, bioinformatics, and supporting information technology (IT). All five laboratories were minimally operational within three weeks, with one complete processing line for the chips in place.

Prior to the start of Silent Guardian, specimen analysis consisted of a single technician running 1-20 samples over 2 days from start to finish. To process the projected 300 specimens/day (with a surge capacity to 450 samples/day), an assembly-line type of operation was established at NRL, operating 24 hours a day, 7 days a week. Laboratory staffing comprised NRL staff (Code 6900 and Code 6100), active duty Air Force staff, NRL contractors, and Navy reservists. The protocol was divided into four operations: receiving/nucleic acid extraction, RNA/DNA processing and amplification, chip hybridization, and data acquisition/analysis, performed in five rooms designated as Labs A-D. Figure 1 shows a flow chart of the protocol and photographs from each room.

The IT systems posed one of the biggest challenges. The Silent Guardian Demonstration required the development of a system to track all samples, from patient through analysis and storage, while maintaining confidentiality and chain of custody. At the time of sample collection, volunteer donors completed a questionnaire that was then entered by MTF personnel into the COHORT system. COHORT notified NRL of arriving samples. The NRL Laboratory Information Management System (LIMS) system then tracked each sample through Labs A, B, and C based on scans of the bar code on each sample tube. In addition, the high-resolution DNA microarray chips produced photolithographically by Affymetrix, Inc., were separately barcoded so that the microarray images could be associated in LIMS with information from the procedure. When the procedure was complete, the image was automatically evaluated to read the gene sequences off the chip and identify the pathogen based on best fit to sequences in the public gene sequence database, GenBank. The final pathogen identification was checked by a senior staff member (notified of a positive result by a beeper) prior to release to COHORT.

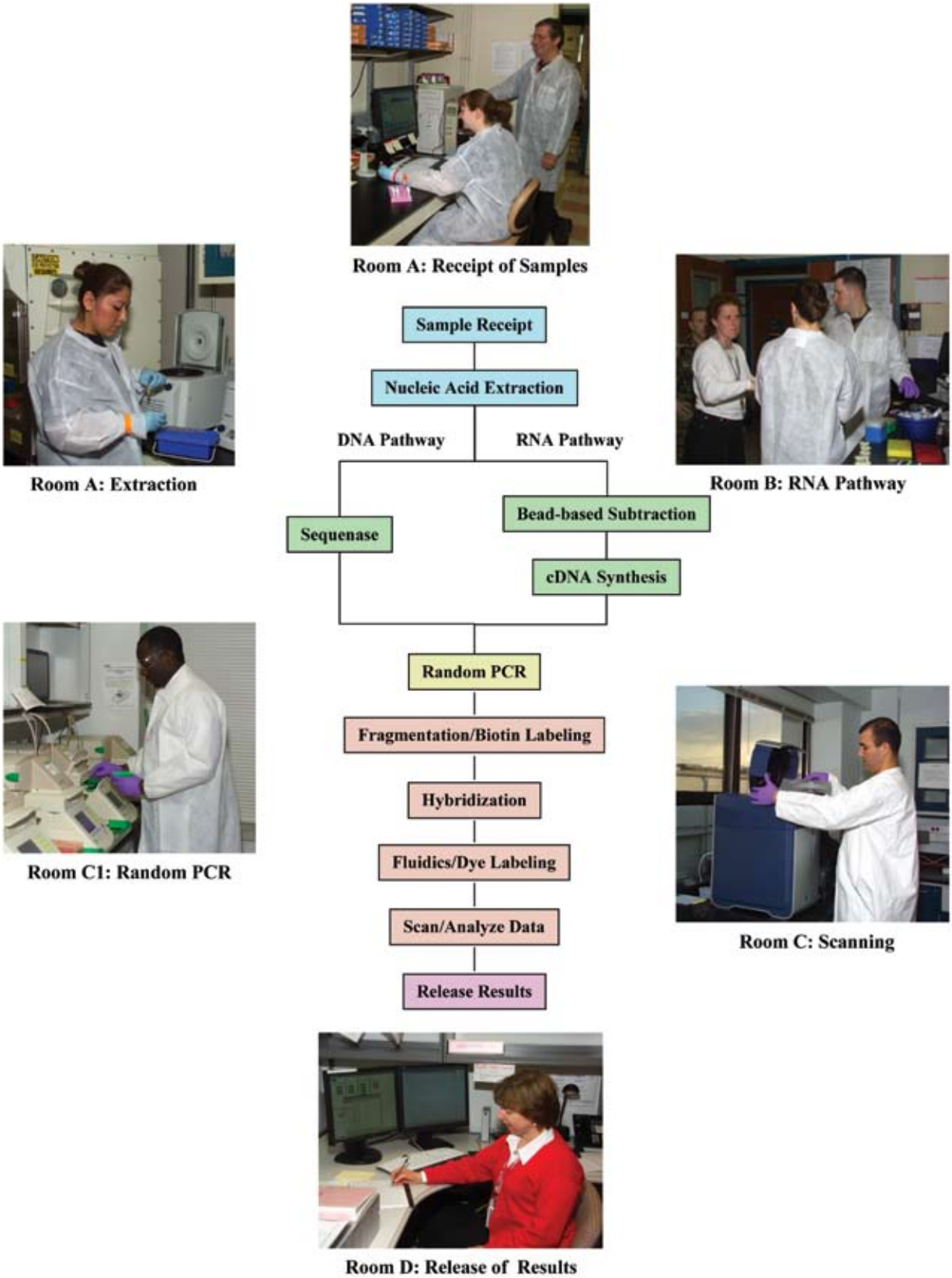

FIGURE 1
The Silent Guardian Standard Protocol. The major steps involved in pathogen identification are diagrammed in the center. Photographs from the five laboratories used in the protocol are shown.

RPM V.1 SAMPLE PROCESSING AND ANALYSIS

Each nasal wash aliquot was subjected to total nucleic acid extraction (Lab A), isolation of pathogen RNA (and conversion to cDNA) and DNA (Lab B), amplification (Lab C1), and microarray hybridization and image analysis (Lab C). Figure 2 shows false color and real images of the microarray chip after hybridization. The false color is used to identify regions on the chip for each pathogen.

Prior to amplification (Lab C1), each sample was split; half of each sample was carried through the rest of the analysis using the random amplification protocol as the standard protocol; the remaining split was frozen for later analysis using a different primer mix. Random amplification without removal of human DNA, prevalent in nasal wash samples, resulted in an increase in background noise. To improve sensitivity, specific primers were added to the unused split for more efficient amplification. Two groups of specific primers were used: UberMix (for all regions on the chip) and BTA (for bioterrorism agents, Adenovirus and Influenza). Use of these "splits" enabled direct comparisons between results obtained with the different amplification protocols.

A rigid set of criteria was imposed for a result to be released to COHORT and thereto back to the MTFs. For a "negative" result to be released, two positive controls, added prior to processing, were required to produce hybridization signals on their respective tiles. Thus, any sample producing a positive pathogen response and/or two positive controls was released to COHORT. If the sample was negative for both pathogen and at least one control, a duplicate aliquot was thawed and reanalyzed.

PATIENT RESULTS

Patient samples were collected at six Military District Washington MTFs from both Emergency Department and clinic settings. Adult patients (active duty

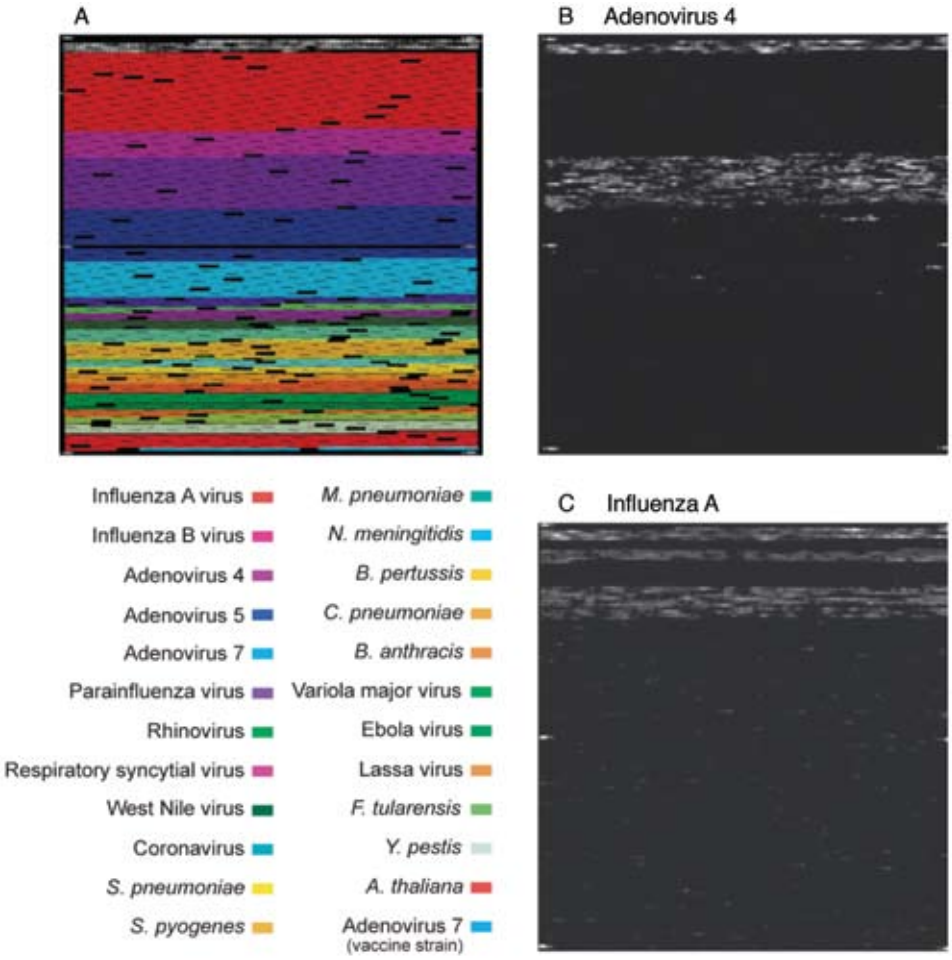

FIGURE 2
Images of RPM v.1 microarray. Panel A is a false color image showing the regions of the chip for different pathogens. Panels B and C are images of a sample positive for Adenovirus 4 and Influenza A, respectively.

military, retired military, and their families) who had a temperature >100.4 deg Fahrenheit and any flu-related symptom(s) could provide consent and donate sample. After the study, individual symptoms were compared to culture and microarray results; there was no statistical correlation between pathogen identity and any individual symptom. This confirms the requirement for a diagnostic test to differentiate between pathogens causing flu-like symptoms.

A total of 565 patients met all study criteria and donated nasal wash; 33 also donated nasal swabs. Samples were tested using the standard random amplification protocol, and the results reported to COHORT. Of these samples, 450 were sent to Naval Health Research Center (NHRC) for culture and PCR characterizations. Hard-to-culture pathogens of interest (Coronavirus, *Mycoplasma pneumoniae*, *Chlamydia pneumoniae*, and *Bordetella pertussis*) were characterized using PCR.

In addition to the results obtained from the standard protocol, further experiments were performed on a subset to examine other modifications. First, 464 replicate patient samples were amplified by multiplex PCR using a specific primer cocktail (UberMix) rather than random amplification. A second set of experiments involved re-analysis of sequence calls using a "relaxed" algorithm in which targets were identified by associating the top sequence similarity ranking instead of satisfying an arbitrary value for goodness of fit. Table 1 show the collective number of positive results obtained using culture, standard protocol (random amplification), the "relaxed criteria" for the sequence calls in the standard protocols, and "relaxed criteria" multiplexed PCR (UberMix). As seen in this table, culture successfully detected Influenza A, Influenza B, *S. pneumoniae* and *S. pyogenes* (Group A Strep), and some Adenovirus from nasal wash specimens. Coronavirus is very difficult to culture; therefore, the positives were determined by PCR. Influenza (A and B) virus was the most commonly identified respiratory pathogen by all methods. Of the 598 samples reported to COHORT, 102 (17%) were identified as positive for influenza when using the Silent Guardian standard protocol. Cultures lasting up to 42 days were performed on 450 of the samples and revealed that 213 (47%) were positive for influenza by culture. Additional pathogens were identified in low incidence.

Three hundred fifty-one "matched" experiments for which there were data for culture, random amplification, and multiplexed amplification were analyzed with the relaxed algorithm. Of the 351 matched experiments, 30-day culture detected Influenza A in 147 (42%) of the specimens. Used in combination with the relaxed algorithm, the random amplification and UberMix amplification protocols resulted in a total of 114 unique positive results for 32% of the total "matched" sets. Overall, modifications to the protocol allowed increased detection of a variety of additional respiratory pathogens without false detection of BT agent genetic sequences. As expected, the use of multiplexed primers (UberMix) increased both the number and types of pathogens detected relative to the standard protocol. Especially noticeable was the large increase in calls for Adenovirus and the bacterial pathogens *N. meningitidis* and *S. pneumoniae*, both of which are known to colonize the nasal passage in healthy individuals. Also observed were the increased detection of *S. pyogenes* and respiratory syncytial viruses A and B. Only this amplification technique gave detection of erythromycin resistance gene markers (plasmid conferred) in 19 individuals.

For standard comparisons of resequencing microarray results to those obtained with culture, the FDA recommendation of using an overall percent agreement (defined as the proportion of sample where both the new test and the imperfect reference test agree) was used. Based on these values, the overall percent agreement for samples tested by both methods was 70%. Additional determinations of agreement for positive and negative samples showed 33% positive agreement and 93% negative agreement. When similar calculations using the "relaxed" data were done, FDA analysis method indicated 70% overall percent agreement. There was 66% agreement for positive analyses and 92% agreement for negative analyses, suggesting that improvements in the resequencing microarray assays and analytical software would be required to meet the clinical thresholds in the future. [NOTE: Recent progress has led to significantly improved sensitivity with clinical agreement of over 90% for a set of over 100 samples we have received from NHRC for Influenza and Adenovirus. Retesting of the samples collected from Silent Guardian is now in progress.]

BLIND *B. ANTHRACIS* SPIKE TESTS

To demonstrate the detection capability for bioterrorism agents and to test the notification system, 11 test samples containing spikes of **certified, inactivated** *Bacillus anthracis* (1 containing Ames strain and 10 containing Sterne vaccine strain) in pooled normal nasal wash. These samples were included with clinical samples through standard sample processing without prior knowledge of the technical staff. Samples were put into the normal patient specimen jars with a special LIMS barcode that appeared to be from an MTF with no indication that they were not clinical samples. Once the sample was analyzed as anthrax-positive, the designated senior staff member at NRL for that shift initiated testing with a standard rapid testing protocol

Table 1 — Positive Results for All Methods

Positives for	Culture/PCR	Standard	Standard "Relaxed"	UberMix "Relaxed"
Influenza A	184	91	108	104
Influenza B	29	11	13	15
Adenovirus	2	0	0	17
Coronavirus	33	4	7	2
Rhinovirus	0	1	3	0
Neisseria meningitides	0	0	0	38
Streptococcus pneumoniae	10	0	0	21
Streptococcus pyogenes	9	0	0	3
Respiratory Syncytial Virus A	0	0	0	1
Respiratory Syncytial Virus B	0	0	1	4
Erythromycin resistance	NA	NA	0	19
Total	**450**	**598**	**598**	**464**

to verify the microarray results. Samples that tested positive for anthrax in both tests were reported directly to the on-duty Air Force Silent Guardian officer. Notifications of spike positives were received by the Air Force Silent Guardian senior staff within 10 minutes of sample analyses. Time from initial receipt of sample in Room A to the staff notification ranged from 17.4 hours to 21.3 hours. All 11 samples showed up as positives for *B. anthracis*.

DETECTION AND DISCRIMINATION OF BIOTHREAT AGENTS AND NEAR NEIGHBORS

Because of a mild flu season, a much smaller-than-expected number of patient samples were obtained during Silent Guardian. This provided an excellent opportunity to perform a systematic assessment of the Silent Guardian protocol to: (a) detect sequences of pathogens across large concentration ranges, (b) withstand challenge from a battery of genetically similar organisms, (c) simultaneously screen for the presence of biothreat agents and operationally significant pathogens in clinical matrices, and (d) assess utility for use in a clinical laboratory setting with routine and surge testing.

More than 2,100 analyses were performed on spiked samples and blank controls using random amplification, BTA mix, or UberMix. Using these specific primer mixes, we detected *B. anthracis* sequences from Sterne strain vegetative cells at the lowest number of cells tested (20 colony-forming units, cfu) and from Ames spores at levels as low as 6×10^4 cfu per sample. *F. tularensis* sequences were also detected in two strains at cell numbers as low as 10 cfu per sample (LVS, *F. tularensis* biovar novicida) and 10^3 cfu per sample (Schu4). *Y. pestis* sequences were detected in samples containing 10-300 cfu of *Y. pestis* target, depending on the source. Sequences specific for Vaccinia virus, a simulant for Variola major virus, were detected at the lowest concentration of spiked Vaccinia tested (10^5 cfu)—while allowing for fine-scale genomic discrimination between Vaccinia and the actual smallpox virus.

CONCLUSIONS

The Silent Guardian Demonstration successfully showed its potential as a bio-surveillance system in the Military District Washington during January and February 2005 for both natural and biothreat pathogens. **Multiple pathogens were identified in clinical samples from the general population in less than 24 hours**. Identifications of >20 naturally occurring pathogens were made at the **strain**, as well as species, level in many cases. None of the sequences from six bioterrorist agents included on the RPM chip were detected in patient samples, although *B. anthracis* sequences from all of the blind samples artificially spiked with anthrax were immediately detected. The results produced a high level of confidence in the reliability of the resequencing approach for bio-surveillance in both military and civilian populations.

Silent Guardian was also a unique demonstration of the capability of the Joint Services to bring research to operation in record time (full operational capability within 6 weeks). It exemplified the amazing synergy possible when individuals with widely diverse capabili-

FIGURE 3
Silent Guardian Demonstration personnel at the Naval Research Laboratory: 1st row: SSgt J. Schuerger, Dr. F. Ligler, Capt F. Lobo-Menendez, Dr. C. Taitt, SSgt P. Chernay, SRA B. Sanchez, Ms L. Shriver-Lake, SSgt(s) A. Lowman, Dr. D. Stenger, SSgt N. Barboza, SSgt S. Cooper, Dr. B. White; 2nd row: SSgt T. Finch, Ms G. Gover, SSgt L. Jones, SSgt V. Lee, TSgt A. Davis, Capt D. Lennon, SSgt A. Krammer, SSgt S. Johnson, Dr. J. Schnur, LtCol S. Harmon, SRA S. Lowman, A1C M. Martinez, Ms. A. Kusterbeck, Dr. B. Lin, Ms. K. Shaffer, Dr. G. Lin; 3rd row: SMSgt C. Alexander, Capt D. Haggerty, TSgt T. Oaks, SSgt R. Tyler, MSgt(s) K. Norton, SSgt C. Stokely, TSgt A. Allison, SSgt R. Sullivan, Dr. W. Dressick. Inset: 1st row: Mr. P. Charles, Dr. A. Malanoski, Dr. B. Ringeisin, Mr. M. Dinderman, Mr. J. Bongard; 2nd row: Mr. B. Weslowski, Dr. K. Mueller, CDR B. Oyofo, Dr. M. Ngundi, LT S. Hakspiel, Dr. S. Pollack. Missing: Dr. G. Anderson, Capt W. DelaCruz, CAPT(s) B. Hardas, Dr. J. Jones-Meehan, Dr. T. Leski, ENS K. Mandell, LT J. McCardle, MSgt A. Sinclair, Dr. W. Straube, and CAPT W. Suiter.

ties are committed to a common endeavor. Figure 3 show the Silent Guardian staff at NRL, including NRL scientists and active-duty Air Force personnel.

ACKNOWLEDGMENTS

The NRL Silent Guardian team owes its success to: Secretaries D. Klein and K. Schafer from The Office of the Secretary of Defense; The Air Force Surgeon General LTG P. Taylor and his Modernization Directorate (COL P. Demitry, COL S. Holt, and LTC L. Difato); the Joint Program Executive Office-Chemical and Biological Defense (M. Walters, K. Korte, D. Cullen, C. Wilhide, C. Cutshall, and L. Greer); NRL Codes 6900, 6100, 6000, 3500, 3400, 3200, 1200, 1001, and 1000; Air Force staff from AFIOH, Brooks AFB, Tyndall AFB, especially LTC S. Harmon and MSgt C. Alexander III; staff from NHRC and CDR K. Russell for coordination of all culture and PCR reference assays; AFRI, Navy Surgeon General's office, U.S. Navy reserves, and the PIs and collection staff at the six MTFs in the Washington, DC area for the sample collection (CAPT E. Von Rosenvinge, LTC J.K. Klingenberger, Dr. J. Baxter, LTC M. Shepard, LTC G. Wortmann, CAPT S. Tasker).

[Sponsored by OSD]

Reference

[1] B. Lin, et al., "Broad Spectrum Respiratory Tract Pathogen Identification Using Resequencing DNA Microarrays," *Gen. Res.* (2006), in press. ★

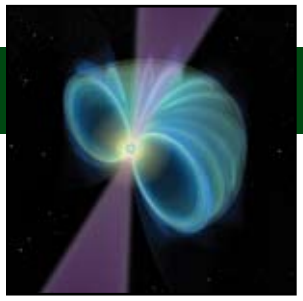

Spacecraft Navigation Using X-ray Pulsars

P.S. Ray, K.S. Wood, and B.F. Phlips
E.O. Hulburt Center for Space Research

Pulsars are the collapsed remnants of massive stars that have become neutron stars, where a mass exceeding that of the Sun is packed into an area about the size of the DC Beltway. Many of these neutron stars spin rapidly (hundreds of times per second) on their axis and emit pulsations at the spin frequency in much the same manner as a lighthouse. These natural "lighthouses" can also be used for navigation, that is, determining the position, time, and attitude of a spacecraft. Because of their enormous mass and relatively simple structure, pulsars are exceptionally stable rotators whose timing stability rivals that of conventional atomic clocks. A navigation system based on celestial sources will be independent of GPS and available in any Earth orbit as well as in interplanetary and interstellar space. NRL has undertaken a program to characterize and model X-ray pulsars and build X-ray detectors for a planned flight demonstration of this technology.

INTRODUCTION

Since prehistoric times, celestial sources such as the stars, Sun, and Moon have been used as navigation aids. Observations of the sky with precision instruments can allow explorers to determine their local time and latitude and longitude with high accuracy. Modern navigators still use some of these techniques. But they have also come to rely on man-made systems such as the Global Positioning System (GPS). These systems can provide a user with position, velocity, and time with exquisite accuracy—regardless of whether it is night or day, or what the weather is.

Over the last decade, GPS has revolutionized the navigation of everything from rental cars, to commercial aircraft, to precision-guided munitions. Nevertheless, there are some situations, particularly involving spacecraft navigation, where GPS does not provide a satisfactory solution. The most obvious situation is for spacecraft that must operate outside the orbit of the GPS constellation, which is at an altitude of 20,000 km. In addition, a spacecraft with a mission of national importance might want to have an additional source of navigation information besides GPS to increase its robustness to threats.

When considering alternative navigation methods, it is instructive to review how GPS works. GPS consists of a constellation of about 24 satellites, each carrying several precise atomic clocks that periodically broadcast a radio signal containing the precise time according to their clock (and ancillary information including the location of each GPS satellite). A GPS receiver receives the radio signal from several satellites and computes the range (technically *pseudorange*) to each satellite based on the time difference between transmission and reception of the signal and the propagation speed of the radio signal. Using information from at least four satellites, the receiver can thus solve for its own position and the precise local time.

The celestial bodies we are familiar with, based on our experience observing the sky with our eyes, are not particularly promising in this regard because they do not broadcast a precise timing signal that can be used for navigation (except for a few isolated examples such as eclipses of the moons of Jupiter). However, the 1967 discovery of *pulsars* changed that situation dramatically by demonstrating that at least some celestial sources *do* broadcast highly regular timing signals. This led to the proposal to use pulsars as the basis for a spacecraft navigation system based on observations of celestial sources, using them as a kind of "natural GPS." It presents a trade of flexibility, high performance, and man-made control on the GPS side vs zero maintenance and universal availability on the side of the natural sources. The achievable level of performance in the latter case is something that can be settled by practical experiments. Hence, it becomes an interesting objective for a research program.

In this article, we describe the properties of pulsars that make them attractive as potential natural navigation beacons and why a practical implementation looks most feasible in the X-ray band. We then describe the history of the X-ray navigation program at NRL up through our current Defense Advanced Research Projects Agency (DARPA) program. Finally, we describe the custom X-ray detector modules we are developing for this program and some of the algorithmic challenges that must be overcome to implement a real system.

PULSARS: NATURE'S BEST CLOCKS

A pulsar is a rapidly rotating neutron star that is observable as a pulsed source of electromagnetic radiation. Neutron stars are formed in the core collapse of a massive star and are the most dense form of matter in the Universe, with central densities that exceed the density of an atomic nucleus! As the core collapses, conservation of angular momentum causes the star to "spin-up" to a rotation period of order 10 ms, and the conservation of magnetic flux drives the magnetic field strength at the stellar surface up to 10^{12} gauss or higher, with magnetic moments up to 10^{32} gauss-cm^3.

The resulting object is simultaneously a massive freely spinning top and a powerful particle accelerator because the rotating magnetic field generates enormous electric fields that accelerate charged particles. These accelerated particles generate electromagnetic waves across the spectrum, from radio waves to gamma-rays, that tend to be beamed along the magnetic axis. If, as it appears true in most cases (including the Earth), the magnetic axis is misaligned with the rotational axis of the star, a distant observer sees a "pulse" of radiation each time the beam crosses the line of sight, much like a lighthouse (see Fig. 1). The energy that powers these cosmic lighthouses is simply the stored rotational energy of the neutron star. As the energy is slowly radiated away, the star "spins down" to longer and longer rotation periods, and thus these sources are referred to as *rotation-powered* pulsars. They shine in this manner for a period of about ten million years, after which time they have slowed down to a period of order 10 seconds and can no longer generate the strong fields necessary to accelerate the particles that produce the powerful radiation beams. These pulsars then turn off and inhabit the "pulsar graveyard."

During their lives, these pulsars make very good clocks; their periods change by only 100 ns or so each year. Nevertheless, even this paltry rate of slowing causes the star to get out of equilibrium as the rotation of the crust gets out of sync with the superfluid interior. This causes timing irregularities, both gradual (the long-term stochastic wandering of the pulse phase, referred to as "timing noise") and sudden (nearly instantaneous "glitches" in the pulse period that happen when crustal strains build up to the breaking point). These unpredictable irregularities limit the usefulness of these "normal" pulsars as navigation beacons. However, another class of pulsars is much more stable and promising, the *millisecond pulsars.*

The millisecond pulsars are formed when a pulsar has a binary companion that is a normal star. At some point, stellar evolution or orbital dynamics brings the two stars into contact, and a large amount of matter is transferred from the normal star onto the pulsar in a process known as accretion. During the mass transfer process, these systems become tremendously bright X-ray sources as the infalling matter is heated to temperatures of millions of degrees. The mass transfer also causes two other effects: it transfers angular momentum to the pulsar, spinning it up to periods near 1 ms, and it causes the magnetic field of the pulsar to decay by about a factor of 10,000. When the accretion process stops, the pulsar is reborn as a millisecond pulsar (also called a "recycled pulsar"). The greatly reduced magnetic fields of these pulsars causes them to spin down much more slowly (their period changes by less than 1 picosecond per year!) and live for far longer (tens of billions of years) than the normal pulsars. As a result, the millisecond pulsars are exceptionally stable clocks, whose stability rivals modern atomic clocks (see Fig. 2)!

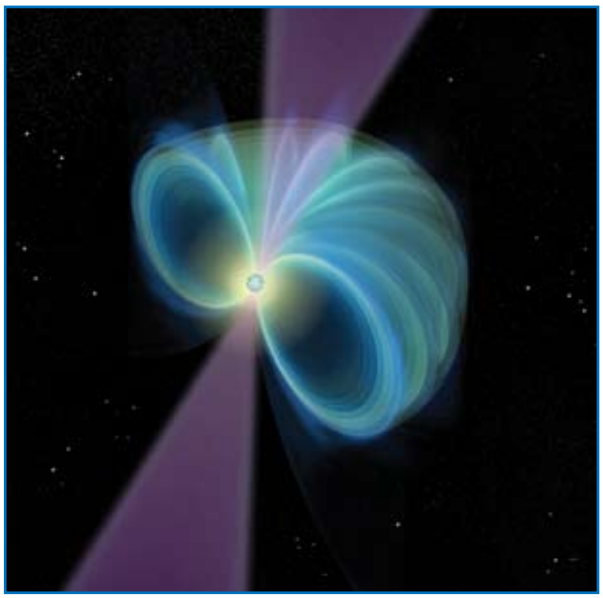

FIGURE 1
Artist's conception of a rotation-powered pulsar.

Why Observe Pulsars in the X-ray Band?

Nearly all pulsars (more than 1500 are now known) are discovered and studied in the radio band, using ground-based telescopes. However, most radio pulsars are very faint and can only be studied with the world's largest radio telescopes, such as the 305-m Arecibo telescope in Puerto Rico, or the 100-m Green Bank Telescope in West Virginia. The requirement for huge antennas makes a navigation system based on radio observation of pulsars impractical for most applications. In addition, propagation of radio signals through the interstellar medium results in phase lags of variable and unpredictable duration, so that they set the limitation on accuracy.

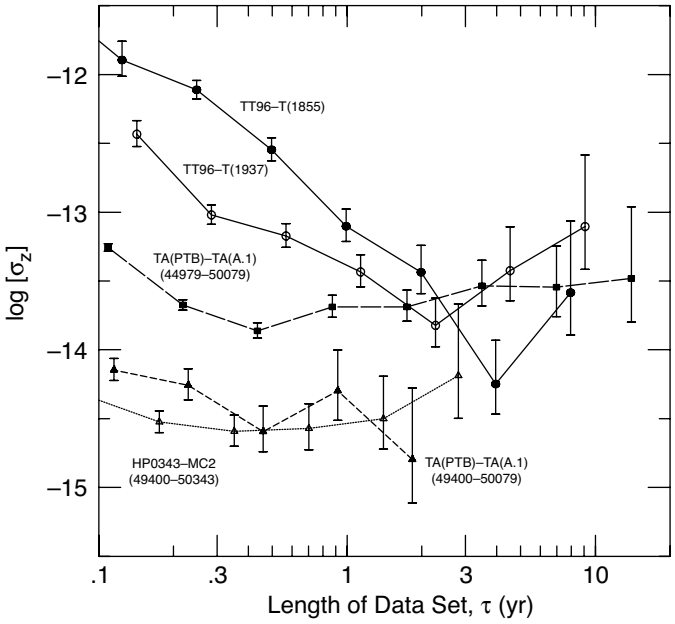

FIGURE 2
A comparison of the stability of two millisecond pulsars with some atomic time scales. σ_z represents the fractional stability of one clock compared to another (it is analogous to the Allan variance used in the clock community). T(1937) and T(1855) are the timescales based on the pulsars PSR B1937+21 and PSR B1855+09, respectively. TT96 is a terrestrial atomic timescale. TA(A.1) and TA(PTB) are free running atomic timescales from the U.S. Naval Observatory and Germany. Notice that at long timescales, the pulsar timing stability approaches that of modern atomic time standards. (Reproduced from Matsakis, Taylor, and Eubanks 1997, *Astronomy & Astrophysics* **326**, 924.)

However, a modest number of pulsars are known to emit pulsed X-rays as well, that can be detected by an X-ray instrument that is less than one square meter (1/70,000th the size of Arecibo!). The X-ray signal, at effectively infinite frequency, is not affected by the interstellar medium like the radio signal, and thus several limitations to the precision of the timing measurements are removed. The primary drawback of using X-ray detectors is that X-rays do not go through the Earth's atmosphere, so the method is limited to space applications. Other drawbacks include the small number of known X-ray millisecond pulsars and their relative faintness, which leads to a requirement for a large X-ray detector to make precision measurements (though still tiny compared to the radio dishes that would be required).

HISTORY OF X-RAY NAVIGATION AT NRL

In the 1980s, the NRL X-ray astronomy group (now Code 7655) was specializing in studies of timing effects in celestial X-ray sources such as pulsars or black holes. In these objects, certain timing signatures were periodic, as in the rotation periods of pulsars or the orbits of binary systems. Others were quasi-periodic or aperiodic; some of these effects are produced by fluid modes involving movement of hot gas in the source systems. Many of the timing studies were conducted with simple instruments of a kind used at NRL since the early work of Herbert Friedman and collaborators, in which a sensor sensitive to X-rays is combined with a collimator that accepts incoming photons from only a small region of the sky, perhaps a square degree. There are no X-ray mirrors in such systems yet they can readily isolate the brightest sources in the sky, say ~1000 of them. It was recognized that the combination of simple detector systems with the outstanding feature of the X-ray sky—an abundance of variable point sources—implied a potential for X-ray navigation.

USA Experiment on *ARGOS* (1999-2000)

During the 1980s, this abstract idea took on a concrete form with the proposal to fly a demonstration experiment called the Unconventional Stellar Aspect (USA) Experiment. When finally realized with launch in February 1999 on the Air Force *Advanced Research and Global Observation Satellite* (*ARGOS*), USA had become an X-ray astronomy experiment with four distinct objectives: astronomy, autonomous satellite navigation, atmospheric diagnostics, and testing techniques for computing in space.[1] It was built by NRL in collaboration with Stanford University, using funding from the Navy, the Department of Energy, and the Ballistic Missile Defense Organization. From the first proposal (1988) to launch took 11 years. Some of that time went into selling the idea, and some went into evolving the multipurpose system concept that was eventually flown.

USA used an X-ray photon sensor as its central element; the sensor was mounted in a 2-axis gimbal for offset pointing from *ARGOS*.[2] The sensor was designed to look at both stars and the Earth, supporting both astrophysics-related observations and experiments in X-ray navigation. For either goal, it was necessary to do offset pointing, which involved onboard computation. There was also a computing experiment involving testing MIPS-3000 class processors in space. The motivating idea was that this could take data from the X-ray sensor and derive navigational quantities onboard, but

it also served as a testbed for space-based fault-tolerant computing techniques. The computing testbed operated independently of the astronomy effort so that comparative (and rather surprising) flight experience was gained with both commercial off-the-shelf and specially radiation-hardened processors. Figure 3 shows the USA instrument, mounted in its 2-axis gimbal and pylon. The overall weight of the USA Experiment was approximately 200 kg, including sensors, pylons, and gimbals.

X-ray Navigation and Aeronomy with USA

The instrument was successfully used for experiments in autonomous attitude determination, position determination, and time-keeping using X-ray sources, all of which fulfilled its navigational objective. It was also used to study the density of the atmosphere at altitudes of roughly 50–80 km using a technique similar to X-ray tomography. The central aim of the navigational part of the program was to explore how well observations of X-ray sources could be used to determine the attitude, position, and local time for a satellite in orbit.

Attitude

As it happened, USA had to be used to diagnose and correct unexpected errors in the performance of the spacecraft attitude control system that initially caused it to miss targets. This was the first use of an X-ray sensor to provide diagnostic attitude information for the control of a satellite in orbit. Since USA was not an imaging system, attitude determination was done using transits of sources through the response of the collimator. When an X-ray source drifts slowly through the field of view, it traces out the angular response function, which is roughly triangular. Early in the *ARGOS* mission, the USA team began doing maneuvers in which the instrument was repeatedly scanned over known sources to measure the accuracy of the onboard attitude determination. To isolate and quantify satellite pointing errors so as to correct the problem, it was necessary to combine observations of several sources, as was done successfully during observations in August 1999. Once the instrument was used to diagnose problems in the attitude reference provided by the spacecraft itself, it became possible to track stars with high accuracy.

Timekeeping

Timekeeping experiments depend on using the best astronomical clocks, isolated pulsars. The pulsar in the Crab Nebula is the brightest in the X-ray sky, although it is not the most stable clock. Nevertheless, its strong signal makes it the source of choice for initial timekeeping studies. Figure 4 shows the pulse profile of the Crab pulsar; it had a period of 33.4033474094 ms at the time of the observation. The photons had their arrival times recorded using an onboard GPS receiver, and the pulse arrival times were compared to those predicted from ground-based radio measurements. The two were found to agree to about 100 μs, approximately the accuracy of the radio ephemeris. The ultimate limits of X-ray pulsar timing methods will be set by more stable pulsars such as PSR B1937+21, whose pulse period is 1.555780646881979 ms.

Position

USA demonstrated a technique for position determination using stellar occultations by the Earth's limb as measured in X-rays, which is distinct from the pulsar-based methods. This works for satellites in low Earth orbit (LEO). The exact time when the source

FIGURE 3
The USA Experiment mounted on the *ARGOS* spacecraft.

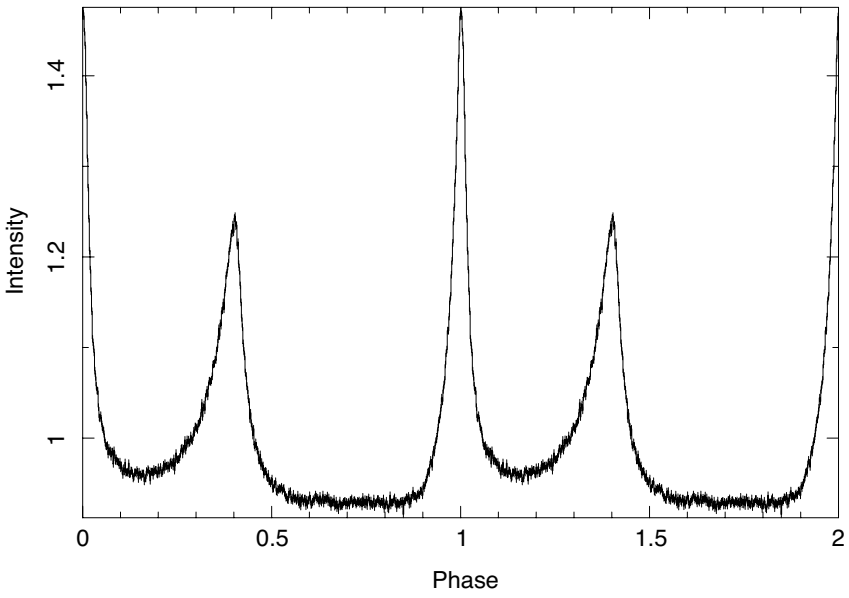

FIGURE 4
Average pulse profile of the Crab pulsar, recorded with the USA Experiment.

is eclipsed (say, when intensity is reduced to 50%), combined with an atmospheric model, will give the satellite position. This is like a classical horizon sensor except that here the sensor uses X-rays, not visible light. X-rays are absorbed at high altitude, not near sea level, and are not refracted or affected by dust or clouds. It is not possible to use the occultation method to determine positions accurately unless the density profile of the upper atmosphere is modeled properly, but work on this is also being done with USA data to fully characterize the technique.

The DARPA XNAV Program

Since the initial navigation concept demonstrations with the USA Experiment, interest in the possibility of X-ray source-based navigation has greatly increased from within both DoD and NASA. In particular, DARPA has initiated a program it calls XNAV. DARPA is funding two teams, one led by our group at NRL, to perform an 18-month Phase I study of the XNAV concept. Our DARPA-funded work at NRL consists of two task areas:

- a detailed study of the most promising pulsar sources for this application, and
- development of laboratory prototype X-ray detectors well matched to the XNAV tasks.

Our collaborators on this effort include Massachusetts Institute of Technology and Brookhaven National Laboratory. At the completion of Phase I, DARPA will decide whether to fund Phase II, which involves the development and launch of a prototype XNAV instrument suite for an on-orbit flight test of the technologies and algorithms involved.

THICK SILICON PIXEL DETECTORS

To make precise timing measurements of these X-ray pulsars, a detector system is required that is low-power, low background, and capable of sub-microsecond timing accuracy on each X-ray photon received. The detectors need to be large because the pulsars of interest are all rather faint. It must also be light weight and highly reliable in the harsh, high-radiation environment of space, and not require heavy and expensive cryogenic cooling. Previous X-ray detection satellite missions have used gas-based detector technology (e.g., HEAO A-1, RXTE, USA). These detectors are prone to leaks in the entrance window (from micrometeorites), as happened with the USA experiment. The detectors, although made of low density gas, can be rather heavy because of the massive frames required to contain the gas. An alternative technology is therefore of interest. As part of our DARPA program, we are developing prototype silicon pixel detectors that achieve all of these capabilities.

Silicon X-ray detectors are silicon PIN (p-type, intrinsic, n-type) diodes that are reverse-biased with high voltage until the entire silicon volume is depleted of free charge carriers. Under these conditions, an incoming X ray that interacts in the silicon will create a high energy electron, whose ionization track will create a large number of secondary electrons and holes. The electrons and holes drift under the electric field to the surface contacts, where they can be collected into preamplifiers and generate signals whose amplitude is proportional to the energy deposited by the X ray. The time response of the detectors is very fast and is dominated by the drift time of the electrons across the

thickness of the detector. The drift time is ~20 ns/mm in silicon at room temperature.

The thickness of the detectors determines the efficiency of stopping higher energy X rays. Since X rays can be quite penetrating, thick wafers are required. For the XNAV program, as many X rays as possible should be detected, to maximize the accuracy for navigation. Therefore, the detector energy range should be maximized, requiring the detectors to be made as thick as possible to stop high energy X rays. The thickest silicon detectors currently manufactured are 2 mm thick, and we chose this thickness for our prototype detectors. Realistic detector configurations will require frontal areas much larger than the largest single pieces of silicon currently available. The instrument must therefore be modular and use large silicon devices to minimize the number of modules required for a particular instrument concept. The largest detector-grade silicon wafers available have a diameter of 150 mm. We are developing detectors that are 95 × 95 mm in area, the largest square device that can be obtained from the 150-mm wafers.

If the entire area of a wafer were read out as a single pixel, the capacitance of that pixel would be very large. The intrinsic noise performance of any preamplifier reading out that pixel would be very poor because the noise in a preamplifier is linearly dependant on the capacitance on the input of the preamplifier. The silicon wafers are therefore segmented into many small pixels, even though the pixels are not used for imaging. As the number of pixels grows, the capacitance of each pixel shrinks and the noise performance improves. But as the number of pixels increases, the power available per pixel decreases, which worsens the preamplifier noise performance. Simulations have shown that the optimal number of pixels per side of a wafer is 35-40, with a power budget of 0.7 W per wafer for the analog electronics. With this power budget, a noise performance for the electronics of ~50 electrons equivalent noise charge (~180 eV energy resolution) is expected with 1-μs filtering. We selected 36 pixels per side, for a total of 36 × 36 pixels per wafer. Figure 5 shows a prototype silicon X-ray detector wafer.

Custom electronics are required to read out all the pixels on a silicon wafer. To interface to all the pixels, the wafer needs to be bump-bonded to the readout electronic card. On this card, pre-amplifiers and amplifiers are connected to each pixel. The required circuit density and power budget demand the development of a custom application specific integrated circuit (ASIC). Such a program was started in collaboration with Brookhaven National Laboratory. Each wafer is to be read out by a 6 × 6 array of ASICs, each of which is connected to a 6 × 6 array of pixels. Each ASIC therefore contains 36 parallel channels of preamplifier, shaping amplifier, discriminator, and peak detection. The

FIGURE 5
Prototype 2-mm thick large-area silicon X-ray detector.

preamplifier amplifies the very small signals of a few thousand electrons by a factor of ~1000 and is followed by a shaping amplifier that filters out low- and high-frequency noise. The discriminator provides an adjustable threshold for signal detection and also provides a timing signal to mark the arrival time of a photon. The peak detection holds the peak amplitude of the transient pulse for later multiplexing and digitization in an analog-to-digital converter (ADC). The ASICs, ADCs, and ancillary electronics are controlled by a field programmable gate array (FPGA) that is in turn controlled from a computer. The amplitude of the pulse and time of arrival of the photon are recorded and stored in the computer for analysis.

ALGORITHMS FOR POSITION AND TIME DETERMINATION FROM PULSAR OBSERVATIONS

The basic measurement that yields position and time information is the arrival time of a pulsar pulse at the detector. This arrival time is then compared to the expected arrival time based on a timing model of the pulsar that has been developed from years of observations at ground-based radio telescopes. The difference between the observed and predicted arrival time can be translated directly into a correction in the position of the detector in the direction of the pulsar being observed (Fig. 6). Observations of multiple pulsars can thus be combined to provide full three-dimensional position information. Similarly, if the position of the detector is known, the time difference can be used to correct the time of the onboard clock. In practice, the spacecraft must keep a continuously updated model of its position and velocity state vector. This model is propagated forward in time using a high-precision orbit propagator; corrections to the model based on the pulsar observations are incorporated using a Kalman filter[3] (Fig. 7).

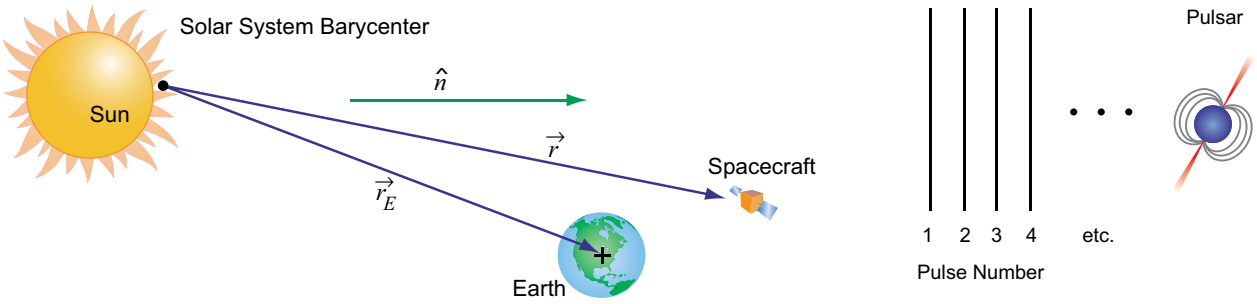

FIGURE 6
Observation geometry for X-ray pulsar-based navigation.

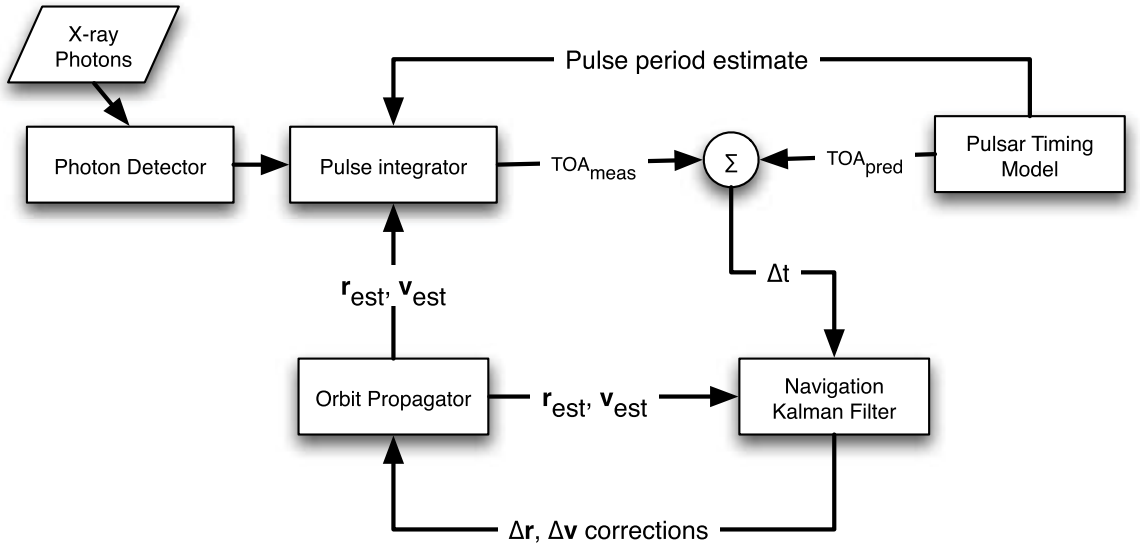

FIGURE 7
Flow chart of the basic algorithm for incorporating pulsar timing information into a navigation Kalman filter.

The details of the algorithm design depend very strongly on the requirements of a particular operational concept. Applications that we have considered include: time synchronization of multiple satellite clocks using a pulsar-based time scale; position and time determination for DoD satellites in highly elliptical or geosynchronous orbit or cislunar space; and precision navigation of spacecraft on interplanetary, or even interstellar, missions.

CONCLUSIONS

The High Energy Space Environments Branch at NRL continues to explore the possibility of using X-ray pulsars as natural navigation beacons to provide time, position, and attitude information for spacecraft under a variety of operational concepts. Our plans for the future include detailed development of the algorithms required for the onboard processing of the raw pulse times-of-arrival and an advanced flight test of the detector system. We are also pursuing additional applications for the X-ray detectors such as a potential future large-area X-ray timing mission with ten times the collecting area of NASA's *Rossi X-ray Timing Explorer*. This could probe the behavior of matter in the strong gravity around neutron stars and black holes in a way never before possible.

ACKNOWLEDGMENTS

We gratefully acknowledge the contributions of our many collaborators at NRL, Stanford University, Massachusetts Institute of Technology, Brookhaven National Laboratory, the University of Maryland, and elsewhere, whose efforts made the USA Experiment and our X-ray navigation program so successful.

[Sponsored by DARPA]

References

[1] K.S. Wood, "Navigation Studies Utilizing the NRL-801 Experiment and the ARGOS Satellite" in *Small Satellite Technology and Applications III*, ed. B. J. Horais, *SPIE Proc.* **1940**, 105 (1993).

[2] P.S. Ray, K.S. Wood, G. Fritz, et al. "The USA X-ray Timing Experiment" in *Proceedings of X-ray Astronomy 1999 — Stellar Endpoints, AGN and the Diffuse Background*, Bologna, Italy, *AIP Conf. Proc.* **599**, 336 (2001).

[3] S.I. Sheikh, D.J. Pines, P.S. Ray, K.S. Wood, M.N. Lovellette, and M.T. Wolff, "Spacecraft Navigation Using X-ray Pulsars," *J. Guid., Cont. Dyn.* **29**, 49 (2005). ★

First Detection of X Rays from the Sun

Achievement: With the launch of an experiment aboard a V-2 rocket on September 29, 1949, NRL directly confirmed that X rays from the Sun are a principal cause of ionization in the E region of the Earth's ionosphere. Additional experiments, aboard a Viking rocket flight and two Aerobee firings, later indicated that the solar X-ray spectrum is adequate to account for all of E-layer ionization. This pioneering research opened the field of solar X-ray astronomy that the Laboratory explored so extensively in the 1950s and thus contributed profoundly to the understanding of the physical processes in the solar atmosphere. A practical benefit of this research includes the improved understanding of the effects of solar disturbances on radio communication and an improved ability to predict the influence of solar particle emissions on the radiation environment of manned space flight.

NRL's H. Friedman led the Laboratory's pioneering efforts in X-ray astronomy. In 1969, he received the National Medal of Science, the U.S.'s highest honor for scientific achievement, for "pioneering work in rocket and satellite astronomy and in particular for his contributions to X-ray astronomy." More recently, in honor of this work he received the coveted Wolf Foundation Prize for Physics in 1987. The Wolf Prize committee recognized Friedman and the other two co-recipients of the award:

> "as the principal founders of X-ray astrophysics, a new field of astronomical science which has proven to be a prolific source of fundamental discoveries and deeper physical understanding about high-energy processes in the universe. Their work has profoundly influenced every area of astronomical research. All agencies engaged in space science are now developing major orbiting facilities for X-ray observations, which will play a vital role in the future of astronomical science."

Impact: Solar X-ray emission is used to predict the state of the ionosphere and its effect on radio frequency transmission, especially at the HF frequencies. This was of major importance to Naval communications. The knowledge gained from the first detection of X rays from the Sun was a major milestone in a continuing endeavor by NRL that began with E.O. Hulburt's theoretical efforts in the late 1920s and continued through the SOLRAD satellite series, as well as other space satellite research programs.

Volumetric Acoustic Intensity Probe

E.G. Williams
Acoustics Division

Introduction: How often have we sat in an automobile or airplane and wondered where an annoying sound source was coming from? In military vehicles and aircraft, or habitation spaces on ships and submarines, annoying sources promote fatigue and may interfere with mission success. Identification of these sources is crucial so that measures may be taken to quiet them. Pressure or vibration sensors are generally not successful in localization and identification of noise sources. Modern metrology has turned to intensity probes for a solution. These probes have had marked success since they measure the direction and magnitude of energy flow at the measurement point. When used to scan over surfaces or in an array configuration, they are also effective at locating noise sources. The ability to locate detrimental noise sources and quantify them has taken a quantum leap forward with the invention at the Naval Research Laboratory (NRL) of a new and radically different type of intensity probe. Called the Volumetric acoustic Intensity Probe (VIP), it works by imaging the acoustic intensity vector in a volume nearly a cubic meter in size using an array of relatively inexpensive microphones. This holographic-like imaging capability is remarkable since it tracks the energy flow throughout this volume at points in space where measurements are not made. Furthermore, energy-flow tracks of multiple noise sources are separated by state-of-the-art, front-end signal processing. This new measurement device can be used to diagnose any complex noise source, whether flow-noise or shock induced, for example.

Description and Theory of Operation: The VIP consists of a nearly transparent spherical array of 50 microphones optimally positioned on an imaginary spherical surface of radius 0.2 m. The VIP uses high-level mathematics (spherical wave-function expansions) to convert the measured pressure field into a vector intensity field in a volume that is 0.8 m in diameter centered at the sphere origin. The operational array is shown in Fig. 1 in front of a window inside a Boeing 777 aircraft. The microphone probes can be seen pointing outwards from the center of the sphere along with an interconnecting framework. The VIP is held by a horizontal attachment boom shown below center on the right of the figure. Time-domain pressure at the 50 microphones and optional reference transducers (placed on suspected sources) are recorded simultaneously. Advanced signal processing based on cross-power spectra and high-level mathematics based on nearfield acoustical holography (NAH), both used for the tracking of the intensity vector, are coded in software on a fast PC with output on a LCD display consisting of frequency domain plots of the power flux (vector intensity) in a volume starting at the origin of the array and extending to a radius twice that of the array, as shown in Fig. 2. Currently, the 50-microphone design works in the frequency band of 0 to 1400 Hz in air with an upper limit of 6 kHz in water. The upper frequency limit can be extended by increasing the number of microphones used in the array.

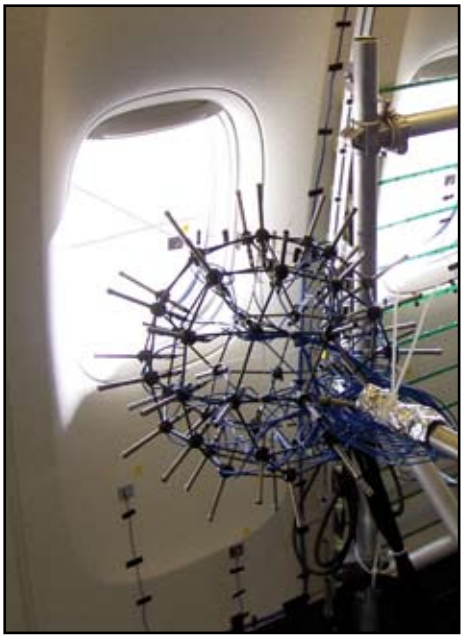

FIGURE 1
Fifty-element spherical array designed and constructed at NRL and mounted on a horizontal beam inside a Boeing 777 aircraft.

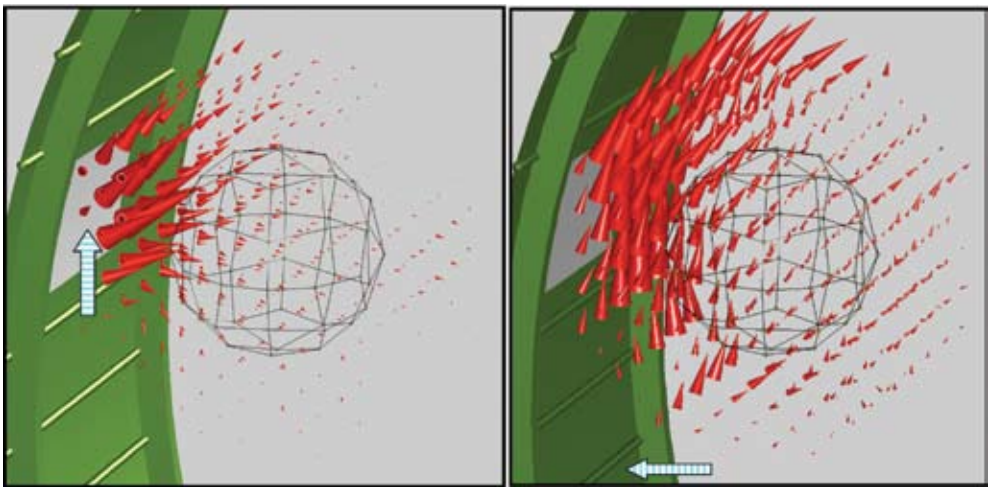

(a) (b)

FIGURE 2
Front-end signal processing successfully separates two independent noise sources. Results are at 732 Hz in front of a bare sidewall of a Boeing 757 aircraft flying at standard speed and altitude reconstructed from a single measurement with the VIP. A sketch of the sphere location (wire frame) as well as one vertical segment (colored green, located between two vertical king frames) of the fuselage sidewall is shown. An acoustic source (not shown) driven by a loudspeaker was located at point (a) and the second source was a fuselage horizontal panel (b), which was exterior-driven by flow noise and was resonant at 732 Hz.

Example of Operation: An in-flight experiment in a Boeing 757 aircraft, carried out in cooperation with NASA Langley and The Boeing Company, tested the operation of the VIP in a complex noise-source environment. Time data was recorded digitally for off-line processing and for testing and development of the capabilities of the VIP. The array was placed close to a bare sidewall (trim panels and insulation removed) of the fuselage similar to Fig. 1. Front-end signal processing using about 3 min of recorded data created pressure holograms (amplitude and phase of pressure in each of 270 frequency bins) correlated to individual references out of a suite of reference accelerometers and microphones used in the measurement. Coherence procedures pick the most important holograms for conversion into intensity fields at each frequency or in third-octave bands. In the sample result shown in Fig. 2, the 757 aircraft was flown at typical speed and altitude; the fuselage sidewall was excited by the exterior flow noise, radiating noise into the interior of the aircraft. A second source of noise was a controlled acoustic point source driven with pseudorandom noise by a loudspeaker and placed very close to the center of a window. A resonance of one of the fuselage panels below the window was identified at 732 Hz. Results from the VIP for the frequency bin at 732 Hz are displayed in Fig. 2. Note the front-end signal processing was successful at separating the two noise sources, displaying the most significant one (correlated highly to the acoustic point source) on the left and the second one (correlated highly to the resonant panel) on the right. The latter intensity field surprisingly follows a tangential path along the fuselage sidewall as it radiates out of the panel at the bottom of the picture. The VIP is very successful at resolving and tracking the energy-flux fields of these two uncorrelated noise sources.

Summary: Although this device has quickly caught the attention of the commercial aircraft industry, it is an ideal tool for the Navy and provides the ability to locate sources of sound in confined interior spaces like the cabins of military vehicles, surface ships, submarines, and aircraft; as well as in exterior spaces such as near a ship hull. The VIP tracking algorithm is very fast so that the probe can be used in real time, with LCD displays on a local laptop locating noise sources as the probe is physically moved, scanning for noise sources in a field application. The underlying technology is not limited to acoustic applications, but with a change from pressure sensors to electromagnetic field sensors, one would be able to image the Poynting (electromagnetic intensity) vector in the volume in the same way.

Acknowledgments: The experimental work was carried out under the direction (and funding) of Richard Silcox of NASA Langley in cooperation with Bernard Sklanka of The Boeing Company. Theoretical development and probe design and construction were supported by ONR.

[Sponsored by ONR]

Sub-Bottom Profiling and Geoacoustic Inversion Using a Ship-Towed Line Array

T.C. Yang, K.B. Yoo, and L.T. Fialkowski
Acoustics Division

Introduction: Bottom properties in littoral water can be very complex (i.e., not horizontally stratified) and are location dependent, as indicated by core samples and seismic surveys taken in some areas. Acoustic signal propagation cannot avoid interacting with the bottom in shallow water areas. Navy operations in littoral regions require some knowledge of the signal propagation loss, which determines the range that a (distant) target can be detected. Knowing the bottom, thus, becomes critical for Navy operations in shallow water. Unfortunately, there exist few direct measurements of the ocean bottom except in some isolated locations, since core sampling and seismic measurements of the bottom are generally expensive and time consuming. Existing data bases often yield incorrect predictions of propagation loss because the data entries are sparse and neglect the variation of the bottom properties along the propagation path. A recent effort at NRL is devoted to developing an acoustic method to invert for the bottom properties (the geoacoustic inversion method) using a horizontal line array towed behind a ship. A ship can cover a wide area in a reasonable time (e.g., 24 km in 2 h). The towed array inversion method can provide snapshots of the bottom properties under the ship as it traverses an area, and in this way, build a data base for the Navy. This article summarizes recent advances made at NRL and experimental verifications of the method.[1,2]

Sub-Bottom Profiling and Geoacoustic Inversion: Geoacoustic inversion correlates the signal calculated using an assumed bottom model with the acoustic data received on an array, and iteratively alters the parameters of the bottom (and other relevant parameters) until there is a good match between model and data. The method has been tested widely using vertical line-array data and works when there is some prior knowledge about the bottom, such as the number of sediment layers in the bottom. It is generally known that geoacoustic inversions can have ambiguous solutions, namely, that often more than one solution can fit the data. For building a database, the inversion method becomes untrustworthy if multiple data measurements of the same area yield different bottom profiles. Additional constraints, such as prior information, are needed to narrow down the inversion results.[1]

In the seismic community, long horizontal arrays are used to survey the bottom using acoustic signals received from a distant source. Focusing on bottom penetrating acoustic rays, the reduced ray travel time is deduced as a function of the ray arrival angle. This relationship can be used to determine the bottom layer thickness and bottom sound speed. In the acoustic community, geoacoustic inversion is preferred to seismic methods for two reasons: The towed sonar array is short compared with the seismic array, and the source-receiver range is fixed at a few hundred meters. The seismic community is interested in very deep bottom structure, whereas a shallow (sub-) bottom structure is more critical for sonar applications. The geoacoustic inversion method determines not only the bottom thickness and sound speed but also the bottom density and attenuation coefficients.

NRL developed a unified signal processing approach that combines a sub-bottom profiling method similar to that used by the seismic community with the geoacoustic inversion method used by the sonar community. By beamforming the towed array data, the beam outputs exhibit an angle and time (or depth) relationship (Fig. 3), from which one can extract a reduce-time-angle (or slowness) relationship similar to that used by the seismic community. Figure 3 shows a direct arrival from the source at an angle of approximately 5°, the surface-reflected arrival at approximately 18°, and bottom interacting arrivals at approximately 30°. The bottom arrivals show a return at the water-bottom interface and a return from the sub-bottom. The time difference is related to the sub-bottom thickness. Figure 4 displays the beam intensity time series at 30° for data collected over a 24-km ship track; this shows a sub-bottom layer structure (right figure) in good agreement with that obtained from a bottom profiler (left figure). The arrival angles and bottom-layer structure provide the needed inversion constraints to define sufficiently narrow parameter search windows, yielding an inverted bottom profile for water depth and sediment thickness, bottom-sound speed, and density and attenuation (Fig. 5). The inverted result at the edge of the track (designated as site 4) is in good agreement with an independent seismic reflection measurement conducted at site 4.

Summary: A method of geoacoustic inversion incorporating the information obtained from sub-bottom profiling is developed for a ship-towed line array. The sub-bottom profile data are deduced from the acoustic data and used to define parameter constraints used for geoacoustic inversion of the same data. The inversion result can be shown to be "unique" given the certainty of the bottom layer structure.[2] The method is being extended to use the ship's own noise as the acoustic source. In this case, the acoustic ray arrival angles are used to constrain the parameter search windows and the inversion results.

[Sponsored by ONR]

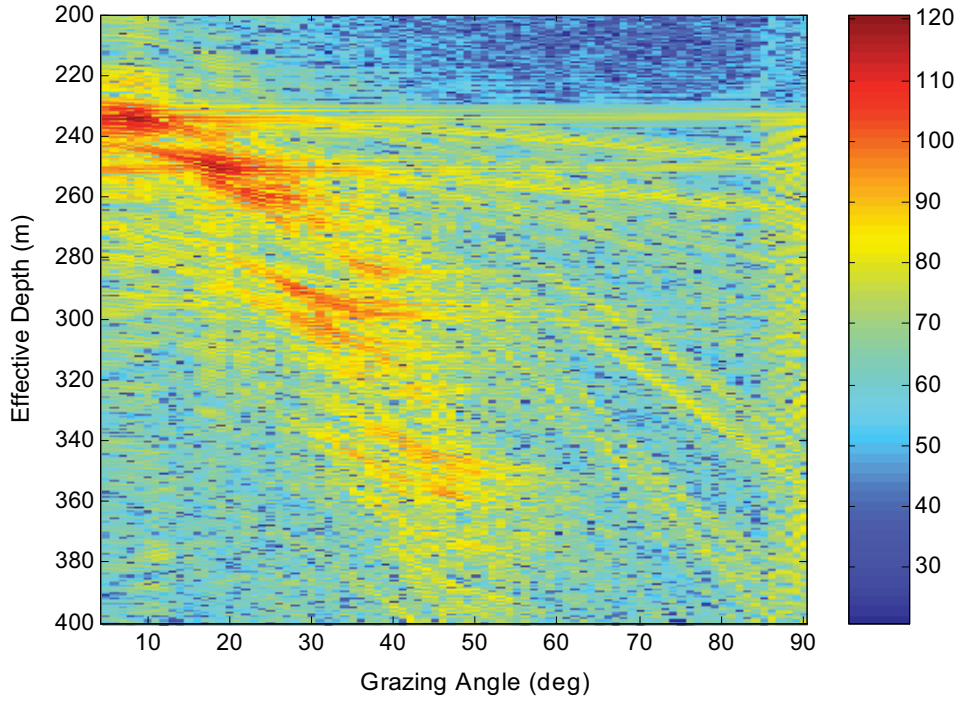

FIGURE 3
Beam-intensity time series at different beam angles measured from the forward endfire. Effective depth is travel time x 1582 m/s.

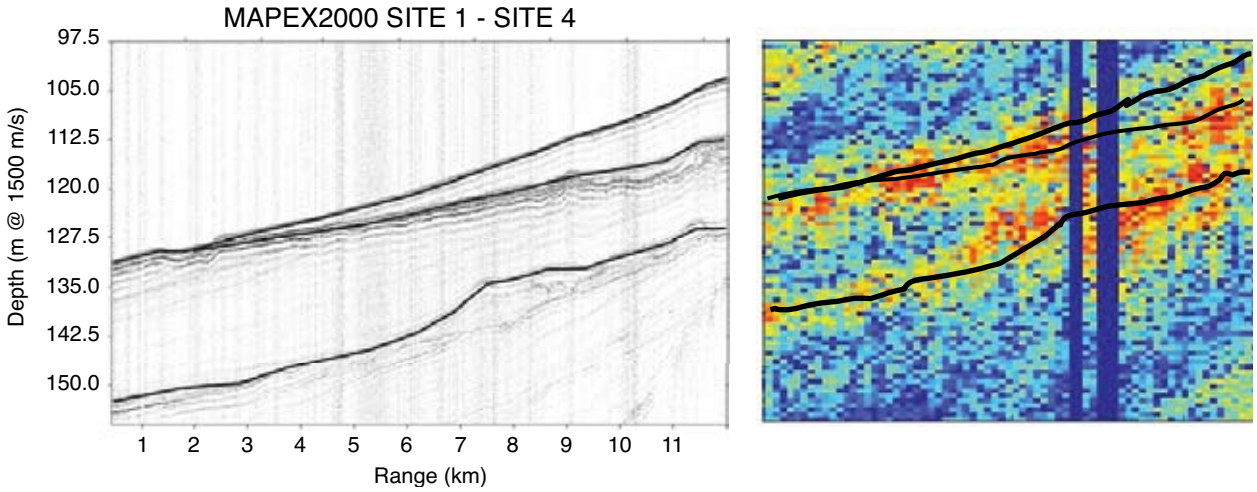

FIGURE 4
Effective depth determined from the bottom profiler (left figure). Effective depth estimated from the towed-array data superimposed with the profiler data.

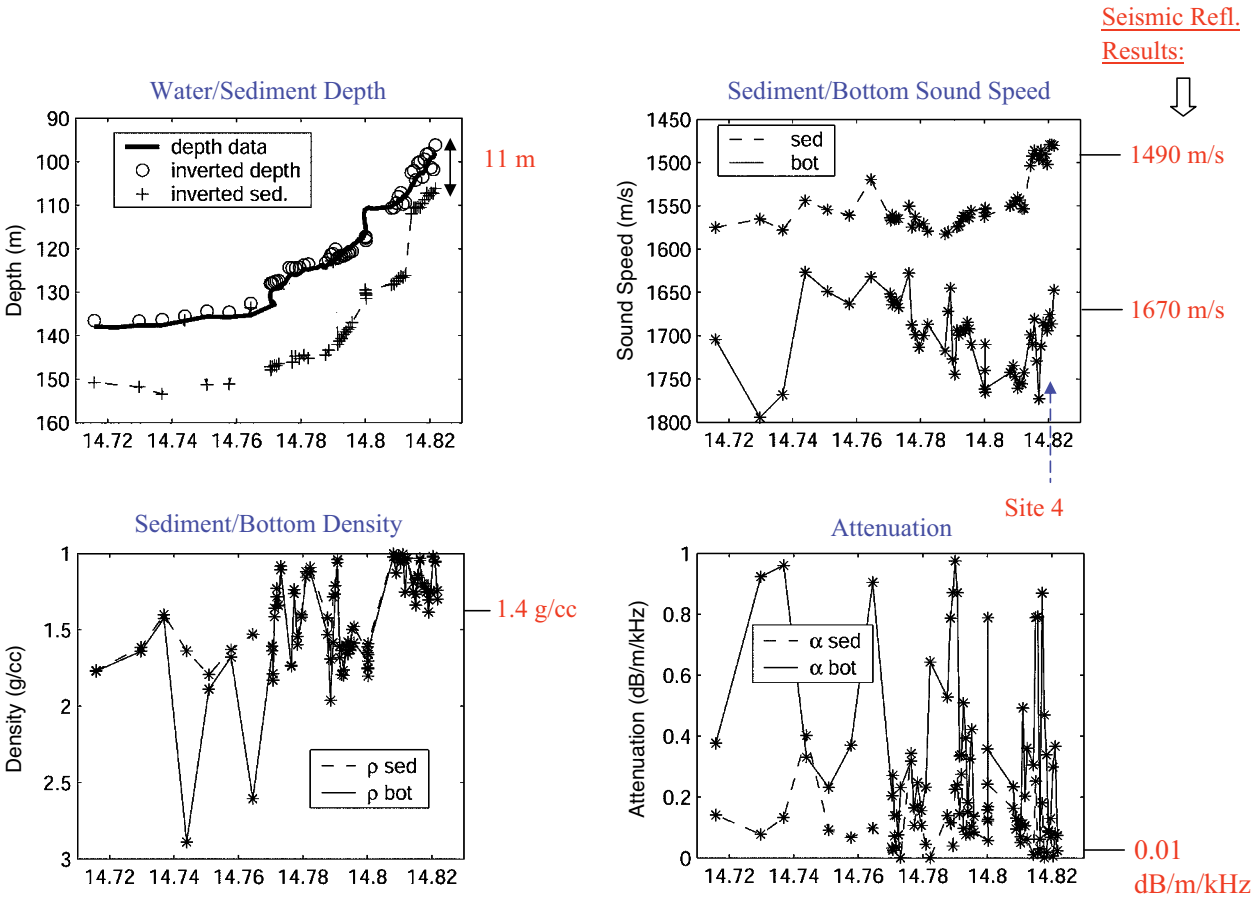

FIGURE 5
Geoacoustic inversion results for the water and sediment depth (upper left), sediment and bottom sound speed (upper right), sediment and bottom density (lower left) and sediment and bottom attenuation (lower right) along the track in longitude. The numbers on the right column are seismic reflection measurements at site 4.

References

[1] L.T. Fialkowski, T.C. Yang, K. Yoo, D.K. Dacol, and E. Kim, "Consistency and Reliability of Geoacoustic Inversions with a Horizontal Line Array," *J. Acoust. Soc. Am.*, in press.

[2] T.C. Yang, K. Yoo, and L. Fialkowski, "Sub-Bottom Profiling and Geoacoustic Inversion Using a Ship Towed Line," *Proceedings of Underwater Measurement and Technology Conference*, June 28-July 2, Crete, Greece (2005). ★

Seismo-Acoustics in Laterally Varying Media

M.D. Collins,[1] D.C. Calvo,[1] H.J. Simpson,[1] R.J. Soukup,[1] J.M. Collis,[2] E.T. Küsel,[2] D.A. Outing,[2] and W.L. Siegmann[2]

[1]*Acoustics Division*

[2]*Rensselaer Polytechnic Institute/Dept. of Mathematical Sciences*

Introduction: Many wave propagation problems in the geosciences involve a nearly stratified waveguide. When lateral variations in the medium (ocean, solid Earth, or atmosphere) are sufficiently gradual, outgoing energy dominates backscattered energy, and solutions can be obtained using an approximate wave equation that only accounts for outgoing waves.[1] This approach, which is known as the parabolic equation method, often improves efficiency by several orders of magnitude with no significant loss in accuracy. For example, outgoing solutions can be obtained in minutes for global-scale ocean acoustics problems[2] that would be out of the question to solve in terms of the full-wave equation.

Improved Techniques: The extension of the parabolic equation method to problems involving solid layers has been an area of great interest for nearly 30 years. Solid layers are governed by the elastic-wave equation and support two types of body waves and interface waves. This vector equation is more complicated than the scalar equation that governs acoustic waves, and the solutions are more prone to instabilities. Due to these difficulties, it was nearly 20 years

between the introduction of the parabolic equation method into ocean acoustics and its first successful application to problems involving elastic layers.[3]

For the past decade, there has been a focus on improving the accuracy of parabolic equation solutions when there are lateral variations in solid layers. One of the key developments in this area was to rederive the elastic parabolic equation in terms of a new set of dependent variables.[4] In order to facilitate the derivation of the parabolic-wave equation from the full-wave equation, it is necessary to choose the dependent variables so that they have certain symmetry properties. Otherwise, it is impossible to derive a parabolic-wave equation. The first derivations were based on an unconventional choice of variables. The fact that one of the variables is not continuous makes it difficult to handle interfaces between solid layers. The new formulation is also based on an unconventional choice of variables, but both of the variables are continuous, and this has made it possible not only to handle arbitrary layering, but also to handle lateral variations more accurately.

We have considered two approaches for handling lateral variations, and both of them have produced promising results. One of the approaches is based on rotating coordinates so that one of the coordinates is aligned with the interface. This approach has proven to be effective for handling a sloping ocean bottom, which is an important and difficult case. Appearing in Fig. 6 is a problem involving two types of interface waves that was solved with this approach. In this example, a Scholte wave propagates along the ocean bottom and onto the beach, where it becomes a Rayleigh wave. We are also developing approaches based on the original coordinate system that can handle a larger class of lateral variations. These approaches are based on making corrections to the field as the properties of the waveguide vary with range. Appearing in Fig. 7 is a seismic problem involving complex layering that was solved with this approach.

Comparison with Data: When possible, we compare parabolic equation solutions with solutions obtained by other means. Since such solutions are very limited, we have also made comparisons with data from tank experiments. Appearing in Fig. 8 is a comparison of the parabolic equation solution with data taken in a carefully controlled experiment involving a slab of poly vinyl chloride (PVC) that was suspended in a tank of water to model a sloping, elastic ocean bottom (Fig. 9).

[Sponsored by ONR]

References

[1] F.B. Jensen, W.A. Kuperman, M.B. Porter, and H. Schmidt, *Computational Ocean Acoustics* (American Institute of Physics, New York, 1994), pp. 343-412.

[2] B.E. McDonald, M.D. Collins, W.A. Kuperman, and K.D. Heaney, "Comparison of Data and Model Predictions for Heard Island Acoustic Transmissions," *J. Acoust. Soc. Am.* **96**, 2357-2370 (1994).

[3] M. D. Collins, "Higher-order parabolic approximations for accurate and stable elastic parabolic equations with application to interface wave propagation," *J. Acoust. Soc. Am.* **89**, 1050-1057 (1991).

[4] W. Jerzak, W.L. Siegmann, and M.D. Collins, "Modeling Rayleigh and Stoneley Waves and Other Interface and Boundary Effects with the Parabolic Equation," *J. Acoust. Soc. Am.* 117, 3497-3503 (2005).

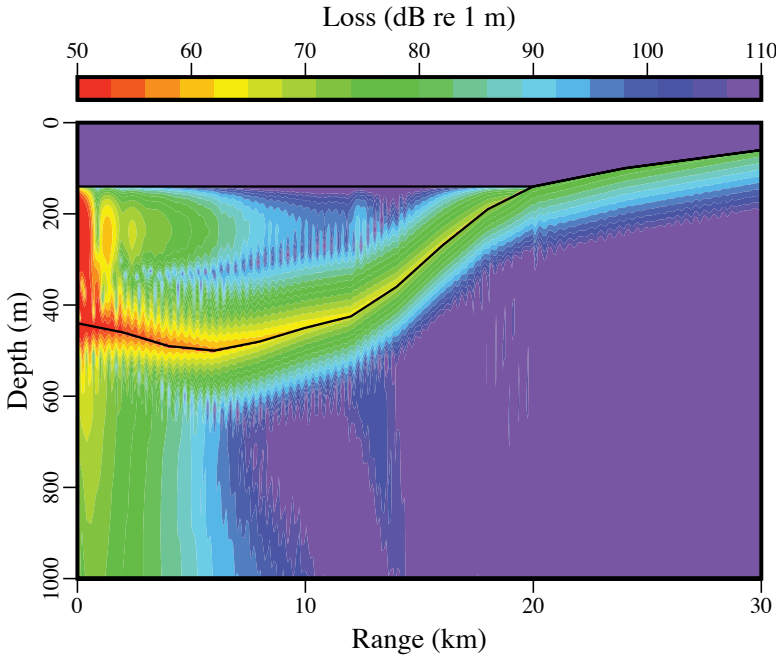

FIGURE 6
Propagation of a Scholte wave along the ocean bottom. This interface wave becomes a Rayleigh wave beyond the beach.

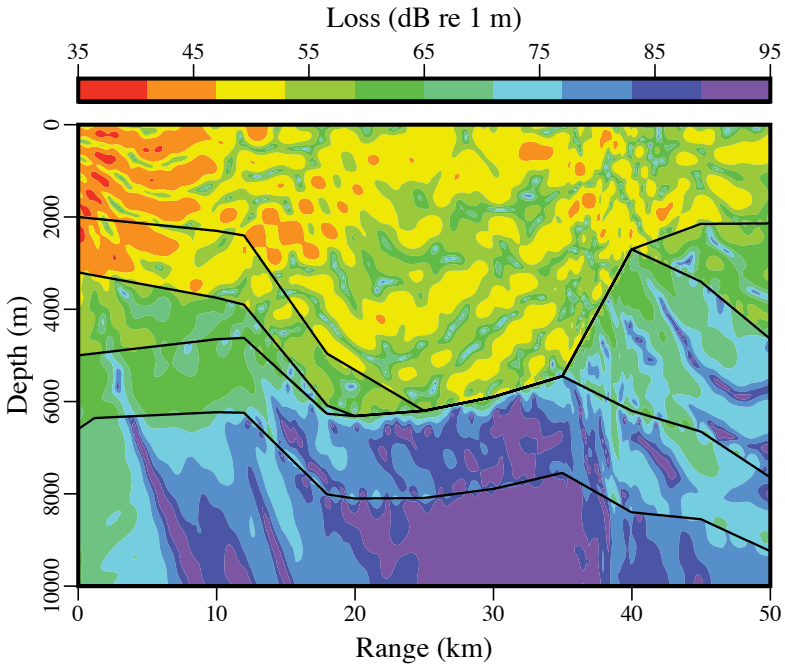

FIGURE 7
Elastic wave propagation in a medium with complex layering. This plot only shows the compressional wave energy.

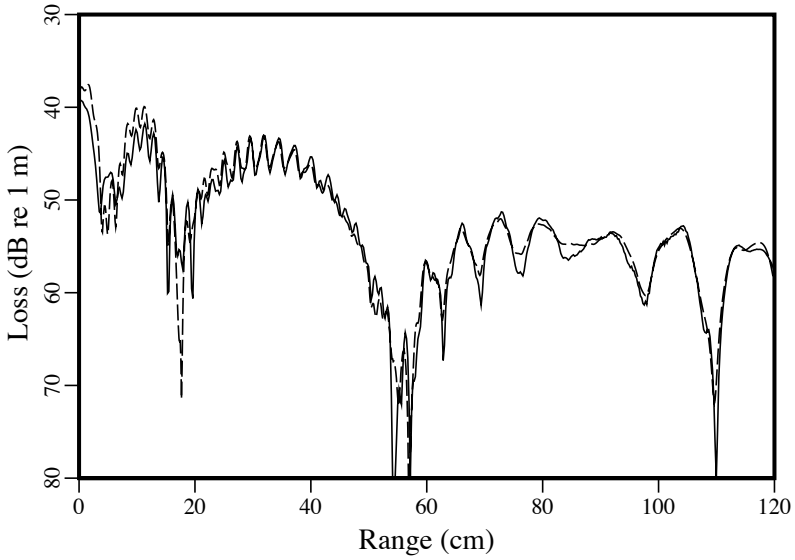

FIGURE 8
Comparison between model results (dashed curve) and tank data (solid curve) along a line at constant depth. The frequency is 225 kHz.

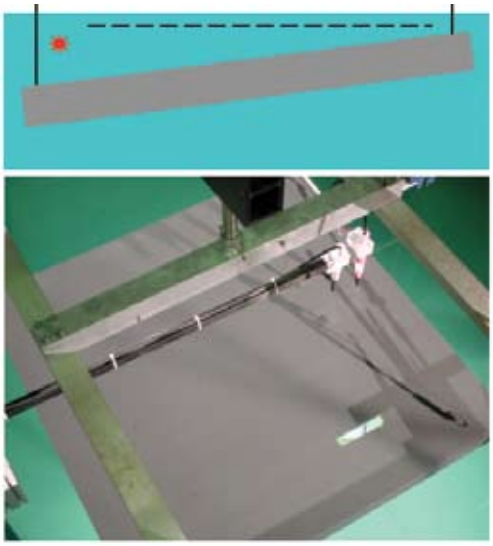

FIGURE 9
Geometry of the tank experiment.

Acoustic Propagation Through Surface Ship Wakes

S. Stanic,[1] T. Ruppel,[1] and R. Goodman[2]
[1]*Acoustics Division*
[2]*University of Southern Mississippi*

Introduction: A ship's wake is a mixture of bubbles and turbulent seawater generated by a ship's hull and its cavitating propellers. These bubble clouds are a common feature of all ship wakes, and the entrapped air bubbles are responsible for the lingering acoustic signatures of a ship's wake. It is well known that bubbles, even in small amounts, cause considerable frequency-dependent changes in the speed of sound and absorption. These bubble-cloud characteristics are driven by the type of ship, its speed, and local oceanographic conditions.

As the wake ages, it goes from a violent breakup and mixing of bubbles due to turbulence to one where, as the turbulence decays, the bubbles begin to rise toward the surface due to their buoyancy and the changes in the buoyancy of the water mass. It is clear that since bubbles of different sizes rise at different rates, as the wake ages, the horizontal and vertical distributions of bubble densities result in changes to both sound-speed profiles and absorption within the wake. These frequency-dependent sound-speed profiles have dramatic effects on propagating acoustic signals.

Field Measurements: A series of across-the-wake acoustic absorption measurements were taken in the summer of 2004. A 10-meter-long, 8-element receiving array and broadband source were towed by separate ships on either side of a wake generated by a small Naval vessel traveling at 15 kt. The vessel, a YDT, was provided by NAVDIVESALVTRACEN Panama City, Florida. The YDT is 131 ft long, 26.6 ft wide, has a draft of 4.95 ft, and displaces 173 light tons.

Figure 10 shows the source-receiver measurement configuration and the receiving array tow ship. The wake width is approximately 10 m and the distance between the measurement systems is 150 m. This range is monitored by a laser system and recorded. The measurement systems are towed at a speed of 4.5 kt. The signal repetition rate of 1 s gave an across-the-wake absorption measurement every 7.5 m.

Figure 11 shows the average acoustic absorption across the wake for a number of frequencies as a function of distance from the time the measurement

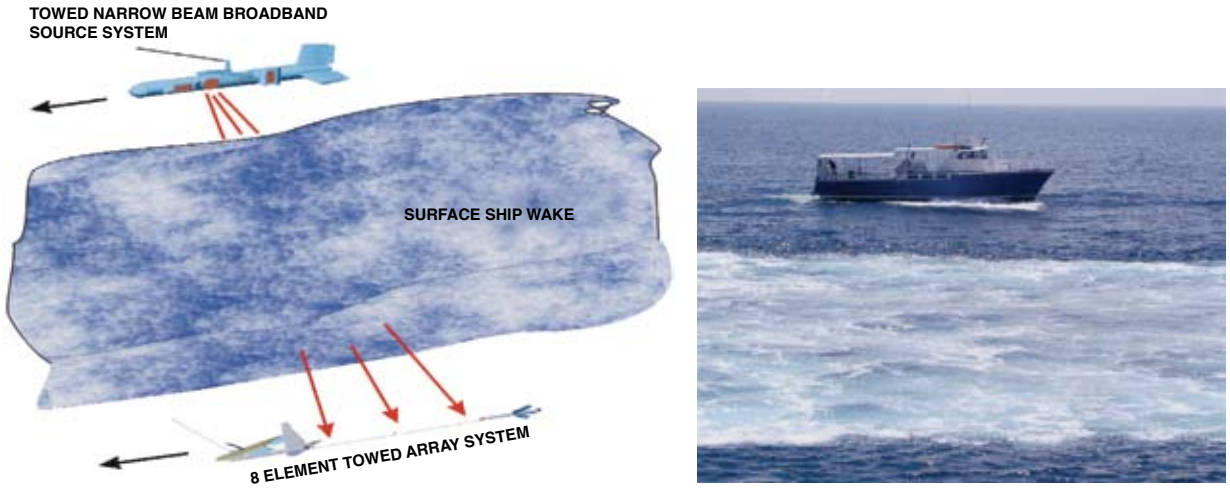

(a) (b)

FIGURE 10
(a) Measurement configuration and (b) generated wake and array tow ship.

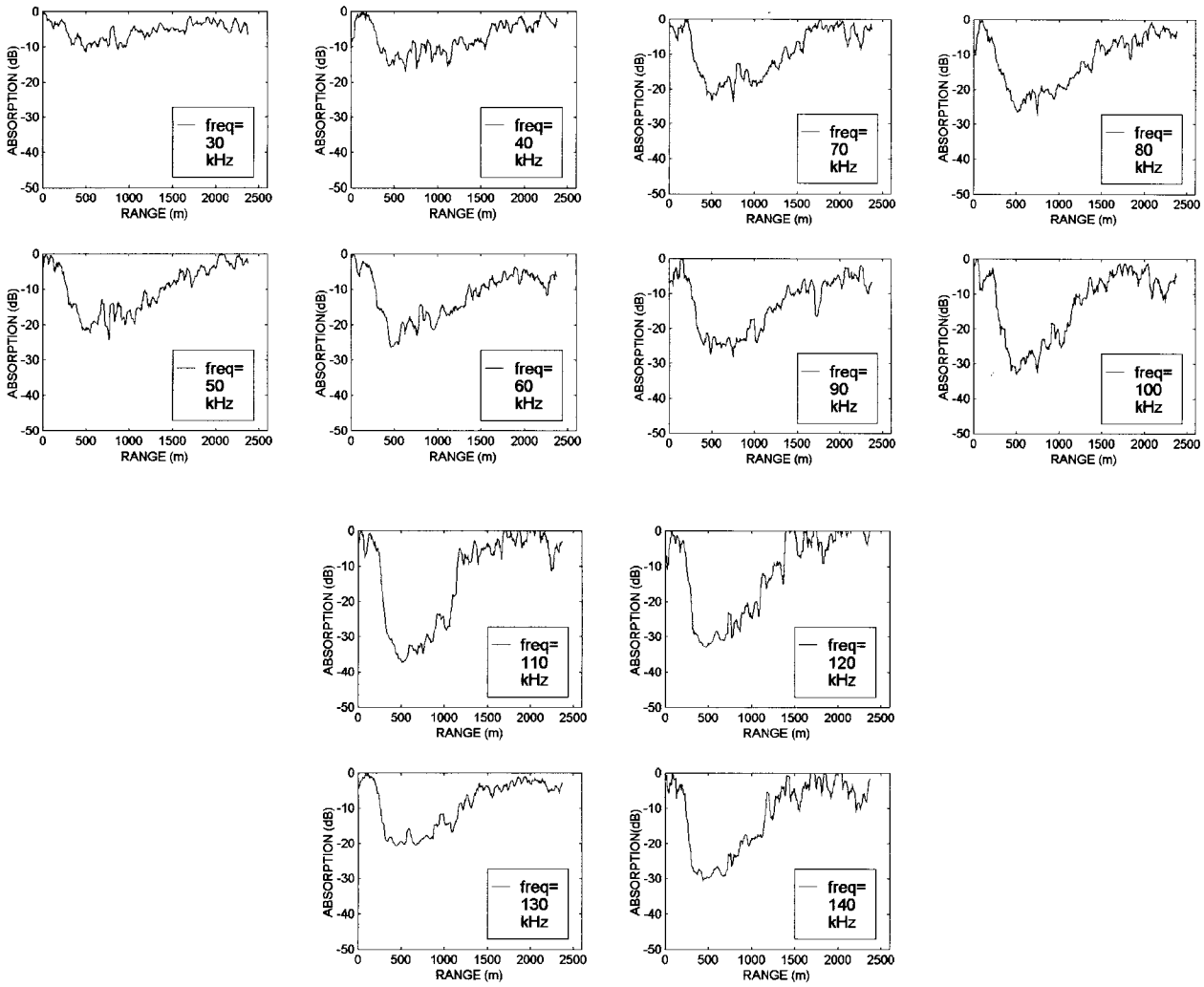

FIGURE 11
Average signal absorption as a function of range and frequency.

sequence began. The maximum absorption clearly occurs at a range of about 500 m after the start of the measurement sequence. This was the most intense part of the wake that occurred about 20 m behind the YDT. The average across-the-wake absorption levels returned to the nonbubble background levels at a distance of about 2 km. In these measurements, the maximum absorption occurs at a frequency of 100 kHz, suggesting a large number of 30-µm-diameter bubbles in that part of the wake.

From the absorption measurements, the void fractions and the sound velocities were calculated for a 10-m deep wake. Figure 12(a) shows the frequency-dependent sound velocity profiles at 5, 20, 60, and 120 kHz that were derived from the absorption measurements and a simple model for the vertical dependence of the bubble densities.

Figure 12(b) shows the ray plots for a source located at a depth of 10 m, which is near the lower portion of the wake. These ray plots clearly show the dispersive effects of the sound velocity profiles. For launch angles of 2.5° and 20°, and at frequencies of 5, 20, and 60 kHz, the acoustic conditions are clearly upward-refracting, while at a frequency of 120 kHz, the conditions are downward-refracting.

Summary and Impact: NRL has developed a method for providing valuable data and performance estimates for target detections in and below a surface ship wake. The varying vertical and horizontal distribution of bubbles and the corresponding fluctuating absorptions provide insight into target detections in and below a surface ship wake.

[Sponsored by ONR] ★

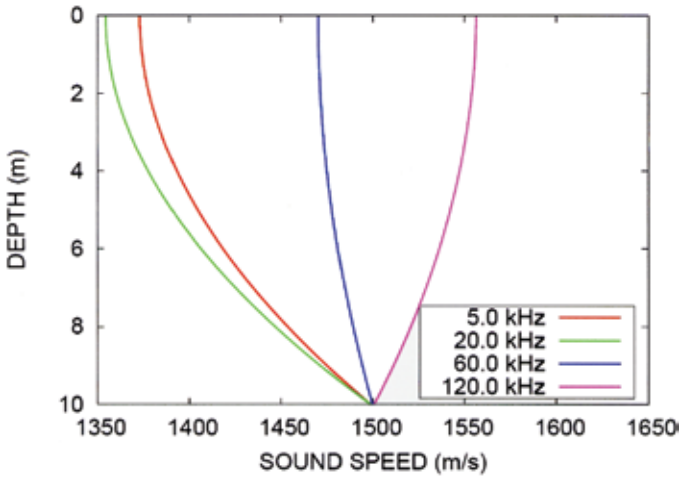

(a)

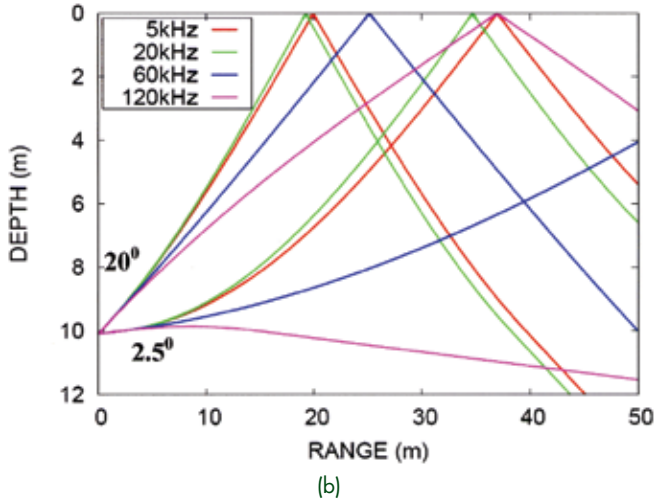

(b)

FIGURE 12
(a) Calculated frequency-dependent sound velocity profiles. (b) Ray paths corresponding to the different sound velocity profiles at launch angles of 2.5° and 20°.

The Principles of Fracture Mechanics

Achievement: Fracture mechanics is a field that recognizes that all structures are manufactured with, or will ultimately contain, flaws that govern the eventual failure of the structure. The study of the stresses caused by the flaws, and the material's resistance to failure from them, forms the basis for the field of fracture mechanics. Fracture mechanics permitted, for the first time, the capability to calculate the strength of structures containing defects, which inevitably occur in fabrication or during service operation. The net result of these new design principles increased the reliability of structures due to improved design capability and an improved predictive capability of in-service damage.

NRL's G.R. Irwin is recognized as the pioneer of modern fracture mechanics. He developed the scientific principles for understanding the relationships between applied stresses and cracks or other defects in metallic materials. Irwin developed, around 1947, the concept that fracture toughness should be measured in terms of resistance to crack propagation. Critical values of the stress intensity describing the onset of fracture, the commencement of environmental cracking, and the rate of fatigue crack growth were established later.

As a consequence of Irwin's scientific work, fracture mechanics is now taught in many graduate schools and remains an active field of R&D today.

Impact: Using these fracture-safe design principles, NRL assisted in the solution of many important military and commercial problems, for example, by solving the catastrophic failures in commercial jet aircraft in 1953, and the fracture problems experienced by the Polaris and Minuteman missile programs in 1957. Fracture mechanics has been applied throughout the world for the design of any structures where sudden, catastrophic failure would cause loss of life or other serious consequences. Examples include nuclear reactor pressure vessels, submarines, aircraft and missiles, and tanks for storage of toxic or flammable materials.

Thermal Dip Pen Nanolithography

P.E Sheehan,[1] W.P. King,[2] A.R. Laracuente,[1] M. Yang,[1,3] and L.J. Whitman[1]
[1]*Chemistry Division*
[2]*Georgia Institute of Technology*
[3]*NRL/NRC Postdoctoral Research Associate*

Introduction: The steady shrinking of integrated circuits demands constant innovation. Though ever-greater resolution remains the foremost goal, many new abilities are also needed—the reduction of toxic by-products ("green chemistry"), integration of heterogeneous materials (e.g., organic and inorganic) into a single structure, and the production of just a few integrated circuits at low cost. We are developing a new lithographic approach, thermal Dip Pen Nanolithography (tDPN), to both achieve greater resolution and address many of these secondary needs.[1,2]

Although tDPN can create nanoscale structures, in principle it works as simply as a soldering iron. The heart of the device is a custom-fabricated *heatable* atomic force microscope (AFM) tip, coated with a material (i.e., the "solder" or "ink") that is solid at room temperature. When melted, the ink flows from the tip onto the surface (Fig. 1). The use of meltable inks has many benefits. Since the ink's fluidity is controlled by the tip temperature, writing may be turned on or off and the deposition rate easily varied. Secondly, one can write new layers on top of previously deposited—now solid—layers to create complicated three-dimensional structures. Finally, tDPN can be performed in vacuum, making it compatible with conventional semiconductor device fabrication.

Current Capabilities of tDPN: We have used tDPN to deposit metals, polymers, and self-assembling monolayers. The technique is particularly powerful for polymer deposition. Because tDPN requires only that the polymer melt before it decomposes, a wide range of polymers may be used. To date, an insulating polymer, Mylar, and two conducting polymers, MEH-PPV and PDDT, have all been successfully deposited.

An important aspect of tDPN is that ink can be deposited with sufficient thermal energy to organize into well-formed monolayers before solidifying. This capability is illustrated in Fig. 2, which shows the deposition of poly(3-dodecylthiophene) (PDDT), a conducting polymer used in organic-based electronics. The coated tip was heated and scanned over a rectangular area to deposit a polymer film, precisely a *single* molecular layer thick onto the SiO_2 substrate. A second pass added a second monolayer without disturbing the first. The stepwise nature of the deposition is clearly seen in the averaged cross-section (Fig. 2(b)). The thickness of each layer is 2.5 nm—the expected thickness for the polymer in the preferred high-conductivity orientation. The smallest features we have written are about 75 nm wide, most likely limited by the sharpness of the current generation of cantilevers (which are relatively dull at approximately a 100-nm radius of curvature). Newer, sharper tips promise even finer features. Nonetheless, such exquisite control over polymer deposition—nanoscale widths and molecular layer thickness control—cannot be achieved by any other additive patterning method.

The large temperature range of the cantilevers, up to 1000 °C, allows many different inks to be used. Our exploration of high-melting-point inks has recently led to the writing of indium metal. As shown in Fig. 3, we have used tDPN to write narrow (< 80 nm) indium metal lines onto glass and silicon substrates. Though many methods have been used to create nanoscale metal lines, it is exceedingly difficult to make them continuously conductive. We wrote an In wire between gold electrodes and measured its resistance in NRL's unique Nanomanipulation and Nanocharacterization Facility. Ohmic contact was achieved, although the conductance was indicative of indium oxide (which is also a conductor). Nanoscale chemical analysis in the Facility confirmed the composition as indium oxide, as expected for an In nanowire deposited on a bench-top apparatus in laboratory air.

The Future for tDPN: Full realization of tDPN will require massively parallel lithography. Fortunately, arrays of 4,096 individually controlled thermal cantilevers, similar to ours, have already been fabricated by

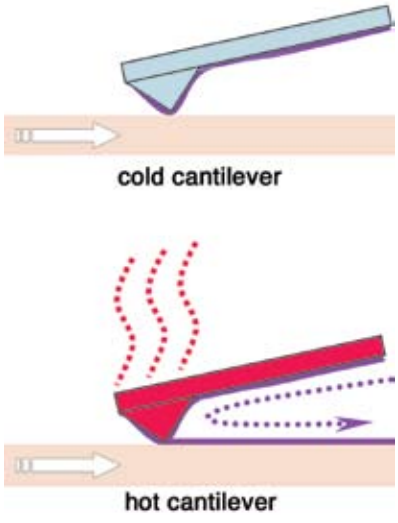

FIGURE 1
Scheme of Thermal Dip Pen Nanolithography. When the cantilever is cool, the ink is solid and does not flow. When the cantilever is heated, the ink melts and flows from the tip onto the surface. Moving the tip writes the ink pattern.

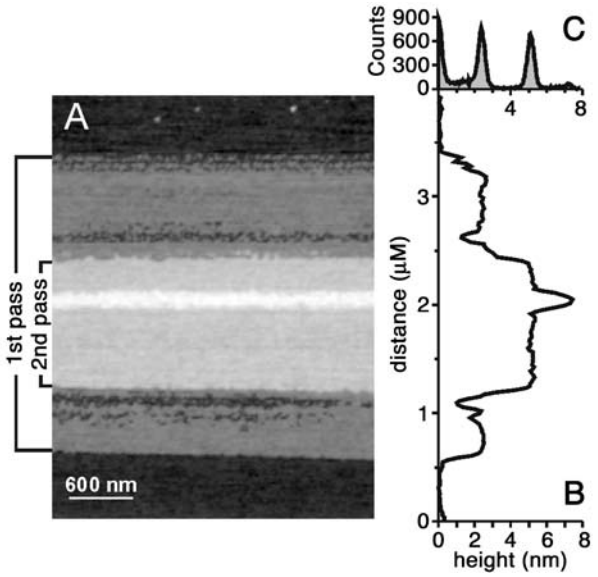

FIGURE 2
(a) Tapping-mode AFM image of a PDDT film deposited on SiO_2. The PDDT pre-coated tip was rastered at 5 μm/s with 47 nm/line while heated above PDDT's melting temperature. The outer pattern resulted from the first pass, which deposited a single monolayer. After 50 s, a second (rectangular) scan deposited a second monolayer without disturbing the first. (b) The average height profile; discrete height changes are apparent for each layer. (c) Height histogram of the film with peaks at 0, 2.4, 5.1, and 7.3 nm.

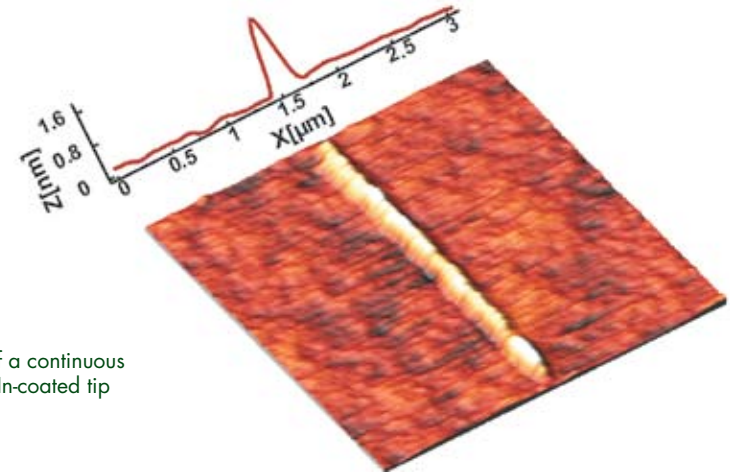

FIGURE 3
A topographic AFM image of a continuous nanowire deposited from an In-coated tip onto a glass substrate.

IBM for use in the "Millipede" memory storage system. Thermal cantilevers may be designed to give rapid heating (1 to 20 μs) and cooling (1 to 50 μs) times. Thus, rapid and highly parallel patterning of surfaces should be possible. Given tDPN's ability to deposit insulators, semiconductors, and conductors, it should one day be possible to write integrated circuits directly using an inexpensive, bench-top apparatus.

Although the immediate benefits of using a multipen tDPN to write integrated circuits will be nanoscale resolution and wafer-scale patterning, we expect many other benefits. For instance, unlike conventional fabrication methods, which etch away material to create small features, tDPN is an additive technique, which requires very little ink to create nanoscale devices. Therefore, the use of expensive inks can be kept to a minimum and the generation of toxic etchant wastes can be greatly reduced. Secondly, tDPN's robust deposition process enables the writing of many different materials onto many different substrates, a key capability needed for heterogeneous integration in microelectronics. Finally, multipen writing should be ideal for the fabrication of low numbers, hundreds to thousands, of integrated circuits without the billion-dollar development costs currently associated with integrated circuit fabrication. This capability, in particular, will be important to a low-volume, high-value customer such as the Department of Defense.

[Sponsored by DARPA and ONR]

References

[1] P.E. Sheehan, L.J. Whitman, W.P. King, and B.A. Nelson, "Nanoscale Deposition of Solid Inks via Thermal Dip Pen Nanolithography," *Appl. Phys. Lett.* **85**, 1589 (2004).

[2] B.A. Nelson, W.P. King, A.R. Laracuente, P.E. Sheehan, and L.J. Whitman, "Direct Deposition of Indium Metal Using Thermal Dip-Pen Nanolithography," *Appl. Phys. Lett.*, in press. ★

Chemical Sensors from Carbon Nanotubes

F.K. Perkins, E.S. Snow, and J.A. Robinson
Electronics Science and Technology Division

Introduction: There exists a clear need in the Department of Defense for small, sensitive, and rapid-response sensors of dangerous chemicals and explosives. To address this need, we are developing devices based on random networks of single-walled carbon nanotubes (SWNTs).[1] The carbon nanotube, a carbon phase that can be described as a hollow tube one nanometer in diameter, one atom thick, and several microns long, is very nearly an ideal material for sensor applications: it is highly nonreactive while at the same time all of the electronically active area is at the surface. We have found that SWNT network-based transducers rapidly and reversibly respond to a wide spectrum of dilute chemical vapors. We are working with colleagues in the Materials Science and Technology Division to improve the specificity of the devices and to turn this novel transducer design into a fieldable and useful sensor technology.

Carbon nanotubes were initially discovered about a dozen years ago. Demonstration of sensitivity of single nanotube conductance to ambient species was only six years ago. However, such single nanotube devices are difficult and expensive to fabricate. A key innovation of our laboratory is the use of networks of randomly grown nanotubes as the active sensor material.[2] Such SWNT network sensors can be fabricated with high yield by using conventional microfabrication technology (Fig. 4). Additionally, the use of SWNT networks dramatically reduces the level of $1/f$ noise, a critical factor for sensor applications, but an intrinsic feature of nanoscale electronic materials.

Transducer Physics: We test the transducer by blowing dilute concentrations of vapor in air from various liquids and solids across the active area and monitoring the capacitance C between the network and the substrate as well as the conductance G across the network.[3] We observe a C and G response to nearly all analytes tested, and further that these responses increase monotonically and smoothly with concentration over a wide range (Fig. 5). Further study has revealed that the dominant physical mechanism behind sensitivity to ambient is adsorption of species on the surface of the nanotubes. Surface coverage by adsorbed species is related not to the concentration of species in the ambient (i.e., the partial pressure P), but rather to the fraction of the equilibrium vapor pressure P/P_0. In other words, our transducer responds to analytes not according to their local abundance (P) but according to their likelihood of condensing on a surface (P/P_0). As a result, our sensor responds equally well to both high and low vapor pressure materials. Since the low vapor pressure of many materials of interest, such as nerve agents, blister agents, and explosives, has made their detection by conventional sensors a challenge, this indicates an area where our sensor offers unique capabilities. Furthermore, equilibrium between surface adsorbates and ambient is rapidly established, implying subsecond response times (which we observe).

Changes in C are primarily associated with the intrinsic dipole moment of the analyte. Changes in G are primarily due to charge transfer interactions between the analyte and the nanotube. The ratio of these two terms is a constant for a given analyte, and can be used to distinguish even closely related species. In Fig. 6, we show that the response of the transducer to doses of $(CH_3O)_2P(O)CH_3$, a simulant for a nerve agent, and structurally similar $(CH_3O)_2P(O)H$, produces two distinct C to G ratios. Thus, the transducer can be used to match a response to a library of values from known materials.

In an effort to increase both sensitivity and specificity, we have modified our devices by applying thin films of certain sorbent polymers or self-assembled monolayers. Many of these materials were developed by the NRL Materials Science and Technology Division for use in surface acoustic wave sensors, and are known to be highly efficient and selective concentrators of materials out of vapor phase. Work in this area is ongoing.

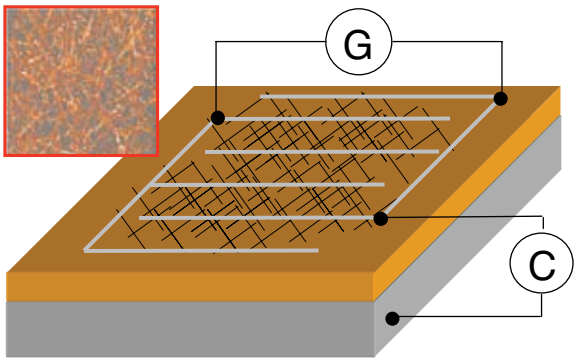

FIGURE 4
Schematic of transducer design and measurement configuration, with an atomic force microscope (AFM) image of the SWNT network shown as an inset. The tubes are about 1 nm in diameter.

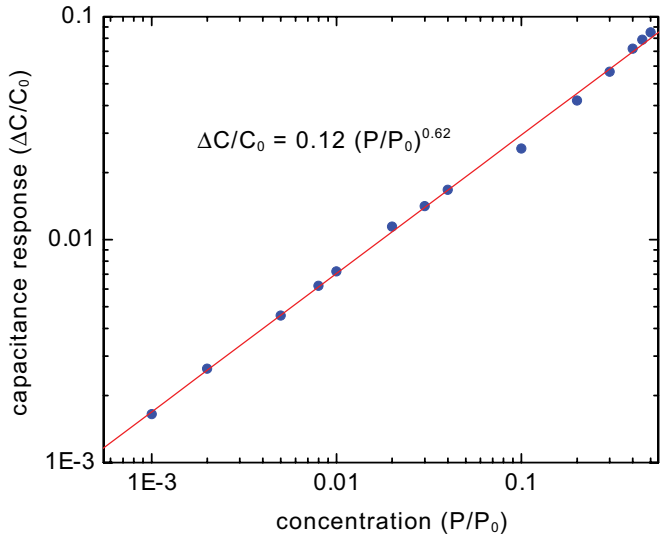

FIGURE 5
Measurements of transducer capacitance response $\Delta C/C_0$ vs fraction of equilibrium vapor pressure for acetone, along with a best fit for a power-law relationship. Our noise floor for $\Delta C/C_0$ is conservatively established as 10^{-4}. This implies a minimum detectable level of $P/P_0 = 1 \times 10^{-5}$ for this material.

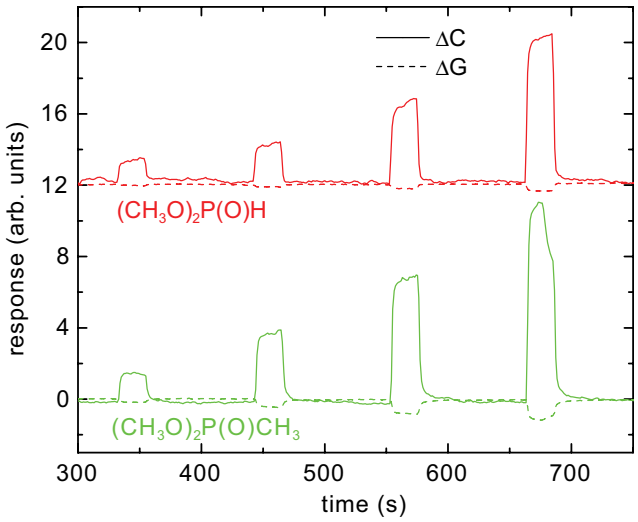

FIGURE 6
Capacitance *C* and conductance *G* responses at four different concentrations for two similar materials. The ratio of *C* and *G* is constant over the concentrations shown, but different for the two materials: –0.04 for DMPH and –0.12 for DMMP, after appropriate normalizations.

Summary: We have found these devices to be rapid and sensitive transducers of chemical exposure, generally exceeding performance of existing commercial devices meeting the same application niche. They are easy to manufacture in large quantities. Strategies are in hand to increase discrimination of agents. Integration with existing sensor units is currently under development, in collaboration with the Materials Science and Technology Division.

References

[1] E.S. Snow, F.K. Perkins, E.J. Houser, S.C. Badescu, and T.L. Reinecke, "Chemical Detection with a Single-Walled Carbon Nanotube Capacitor," *Science* **307**(5717), 1942-1944 (2005).
[2] E.S. Snow, J.P. Novak, and P.M. Campbell, "Interconnected Networks of Single-Walled Carbon Nanotubes" U.S. Patent No. 6,918,284.
[3] E.S. Snow and F.K. Perkins, "Capacitance and Conductance of Single-Walled Carbon Nanotubes in the Presence of Chemical Vapors," *Nano Letters* **5**(12), 2414 -2417 (2005). ★

Self-Assembled Modular TNT Biosensor

I.L. Medintz,[1] E.R. Goldman,[1] A.W. Kusterbeck,[1] and J.R. Deschamps[2]
[1]*Center for Bio/Molecular Science and Engineering*
[2]*Laboratory for the Structure of Matter*

Introduction: Increasing demand is being placed on the biosensor community to deliver sensors for military and security purposes. The Navy and Homeland Security are particularly interested in detecting explosives underwater, especially in marine and port environments. Rather than developing a unique sensor for each analyte of interest, a generalized sensing strategy that is readily adaptable to a variety of small analytes in many challenging environments would be extremely useful, but this has been lacking until now. We developed a general biosensing strategy that is based on a modular design and employs multifunctional surface-tethered components. Biosensors built on this strategy are designed to be fully reversible, reagentless, and capable of self-assembly on surfaces.[1] The first prototype targeted the nutrient sugar maltose and utilized *E. coli* maltose binding protein and a flexible biotinylated DNA oligonucleotide that contained both a fluorescent dye and an analog of maltose.[1] A key criterion in the overall sensor design is modularity with the idea of facile adaptation to target other analytes. We demonstrate here that this same self-assembled modular-sensing strategy can be applied for the sensitive and specific detection of 2-, 4-, and 6-trinitrotoluene (TNT) in aqueous environments.[2]

Sensor Self-Assembly and Function: The TNT sensor consists of a dye-labeled, TNT-binding, single-chain antibody fragment (α-TNT scFv), which interacts with a multifunctional DNA arm. The arm contains a TAMRA dye attached to a modified internal base and is terminally labeled with the TNT analog 1,3,5-trinitrobenzene (TNB), (Fig. 7). The α-TNT fragment, dye-labeled with AlexaFluor 532 dye on a unique cysteine residue, is allowed to bind the TNB analog on the DNA arms' terminus, bringing both the AlexaFluor and TAMRA dyes into close proximity and establishing a baseline level of fluorescence resonance energy transfer (FRET). In this configuration, selective excitation of the AlexaFluor donor dye results in significant energy transfer to the TAMRA acceptor dye. This complex is then self-assembled on a NeutrAvidin (NA) covered microtiter well. Addition of TNT to the sensor solution displaces the TNB from the α-TNT fragment binding site, altering the proximity of the dyes and resulting in a concentration dependent change in FRET, which is monitored for signal transduction. The sensor can be washed free of analyte and regenerated for subsequent detection events.[2]

Sensor Testing and Specificity: TNT was tested for in phosphate buffered saline (PBS), a matrix more saline than seawater (Fig. 8). The resulting loss of FRET-based fluorescence at 600 nm was plotted against the concentration. A lower limit of detection of 1 mg/L TNT (1 ppm) was noted for this sensing assembly. The binding curve appears as a relatively linear function over the concentrations tested. The sensor assembly was washed using 10 volumes of PBS and then regenerated in PBS. A second TNT titration was performed; the sensor was washed, regenerated for 1 hr at room temperature, and then a third titration was performed. Similar control experiments were performed using sensor assemblies, incorporating a dye-labeled DNA arm, lacking the TNB moiety by substituting a control myoglobin protein, which resulted in no change in fluorescence upon TNT addition.

To determine specificity and cross-reactivity, sensor assemblies were tested against several TNT structural analogs (Fig. 9). TNB, used for the original antibody fragment selection, elicited the highest sensor response and was the most effective competitor for binding sites. Other explosives tested included RDX (hexahydro-1,3,5-trinitro-1,3,5-triazine) and 2-amino 4,6 DNT (2-amino-4,6-dinitrotoluene), which caused significantly less response. The least response was seen with 2,4 DNT. The dynamic sensing range of this sensor assembly was modulated by "stiffening" the tether arm through the addition of a DNA complementary to the DNA linker (Fig. 7(b)). Although the binding constant essentially remained the same, the binding curve of the modulated prototype became broader, significantly increasing the useful sensing range. The lower limit of TNT detection dropped approximately tenfold from 1 mg/L to 0.1 mg/mL (100 ppb). This sensitivity approaches that of whole antibodies, selected specifically against TNT, but whose bulk size has precluded use in the current sensor configuration.

Discussion: The TNT sensing assembly demonstrated here has several desirable features. These include the use of robust avidin-biotin chemistry for surface tethering, ease of self-assembly in a microtiter plate format, and analysis by readily accessible fluorescent plate readers. The sensor can be regenerated for subsequent reuse and an upper limit of 6 to 8 regenerations was obtained. This also suggests that real-time sensing in a flow cell is feasible. The current results validate the modular nature and adaptability of the sensor design. Comparison to the original maltose sensor[1] confirms the design can easily be adapted to target another analyte and yet remain functionally robust. The many choices of biorecognition elements available, including other binding proteins, receptors and antibody fragments that can fit directly into the current format, suggest that this design could be easily adapted to

FIGURE 7(a)
Schematic of the modular biosensor illustrating its targeting of the explosive TNT. The sensor consists of two modules: (1) the biorecognition module, a single-chain antibody fragment specific for TNT (α-TNT scFv); and (2) a modular arm (DNA). Both modules are specifically attached to a surface in a particular orientation using biotin-avidin chemistry and metal-affinity coordination. The surface of the microtiter well plate is coated with NeutrAvidin (NA), and the dye-labeled TNB DNA arm (2. modular arm) is attached to the NA via complementary hybridization to a biotinylated flexible DNA linker. The dye-labeled α-TNT scFv (1. biorecognition module) is attached to the surface with Bio-X-NTA (Biotin-spacer-nitrilotriacetic acid), coordinating the fragments 12-histidine residues and orienting the protein on the NA. Both modules are added together in equimolar amounts and then self-assembled on the surface to form the final sensor. ScFv binding of the TNB analog brings the protein-located dye and DNA-located dye into close proximity, establishing efficient FRET. Addition of TNT displaces the TNB analog and DNA arm disrupting FRET in a concentration dependent manner. The sensor is washed and regenerated for subsequent detection events. Rigidifying the DNA arm can modulate or usefully improve the dynamic sensing range.[1,2]

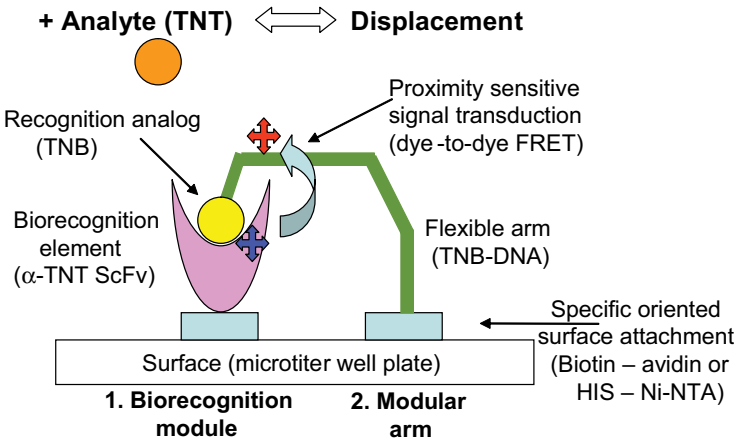

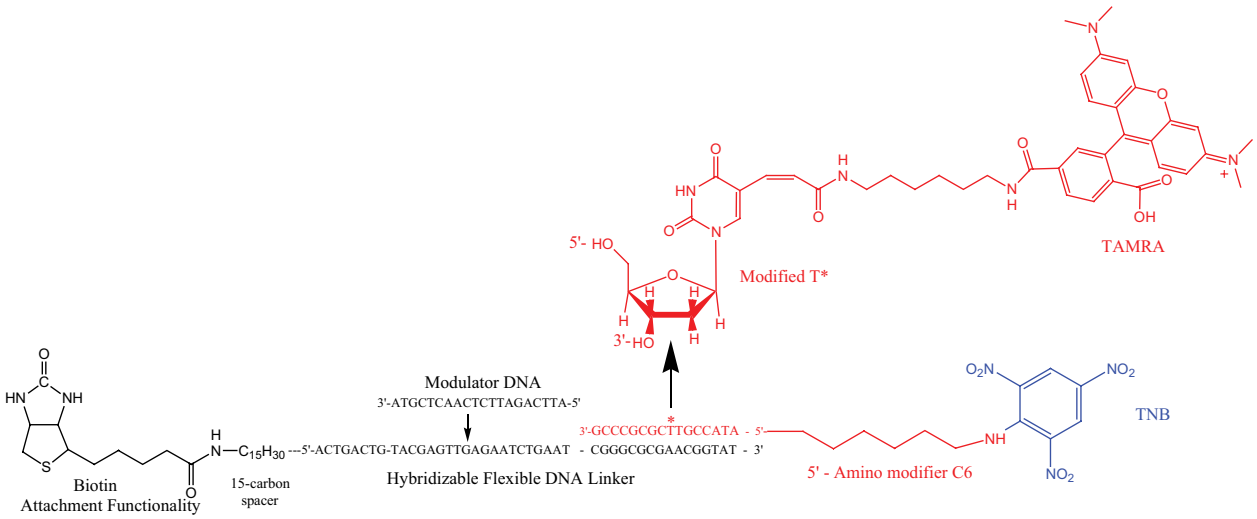

FIGURE 7(b)
Structure of the dye-labeled TNB DNA arm. The precursor DNA modified with a TAMRA dye on an internal T* and the 5′ amino modifier C6 is shown in red. The amine was subsequently modified with TNB (blue). The flexible DNA linker and modulator DNA aligned with its complement are shown in black. Hybridization of the linker to the TNB containing oligonucleotide completes the arm and allows it to be attached to the NA surface by the biotin.[2]

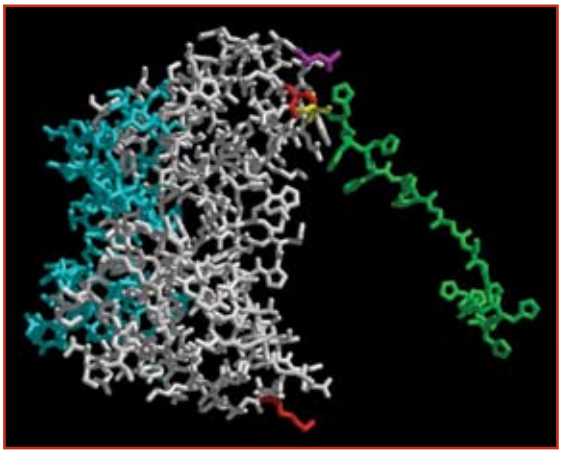

FIGURE 7(c)
Model structure of the α-TNT scFv fragment. The $(His)_6$-spacer-$(His)_6$ carboxy terminus is shown in green. The sites of cysteine mutations tested are shown in yellow, red, and magenta. Only the magenta site yielded a viable fragment. The "TNT binding region" as defined by the hypervariable regions of the scFv is colored cyan.[2]

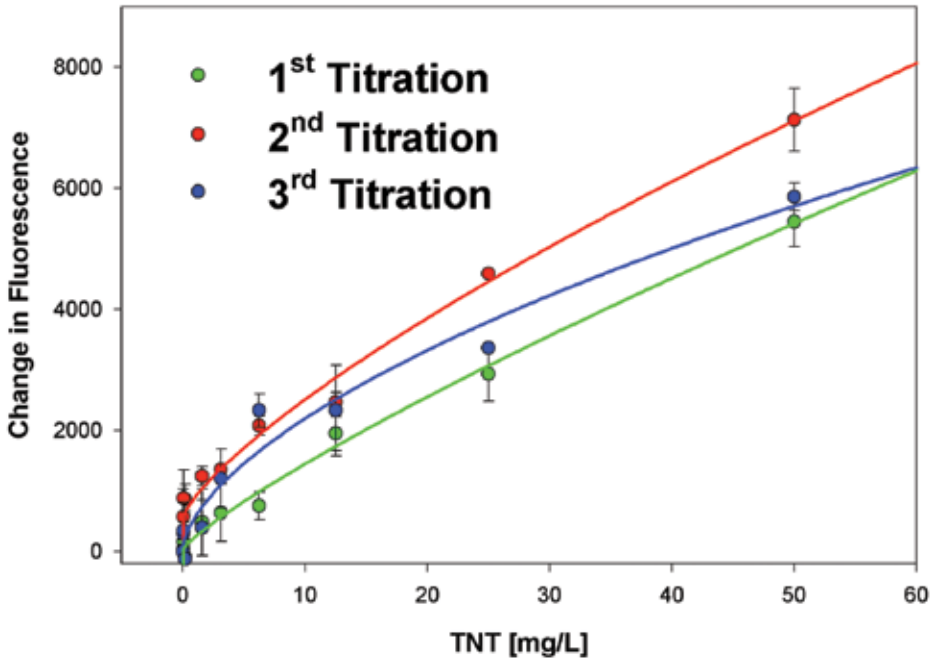

FIGURE 8
Repetitive testing of the sensor assembly with TNT. The sensor was self-assembled, challenged with TNT, washed, regenerated, and tested again. Samples were excited at 510 nm and emission monitored at 600 nm. The change in fluorescence is plotted on the vertical axis versus TNT concentration in the horizontal axis. TNT concentrations are in mg/L, which corresponds to ppm. In this configuration, a maximum of 6 to 8 consecutive sensings were attained.[2]

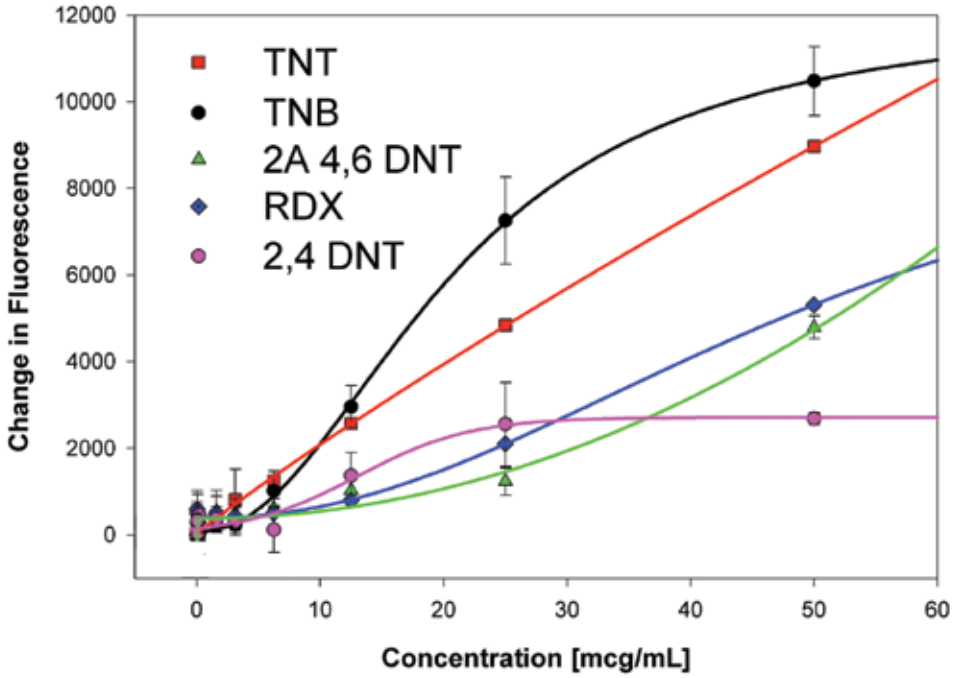

FIGURE 9
Sensor specificity. Sensor assemblies were tested against the indicated explosives. Only TNT and its closest analog TNB resulted in significant changes in sensor fluorescence. As the antibody fragment was generated against TNB it resulted in the largest changes.[2]

target further analytes. Experiments with the original maltose-sensing prototype showed that sensor assemblies could be dried, stored, and reconstituted for later use. This would allow sensors to be manufactured in one location and reconstituted for use at other locations or remote field sites. Multianalyte or "multiplex" sensing formats that screen for multiple analytes may also be possible. Current research is focused on adapting this sensor to target other analytes of priority to the Navy.

Acknowledgments: The authors acknowledge NRL base funding and thank Andrew Hayhurst of the Southwest Foundation for Biomedical Research for providing the original single-chain antibody fragment. Figures reprinted with permission from the American Chemical Society.

[Sponsored by ONR]

References

[1] I.L. Medintz, G.P. Anderson, M.E. Lassman, E.R. Goldman, L.A. Bettencourt, and J.M. Mauro, "General Strategy for Biosensor Design and Construction Employing Multifunctional Surface-Tethered Components." *Anal. Chem.* **76**, 5620-5629 (2004).

[2] I.L. Medintz, E.R. Goldman, M.E. Lassman, A. Hayhurst, A.W. Kusterbeck, and J.R. Deschamps, "Self-Assembled TNT Biosensor Based on Modular Multifunctional Surface-Tethered Components." *Anal. Chem.* **77**, 365-372 (2005). ★

TNT Detection Using Multiplexed Liquid-Array Displacement Immunoassays

G.P. Anderson,[1] P.T. Charles,[1] I.L. Medintz,[1] E.R. Goldman,[1] M. Zeinali,[1] C.R. Taitt[1] and S.C. Moreira[2]
[1]*Center for Bio/Molecular Science and Engineering*
[2]*University of Puerto Rico at Arecibo*

Introduction: The presence of trace environmental contamination of soil and ground water is an ongoing concern. Historically, improper practices during the manufacture and storage of explosives, such as 2,4,6-trinitrotoluene (TNT), were the primary causes. Now, the need for trace detection of explosives is further heightened by current homeland security concerns. Required are easy-to-use, sensitive, and fast methods to facilitate the detection and quantification of these contaminants, whether to monitor remediation or provide surveillance. Biosensors have been found effective for solution-phase detection of environmental contaminants, with NRL pioneering the use of flow displacement immunoassays.[1,2] Our work utilized the Luminex[100] (a commercial flow cytometer), which can perform highly multiplexed assays by discriminating between up to 100 different bead sets, each of which can be used to test for a different target. While the Luminex[100] has been shown to be a highly effective biosensor for sandwich or competitive immunoassays, the goal of this project was to demonstrate for the first time a displacement immunoassay on this platform, and to test its suitability for TNT detection in the marine environment.

We evaluated four different TNT monoclonal antibodies, two recombinant TNT antibodies, and a control antibody simultaneously for the rapid detection of TNT and other nitroaromatics. TNT was detected at 0.1 ppb and could be quantified over the range of 1 ppb to 10 ppm. In addition, the assay was shown to be effective in various matrixes such as lake water, sea water, and soil extracts. This ability to function in the maritime environment is critical for Naval applications, such as trace detection of explosive materials onboard interdicted vessels, anti-mine operations, or detection of unexploded ordinance. In addition, the assay methodology can be applied to address the whole scope of small-molecule detection needs, from environmental pollutants to identification of illicit drugs.

TNT Displacement Immunoassay: The Luminex[100] is a specialized flow cytometer that performs multiplexed immunoassays by using a red laser to differentiate up to 100 different types of fluorescent latex microspheres, while a green laser quantifies a shorter wavelength fluorophore or fluorescent target molecule bound to the surface of each microsphere during the assay. Luminex microspheres (seven types, each coated with a different antibody) were incubated with a high concentration of the fluorescent analog of TNT, Alexa Fluor 555-TNB (AF-TNB). Afterwards, the excess AF-TNB was removed, the beads added to the samples, and immediately processed in the instrument to analyze for TNT. If TNT was present, AF-TNB was displaced in a TNT concentration dependent manner from the bead surface (Fig. 10), resulting in a lower measured signal on each bead. By measuring the loss in signal on each bead set and plotting median fluorescent intensity vs TNT concentration, we could quantify the concentration of TNT over the range of 10 ppm to 1 ppb (Fig. 11). The limit of detection for TNT varied for the different antibodies tested, with Mab A1.1.1 being the most sensitive at 0.1 ppb.

The relative cross-reactivities of all the TNT antibodies to a panel of nitroaromatic or nitramine compounds were also determined. In this displacement assay, the cross-reactivity factor was calculated by first determining the concentration of each compound required to produce 50% displacement of the AF-TNB from the beads. This concentration was compared to the amount of TNT required to induce 50% displacement (Table 1). The magnitude is indicative of how much more of each compound is required to generate the same displacement of AF-TNB as TNT. For the

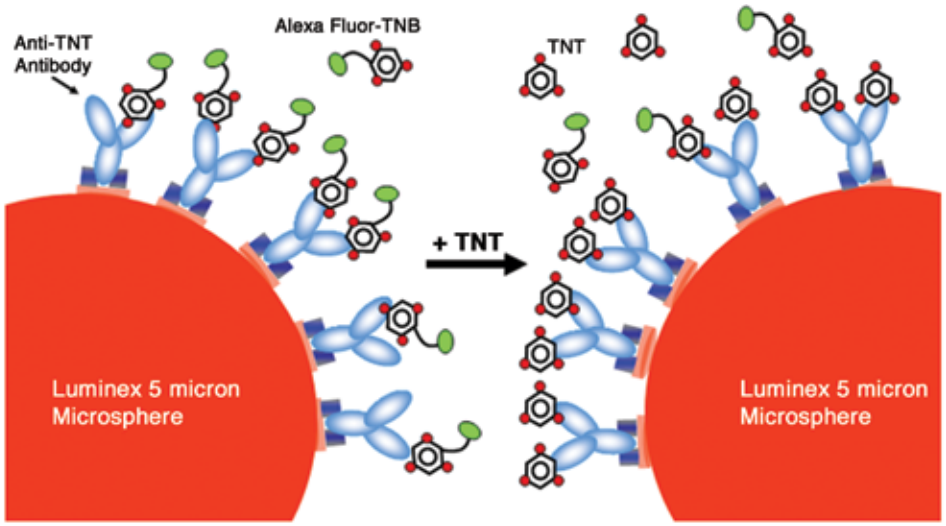

FIGURE 10
Fluid-array displacement TNT immunoassay schematic. First, the Luminex beads are saturated with Alexa Fluor-TNB, making them highly fluorescent. When TNT is added, AF-TNB is displaced and the beads become less fluorescent, causing the measured signal to decrease.

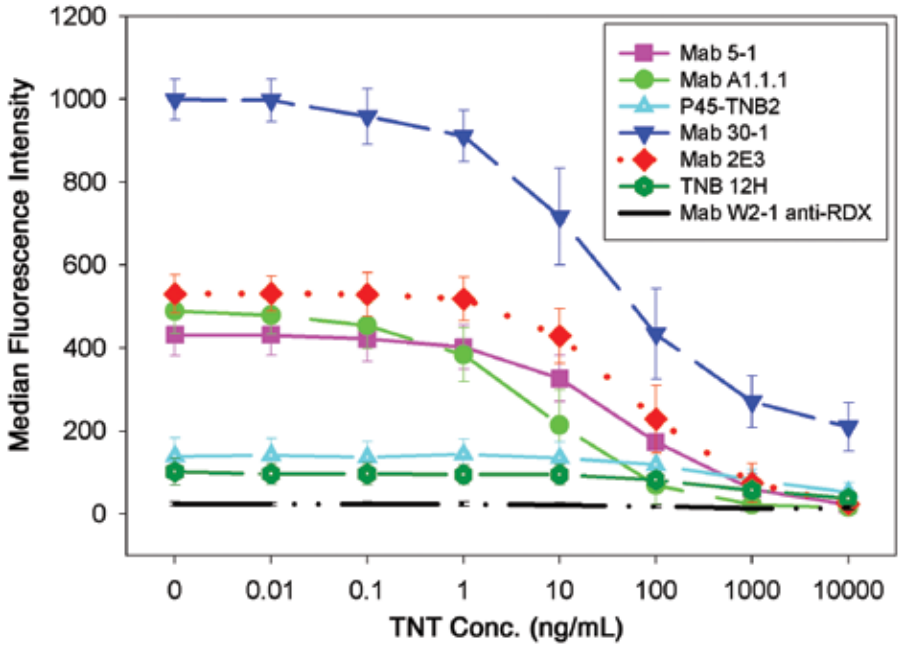

FIGURE 11
This figure shows the median fluorescence value obtained upon measuring each anti-TNT antibody coated Luminex bead set exposed to TNT of various concentrations, which induces displacement of a previously bound AF-TNB tracer molecule.

Table 1 — Cross-Reactivity to Nitro Compounds

Explosive Compound	Anti-TNT Antibodies					
	5-1	A 1.1.1	P45-TNB2	30-1	2E3	TNB12H
TNT	1	1	1	1	1	1
TNB	14	26	1.2	4	17	1.2
Tetryl	0.3	0.1	11.2	0.5	0.3	23
2-A-4,6-DNT	71	91	11	172	108	25
2,4-DNT	108	555	42	625	86	22
RDX	277	3333	10	909	476	111

Cross-reactivity factors of the anti-TNT antibodies to nitroamines and nitroaromatics. Values were calculated by taking the concentration of each compound required to cause 50% dissociation of the AF-TNB, then dividing by concentration of TNT to achieve 50% dissociation. Cross-reactivity factors greater than one indicate that the compound is less effective than TNT at displacing AF-TNB from the antibody-coated beads.

Table 2 — TNT Quantitation in Soil Samples

Soil Sample	Antibody-Coated Bead Type				Avg	HPLC
	5-1	A1.1.1	30-1	2E3		
G18-L1-A	28.9	24.4	19.4	16.1	22.2	16.2
G16-L2-A	17.9	9.4	7.0	10.4	11.2	6.2
G18-L3-A	7.6	6.9	3.9	5.2	5.9	1.7
G51-L1-A	3.4	4.1	1.1	2.7	2.8	1.5
G55-X-A	350	261	82	291	246	238

The concentration of TNT in each of the soil samples was determined in the displacement assay using several monoclonal antibodies. TNT concentrations in the same samples were also determined using the HPLC standard method employed by the EPA.

monoclonal antibodies, tetryl was found to be more effective, while unrelated compounds like RDX gave essentially no cross-reactivity.

Tests were also performed on acetone extracts of soil samples collected from areas contaminated with TNT. Table 2 shows the results of these analyses and compares them to analyses of these same acetone extracts by the EPA standard high-performance liquid chromatography (HPLC) method.

Summary: We demonstrated the potential of the multiplexed fluid-array displacement immunoassay to detect the explosive TNT and related compounds. This assay was highly sensitive with a large dynamic range. The test was rapid, taking only a few minutes to complete, and user-friendly, requiring the addition of only a single reagent prior to measurement. This method was found very useful for choosing the best anti-TNT antibody, and also made possible the rapid comparison of their cross-reactivities for various explosive compounds. By using antibodies with complementary cross-reactivities and a pattern recognition algorithm, both the identity and concentration of the explosive could potentially be determined. The next step is to demonstrate that this assay can monitor a range of unrelated explosive targets, using one or more antibody-coated microspheres and suitable fluorescent analogs for each target to be detected. This ability to simultaneously monitor for a range of environmental contaminants in a rapid, high-throughput manner may make multiplexed fluid-array displacement immunoassays the analytical method of choice in the future.

[Sponsored by ONR and NSF Historically Black Colleges and Universities — Tribal College or University Internship Program]

References

[1] J.P. Whelan, A.W. Kusterbeck, G.A. Wemhoff, R. Bredehorst, and F.S. Ligler, "Continuous-Flow Immunosensor for Detection of Explosives," *Anal. Chem.* **65**, 3561-3565 (1993).

[2] P.T. Charles, L.C. Shriver-Lake, S.C. Francesconi, A.M. Churilla, J.G. Rangassammy, C.H. Patterson, J.R. Deschamps, and A.W. Kusterbeck, "Characterization and Performance Evaluation of In vivo and In vitro Produced Monoclonal Anti-TNT Antibodies for the Detection of TNT," *J. Immunol. Methods* **284**, 15-26 (2004).

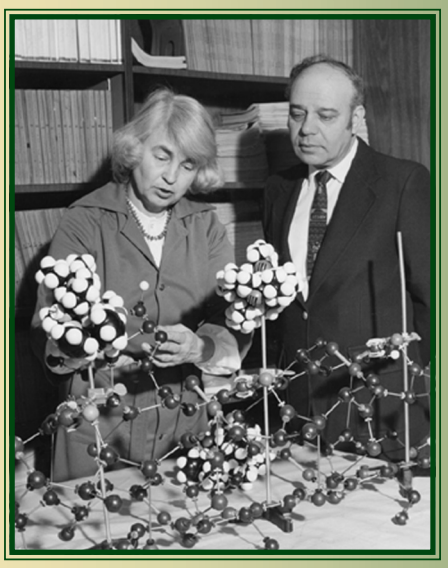

Molecular Structure Analysis and the Nobel Prize

Achievement: NRL has produced two Nobel Laureates, J. Karle and H. Hauptman, who each received the Nobel Prize for Chemistry in 1985 for devising direct methods employing X-ray diffraction analysis in the determination of crystal structures. The seminal research paper, "The Phases and Magnitudes of the Structure Factors," was published in 1950. The major events leading to these new methods were: quantitative molecular structure analysis in 1948; foundation mathematics for the X-ray phase problem in 1949; and the first general procedure for solving crystal structure problems in 1963. As experience with applications developed, I. Karle, another NRL chemist, made a major contribution to the development of analytical techniques of broad applicability to all types of crystals, whether they had a center of symmetry or not. It was a considerable step to bridging the gap between theory and practical application.

X-ray diffraction analysis involves the determination of the arrangement of atoms in crystals from which the molecular formula is derived directly. Determination of the molecular structure is important in that once the structural arrangement is understood, the substance itself can then be synthesized to produce useful products. This research occupies an almost unique position in science because the information it provides is used continuously in other fields. In fact, many phenomena in the physical, chemical, metallurgical, geological, and biological sciences are interpretable in terms of the arrangements of atoms.

J. Karle and I. Karle are still conducting research at NRL since joining the Laboratory in 1946. Their research plays a large part in the Navy's energetic materials program, which focuses on making explosives and propellants that are safer, more powerful, or both.

Impact: Methodologies for determining molecular structures are major contributions to science and technology. For example, they form the basis for the computer packages used in pharmaceutical laboratories and research institutions worldwide for the analysis of more than 10,000 new substances each year. A significant portion of structural research has direct application to public health, including the identification and characterization of potent toxins found in animals and plants, antitoxins, heart drugs, antibiotics, anti-addictive substances, anticarcinogens, and antimalarials.

Demonstration of a 600 kW Multiple-Beam Klystron Amplifier: A First-Pass Design Success

D.K. Abe,[1] K.T. Nguyen,[2] D.E. Pershing,[3] F.N. Wood,[3] R.E. Myers,[3] E.L. Eisen,[4] M. Cusick,[4] and B. Levush[1]
[1]*Electronics Science and Technology Division*
[2]*Beam-Wave Research, Inc.*
[3]*ATK Mission Research*
[4]*Communications and Power Industries, Inc.*

Introduction: Multiple-beam klystrons (MBKs) are a class of vacuum electronic amplifiers, in which the kinetic energy of axially streaming electron beams is converted to electromagnetic energy through the interaction of the beams with a series of resonant microwave cavities. With their potential to efficiently produce coherent, broadband, high-power microwave radiation in a compact package, MBKs are a promising device technology to provide the low-noise transmitter performance required by shipboard radar systems to operate in high-clutter environments (e.g., littoral zones) and to keep pace with evolving antiship cruise missile (ASCM) and tactical ballistic missile (TBM) threats. Nondefense applications of this technology include civilian radar, communications, and accelerators for high-energy physics.

As the name implies, MBKs make use of multiple electron beamlets, each of which propagates in a separate, parallel beam tunnel, but interact with electric fields in common regions such as cavity gaps. In this manner, the perveance of the individual beamlets can be low, facilitating stable-beam propagation and efficient beam-wave interaction without the adverse space-charge effects that could debunch the beam, while the total beam current can be high, facilitating high-power and broad-bandwidth operation.

In addition, MBKs possess a number of advantages over conventional single-beam klystrons of comparable power, including reduced operating voltages (typically 50% to 80%) which leads to shorter circuit lengths (typically 30% to 60%) and significantly lower weight. Furthermore, MBKs possess the low phase noise performance that is desirable for radar and communication applications.

MBK Design and Experiment: The inherent three-dimensional nature of the MBK creates design challenges for multiple-beam generation and transport, and the development of efficient radio-frequency (RF) interaction circuits. To address these issues, personnel from NRL and the U.S. industry formed a team to start an MBK development program in 2002.

In the first of a series of planned experiments, we have designed and successfully demonstrated a 600 kW, 40% efficient, S-band (3.24 to 3.30 GHz) fundamental-mode MBK[1,2] (Fig. 1). The eight-beam, four-cavity device was only 60 cm long and weighed approximately 23 kg (without the magnet). This is the first such device developed in the U.S. and is significant not only for the high-peak RF power achieved at a low cathode voltage (approximately 45 kV) and extremely compact size, but for the fact that all of the performance goals were met in a single hardware design pass.

To achieve such a "first-pass" design success, we have developed a simulation-based design methodology. Enabled in large part by advances in low-cost computer power, this methodology makes extensive use of a combination of NRL-developed and commercial two- and three-dimensional computational tools to model realistic device geometries. These new tools have sufficient accuracy and resolution to assess potential designs for their sensitivity to mechanical tolerances and fabrication methods, replacing costly, hardware-intensive "cut-and-try" methods.

The resulting MBK performed very close to design expectations.[3] Beam generation and transport were key technical challenges. We made extensive use of MICHELLE 3D, an NRL-developed electron gun/collector code, to design the beam optics in the cathode-anode region of the gun (Fig. 2(a)), model the transport of the beamlets through the interaction circuit (Fig. 2(b)), and design the electron beam collector

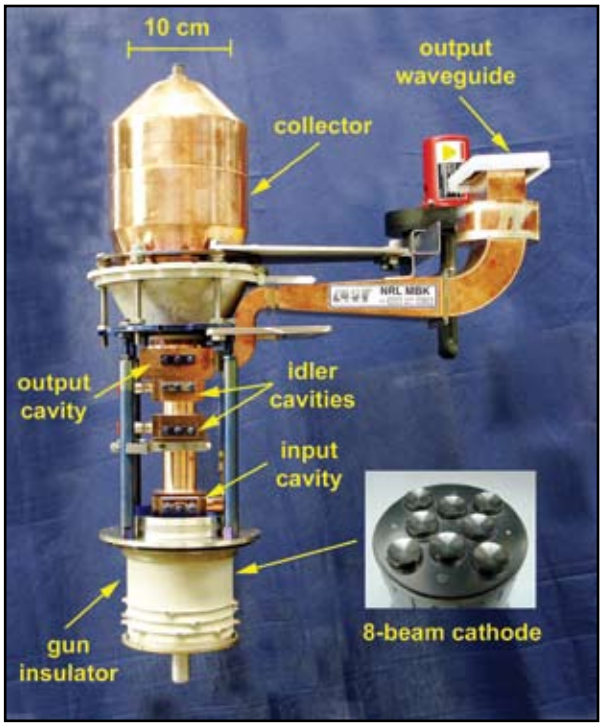

FIGURE 1
The NRL eight-beam, four-cavity, 600-kW MBK with a detail of the eight-beam cathode shown in the inset.

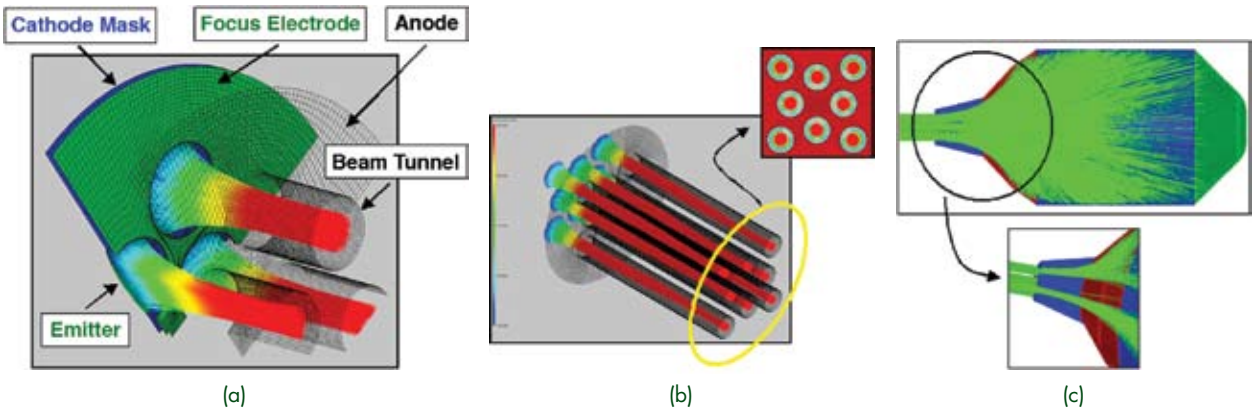

FIGURE 2
MICHELLE 3D electron-beam simulations: (a) quarter section of the eight-beam electron gun; (b) nonintercepting eight-beam transport in an axial magnetic field (inset: cross-sectional view showing the beamlets well-centered on the beam tunnels); (c) spent beam distribution in the collector, showing uniform deposition on the walls without particle reversals.

(Fig. 2(c)). To avoid electron interception on the walls of the beam tunnels, an external solenoidal magnetic field guides the eight off-axis beamlets. An innovative iron pole-piece design at the interface of the gun and circuit matches the beamlets into the highly uniform axial magnetic field in the interaction region (less than 0.2% measured variation in B_z). Very few beam electrons were lost to the walls: we measured greater than 99% beam transmission in the absence of an RF drive and greater than 97% transmission at saturation (maximum energy extracted from the beams). A reentrant pole piece shapes the magnetic field lines as they enter the collector, preventing potentially catastrophic virtual cathode formation and particle reversals.

The MBK generated a peak RF power of 600 kW at a frequency of 3.26 GHz with a corresponding gain of 25 dB and an electronic efficiency of 40%. Simulations using TESLA, an NRL-developed 2.5-D large-signal klystron code, are in excellent agreement with experiment. For example, Fig. 3 plots the measured and simulated output power vs frequency. The model accurately predicts the response of the MBK over a wide range of frequencies and in two very different regimes of amplifier operation (linear and nonlinear), validating our understanding of this complex nonlinear beam-wave interaction.

Summary: The successful demonstration of this eight-beam fundamental-mode MBK is an important first step in the development of a class of compact, high-power, broadband, low-noise amplifiers to improve the capabilities of Navy radar and communi-

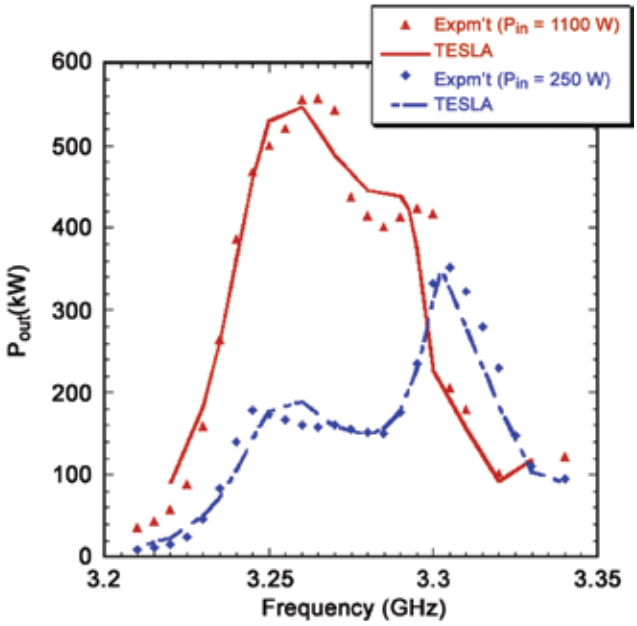

FIGURE 3
MBK output power vs frequency for drive powers corresponding to the linear (blue) and nonlinear (red) amplifier regimes of operation. The solid lines represent TESLA simulations and the discrete points are measured data.

cations systems. With the development of a validated complement of computational tools and a simulation-based design methodology, we are building the technological foundation to produce optimized, high-performance designs in a rapid and cost-efficient manner.

[Sponsored by NRL and ONR]

References:

[1] K.T. Nguyen, D.E. Pershing, D.K. Abe, B. Levush, F.N. Wood, J.P. Calame, J.A. Pasour, J.J. Petillo, M. Cusick, M.J. Cattelino, and E.L. Wright, "Electron Gun Design for Fundamental Mode S-band Multiple-beam Amplifiers," *IEEE Trans. Plasma Sci.* **32**(3), pp. 1212-1222, June 2004.

[2] K.T. Nguyen, D.K. Abe, D.E. Pershing, B. Levush, E.L. Wright, H. Bohlen, A. Staprans, L. Zitelli, D. Smithe, J.A. Pasour, A.N. Vlasov, T.M. Antonsen, Jr., K. Eppley, and J.J. Petillo, "High-power Four-cavity S-band Multiple-beam Klystron Design," *IEEE Trans. Plasma Sci.* **32**(3), pp. 1119-1135, June 2004.

[3] D.K. Abe, D.E. Pershing, K.T. Nguyen, R.E. Myers, E.L. Eisen, M. Cusick, and B. Levush, "Demonstration of an S-band, 600 kW Fundamental-mode Multiple-beam Klystron," *IEEE Electron Device Lett.* **26**(8), pp. 590-592, August 2005. ★

Improving Clutter Suppression in Navy Legacy Radars

M.T. Ngo,[1] V. Gregers-Hansen,[1] and H.R. Ward[2]
[1]*Radar Division*
[2]*HRW Consultant*

Introduction: New Navy missions in littoral regions have accentuated the need for improved radar performance in a heavy clutter environment. While new solid-state phased-array radars, currently under development, are specified to have a much improved clutter suppression capability, a large number of ships using older tube-based transmitters will continue to have a major role in Naval operations for years to come. For many of these radars, the ability to suppress clutter is limited by intra-pulse noise generated in the Crossed-Field Amplifiers (CFA) used as the final power amplifiers of the transmitter. The cost of replacing such transmitters with more stable and lower-noise alternatives is usually deemed much too costly.

In an effort directed at improving clutter suppression in such Navy Legacy radars, without the need for major transmitter modifications, NRL has been pursuing the development of a new signal processing technique, referred to as transmitter noise compensation (TNC). This technique compensates for intra-pulse transmitter noise, as well as power supply instabilities, by capturing and processing an accurate replica of each transmitted pulse in real time. Subsequently, through pulse-to-pulse comparisons, the measured transmit errors are used to derive a digital filter, which compensates for the transmitter instabilities in the digital signal processor (DSP), thus improving the suppression of returns from strong clutter.

A preliminary feasibility study proved that this technique should be capable of providing more than a 10-dB improvement in clutter suppression. This paper describes the TNC technique and outlines the results of an experimental study on the AN/SPY-1B radar aimed at demonstrating the practical feasibility of the TNC technique.

Transmitter Noise Compensation: In simple terms, the TNC technique is similar to the classical "coherent-on-receive" moving target indicator (MTI) approach,[1] but instead of making a single complex correction to all the received clutter returns, specific corrections are made on all the samples across the duration of the radar pulse width, based on a direct measurement of the waveform of each transmitted pulse. Since once the transmit signal is radiated it is deterministic, the samples of each pulse can be used to equalize received signals within a coherent processing interval (CPI), resulting in a significantly improved clutter suppression. The errors on each transmitted pulse can be referenced either to the ideal waveform or to the first transmitted pulse in a coherent dwell. Challenges with this technique are to obtain a high-quality sample of the transmitted pulse and to implement efficient signal-processing algorithms, which equalize the returns over an entire coherent dwell.

A block diagram describing the basis of the TNC principle is shown in Fig. 4, and the corresponding mathematical approach is summarized by the following equation:

$$Output = [C \otimes SE] \otimes \left[F^{-1} \left\{ (F(S)^*) \cdot \frac{F(S)}{F(SE)} \right\} \right].$$

A sample, *SE*, of each of the transmitted radar signals in the CPI is down converted, filtered, and digitized in a separate receive channel. The total radar return is the convolution of the transmitted signal, *SE*, and the clutter reflectivity, *C*. Pulse-to-pulse differences are defined by their spectral ratio, $F(S)/F(SE)$, which is multiplied by the matched filter function, $F(S^*)$, and then transformed into an error-correcting finite-impulse-response by taking the inverse Fourier transform. Here S denotes the ideal desired radar waveform and $F(\cdot)$ is the Fourier transform. This error-correction/matched filter response is convolved with clutter returns to obtain the corrected output, which is sent to the MTI filter or pulse Doppler processor.

Experimental Study: For the experimental study, data was collected on the AN/SPY-1B radar at the U.S. Navy Surface Combat Systems Center (SCSC)

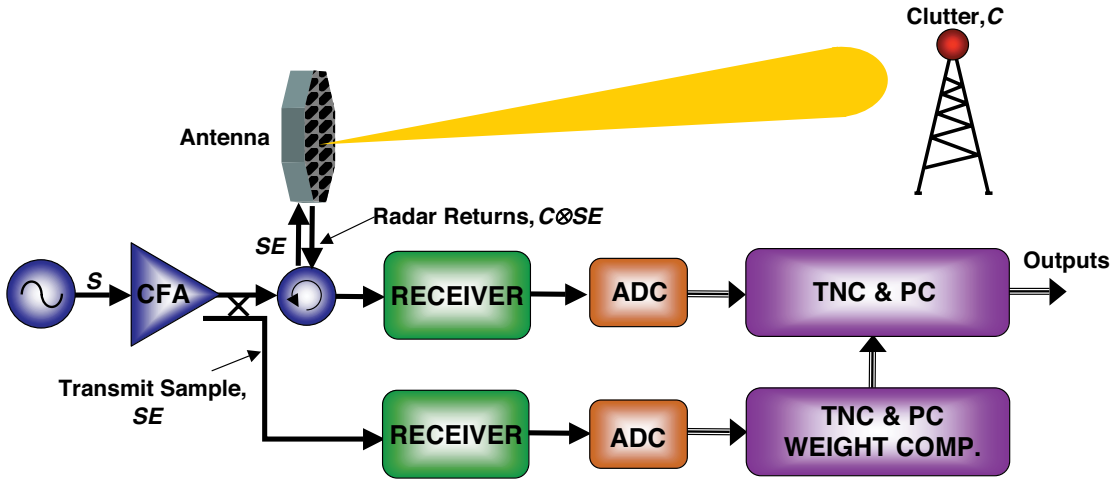

FIGURE 4
Transmitter noise compensation functional block diagram. TNC: Transmitter Noise Compensation, PC: pulse compression.

at Wallops Island, VA, using a data recording system developed and operated by the Naval Surface Warfare Center (NSWC). Referring again to Fig. 4, both the transmit sample and radar returns, from nearby clutter sources, were recorded after the analog-to-digital converters (ADCs) for a large number of consecutive MTI dwells in each beam position. The transmit sample is the combined output of the 32 CFAs in the AN/SPY-1B. Due to significant levels of transmitter leakage into all the receiver channels during the transmit pulse, a 10-km optical delay line was used to delay the transmit sample. The clutter return signals from actual clutter sources were fed directly to the receiver without the use of an optical delay line, since the clutter sources were located 4 to 5 nmi from the radar. The outputs from the receiver were sent to the data recording system where each was digitized in 14-bit, 100-MS/s ADCs.

Data Analysis: A Matlab program was used to compute the clutter improvement factor (CIF) with and without TNC, as described by the functional diagram in Fig. 4. Gated transmit and clutter samples were input to the calculation and filtered to separate the individual subpulses. The filtered pulses were then compressed and compensated for the transmitter noise, and a three-pulse dwell was used to compute MTI residue.

Figure 5 shows an example of the outputs from the analysis program based on a single CPI. The single-pulse compressed output is plotted in black at the top and its peak value serves as the amplitude reference. The normal MTI output is plotted in blue and the TNC-compensated MTI output is plotted in red. Notice that the compensated residue has much less energy, but it is spread farther in time. The improvement CIF value given in this figure is the difference of the total integrated energy under the MTI and MTI + TNC waveforms across their total time duration. Figure 6 shows histograms of more than 300 dwells with and without the TNC technique. With the TNC technique applied, a median improvement of more than 15 dB was achieved in this particular case.

Conclusions: Based on the analysis of experimental data taken with the AN/SPY-1B radar, it has been shown that the proposed TNC technique can improve radar detection of small targets in clutter by more than 10 dB. This agrees well with initial theoretical predictions. While the TNC technique only works in a single designated unambiguous pulse repetition interval (PRI) following the transmitted pulse, it would be well suited for medium pulse-repetition-frequency (PRF) radars where significant clutter is unlikely to extend over more than one PRI interval. The TNC processing can be easily adapted to future radar upgrades and should be extremely cost competitive compared to alternative transmitter improvements, in particular, if it can be implemented as part of an overall radar signal processor upgrade.

Acknowledgments: The work presented here was spawned by an earlier NRL effort, dating back to 1995.[2] Valuable assistance during the experimental program was provided by NSWC-DD (Steve Beasley), TSC (Rick Jones), and SEG (Glenn Leite).

[Sponsored by PEO IWS 2RI2]

References:

[1] H. Li, A. Illingworth, and J. Eastment, "A Simple Method of Dopplerizing a Pulsed Magnetron Radar," *Microwave Journal*, pp. 226-234, April 1994.

[2] B. Cantrell, "Low Cost SPY-1B/D ORDALT Proposal for Operation in Littoral Environment," NRL presentation, August 1995.

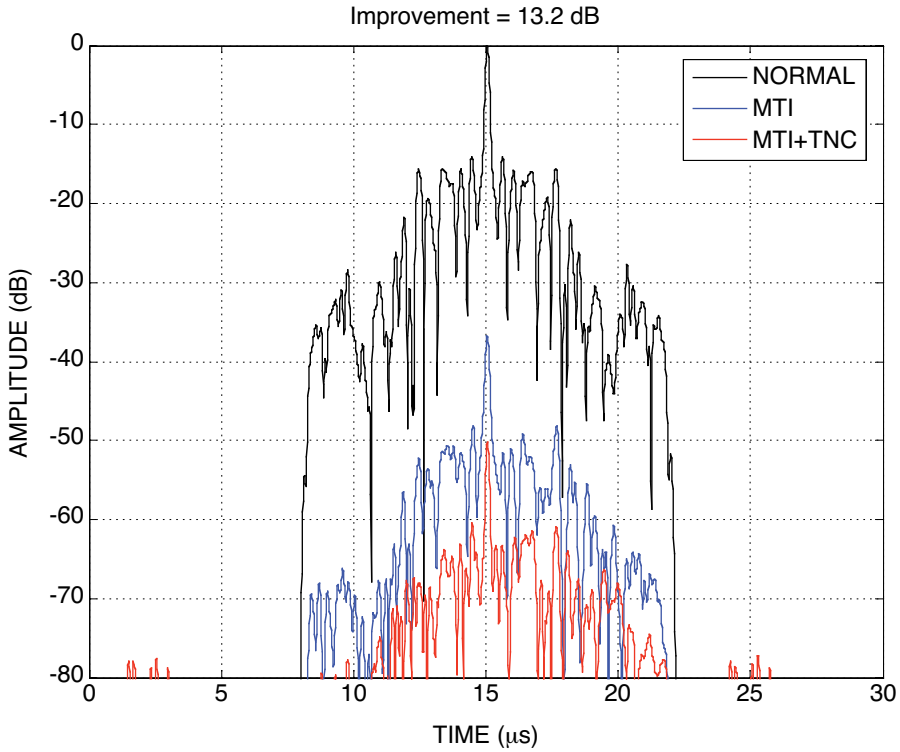

FIGURE 5
Sample output of the data analysis program.

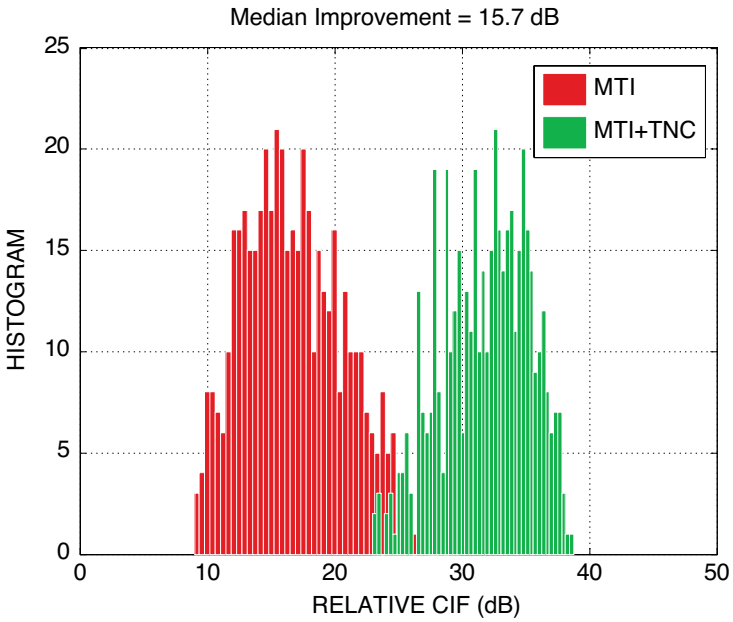

FIGURE 6
Histogram of CIF with and without TNC using a TV tower on Chincoteague Island as a clutter source.

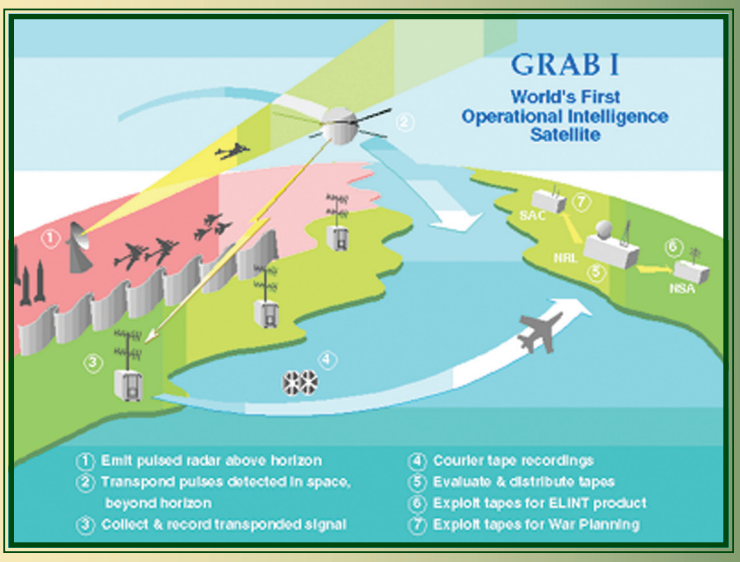

America's First Operational Intelligence Satellite

Achievement: The now unclassified Galactic Radiation and Background I (GRAB I) payload, an acknowledged co-flyer with the publicly recognized Solar Radiation I (SOLRAD I) scientific payload, was America's first operational intelligence satellite. In June 1960, fifty-two days after a U-2 aircraft was lost on a reconnaissance mission over Soviet territory, the GRAB I satellite soared into orbit and began transponding space-intercepted electronic intelligence signals to Earth-bound signals intelligence stations.

GRAB I was the unique application of many emerging technologies. NRL's M.J. Votaw, previously with Project Vanguard, brought the technical experience and resources necessary to design, build, launch, and operate a satellite in space. R.D. Mayo supervised the design and development of the S-band antenna with crystal video receiver and ground receive equipment to collect signals from Soviet air defense radar. H.O. Lorenzen provided the overall technical direction, obtained intelligence community sponsorship, and led transfer of the technology into operational deployment. The notion of operating the antenna/detector reconnaissance technology in an orbiting satellite and collecting its transponded signal on magnetic tape was a breakthrough answer to CNO ADM Arleigh Burke's request for naval material bureaus and laboratories to consider how they could use space in their design ideas for the Navy.

With mission sponsorship by the Office of Naval Intelligence, NRL completed development of the satellite and its network of overseas ground collection sites. President Eisenhower approved the electronic intelligence (ELINT) program and its SOLRAD scientific experiment cover. The GRAB/SOLRAD payloads shared a ride into space with the Navy's third Transit navigation satellite as part of the world's first multiple-satellite launching. Field sites recorded GRAB I signals on magnetic tapes, which were couriered to NRL for evaluation and duplication. The National Security Agency (NSA) and the Strategic Air Command exploited the tapes for technical ELINT data and to support the Single Integrated Operations Plan.

Impact: The GRAB project provided proof-of-concept for satellite-collected ELINT. This was accomplished by demonstrating that a platform in outer space could collect as much as all other sea, air, and land-based reconnaissance platforms operating within the satellite's field of view, at a fraction of their cost, and at no risk to personnel. The output, initially overwhelming, stimulated invention by NRL and NSA of machine processing of digitized data using commercial computers. In searching the tapes for new and unusual signals, NSA found the Soviets were already operating a radar that supported a capability to destroy ballistic missiles. Such information could not be obtained by airborne reconnaissance, nor without enormous risk to human sources. The intelligence information gained from GRAB I had a profound impact on national security decisionmaking and on deterrence of nuclear war with the Soviet Union.

Identifying Virtual Technologies for USMC Training

R.M. Stripling,[1] J.N. Templeman,[1] L.E. Sibert,[1] J. Coyne,[2] R.G. Page,[1] Z. La Budde,[3] and D. Afergan[2]
[1]*Information Technology Division*
[2]*Strategic Analysis, Inc.*
[3]*CACI*

Virtual Environments (VE) provide safe, low-cost training opportunities for many different tasks. However, the actual training benefits achieved, and thus the true cost-benefit ratio, depends on many variables. One of these variables is the interface system used to control the trainee's movement within VE. Efficient, intuitive interfaces allow the trainee to focus on the skills and knowledge to be acquired, while awkward systems require the user to concentrate on performing basic actions (such as avoiding furniture). Most commercial producers of VEs do not test their systems for training effectiveness. Instead they use devices, such as joysticks, that users accept even when they are inferior control devices.

The Warfighter Human-System Integration Laboratory (WHSIL) and the Immersive Simulation Laboratory (ISL) are jointly developing an empirically based mapping between interface technologies and the requirements of desired training objectives. A challenge to the validity of this effort is the pace of technological development. Arguably, system-specific evaluations become obsolete when new technologies are made available. To overcome this limitation, WHSIL and ISL are pursuing experiments designed to identify the underlying principles that determine interface effectiveness. The current focus of this effort is the evaluation of VE systems that were designed to train dismounted infantry Close Quarters Battle (CQB) tactics in urban terrain.

Three control interfaces are being tested in these studies: a standard joystick; Gaiter, invented by ISL, in which the full body and replica rifle are tracked; and a rifle-mounted joystick system that tracks the rifle and upper body position. With the standard joystick, all translations are made by pushing the stick in the desired direction of movement; rotations are achieved by twisting the joystick in the desired direction of rotation. In Gaiter, users make translations by raising their legs in the desired direction of movement once for each step taken (basically, walking in place), while rotations are made by rotating their bodies as they would in the real world. In the rifle-mounted joystick system, users make translations by pushing the thumb-joystick mounted on the replica rifle in the desired direction of movement, while rotations are made by rotating their body as they would in the real world.

A pilot study was conducted to confirm that users could navigate effectively using these systems. Volunteers followed a computer-generated avatar through a large warehouse and through an office space with a narrow hallway and several rooms. This study found that these systems supported precision movement in the warehouse, but that for those tracking the position of a replica rifle carried by the user, moving through doorways was difficult when the weapon was not carried correctly. Thus, from a purely data-driven perspective, people using a standard joystick exhibited better performance when in the office space. However, from a training perspective, these results indicate that the interfaces tracking a real-world (replica) rifle actually reinforced good CQB weapon handling techniques.

More recently WHSIL and ISL completed a study to determine whether the increased proprioceptive/kinesthetic feedback offered by systems like Gaiter, and to a lesser extent the system using the rifle-mounted joystick, enhanced the user's ability to maintain awareness of his/her relative position and orientation within a VE. In this study, participants had to complete a series of tasks that included moving to the location where an object was recently viewed or rotating in place by a specific angle—without visual feedback. An additional maze navigation task with visual feedback was conducted to determine whether proprioceptive/kinesthetic information was necessary for this type of task. In this maze task, volunteers moved through a short series of rooms and hallways and then were asked to indicate where they stood relative to the start location.

Results from the maze task indicated that when visual cues were present, a standard joystick was associated with performances as good as, or better than, the two body-tracked interfaces. In a task where users viewed a target and then sought to move to it in the dark, users consistently overshot the target by a factor of about two using Gaiter, and were more accurate with both joystick-based interfaces. This suggests that users of Gaiter misperceived the mapping from their real-world walking-in-place actions to their virtual movement: in-place steps were interpreted as half-steps. In contrast, accurate rotations required interfaces that provide more proprioceptive/kinesthetic information than the standard joystick. These experiments have led ISL to develop "Pointman," a new way of providing a proprioceptive sense of course, heading, and displacement using game controls.

In CQB training scenarios, there are many instances where users may find themselves in locations with little or no visual cues—for example, unlit stairwells or when moving from well-lit to dark areas. Our data suggest that for training scenarios such as these, interfaces that provide better proprioceptive/kinesthetic information should be used. However, in

other situations, a standard (and much less expensive) joystick may be sufficient.

[Sponsored by ONR] ★

Self-Optimizing Adaptive Antenna

C.K. Oh and B.K. Hanley
Tactical Electronic Warfare Division

Introduction: Currently, in dynamically changing and highly uncertain electronic warfare (EW) environments it is not possible to design in advance EW hardware that can adapt in real-time to these complex environments autonomously. Particularly, the real-time adaptation of EW to rapid changes in hostile activity poses a technological challenge. The ability of combining reconfigurable hardware devices with optimization software capable of executing real-time autonomous reconfiguration opens up a new approach to many difficult EW problems. This paper describes a real-time implementation of Genetic Algorithms (GAs)[1] demonstrated in a specific hardware configuration.

Background: We assume that the structure of a reconfigurable hardware device or system can be changed in real-time through altering bit strings ("configuration bits"). GA theory indicates that an optimal solution can be found over a vast and diverse nonlinear space at reasonable computational costs. The GA treats the "configuration bits" of the reconfigurable hardware devices as a chromosome and optimizes the chromosome through evolutionary computation. If the GA fitness function is properly designed for the task, then the GA can autonomously find the best hardware configuration in terms of chromosomes (i.e., configuration bits). Since the fitness landscape unpredictably changes in EW environments, the sensors that detect the changes in the environment should be in the loop of a real-time adaptable EW system. In this study, a low cost V-dipole ("rabbit ear") antenna system was used to demonstrate this real-time approach in a readily available, inexpensive three degrees of freedom hardware.

Self-Optimizing Adaptive Antenna System Validation: The V-dipole antenna system consists of two elements that can rotate through two different axes (two degrees of freedom) on a rotating mount (one degree of freedom). In this demonstration we used the V-dipole antenna for television reception. Even though the antenna has a simple structure, finding the optimal position of the two telescoping elements for the best signal reception on a rotating mount is a complex task because the three degrees of freedom encompasses a very large set of possible position combinations. Also, the V-dipole antenna system must adapt to changes in the signal environment due to weather, terrain, and other interference. Figure 1 is a diagram of the real-time self-optimizing adaptive antenna system. The GA on the computer

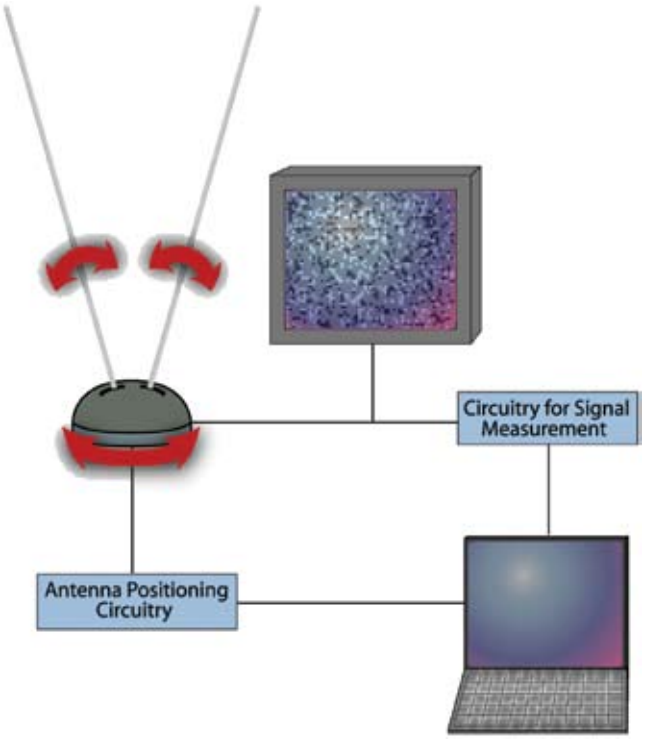

FIGURE 1
Self-optimizing adaptive antenna system.

controls the positions of three servo motors through the servo controller in antenna positioning circuitry. The conventional GA, which typically requires off-line, non-real-time processing, was modified to provide a real-time computational capability. The computational flow chart of the modified GA is shown in Fig. 2. The modifications to the standard GA flow are shown in the yellow blocks. These modifications allowed the GA to be implemented in real time in the feedback circuit. The three angular positions of the servo are encoded in a chromosome of the GA population. The raw value of signal strength is measured as a fitness to estimate the performance of each position. This single value can incorporate all interference and noise in the signal. The raw signal value is digitized to provide discrete values to the new real-time GA algorithm. At the end of the computation, the system moves the elements to the best position as determined by the GA. In the validation experiment, as the television channels were changed, the GA adjusted the V-dipole antenna position to find optimal reception. The initial test hardware of the antenna system that validates this novel real-time solution is shown in Fig. 3.

Summary: An autonomous, real-time adaptive system combining GA and reconfigurable hardware was demonstrated using a low-cost, simple V-dipole antenna system. This system was controlled through a feedback loop that used evolutionary computation in real time to find antenna positioning that optimized received signal strength. Although this application was rudimentary, we project that chip-level real-time GA processing can be applied to more complex reconfigurable hardware such as field

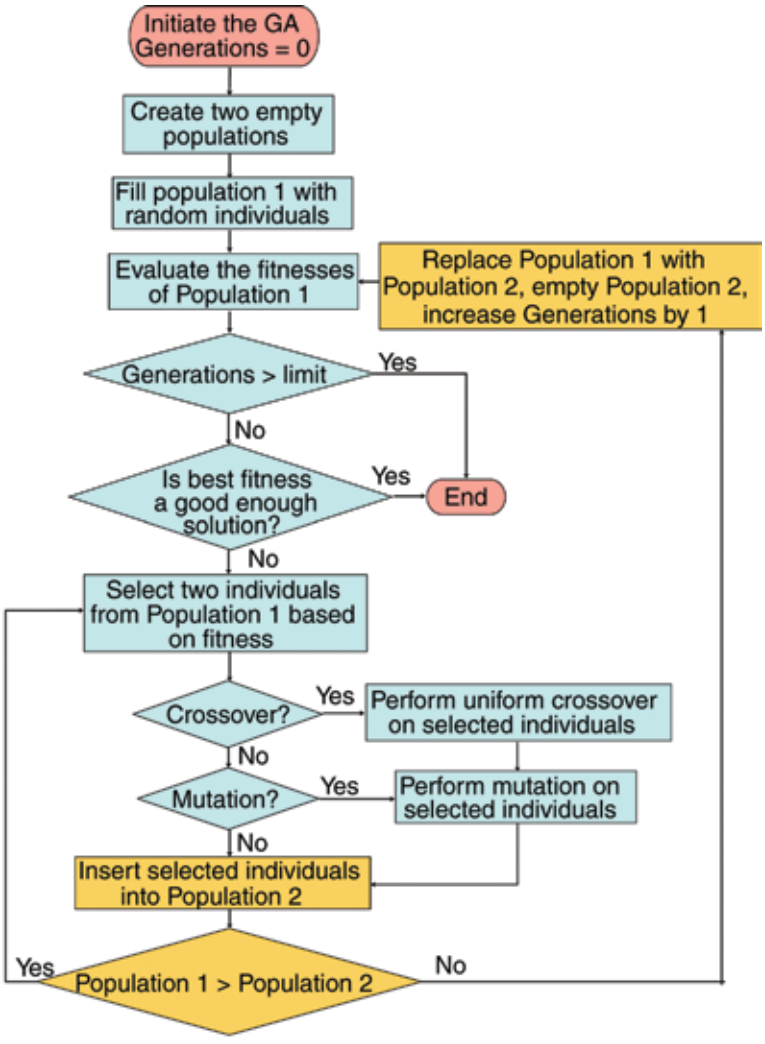

FIGURE 2
Flow chart of compact GA computational procedures.

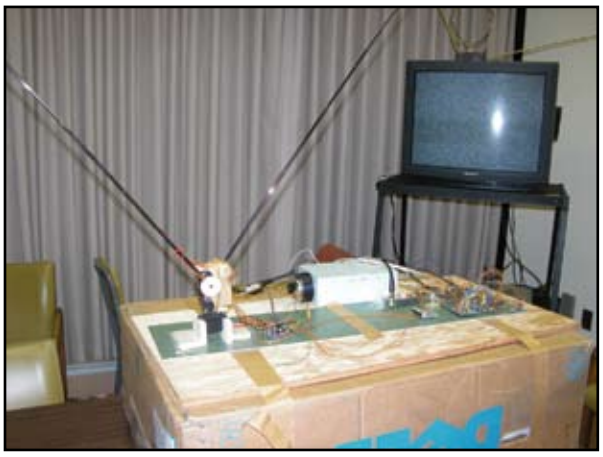

FIGURE 3
The initial test hardware of the self-optimizing antenna system.

programmable gate arrays (FPGAs) to support more complex applications in autonomous and adaptable EW systems.

[Sponsored by ONR]

Reference

[1] D.E. Goldberg, *Genetic Algorithm in Search, Optimization & Machine Learning* (Addison-Wesley, 1989). ★

Multicasting Within Mobile Ad hoc Networks

J.P. Macker, R.B. Adamson, J. Dean, W. Chao, I.T. Downard, J.W. Weston, and R.D. Lee
Information Technology Division

Background and Problem Area: The development of mobile ad hoc networking (MANET) technology for DoD use presents formidable challenges.[1] The Naval Research Laboratory (NRL) has been a technology leader in the conception, development, and standardization of MANET technologies. MANET technology is evolving and will allow future DoD network systems to self-organize and operate more autonomously without reliance upon a fixed infrastructure. Despite recent advances in this technology, there remains little work in adapting or standardizing multicasting forwarding in MANET.[2] Multicasting provides efficient network group communications, a feature important in future DoD tactical edge and network-centric scenarios. This article briefly describes recent NRL work advancing the state of the art in multicast forwarding capabilities for MANETs.

A Simplified Multicasting Process for MANETs: Previous research in MANET technology has developed techniques for optimizing the process of flooding control information often applied to specific routing protocol designs and requirements.[3] There is recent interest in applying these techniques to forward multicast user data in mobile, wireless data networks. Within MANETs, a simpler multicast forwarding model that optimizes the forwarding of multicast traffic to all participating nodes in a routing area is often useful. One such solution is the Simplified Multicast Forwarding (SMF)[4] specification design within the Internet Engineering Task Force (IETF). SMF is a flexible common framework for MANET multicast forwarding independent of any unicast routing specification. It includes a duplicate packet detection mechanism and supports multiple forwarding optimization methods. A recognized research challenge has been to better characterize the traffic loading performance of various algorithms within multicast mobile wireless networks.

CDS Algorithm Improvement: Algorithms that help form and minimize a Connected Dominating Set (CDS) are often considered as design frameworks for MANET multicast forwarding to minimize forwarding relay sets. Figure 4(a) represents a wireless network of 100 nodes and the related topological links between the nodes. Classical flooding (CF) or legacy wireless forwarding algorithms use all red nodes in Fig. 4(a) to retransmit network packets at least once, leading to the well-known broadcast storm problem.[5] To illustrate the value of CDS algorithms, Fig. 4(b) shows a connected graph containing only a subset of the total links and relay nodes obtained using a distributed CDS algorithm. The smaller number of red relay nodes (i.e., 12 vs 100) clearly demonstrates a significant reduction in the relay set size required to reach all destinations vs the CF approach.

Our research goes beyond CDS efficiency analysis predicted from static graphs, as illustrated in Fig. 4. We are developing operational models and exploring the robustness of multiple techniques under emulated and simulated mobile, wireless network conditions. Figure 5 is a sample of a simulation analysis comparing several CDS algorithms against CF within an increasingly congested mobile network. As shown in Fig. 5, CDS algorithms can improve network goodput (i.e., usable received network data) over CF as load increases. Due to inefficient relaying, the CF algorithm causes network contention and congestion under lighter source traffic loading than more optimized CDS algorithms.

Summary: NRL research is characterizing the complex behavior of various distributed relay set algorithms being considered for future MANET multicast forwarding. NRL also acts as a technical leader in a related Internet protocol standardization process and is

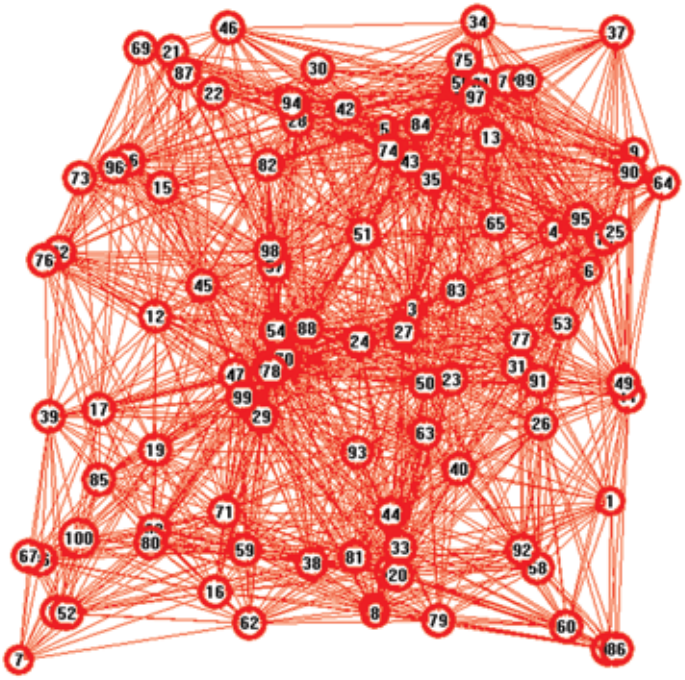

(a)

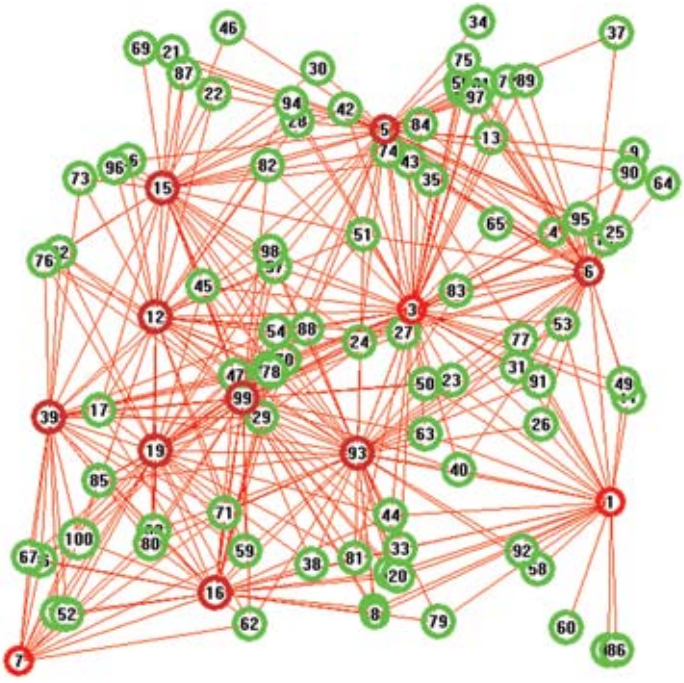

(b)

FIGURE 4
(a) 100-node network (fully connected no CDS) and (b) 100-node network (MPR-based CDS algorithm).

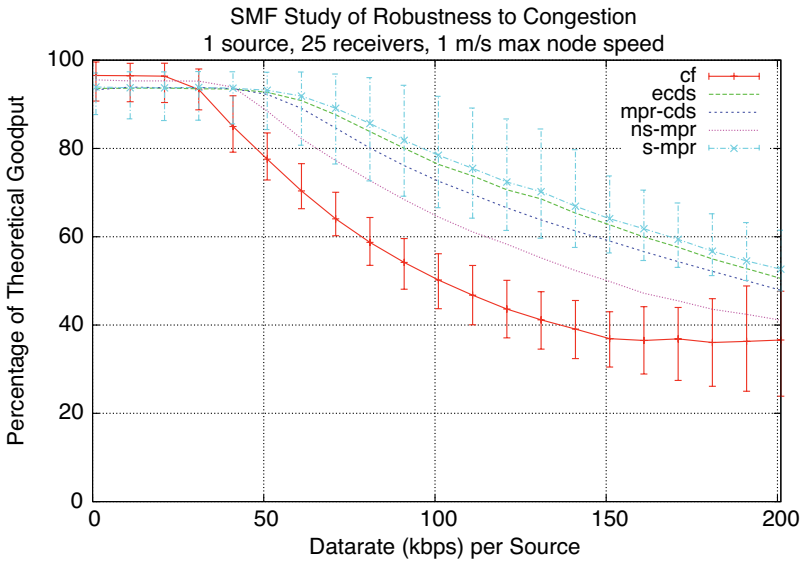

FIGURE 5
CDS algorithm study with mobility and increasing traffic volume.

transitioning lessons learned from this research within that forum. Research products are also expected to aid in supporting the complex design tradeoffs needed in developing future tactical Navy and DoD mobile wireless networks. Future plans include extending this work by researching the performance of reliable multicast transport mechanisms within SMF-enabled MANET models.

[Sponsored by NRL and ONR]

References

[1] J.P. Macker and M.S. Corson, "Mobile Ad Hoc Networking (MANET): Routing Protocol Performance Issues and Evaluation Considerations," IETF RFC 2501, Jan. 1999.

[2] J.P. Macker and M.S. Corson, "Mobile Ad Hoc Networks: Routing Technology for Dynamic, Wireless Networks," S. Basagni et al., eds., *Mobile Ad Hoc Networking*, Chapter 9, IEEE Press, 2003.

[3] J.P. Macker, J. Dean, and W. Chao, "Simplified Multicast Forwarding in Mobile Ad Hoc Networks," IEEE MILCOM 2004 Proceedings, 2004.

[4] J.P. Macker, et al., "Simplified Multicast Forwarding for MANET," specification work in progress, IETF MANET Working Group, http://www.ietf.org/, Oct. 2005.

[5] S. Ni, Y. Tseng, Y. Chen, and J. Sheu, "The Broadcast Storm Problem in Mobile Ad Hoc Networks," Proceedings of ACM Mobicom 99, 1999.

Multi-Source Maritime Vessel Tracking

M.D. Bell, S.M. Elliott, T.Y. Yang, and P. You
Space Science Division

Introduction: NRL Code 8100 is developing the Common Distributed Virtual Database/Information Extraction (CDVD/IE) System for the U.S. Coast Guard (USCG) Maritime Intelligence Fusion Center (MIFC) in Dam Neck, Virginia. The CDVD/IE semiautomatically identifies vessels via multisource data. This provides the USCG with maritime domain awareness of vessels operating in an area of responsibility (AOR) encompassing the Atlantic Ocean, north of the equator, and the Gulf of Mexico/Caribbean Sea. NRL system and software engineers have designed an architecture that implements a multilevel data aggregation and semiautomated tracking system. The CDVD/IE enables the MIFC to monitor potential vessels of interest (VOIs) and automatically generates alerts when behaviors meeting user-defined parameters are detected.

The CDVD/IE Program is sponsored by the U.S. Navy (USN) Office of Naval Research (ONR) and is scheduled for delivery to the MIFC during summer 2006. During fiscal year 2007, NRL and the USCG will exercise the system and assess suitability to support an upgradable path using multiple CDVD/IE installations to form a distributed maritime community grid. The CDVD/IE System uses a suite of commercial and NRL-developed computing technologies and resources to address two main areas:

- Multilevel Security Architecture
- Data Aggregation and Semiautomated Tracking Capability

Multilevel Security Architecture: NRL is developing multilevel security architecture to leverage data available at Sensitive Compartmented Information (SCI), GENSER Secret, and Sensitive But Unclassified (SBU) levels. The design makes this multilevel data available as a SIPRNet web service. The CDVD/IE will enable users to access information from multiple security levels using available DoD and NRL network

interconnections, providing a more complete intelligence picture to the USCG.

NRL security engineers established a Memorandum of Agreement with the Defense Information Systems Agency (DISA) to implement a bidirectional SIPRNet to NIPRNet controlled interface device (security guard). NRL CDVD/IE personnel, along with DISA and accrediting agency personnel, have designed an interface approach that permits high-value open-source data to be transferred to the GENSER Secret level. For National Technical Means data sources, NRL communications engineers are implementing an approved one-way controlled interface device and performing associated certification and accreditation.

Data Aggregation and Semi-Automated Tracking: Aggregated data from multiple disparate sources provide far more opportunity to positively identify vessels and construct tracks than nonaggregated, individual source data. Each data source, comprising vessel "metadata" (data about a vessel) and tracks/position data (posits), has the potential to contribute to solving the vessel identification puzzle, Fig. 6.

NRL designers developed a generic data extraction framework that simplifies efforts required to access and make use of differing data sources. This open approach is critical as additional maritime sources become available that will support future requirements to report on smaller vessels, vessels in other AORs, and

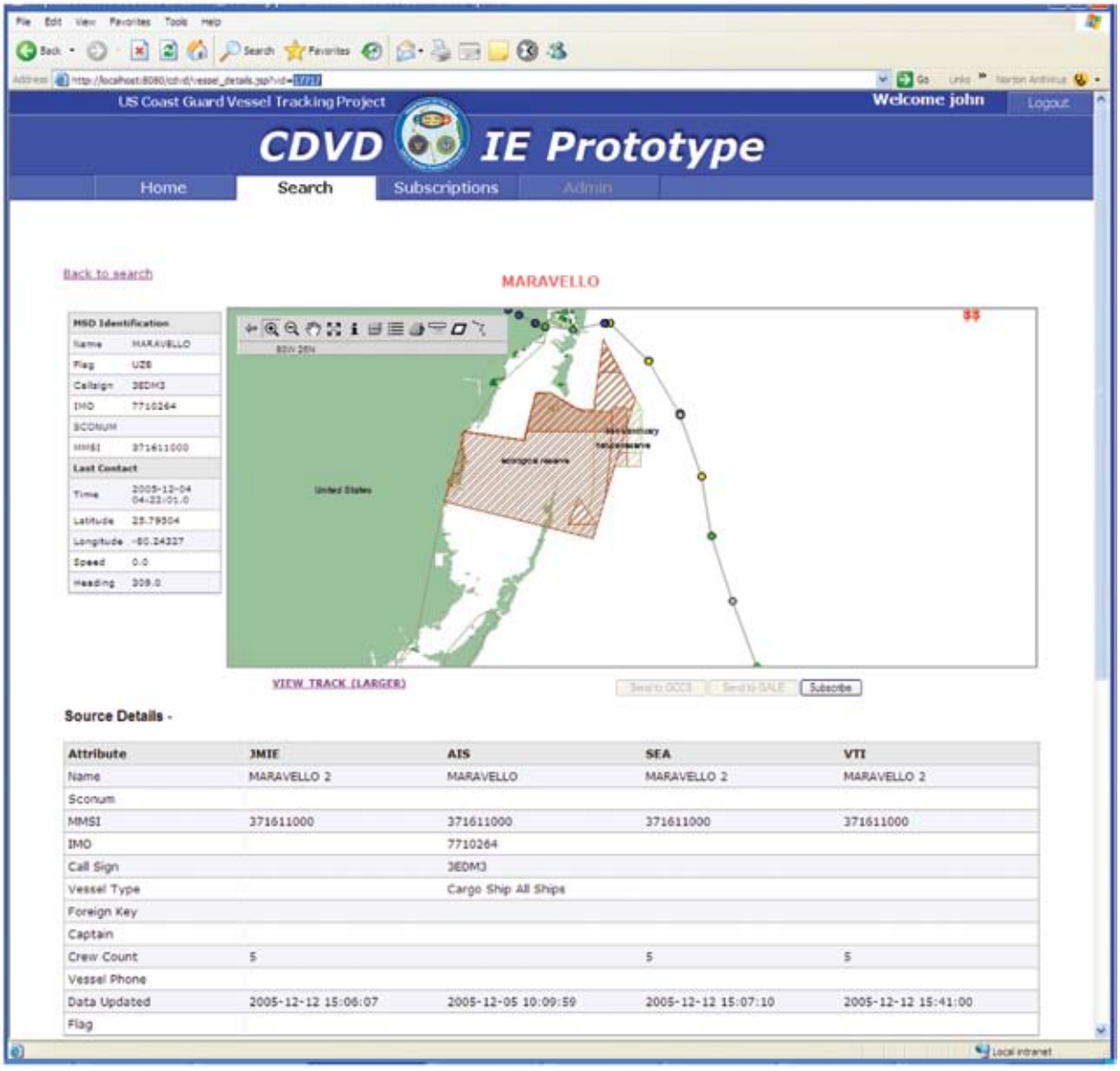

FIGURE 6
Single vessel track and associated multisource data.

cargo. CDVD/IE's semi-automatic track stitching and its ability to aggregate data from as many sources and sensors as possible enhances vessel tracking capabilities without increasing the existing analyst base.

The CDVD/IE software architecture implements an "inherent" query, notification, and alert system. The system automatically detects and alerts the operator to activity that falls within user-defined parameters using two key elements known as MyVessels and MyPlaces. These features enable specific vessels and areas to be added to a watchlist (both at the operator level and at the analysis cell level). A vessel listed in MyVessels is automatically updated when new information associated with that particular vessel enters the CDVD/IE environment. For MyPlaces, CDVD/IE invokes a "tripwire" approach. A user can define specific areas of interest within the AOR so that a vessel will trigger an alert if it enters the area. System search capabilities support queries into the CDVD/IE System by geographical location, by metadata attributes, and by alerts. The CDVD/IE System uses existing ELINT (Electronic Intelligence) and AIS (Automatic Identification System) tracking tools and introduces new capabilities to aggregate and stitch track segments from multiple sources. This stitching process encompasses the following functions:

- Metadata stitching
- Track position filtering
- Track candidate determination
- Track comparison (geographical and parametric)
- Spatial database update

As the CDVD/IE acquires new position data (single-source track data), it performs the above functions and conducts quality checks, Fig. 7. The final step in the process results in a database update reflecting the merged track data and metadata. Over time, updates to the database begin to build a robust repository of known vessel data, reducing the load on the analyst to "start from scratch."

Summary: The CDVD/IE system will provide a leading maritime domain awareness capability for the USCG with future applicability to the USN and Intelligence Community. This system paves the way for rapid aggregation of disparate sources across security domains, with architecture adaptable to modern web services technologies and commercial standards.

[Sponsored by ONR] ★

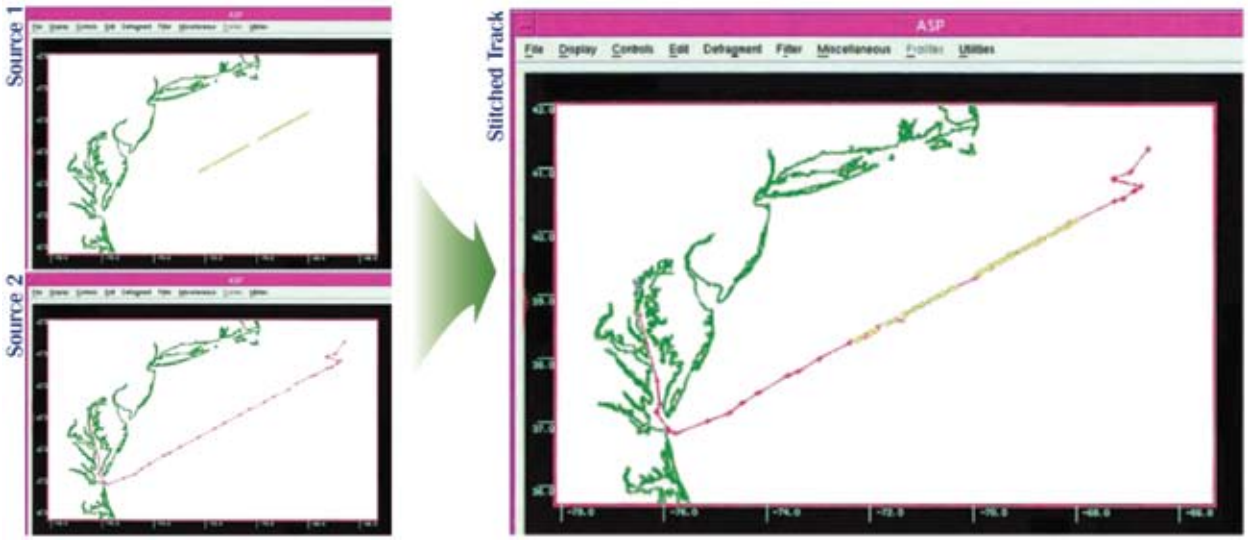

FIGURE 7
Track stitching with two data sources.

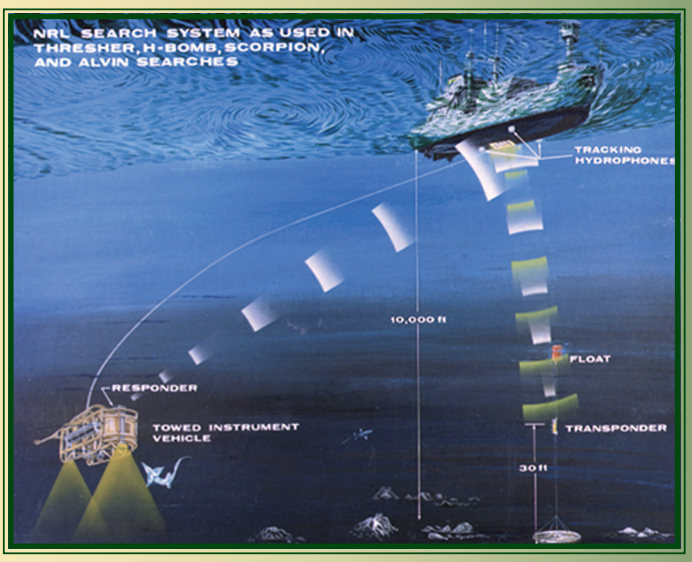

Deep Ocean Search

Achievement: On April 10, 1963, the nuclear submarine USS *Thresher* (SSN 593) was lost in deep water 260 miles east of Boston, Massachusetts, with 112 crew and 17 civilian technicians. The loss of the submarine and its complement was a deep shock to the Navy and to the country.

In an effort to determine the reasons for the loss, NRL applied deep-towing technology, developed years earlier for underwater acoustic research, to the deep seafloor search for *Thresher*. However, the search was terminated in September 1963 with the onset of bad weather. On May 18, 1964, the task group began new search operations. To augment its search capability, NRL had acquired the USNS *Mizar*, a retired cargo ship suited for launching and towing the deep-towed instrument vehicle, or "fish" as it was called. NRL's "fish" included a set of three cameras to photograph the wreckage, a side-scanning sonar to probe beyond camera range, two strobe lights, a magnetometer to locate the *Thresher* pressure hull, a transponder, a sonar pinger to measure the "fish's" altitude, and a telemetry system. This unmanned vehicle, towed by *Mizar*, detected the *Thresher* hull after only eight hours of bottom operations. NRL's photographs were later assembled into a photomosaic of most of the major parts of the sunken submarine.

After NRL's success in the *Thresher* search, the Laboratory was called upon to locate and recover a lost H-bomb off the coast of Spain in 1966, locate and photograph the lost submarine USS *Scorpion* (SSN 589) in 1968, assist in the recovery of the deep submersible *Alvin* in 1969, and locate and photograph the lost French submarine *Eurydice* in 1970. NRL's emergency search mission was transferred to other Navy organizations in 1980.

Impact: NRL-developed ocean search technology now resides in other government and private organizations. According to a 1966 commendation from the Marine Technology Society, NRL was responsible for "pioneering new techniques" and had "established a methodology for future ocean engineering." Years later, after the *Titanic* was located by Dr. Ballard's team, a former Navy Supervisor of Salvage stated before Congress that "the superb work of the scientific teams from NRL...led the way for the [*Titanic*] search operation in the North Atlantic."

High Temperature Superconductors for Naval Power Applications

R.L. Holtz,[1] R.J. Soulen,[1] M. Osofsky,[1] J.H. Claassen,[1] G. Spanos,[1] D.U. Gubser,[1] R. Goswami,[2] and M. Patten[2]
[1]*Materials Science and Technology Division*
[2]*SAIC*

Background and Significance: As the Navy moves to the all-electric warship, superconducting materials will play a key enabling role. High temperature superconducting (HTS) motors and generators will enable extended range, high-efficiency, high-power-density naval propulsion, and compact generators for weapons and ship systems. Compact mobile HTS generators also may provide portable/mobile power for littoral and expeditionary operation, naval air, and homeland security.

The "second generation" high-temperature superconductors (2G-HTS) based on yttrium-barium-copper-oxide (YBCO) "coated conductor" architectures are undergoing a processing technology breakthrough that will lead to large-scale manufacture by 2008. NRL is working with manufacturers to address key issues in the processing and performance of these conductors during this fast-paced stage of technology development.

In particular, 2G-HTS process development is accelerated by fundamental understanding of the materials microstructures gained at NRL. Key goals include reduction of AC losses in the HTS motors and generators, as well as novel inductor designs for power electronics. Ensuring superior fatigue properties of the HTS materials compatible with the lifecycle of naval machinery is a key objective.

Functional Performance: Figure 1 shows a schematic representation of the structure of a typical 2G-HTS tape. The superconductor is the thin (1 micron) layer of YBCO which is deposited by coating or thin-film techniques. The substrate for this superconducting layer is a series of ceramic buffer layers deposited onto a crystallographically textured nickel-alloy foil. For structural stability, laminations of copper-alloy foils are applied.

The superconducting properties depend upon the composition and processing of the YBCO layer. In particular, substitutions of rare-earth elements such as holmium for yttrium results in improvements in how the superconducting critical current Ic depends on magnetic field. In motor and generator coils, the magnetic field varies in direction, and thus the minimum value of Ic at any angle can be more limiting than the highest Ic value. NRL performs sophisticated high-resolution electron microscopy studies of 2G-HTS materials to determine what types of microstructural features form and how they are associated with desirable features of Ic vs field angle behavior. Figure 2 depicts some recent results, showing an Ic curve for a pure YBCO layer, with the sharp peak in Ic for magnetic field parallel to the layer, versus a holmium-doped YBCO layer, with a lower, but more uniform Ic. The most important types of microstructures detected by NRL are shown.

Fatigue Tolerance: High-power naval rotating machinery imposes more severe mechanical conditions than corresponding civilian applications. This is because reduced weight and volume are key drivers for this technology in the Navy, thus structural design of HTS coils is every bit as important as their functional capabilities. In particular, to ensure prospective service life of 30 years or more, potential for fatigue damage must be considered. One premier task area of the NRL program is evaluation of electromechanical properties of HTS tapes and coils, with special emphasis on fatigue tolerance. Figure 3 shows an example of an evaluation performed by NRL on a typical conductor. Figure 3(a) shows how the superconducting critical current Ic decreases with increasing peak applied stress. There is a critical stress below which the Ic changes are at least 95% reversible. Figure 3(b) shows the same conductor subjected to cyclic (fatigue) loading, indicating that cumulative degradation occurs with repeated loading. However, the change of Ic with cyclic loading eventually stabilizes, so that the conductors do not degrade indefinitely.

Cryogenic Inductors: Another element of the NRL program is development and demonstration of HTS inductors for cryogenic power electronics. Conceptually, if the generator and motor are both superconducting, then significant system efficiency benefits could be achieved if the power electronics converters and transmission lines between the generator and motor also operate in the cryogenic environment. Additionally, in conventional ship-drive-power electronics, inductors account for as much as 40% of the volume, 50% of the weight, and are the main source of power losses. Air-core superconducting inductors, however, by virtue of higher current density, can be made smaller and lighter than conventional iron-cored copper inductors. NRL is studying the loss mechanisms of HTS tapes and coils, as well as exploring novel inductor designs for minimizing losses.

Impact: Results of NRL's current program have influenced HTS manufacture for optimizing superconducting properties as well as validated conductor structural architectures for fatigue risk mitigation. Prototype coils are being evaluated for structural integrity

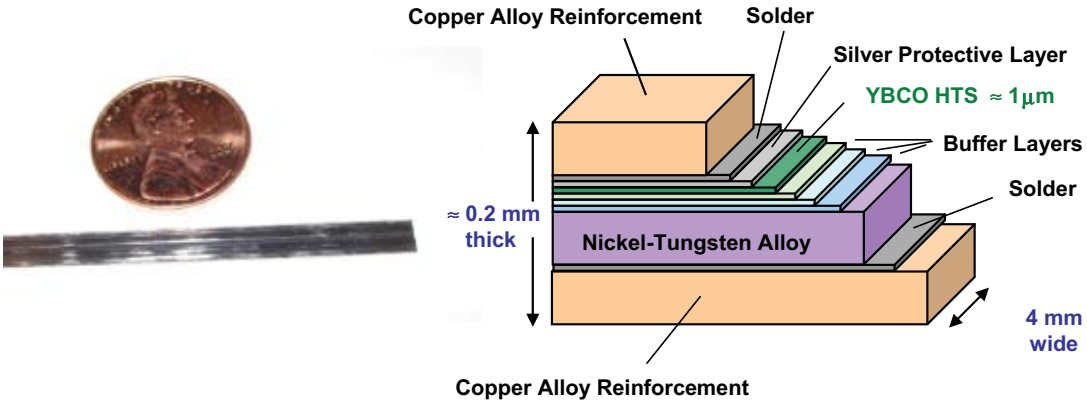

FIGURE 1
A typical 2G-HTS tape about 4 mm wide and 0.2 mm thick is capable of carrying as much as 80 A DC current at 77 Kelvin. Typical architecture of 2G-HTS tapes is shown schematically. The superconducting functionality is provided by the 1 μm-thick YBCO layer. The other 99% of the composite tape determines the mechanical properties.

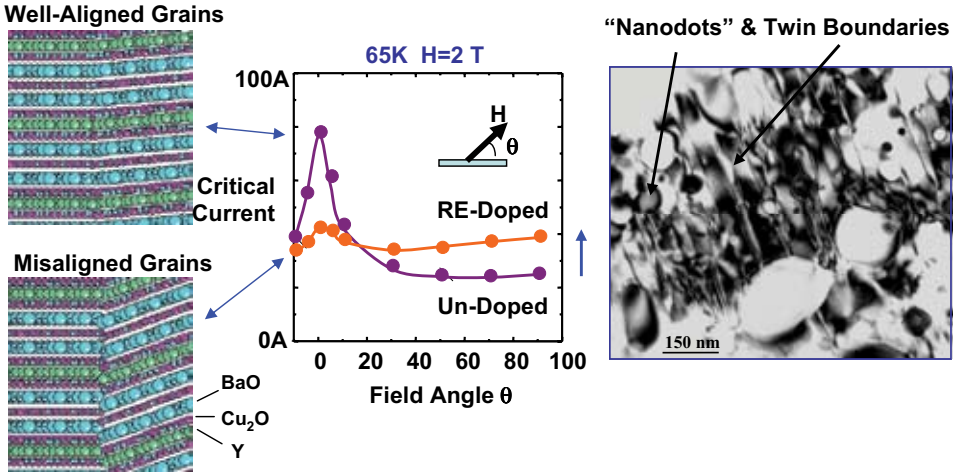

FIGURE 2
Relationship of microstructural defects to superconducting critical current behavior of 2G-HTS tapes in magnetic field, H. Maximum Ic for magnetic fields parallel to the tape is determined primarily by crystallographic alignment of the grains, while defects such as "nanodots" and twins improve the Ic for fields perpendicular to the tape. In this particular case, rare-earth doping decreased Ic for parallel fields due to reduced crystallographic alignment, but the nanoparticles and twin boundaries improve the perpendicular field performance.

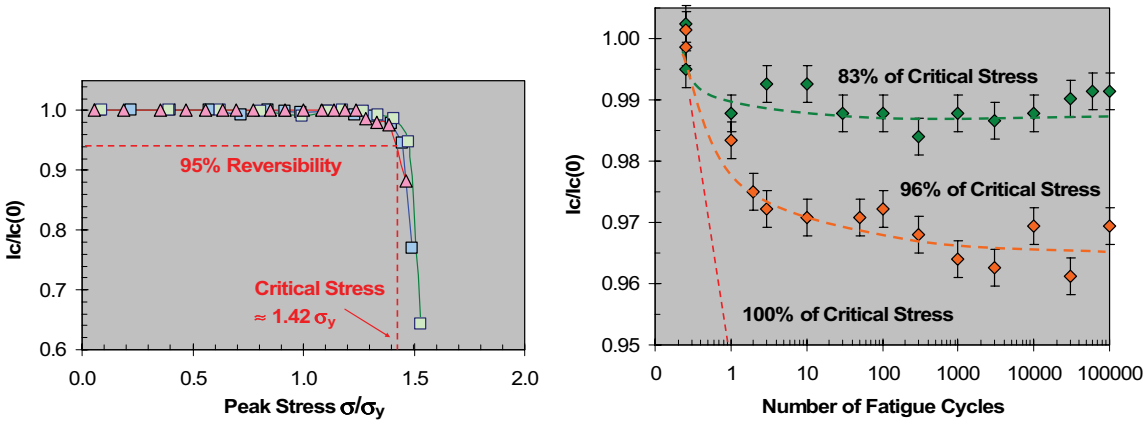

FIGURE 3
Typical electromechanical properties of 2G-HTS tapes. Critical current drops as a function of maximum applied stress as shown in (a) for several tapes, but this effect is at least 95% reversible for stresses below some critical stress limit. Cyclic loading, (b), can cause additional fatigue degradation of Ic for stresses below the critical stress, but the properties stabilize after enough loading cycles. In these plots, Ic is normalized to its initial stress-free value Ic(0) and stress is normalized to the yield stress σ_y.

and AC loss performance. As the technology matures, NRL's contributions will include demonstration of practical inductors, composite coil design, and ultimately participation in large scale motor and generator demonstrations.

Acknowledgments: Superconducting tape and coil specimens used in this work are provided by American Superconductor Corporation, IGC Superpower, Inc., and Sumitomo Electric Industries.

[Sponsored by NRL and ONR] ★

Carbon Nanofiber Reinforced Polymers

J.N. Baucom, A. Rohatgi, W.R. Pogue III, and J.P. Thomas
Materials Science and Technology Division

Introduction: Advanced defense platforms increasingly demand lighter-weight and higher-performing materials. The benefits of lightweight structural components are apparent in the form of increased fuel efficiency, improved mobility, and so on; however, savings in component weight must not come at the expense of functional performance. Whereas aluminum and titanium alloys can be used to reduce weight in many structural applications, even greater weight savings are possible through the use of high-strength polymer composites. The current thrust of our research is to determine the potential benefits of hierarchical structuring to achieve better functional performance. Hierarchical structuring is common in biological material (e.g., nacre, tendon, bone, and wood), yet the general principles and mechanisms by which hierarchical structuring influences functional performance is poorly understood. In this investigation, we examine the structural properties of a polymer nanocomposite whose matrix constituent exhibits an intrinsic hierarchical structure at length scales from 10^{-9} to 10^{-6} m.

Another strategy to achieve weight savings involves the consolidation of multiple functionalities into a single material system resulting in more efficient use of material and reduction of parasitic structural mass. Our group at NRL is actively pursuing the development of materials that simultaneously perform multiple roles, such as structure plus thermal or electrical conduction. The driving force behind the interest in structure/conduction multifunctionality is partly due to the widespread incorporation of densely packed electronic components in shipboard systems. These components produce large amounts of heat that, if not adequately managed, can magnify thermal signature and reduce the life or impair the efficiency of the components themselves. Multifunctional structure-conduction polymer composites might be a lightweight alternative to the thermal management approaches in use today (e.g., aluminum heat sinks).

Technical Approach: We propose the use of mass-produced and inexpensive, *discontinuous* carbon nanofibers to create a percolated fiber network within a polymeric matrix that will result in a nanocomposite material with enhanced mechanical, thermal, and electrical properties.

For the matrix material, we have selected a thermotropic liquid crystalline polymer (LCP) known com-

mercially as Vectra A950. Liquid crystalline polymers exhibit liquid crystalline phases in regions of high shear of the polymer melt (thermotropic LCP) or at sufficiently high concentration in solution (i.e., lyotropic LCPs, a well-known example of which is the aramid Kevlar). This thermotropic LCP was selected owing in part to its processibility using standard thermoplastic processing equipment. More importantly, Vectra A950 is a main-chain LCP that produces a nematic liquid crystalline phase under shear deformation. An interesting result of the molecular alignment is the parallel formation of hierarchically ordered fibrillar structures with diameters ranging from 10^{-9} to 10^{-6} m. Because molecular alignment is induced by the deformation field, this material allows us to explore the influence of hierarchy on functional performance through control of deformation conditions during processing.

We initially selected vapor-grown carbon nanofibers (VGCF) as the reinforcing and conductive second phase because they are inexpensive (25¢/g) yet possess high mechanical and conduction properties akin to their much more expensive cousins, single-wall carbon nanotubes (SWNT - $500/g). This has enabled us economically to develop and refine our processing, testing, and characterization techniques.

A Brabender twin-screw extruder was used to fabricate LCP-VGCF filaments (up to 1.6-mm diameter at 0, 1, 2, 5, and 10 wt% VGCF). The filament diameter was controlled by varying the uptake speed of the semi-molten extrudate. Filaments were tested in quasi-static tension at room temperature. The tensile modulus of elasticity was calculated from the initial slope of the stress-strain curve, and the strength was calculated at the fracture load. Fracture surfaces of the tested samples were observed at high magnification using scanning electron microscopy (SEM).

Results/Summary: From the stress-strain histogram in Fig. 4, we can see that the addition of 1-2 wt% VGCF increased the modulus and strength of our LCP-VGCF nanocomposite by 40% and 20%, respectively. This magnitude of increase in mechanical performance with the addition of such small amounts of VGCF suggests that good interfacial strength is developing between the VGCF and LCP. This is also evident in the SEM images of the fracture surfaces (Fig. 5).

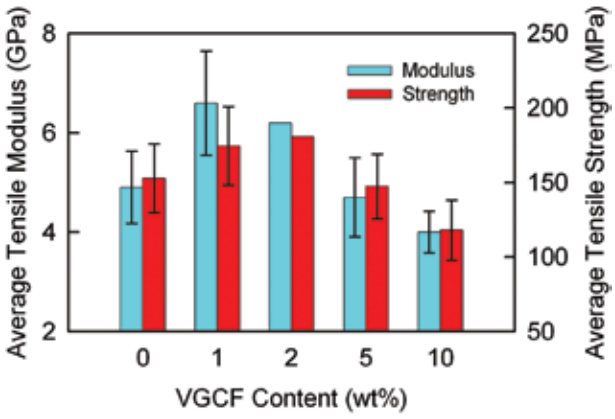

FIGURE 4
Average modulus and strength as functions of VGCF concentration.

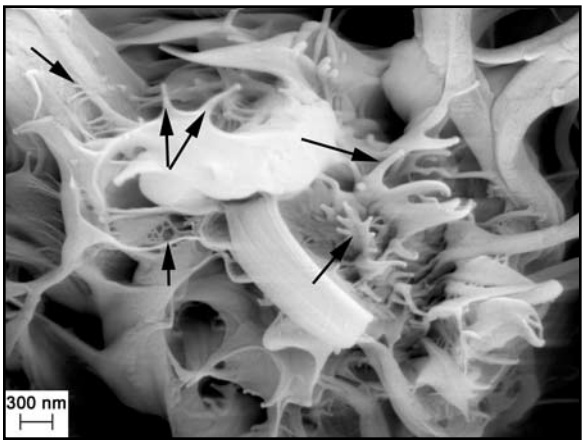

FIGURE 5
SEM image of the fracture surface of an extruded LCP-VGCF filament. The hierarchical nature of the LCP is demonstrated by the presence of numerous smaller-scale fibrils (indicated by arrows) formed by the splitting of larger-scale fibrils.

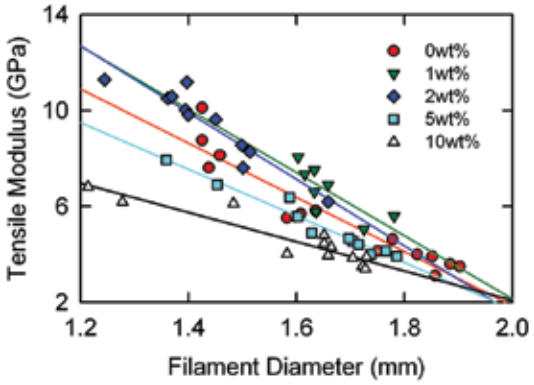

FIGURE 6
Tensile modulus as a function of extruded filament diameter.

In Fig. 6, we see that the tensile modulus increases as the extruded diameter decreases. The largest diameter effects also occur at the 1-2 wt% VGCF levels. This dependence on filament diameter is interesting and likely due to a combination of VGCF and LCP molecular alignment. Stretching the LCP into thinner filaments forces a greater proportion of its molecules to align along the stretch direction, resulting in higher strength and stiffness. We also believe that the LCP molecular alignment process influences the alignment of VGCF resulting in improvement of its stiffening and strengthening effectiveness in the extrusion direction. Transmission electron microscopy, X-ray diffraction, and nanoindentation measurements are being made to assess quantitatively the connection between processing and LCP and VGCF alignment. Thermal and electrical conductivity measurements are also being made to assess the multifunctional potential of these hierarchically structured polymer nanocomposite materials.

[Sponsored by NRL] ★

Railgun Materials Science

R.A. Meger
Plasma Physics Division

Introduction: NRL has initiated a program in electromagnetic (EM) launcher technology focusing on railgun materials science issues. A railgun consists of a power supply that drives current through a pair of conductors or rails to accelerate a projectile to high velocity. The rails and their insulators are contained in a barrel mounted on a platform. The platform must house the power supplies, controls, and projectile loader for the EM Gun (EMG). The conditions within the barrel for high-velocity launch of a multi-kilogram projectile are extreme. They can reach 10,000 atmospheres pressures, megampere currents, and tens of kilo gees acceleration. The barrel must withstand these conditions for up to several rounds per minute for thousands of shots without failure or significant degradation. These parameters are well beyond the state of the art in materials science. NRL scientists are studying the rail, armature, sliding interface, and insulators under these conditions. Initial results from moderate power railguns have shown problems due to rail surface erosion, alloying of materials, arc formation, and localized heating effects. The NRL program is focused on understanding the conditions within the barrel and developing techniques to mitigate damage. A consortium of pulsed power and materials scientists from the Plasma Physics, Materials Science and Technology, and Chemistry Divisions are conducting the research.

Electric Launchers and the Navy: Electric launch offers significant advantages over chemical propellant launch. Conventional guns are limited to velocities comparable to the sound speed of the propellants in the barrel, which limits their effective range to less than 20 nmi. They also require handling of large quantities of energetic materials (propellant and explosive payload) both in the supply chain and on-board ship. This impacts the ship design and the number of shells that can be stored in the ship's explosives magazine. An EMG offers the potential to launch projectiles at higher velocity, which translates into short delivery time and ranges up to 200 nmi, and to use shipboard electric generating capability to launch rather than chemical propellants. The projectile would also be a kinetic energy round with little or no explosives, which simplifies both the supply chain and the magazine requirements. The NRL program is designed to address the barrel materials issues associated with this gun.

Railgun Technology: A railgun consists of parallel conducting rails connected by a sliding contact called

an armature. The launch package, consisting of the armature and payload, is initially pressed between the rails at the breech end. When current is driven through the rails and armature, as shown in Fig. 7, the armature is accelerated by the magnetic field. The accelerating force is proportional to the square of the current driven in the system. This allows one to control the acceleration by programming the current waveform. The launch velocity is limited by the electrical power available, barrel geometry, and the materials properties of the barrel and armature.

NRL is focusing on the barrel materials science issues associated with the Navy railgun. A new railgun Materials Testing Facility (MTF) is being built to allow barrel research at the appropriate power levels. The lab will contain a 6-m long railgun powered by an 11-MJ capacitive energy store using solid-state opening and closing switches. Up to 2 MA of current will be available to launch 1-kg projectiles to greater than 2 km/s velocities. The containment is designed for maximum diagnostic access, rapid turnaround, and easy reconfiguration. NRL has an extremely wide range of bulk and surface materials diagnostics for application to the problem.

Barrel Materials Analysis: Prior to the operation of the MTF railgun NRL scientists have been analyzing rail materials generated by Navy tests at the Institute for Advanced Technology (IAT) located at the University of Texas at Austin.[1] Figure 7 represents a simplified schematic of the rails and armature used for these tests. The launcher has a 3.5-m long square bore with 40-mm-wide rails separated by epoxy-glass laminated insulators. The armature was made of aluminum alloy with a polycarbonate bore rider in front to keep it aligned with the rails. The 500 g package was launched at greater than 2 km/s velocity with 1 MA peak, 6-ms-long current pulse generated by a 10-MJ capacitor bank. NRL has been analyzing single and multiple shot rails from the tests, evaluating rail damage, developing empirical scaling relationships, and trying to understand the launch physics. Figures 8 and 9 contain examples of some of the post-shot analysis of a 20-shot rail. The pictures in both figures come from the vicinity of 40 cm from the start point in the railgun. The current at the time the armature passed this location was approximately 1 MA and the velocity was 1 km/s.

Figure 8(a) shows the rail top surface. The gray colored material is aluminum that has melted off the sliding armature. The three boxes (Fig. 8(b)) show increasing magnification scanning electron microscope (SEM) photographs of the aluminum deposit at one edge. The images at 200-, 30-, and 10-μm scales show the top surface of a thin aluminum layer on the copper rail. Figure 8(c) shows the spectrum generated by Energy Dispersive Spectrocopy (EDS) from near one of the 5-μm sized voids in the aluminum. EDS allows one to determine the atomic constituents near the surface of the material. The spectrum shows a large peak where aluminum is expected. Likewise there are peaks from zinc, copper, oxygen, and carbon.

Figure 9(a) shows a scan from a stylus profilometer of the surface at the 39-cm location. The scan shows that the surface has been eroded by approximately 150 μm near the edge of the rail and to a lesser depth on the other side. In between there appears to be a deposit, found to be a mixture of aluminum and copper, of 200 to 250-μm thickness. Figure 9(b) shows a high-resolution image of the edge of the rail near the 40-cm location approximately where the rectangle in Fig. 8(a) is located. The erosion of the copper near the edge is clearly visible. Figure 9(c) shows SEMs of the ~15 to 20 μm thick edge inside of the groove region. There is evidence of copper dendrites forming near the interface and copper-aluminum crystal formation within the deposit. In the thick deposit region, layers of aluminum were clearly visible in the SEM photographs, showing that the thickness grew from shot to shot. In addition, there have been a variety of X-ray diffraction, X-ray fluorescence, surface stress, material hardness, and other diagnostics applied to the surfaces and cross sections of these rails. From the different diagnostics, a picture of the rail-armature interface under high-power conditions during the acceleration process is being developed.

Conclusion: The development of an EMG for a future Navy platform will be a significant accomplishment. The new NRL facility will provide a testbed to explore the technology at high power. The preliminary work on analysis of rails from other laboratories has both demonstrated the capabilities of the NRL materials analysis and illustrated the effects of a high power launch. NRL hopes to understand and solve some of these problems over the next few years.

Acknowledgments: Contributors to the NRL railgun program include J. Neri, C. Boyer, (L3-Titan Corp., Reston, VA) and R. Hoffman, Plasma Physics Division; J. Sprague, S. Qadri, K. Cooper, and H. Jones from the Materials Science and Technology Division; and I. Singer from the Chemistry Division.

[Sponsored by NRL and ONR]

Reference

[1] R.A. Meger, K. Cooper, H. Jones, J. Neri, S. Qadri, I.L. Singer, J. Sprague, and K.J. Wahl, "Analysis of Rail Surfaces from a Multishot Railgun," *IEEE Trans. on Magnetics* **41**(1), pp. 211-213 (2005). ★

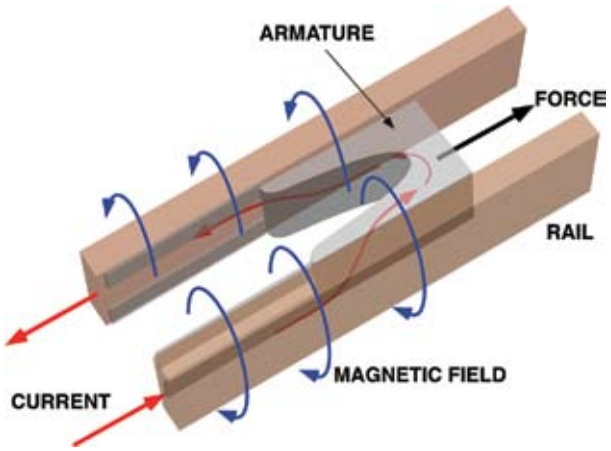

FIGURE 7
Sketch of railgun geometry. Current is driven through one rail, across the armature, and back through the other rail. The magnetic field drives the armature along the rails.

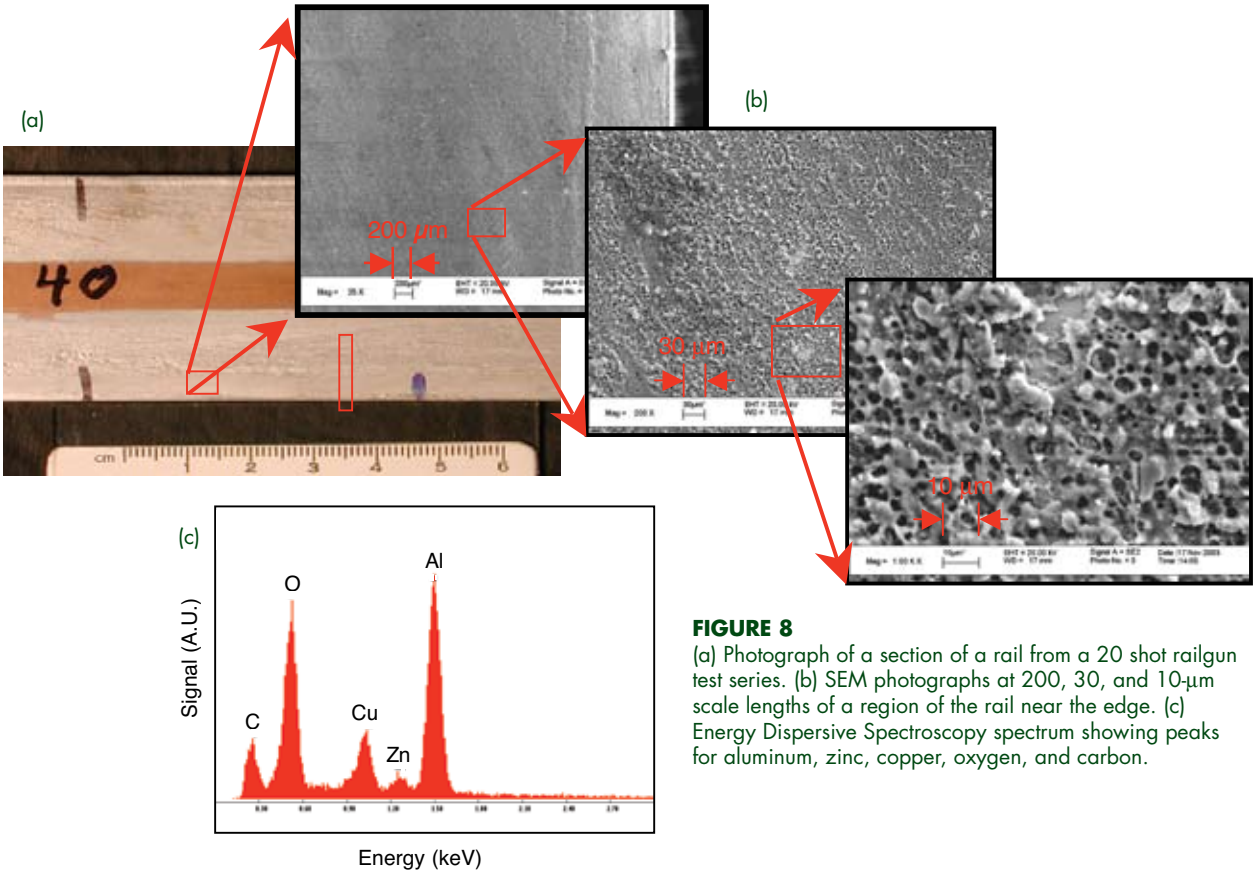

FIGURE 8
(a) Photograph of a section of a rail from a 20 shot railgun test series. (b) SEM photographs at 200, 30, and 10-μm scale lengths of a region of the rail near the edge. (c) Energy Dispersive Spectroscopy spectrum showing peaks for aluminum, zinc, copper, oxygen, and carbon.

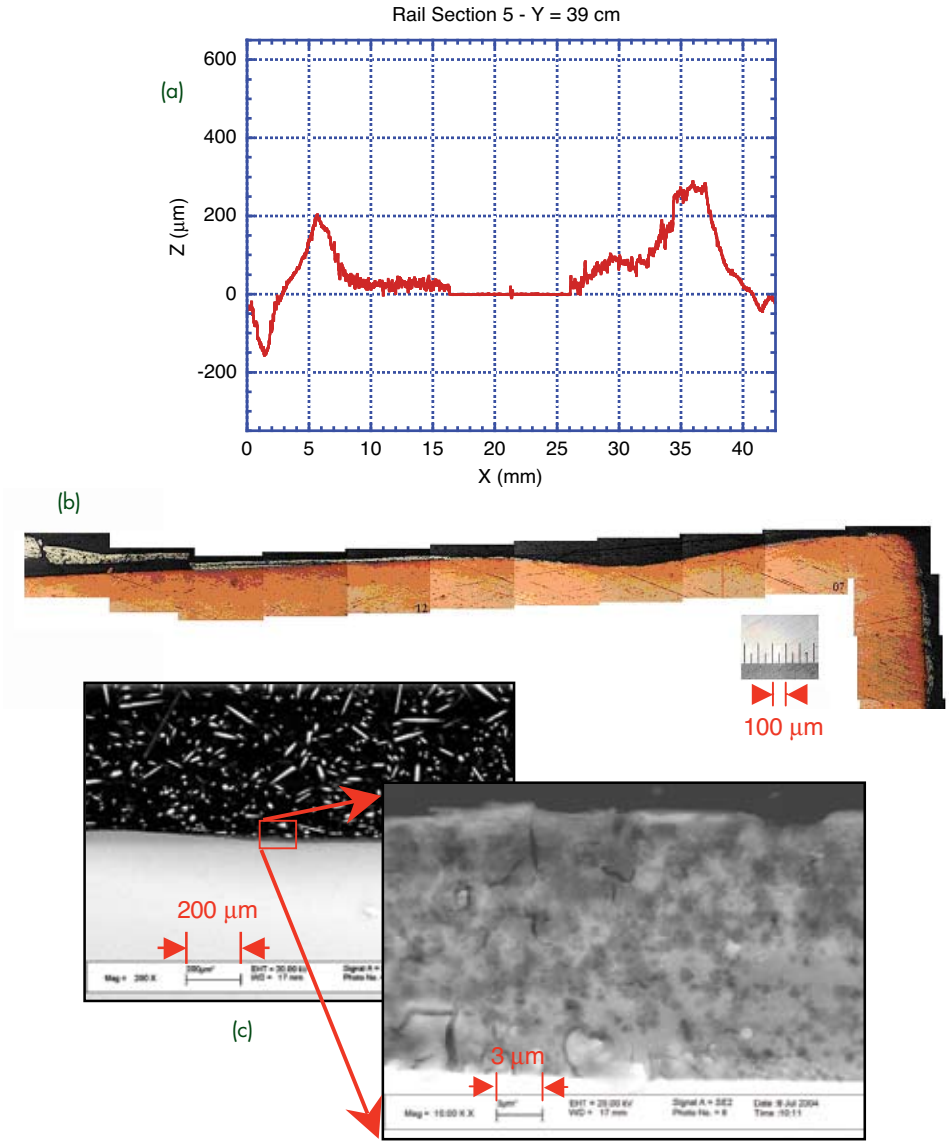

FIGURE 9
(a) A scan from a stylus profilometer at the 39 cm location on the rail section shown in Fig. 8(a). (b) A montage of high-resolution photographs of the cross section near the edge of rail segment in Fig. 8(a). (c) SEM photographs of the deposit on the copper rail in the vicinity of the groove on the edge of the rail.

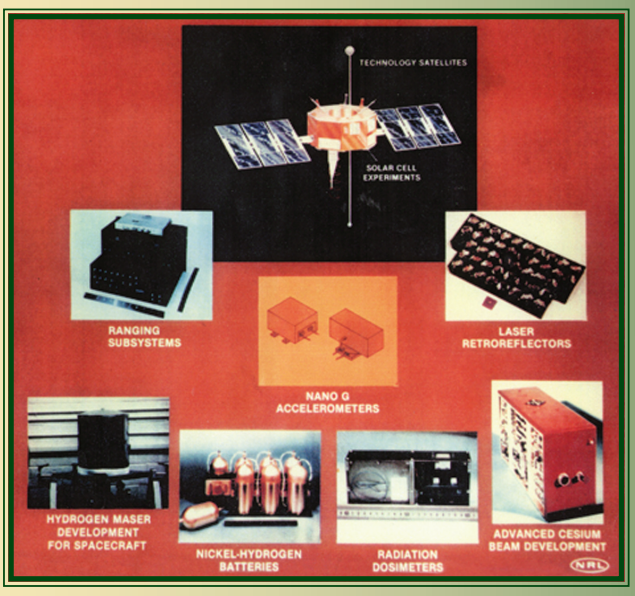

NAVSTAR GPS

Achievement: The NAVSTAR Global Positioning System (GPS) is designed to provide precise navigation data to military and civilian users by means of a constellation of 24 satellites. NAVSTAR is based on NRL's TIMATION (TIMe/navigATION) research program, begun in 1964. R. Easton is recognized for conceiving the idea of the time-based navigational system, which eventually led to the GPS. NRL tested TIMATION concepts by developing and launching two small experimental satellites, TIMATION I and TIMATION II.

NRL launched the TIMATION I satellite on May 31, 1967, and the TIMATION II satellite in 1969. TIMATION I demonstrated that a surface vessel could be positioned to within two tenths of a nautical mile and an aircraft to within three-tenths of a nautical mile using range measurements from a time-synchronized satellite. The TIMATION program proved that a system using a passive ranging technique, combined with highly accurate clocks, could provide the basis for a revolutionary navigation system with three-dimensional coverage (longitude, latitude, and altitude) throughout the world.

In 1973, NRL's program was merged with an Air Force program that was investigating similar requirements to form the NAVSTAR GPS program. TIMATION III was redesignated the Navigation Technology Satellite One (NTS-1), and was launched in 1974 in connection with the new NAVSTAR effort. NTS-1 had the distinction of carrying the first atomic clocks into orbit. NTS-2 was launched in June 1977 as the first NAVSTAR satellite.

Impact: NAVSTAR's military and commercial applications are revolutionary and too numerous to list here. In 1993, the National Aeronautic Association selected the GPS Team composed of NRL, the U.S. Air Force, Aerospace Corp., Rockwell International, and IBM Federal Systems Co. as winners of the 1992 Robert J. Collier Trophy, the most prestigious of all aviation awards in the U.S. The citation accompanying the trophy honors the GPS Team "for the most significant development for safe and efficient navigation and surveillance of air and spacecraft since the introduction of radio navigation 50 years ago." In 2005, Roger L. Easton received the National Medal of Technology from the President for "his extensive pioneering achievements in spacecraft tracking, navigation and timing technology that led to the development of the NAVSTAR - Global Positioning System."

Finite Element-Based Coastal Ocean Modeling: Today and Tomorrow

C.A. Blain, T.C. Massey, R.A. Arnone, and R.W. Gould
Oceanography Division

Introduction: The continued necessity of military special forces operations in riverine and coastal environments along with increasing civilian concerns related to sediment transport, search and rescue, pollutant dispersal, and coastal restoration, have resulted in the need for detailed knowledge of currents and water levels in coastal, estuarine, and riverine environments. This demand for information at highly resolved spatial and temporal scales and the availability of massively parallel computer resources has brought to the forefront the capabilities of finite element (FE)-based coastal ocean circulation models. The use by these models of unstructured triangular meshes permits a large degree of flexibility in representing the complexities of coastal environments associated with convoluted shorelines, and steep gradients in currents or bathymetry. Ultimately this flexibility results in model predictions over periods of hours or less at spatial scales that range from meters to kilometers.

A Model for Coastal Mississippi and Louisiana: Unstructured meshes containing upwards of 281,800 computational points and 540,000 triangular elements are constructed to represent riverine and coastal currents off the shores of southeast Louisiana and Mississippi (Fig. 1). Spatial resolution is 50 m in rivers and decreases to 100 to 200 m offshore. The need for remote boundary forcing is accomodated by including the Gulf of Mexico and extending the mesh into the north Atlantic ocean. The applied forcing includes tides, wind stress at the water surface and river discharge from the Atchafalaya and Mississippi Rivers.

Connecting Mississippi River Currents and Observed Optical Properties: The underlying physical processes that influence observed optical distributions as derived from remotely-sensed ocean color data are often too complex and are manifest at space and time scales that preclude full understanding from imagery alone. But when coupled with highly resolved, dynamically advanced numerical models, understanding increases and the prediction of dynamical processes and optical patterns in coastal waters is possible. During March 2004, magnitudes of the depth-averaged currents computed at the mouth of the

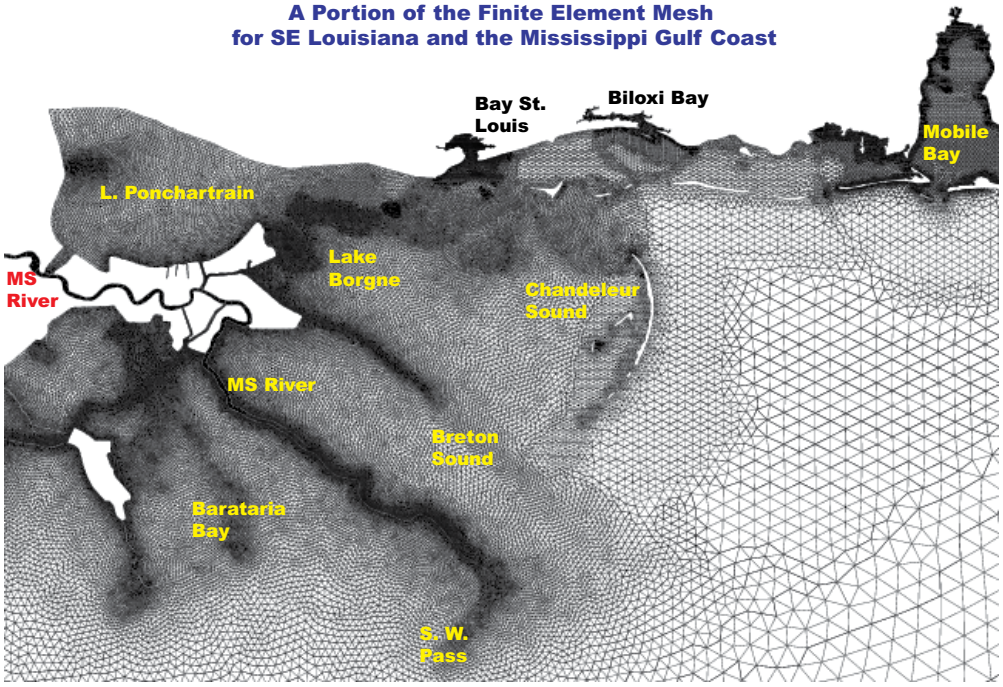

FIGURE 1
Detail of the unstructured computational mesh constructed for Louisiana and Mississippi coastal waters. The mesh, containing 281,528 computational points and 455,203 triangular elements, has 50-m resolution of the Mississippi and Atchafalaya rivers, 100-m resolution of nearshore areas, and includes the entire Gulf of Mexico extending to 60 deg W in the north Atlantic ocean to accommodate remote tidal forcing from a global tide model.

Mississippi River and westward are correlated to the spatial distribution of the beam attenuation coefficient (a sum of the total absorption and scattering) derived from the MODIS 250-m ocean color data.[1] The plume of high beam attenutation (an indication of more sediment particles in the water) found westward of the Mississippi River outflow is a response to the stronger, undulating westward moving coastal currents (Fig. 2). Comparisons of the same currents with observed chlorophyll are not as striking; this is expected since many unmodeled biological and optical processes contribute to the distribution of chlorophyll in coastal waters. Remotely sensed ocean color data are often the only observational window on ocean processes in denied areas of military interest, making the coupling of satellite imagery with numerical models imperative for developing a preditive capability in such regions.

Predicting Hurricane Katrina Storm Surge: Tidal variability combined with the best available NOAA reanalyzed surface winds representing the evolution of Hurricane Katrina force the FE-based coastal model in a hindcast of the surge elevation experienced along the Mississippi Gulf coast. Model predictions (Fig. 3, top) at landfall on August 29, 2005, 5:30Z indicate maximum surges are in the range of 9 m and occur several hours after the peak winds (Fig. 3, lower panels). The unstructured mesh includes such features as levees along the Mississippi River, channels, inland topography, and a capability for surge overtopping of barrier islands.

A New Approach for the Future: While the current FE methodology leads to robust computations of tide and surge dynamics, limitations on local conservation properties are motivating development of the next generation of FE-based coastal models. NRL is implementing a new and promising class of FE methods, the discontinuous Galerkin (DG) methods, which have seen very rapid development over the last several years. The primary advantage of DG methods is their local (element by element) enforcement of the conservation laws, which pave the way for accurate transport of temperature and salinity, or other conservative tracers. Findings from comparisons between the existing FE-based model and a model using the new DG methodology[2] show that the DG formulation is able to retain the robustness of existing model solutions while more sharply resolving gradients and other small-scale circulation features. Furthermore, the local nature of the DG method is advantageous in permitting 1) elemental specification of the order

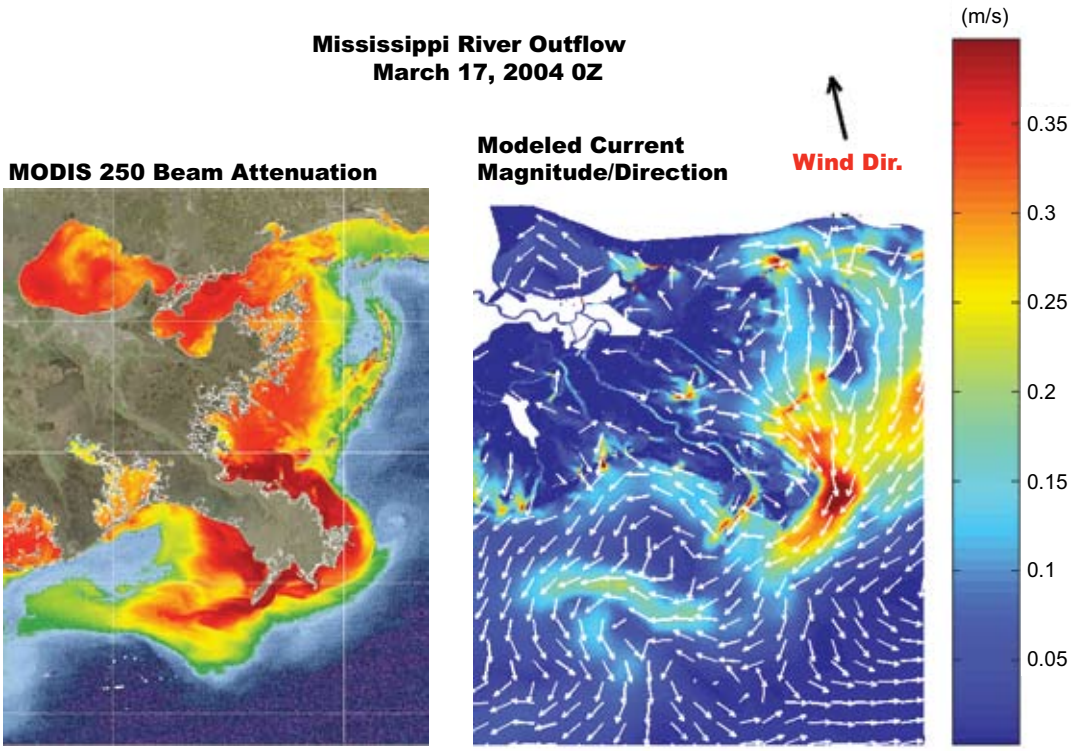

FIGURE 2
The beam attenuation coefficient derived from the MODIS 250-m ocean color data (left) is well correlated to 2D finite element model-predicted barotropic currents (right) on March 17, 2004. The westward movement of the sediment plume (high beam attenuation/high particle concentration) from the Mississippi River can be attributed in part to the underlying westward movement and undulation of the currents.

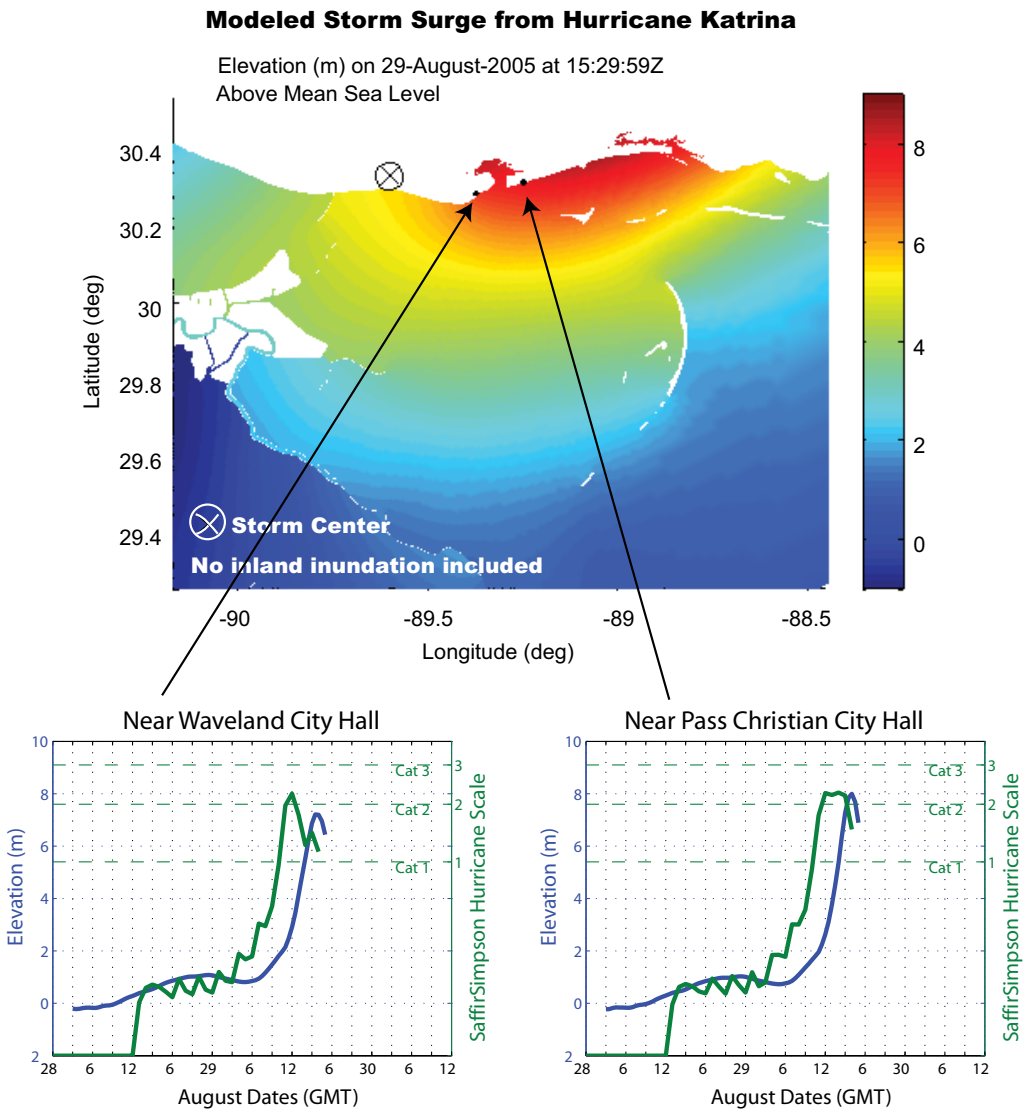

FIGURE 3
Hindcast of Hurricane Katrina storm surge elevations near the time of landfall August 29, 2005, 5:30Z. Time series evolutions of the wind and surge at Waveland, MS and Pass Christian, MS.

of approximation, thereby allowing for the capture of frontal and sharp gradient regions, 2) nonconforming unstructured meshes that simplify development of adaptive meshing strategies, and 3) a reduction in the computational footprint to an element and immediate neighbor elements, a necessity for efficient parallel processing on distributed memory machines. The potential of this new methodology to revolutionize coastal ocean modeling is significant and NRL is leading the way in its development and application to complex ocean dynamics problems.

Acknowledgments: The authors recognize Dr. Joannes Westerink at the University of Notre Dame for contributing an early version of the developed finite element mesh and Dr. Frank Giraldo of NRL's Marine Meteorology Division for his contributions to the future DG-based model.

[Sponsored by NRL]

References

[1] R.A. Arnone, Z.P. Lee, P. Martinolich, and S.D. Ladner, "Characterizing the Optical Properties of Coastal Waters by Coupling 1 km and 250 m Channels on MODIS – Terra," Ocean Optics XVI, 2002.

[2] C.A. Blain and T. C. Massey, "Application of a Coupled Discontinuous-Continuous Galerkin Finite Element Shallow Water Model to Coastal Ocean Dynamics," *Ocean Modeling* **10**, 283-315, 2005. ★

Sea Floor Sediment Mapping from Multibeam Sonar: SediMap®

F.W. Bentrem, W. Avera, and J. Sample
Marine Geosciences Division

Introduction: NRL's Marine Geosciences Division has developed a capability (SediMap®) to characterize the sediment on the sea floor using the acoustic backscatter information from multibeam bathymetric sonars. Sea floor properties play an important role in mine warfare and antisubmarine warfare, as well as in nonmilitary applications, such as laying communication cables along the ocean floor. Of particular interest is the ability to distinguish between mud, fine sand, coarse sand, and gravel or rock. Ocean-survey operations use multibeam sonars to acquire acoustic data for measuring water depth (bathymetry) worldwide. These sonars also measure acoustic backscatter from many incident angles with respect to the sea floor. Since the angular response of the backscatter largely depends on the type of sediment on the sea floor sediment, this same data also provides a means to classify the ocean bottom.

Multibeam Sonar: The Naval Oceanographic Office (NAVOCEANO) conducts surveys to measure water depth and other ocean properties worldwide using their TAGS-60 survey vessels. The water depth is measured by two sonars, EM 121A and EM 1002, each with more than 100 sound beams aimed at different angles below the ship as shown in Fig. 4. The multibeam sonars emit sound frequencies of 12 kHz and 95 kHz, respectively. Strength of the sonars' echo from a particular spot on the bottom returning in the direction of the sonar is known as the backscattering strength and depends on both the incidence angle of the beam with the sea floor and the acoustic properties of the sediment.

Scattering Model: For the purpose of acoustic scattering, the sea floor is sometimes modeled by treating it as a fluid. The scattering is then a result of the roughness and acoustic impedance (reflectivity) of the water-sediment boundary and interaction with the underlying sediment. The backscatter model used in SediMap® was developed by the Applied Physics Laboratory at the University of Washington (APL-UW)[1] and predicts backscattering strength as a function of

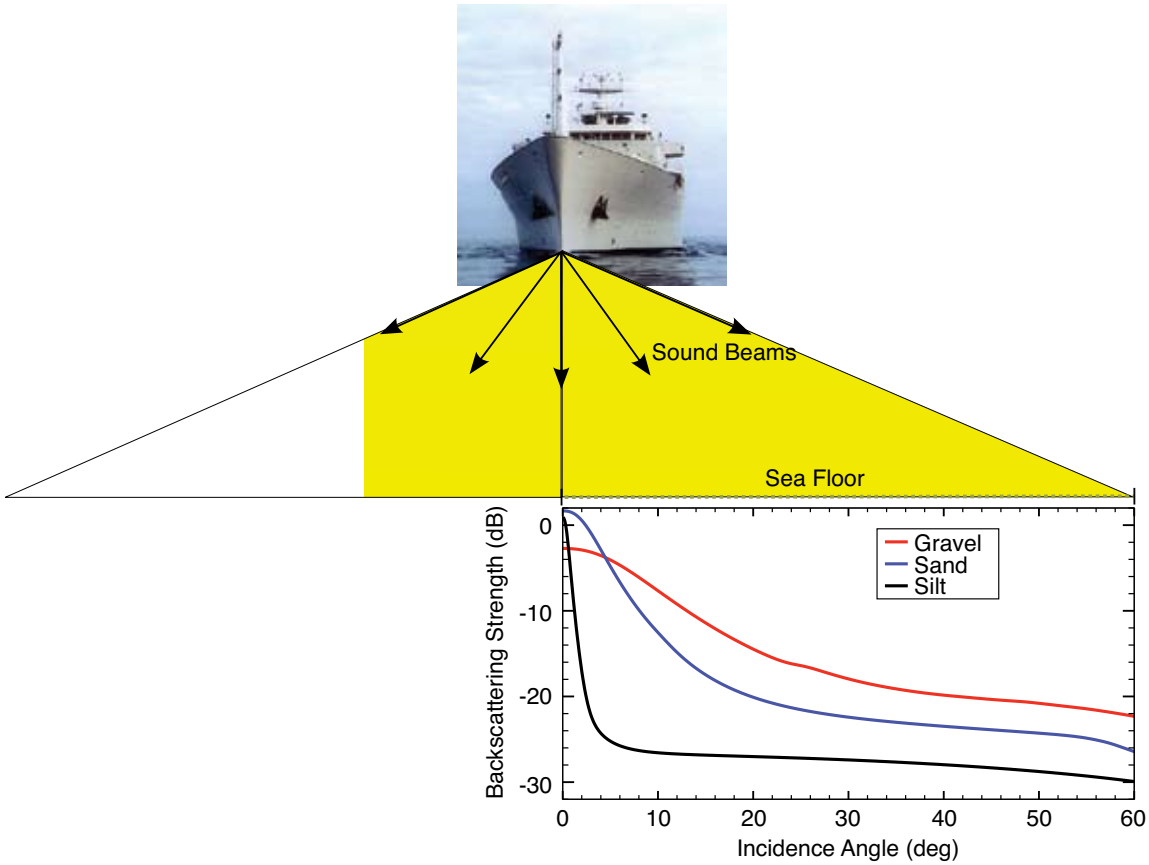

FIGURE 4
(Top) Representation of multibeam sonar from a TAGS-60 survey vessel. (Bottom) Plots showing backscattering strength varying with incidence angle for typical gravel (red), sand (blue), and silt (black).

both the incidence angle and geo-acoustic sea floor properties.

Optimization: SediMap® fits backscattering strength vs incident angle data to the APL-UW scattering model and yields estimates for sediment mean-grain-size.[2] First, a global optimization technique, simulated annealing, is used to find the set of geo-acoustic parameters that best match the backscatter data. Based on empirical correlations in geo-acoustic properties from historical sediment data, these parameters are then associated with a mean-grain-size for the surface sediments.

Naval Survey Testing: Validation tests conducted by NAVOCEANO demonstrate strong correlation with ground truth samples. Testing was performed for water depths ranging from 5 to 500 m with sediment ranging from mud (very fine sediment) to gravel (very coarse sediment). The survey data were available in a number of regions including the Persian Gulf (see Fig. 5), the Gulf of Mexico, and off the coast of Ft. Lauderdale, Florida. In some cases, the ground truth samples were collected during the same survey as the acoustic data. Otherwise, ground truth was obtained from archived data sources. NAVOCEANO is using SediMap® products to improve the Navy's sea floor environmental databases. This new methodology provides a means to rapidly assess and map sea floor sediments using existing bathymetric sensors by simply adding an additional processing step.

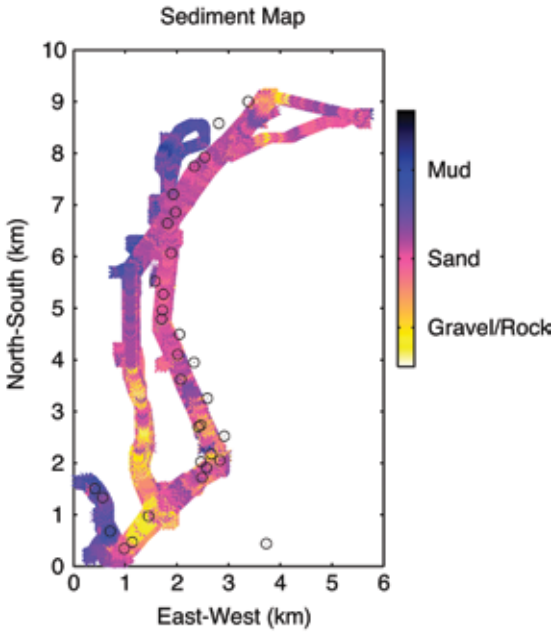

FIGURE 5
SediMap®'s indication of ocean sediments in the Persian Gulf exhibiting strong correlation with the grab samples (in circles). The correlation coefficient is 0.77.

Acknowledgments: We gratefully acknowledge Peggy Haeger (NAVOCEANO) for providing acoustic data. We also thank Gene Kelly (NAVOCEANO) for providing core sample analyses and for arranging a field test in the Gulf of Mexico.

[Sponsored by ONR]

References

[1] Applied Physics Laboratory at the University of Washington, "High-Frequency Ocean Environmental Acoustic Models Handbook," Technical Report APL-UW TR 9407, October 1994, Seattle, Washington.

[2] F.W. Bentrem, J. Sample, M.T. Kalcic, and M.E. Duncan, "High-frequency Acoustic Sediment Classification in Shallow Water," *Proceedings of Oceans 2002 MTS/IEEE Conference and Exhibition*, Biloxi, MS, October 2002, Volume 1, pp. 7-11. ★

A High-Resolution Urban Canopy/Land-Surface Modeling System

T.R. Holt
Marine Meteorology Division

Introduction: Heterogeneities in land-surface characteristics that occur in transitions from a large coastal city to the suburbs and then to the rural countryside can significantly alter the lower portion of the atmosphere through mechanical and thermodynamical interactions. For example, urban-rural interfaces, both upwind and downwind of the urban region, are often preferred zones for the initiation of atmospheric convection or modification of ongoing convection.[1] Changes in the vertical profile of atmospheric static stability in the lowest portion of the atmosphere due to such heterogeneous surface forcing can have an important impact on transport and dispersion of potentially harmful chemical/biological agents. Thus, with a large percentage of the world's population living in coastal urban areas and an increasing emphasis of Naval fleet operations in coastal regions, an accurate characterization of high-resolution processes in numerical weather prediction models will greatly improve local forecasts for populations at risk as well as military operations.

Modeling System: To address these issues, the Marine Meteorology Division has developed new urban canopy and land-surface sub-models that are integrated into the Navy operational mesoscale numerical weather prediction model COAMPS®.* The sub-models use high-resolution land-surface databases characterizing differing vegetation and soil types,[2] time-varying sea surface temperature (SST), as well as

*COAMPS® (Coupled/Ocean Atmosphere Mesoscale Prediction System) is a registered trademark of the Naval Research Laboratory.

building morphologies, anthropogenic heating, and street and roof characteristics.[3] The vegetation and soil component uses an advanced canopy resistance formulation to accurately determine the effectiveness for soil moisture to be released to the atmosphere via transpiration, which is one of the most efficient means of water loss from the vegetated land surface. The urban canopy acts as a friction source, represented via modified aerodynamic drag in the momentum equations, as well as a source of turbulence production to account for turbulence wake generation of turbulence kinetic energy. The urban thermal effects are from heat fluxes from rooftop, street, and building wall reflections.

Results: Because of its complex coastal land-surface characteristics, spatially and temporally varying atmospheric conditions, and prominent threat profile, the New York City (NYC) metropolitan area is chosen as a test bed to evaluate the new system. One particular feature of interest is the evolution and interaction of the sea breeze with the urban environment. Figure 6 shows a COAMPS® simulation of transport in the NYC region of five near-surface tracers continuously released starting at 00 UTC for a period in April 2005. This simulation clearly illustrates the complexities that can result in less than 24 hours. Winds generally from the west at 03 UTC transport all plumes rather uniformly to the east. However, winds shift to southeasterly by 21 UTC with the onset of the sea breeze and the plumes, though generally transported to the northwest, display significant differences. The influence of differing land and urban forcing on vertical velocity and stability profiles is clearly indicated in the increased vertical dispersion of the plume originating from Rockefeller Center as compared to the Financial District. Further evidence of the land-surface and urban effects is shown in Fig. 7, which illustrates the deformation and horizontal retardation of the propagation of the sea breeze front in Brooklyn and the vicinity of JFK airport. A vertical cross-section of two COAMPS® simulations (with and without the urban component of the sub-system) through the southern tip of Manhattan (Fig. 8) illustrates the urban canopy effects on the vertical stability and low-level wind flow. The local vertical circulation in the boxed region is enhanced using the urban component. In addition, high-resolution SST variations, such as induced by river run-off from the Hudson and East Rivers along with local discharge from storm drains, can result in SST anomalies that further alter the overlying atmospheric circulation.

Summary: The Marine Meteorology Division has developed new urban canopy and land-surface submodels within COAMPS®. With this new modeling

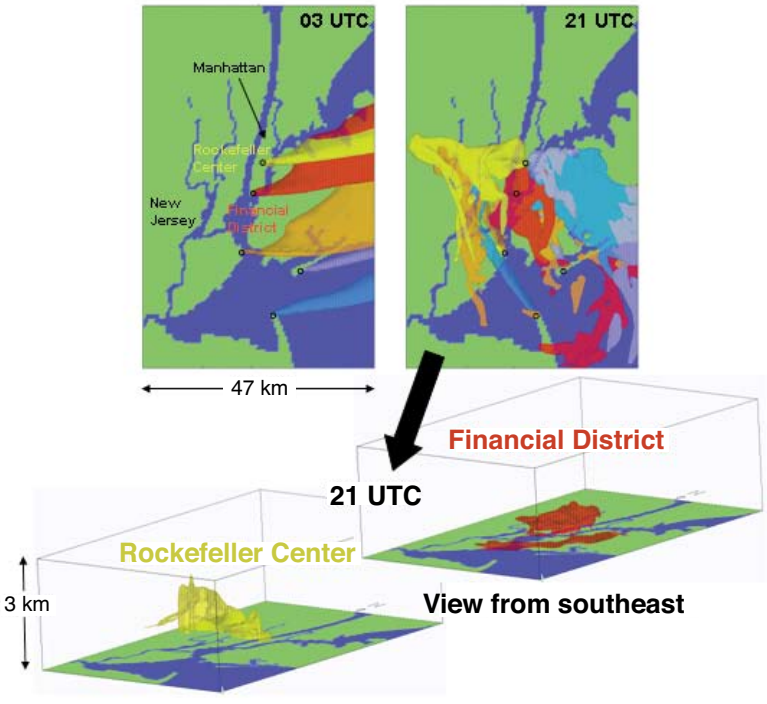

FIGURE 6
COAMPS® simulations of the 10 mg m^{-3} concentration isosurface at 03 and 21 UTC for continuous passive tracer releases at 2 m above ground level for five locations in the New York City region starting at 00 UTC April 18, 2005 (top), and the view from the southeast at 21 UTC for Rockefeller Center and the Financial District (bottom).

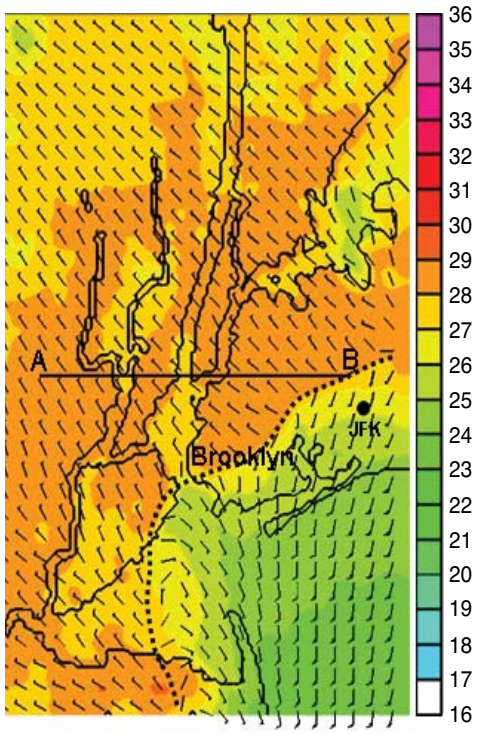

FIGURE 7
COAMPS® simulation of the 10-m winds and 2-m air temperature (deg C; color) valid 00 UTC August 5, 2004. The sea breeze front is indicated by the dashed line. The horizontal grid spacing is 444 m and every fifth wind barb is shown.

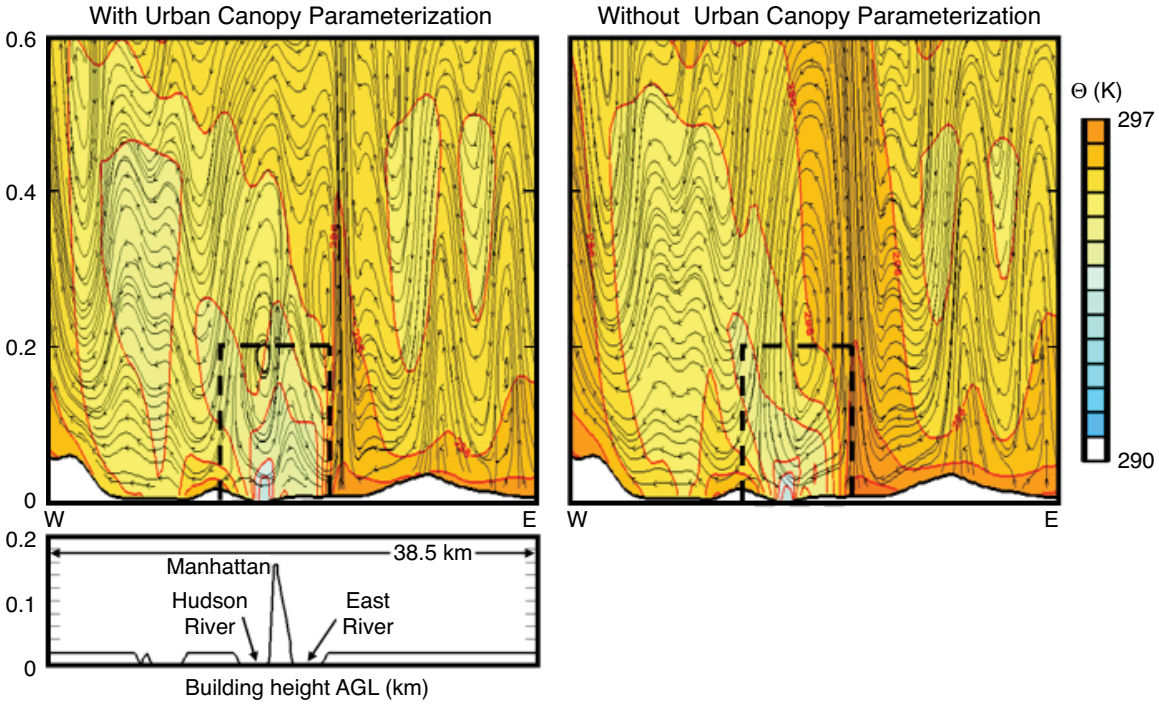

FIGURE 8
COAMPS® simulation of the wind streamlines and potential temperature (color) for the east-west cross section (A-B shown in Fig. 7) through the southern tip of Manhattan valid 17 UTC July 4, 2004. The left panel uses the COAMPS® urban parameterization with the building profile as shown below. The right panel does not use the urban parameterization. Note the differences in structure in the dashed region over the lowest 200 m of the atmosphere in the vicinity of the Hudson and East Rivers.

capability, the Navy will be able to analyze and predict atmospheric conditions in urban coastal areas at very high spatial resolution (~1 km) that has not been achieved before, thereby improving the prediction of the transport and dispersion of chem-bio agents, the performance of naval weapon sensors and systems, and human well-being and security. In addition, the Marine Meteorology Division participated in the second field experiment of the Department of Homeland Security New York City Urban Dispersion Program that occurred on August 6-24, 2005, in midtown Manhattan. This program provides a dense array of high resolution observations in a complex urban environment to better validate the new system. We will be using the observations taken in the NYC experiments and other upcoming field experiments to further our understanding of the complex urban environment and to improve our capability to model the processes that generate these complex environmental states.

Acknowledgments: The core development for the system was performed under NRL base-funded program element number 0602435N. Special thanks to the Department of Homeland Security Urban Dispersion Program that funded our participation through grants P4CF40592 and P5CH40318.

[Sponsored by NRL and the Department of Homeland Security]

References

[1] A.F. Gero, A.J. Pitman, G.T. Narisma, C. Jacobson, and R.A. Pielke, Sr., "The Impact of Land Cover Change on Storms in the Sydney Basin," *Global and Planetary Change*, in press, 2006.

[2] T. Holt, D. Niyogi, F. Chen, K. Manning, M. LeMone, and A. Qureshi, "Effect of Land-Atmosphere Interactions on the IHOP 24-25 May 2002 Convection Case," *Mon. Wea. Rev.*, in press, 2006.

[3] H.-N.S. Chin, M.J. Leach, G.A. Sugiyama, J.M. Leone, Jr., H. Walker, J.S. Nasstrom, and M.J. Brown, "Evaluation of an Urban Canopy Parameterization in a Mesoscale Model Using VTMX and URBAN 2000 Data," *Mon. Wea. Rev.* **133**, 2043-2068, 2005. ★

The United Arab Emirates Unified Aerosol Experiment (UAE^2)

J.S. Reid, D.L. Westphal, E.A. Reid, A.L. Walker, M. Liu, S.D. Miller, and A.P. Kuciauskas
Marine Meteorology Division

Introduction: The Southwest Asian region surrounding the Arabian Gulf is one of the most difficult environments in the world to characterize, model, and monitor. Frequent dust storms, high pollution levels, and complex flow patterns dominate the region. The atmosphere is heavily impacted from air masses from five subcontinents (Central-North Africa, Europe, Arabian Peninsula, Central Asia, and the Indian Subcontinent), and at the same time influenced by very strong micro to mesoscale circulations that form around the hot deserts, warm waters, and mountain ranges. Previous generations of remote sensing systems and meteorology models have had tremendous difficulty coping with the bright, hot, and variable desert landscape as well as the shallow and warm coastal waters. The interests in Southwest Asia are obvious for military and civilian research communities. The poor visibility and complicated meteorology converge to disrupt operations in Iraq and Afghanistan as well as navigation and air operations in the Arabian Gulf. The Arabian Gulf region is an excellent natural laboratory for the study of micrometeorology, air-sea interaction, atmospheric chemistry, radiative transfer, cloud microphysics, aeolian processes, climate change, and the development of atmospheric remote sensing and modeling systems in complicated environments. The research program described here was developed to address these topic areas and is an excellent link between DoD and civilian research interests.

The UAE^2 Campaign: Beginning in the summer of 2004, the Marine Meteorology Division led the United Arab Emirates Unified Aerosol Experiment (UAE^2), funded by NASA, ONR, and NRL, to study the atmospheric phenomenology of Southwest Asia and the Arabian Gulf. Hosted in country by the UAE Office of His Highness the President, Department of Water Resource Studies (DWRS, now the UAE Department of Atmospheric Studies), the eight-country, 50-member science team focused on the mesoscale meteorology, aerosol microphysics, and remote sensing of Southwest Asia. The deployment was organized to intensely monitor the strong gradients in atmospheric parameters over the entire southern Gulf region (Fig. 9). Included were 2 research aircraft, 15 satellite sensors, 5 atmospheric models, and 15 AERONET Sun photometers—the densest such network ever deployed. The UAE DWRS provided data from 52 meteorological stations, the only surface mesonet in Southwest Asia. The mission also included the deployment of NRL's Mobile Atmospheric Aerosol and Radiation Characterization Observatory (MAARCO, Fig. 9) at a coastal site. At MAARCO, a complete set of meteorology, aerosol, and radiation information was obtained during the experiment. A secondary station was deployed in the interior desert by NASA to study radiative transfer. A complete description of the first year's study accomplishments can be found in Ref. 1.

Significant Advances in Aerosol Chemistry and Meteorology by NRL: While large dust events do

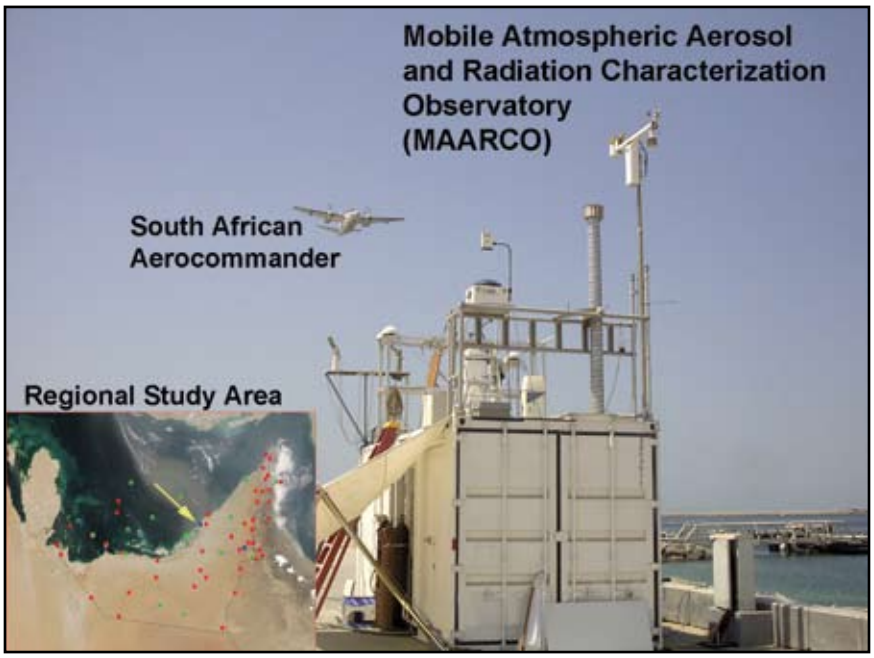

FIGURE 9
The NRL MAARCO with the South African Research Aircraft performing an overpass. Also included is a map of the study region with locations of DWRS weather (red), AERONET Sun photometer (green), and super sites (blue). MAARCO is indicated by a yellow arrow.

occur regularly in Southwest Asia, one of our primary findings was that the smaller mesoscale dust events and atmospheric pollution had the most widespread influence on the atmospheric radiative balance or visibility. Consider Fig. 10, where the Coupled Ocean Atmosphere Mesoscale Prediction System (COAMPS®) surface wind fields for September 12, 2004, are overlaid on the NRL MODIS Dust Enhancement Product.[2] The wind directions clearly show the area where the easterlies interact with the regional southwest monsoonal winds over the Arabian Gulf causing a large convergence zone to form, as evidenced by the region of heavy dust concentration (red shade). On this day, aircraft measurements over the Gulf of Oman and Arabian Gulf revealed the westward advection of high pollution content from the Indian subcontinent into the Gulf of Oman, with associated surface visibilities below 2 km. Similarly, oil platforms in the Arabian Gulf (lower right panel in Fig. 10) also contributed to significant pollution events within the region.

Case studies such as these have led us to a principal area of study: how do atmospheric, land, and ocean scales on the order of kilometers impact the mesoscale and in turn the larger synoptic scale? Indeed, we found that close attention to these smaller scale events is of importance in trying to model aerosol budgets, lifecycle, and impacts. Figure 11 provides an excellent illustration of how NRL satellite-derived products assist in small-scale research efforts. In this example, the Defense Meteorological Satellite Program/Operational Linescan System (DMSP/OLS), METEOSAT-5/IR, Terra/Moderate-resolution Imaging Spectroradiometer (MODIS), and National Ocean and Atmospheric Administration/Advanced Very High Resolution Radiometer (NOAA/AVHRR) captured a massive dust event that formed within the outflow of a thunderstorm (called "Haboobs"). The NRL dust enhancement products (upper and middle right panels) clearly illustrate the dust front ahead of the thunderstorm. Photographs within the lower 2 panels dramatize the onset of the Haboobs; these events occurred with frequency during UAE^2. In combination with other mesoscale flows, such as the strong sea-land breezes and orographically induced winds, haboobs ultimately manifested themselves at a scale once thought to be dominated by much larger-scale synoptic patterns.

Acknowledgments: We thank our partners in this mission including the UAE Office of His Highness the President, the Department of Water Resource Studies, NASA laboratories, the University of Witwatersrand, and numerous other international groups. Funding for NRL participation came from the Office of Naval Research, NASA Radiation Sciences Office, and the NRL 6.1 Base funding and Platform support program.

[Sponsored by ONR, NASA, and NRL]

References

[1] J.S. Reid, S.J. Piketh, R.T. Bruintjes, R.A. Kahn, and B.N. Holben, "A Summary of First Year Activities of the United Arab Emirates Unified Aerosol Experiment: UAE^2," NRL/MR/7530--05-8899, August 2005.

[2] S.D. Miller, "A Consolidated Technique for Enhancing Desert Dust Storms with MODIS," *Geophys. Res. Lett.* **30**(20), 2071-2074 (2003).

[3] S.D. Miller, et al., "MODIS Provides a Satellite Focus on Operation Iraqi Freedom," *Int. J. Rem. Sens.*, in press. ★

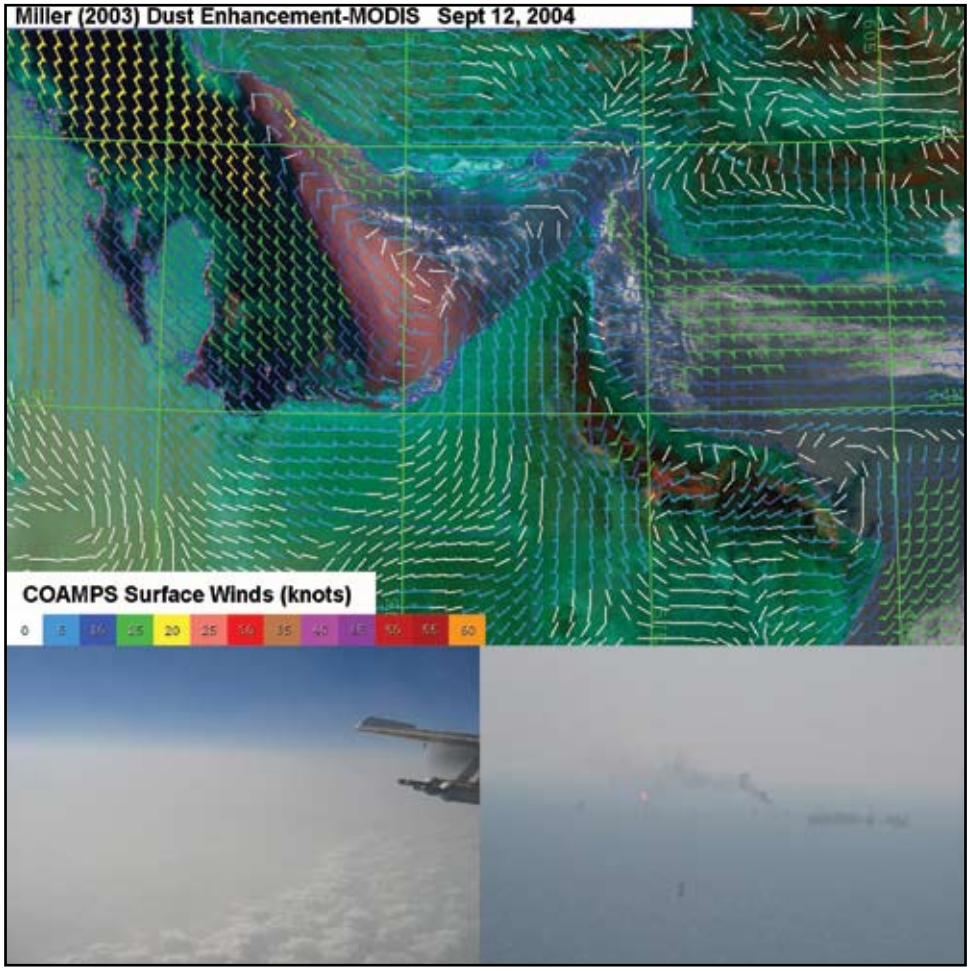

FIGURE 10
NRL Dust enhancement product with COAMPS® surface winds overlay for the September 12, 2004, case. Overlaid is the research aircraft flight track for this day. Here we see two air masses colliding, where pollution from the Indian Subcontinent meets dust from Iraq. Lower left, view of this dust event from a 10,000-ft altitude. Lower right, hazy conditions from pollution in polluted region of the Arabian gulf.

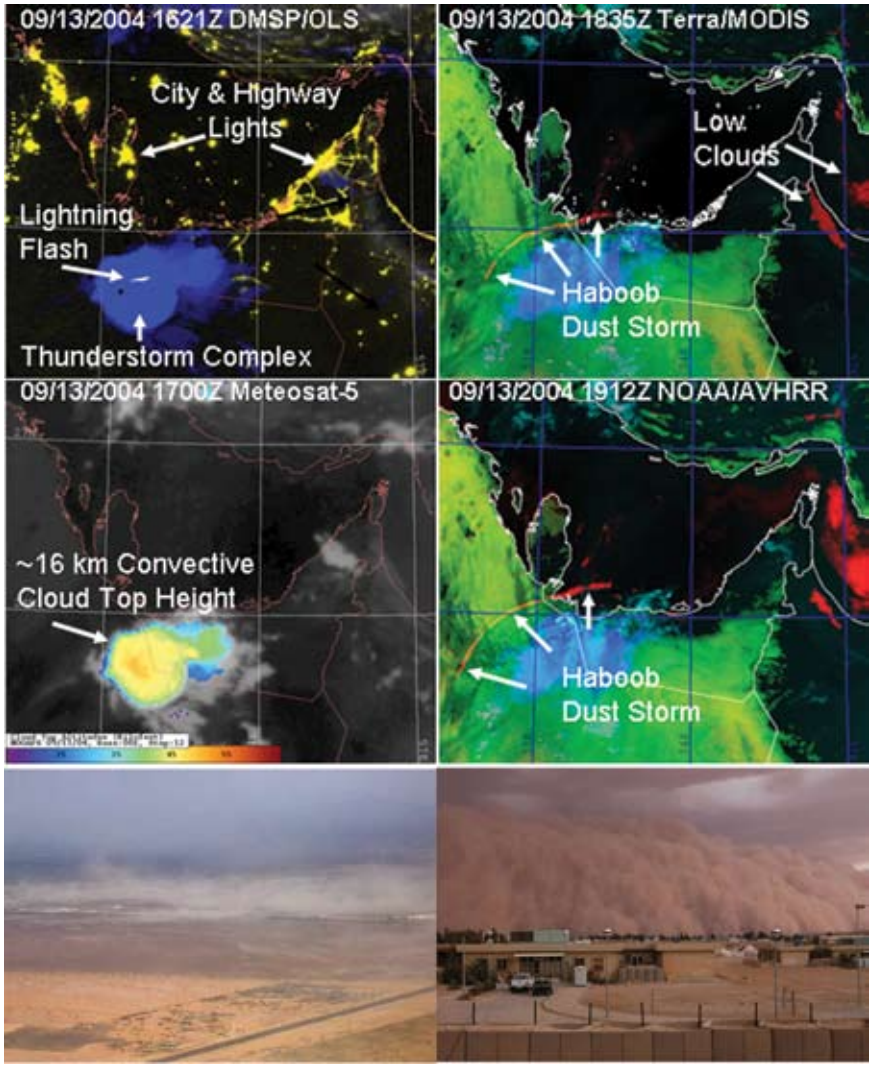

FIGURE 11
Multisensor panel of the observation of a massive Haboob event for September 13, 2004.[3] In this case, the OLS shows storm electrification (proxy for intensity), Meteosat-5 shows substantial vertical development and provides high-temporal resolution, and the MODIS/AVHRR sensors provided enhancement of the dust front itself. Lower left, a Haboob event in its formation in the interior of the UAE. Lower right, a massive Haboob event in Iraq. (Photograph by Sgt. Shannon Arledge, U.S. Marine Corps Story Identification No. 2005426134811.)

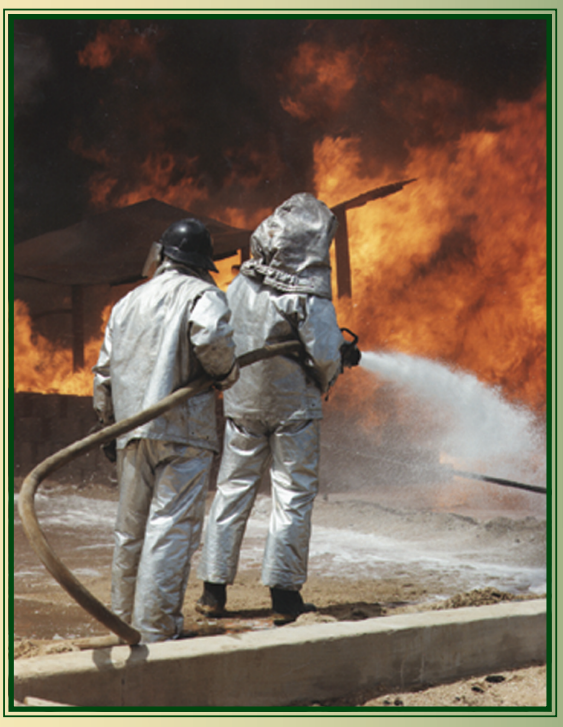

Aqueous Film-Forming Foam

Achievement: NRL, beginning in the early 1960s, conducted research on fire suppression that eventually led to one of the most far-reaching benefits to worldwide aviation safety — the development of Aqueous Film-Forming Foam (AFFF). AFFF achieves rapid extinguishment of hydrocarbon fuel fires and has the additional property of forming an aqueous film on the fuel surface that prevents evaporation and, hence, reignition of the fuel once it has been extinguished by the foam. The film also has a unique, self-healing capability whereby scars in the film layer caused by falling debris or firefighting activities are rapidly resealed.

The initial concepts for AFFF came from NRL's R.L. Tuve and E.J. Jablonski, who patented the first formulation for use in a twinned agent firefighting apparatus that combined Purple-K-Powder (an earlier NRL development) and AFFF. Although NRL was responsible for the original concepts and formulations, it was necessary to elicit the aid of the chemical industry to synthesize the fluorinated intermediates and agents to achieve improvements in formulations. The Minnesota Mining and Manufacturing Co., now 3M, contributed considerably to the success of the development of AFFF.

In honor of his work in developing AFFF, the Society of Fire Protection Engineers International awarded (posthumously) the Arthur B. Guise Medal to E.J. Jablonski in 1990 for "eminent achievement in the advancement of the science and technology of fire protection engineering."

Impact: Following the destructive fires aboard the aircraft carriers USS *Forrestal* and USS *Enterprise*, the Navy sought more effective firefighting agents. NRL met this Fleet requirement with the development of AFFF. In the military, AFFF firefighting foam is now on all Navy aircraft carriers, and is used by all branches of the U.S. armed forces and NATO members. The agent is also recognized by international standards organizations for the protection of civilian airfields, refineries, and fuel tank farms, where potentially catastrophic fuel fires can occur. AFFF is in the inventory of almost all fire departments in the United States and in many fire departments throughout the world.

Rocket Artillery Launch Spotter (RLS)

R.M. Mabe,[1] K.A. Sarkady,[1] H.A. Romero,[1] J.G. Lynn,[1] D.M. Cordray,[1] A. Cross,[2] J.F. Mackrell,[2] J.R. Southwick,[2] K. Strothers,[3] J.A. Schlupf,[3] R.C. Cellucci,[3] M.W. Schuette,[4] and R. Eber[5]
[1]*Optical Sciences Division*
[2]*Tactical Electronic Warfare Division*
[3]*Raven, Inc.*
[4]*SFA, Inc.*
[5]*ITT, Inc.*

The Threat: A common form of attack during current operations in Afghanistan and Iraq is the use of hit-and-run mortar and/or rocket strikes on coalition forces and bases, or on locations associated with the provisional governments in these countries. The insurgents fire mortars or rockets and then quickly escape before their presence is noticed. Rocket artillery can be exceptionally deadly, since the supersonic speeds of these weapons often result in an impact well before the launch is detected acoustically.

Rocker Launch Spotter (RLS): Shortly after entering Iraq, the U.S. Marine Corps issued an Urgent Needs Statement requesting an affordable, expeditionary, and unattended system to rapidly detect, provide warning, and report the point-of-origin (POO) of a rocket launch. The system was needed for Forward Operating Base (FOB) protection in Iraq and Afghanistan. The Office of Naval Research (ONR) Swampworks funded NRL for the rapid development and testing of an Operational Experimentation Article for launch detection. The selected design uses tower-based infrared and acoustic subsystems. The system leverages technology designed for use in another NRL project, Tactical Aircraft Directed Infra-Red Countermeasures (TADIRCM). The two-color infrared sensors are designed to detect surface-to-air missiles for TADIRCM and are used to detect rocket artillery in RLS. Other TADIRCM components used in RLS include the computer processors, inertial navigation units (INU), and detection and tracking algorithms. The RLS system uses two TADIRCM sensors, an INU, and a smaller field-of-view single-color forward-looking infrared (FLIR) camera on each tower. Figure 1 shows a typical arrangement. The sensors are aligned to the INU to provide accurate azimuth and elevation of any potential threats detected. The INU includes a GPS receiver to provide accurate location of the tower. The system uses three towers separated by a distance of 2-3 km in a configuration that provides 360° coverage of the area to be protected. Figure 2 shows a typical arrangement. The towers are connected to a control station via a wireless network. From its sensors, each tower reports potential threats to the control station. The control station compares potential threats detected on one tower to potential threats detected on one of the other towers. For threats that correlate, the system designates a correlated threat, triangulates to provide the POO, and reports the POO to an operator via a map display. When a correlated threat is designated, the system automatically cues the FLIR camera on the nearest tower to the correct elevation and azimuth. This provides the operator with video of the launch location within 2 s. When not in a threat condition, the FLIR cameras are available to the operator as surveillance cameras.

To detect mortar launches, the RLS system uses an acoustic subsystem. The acoustic subsystem consists of an Unattended Transient Acoustic Measurement and Signal Intelligence (MASINT) System (UTAMS) developed by the Army Research Laboratory that is currently in use in Iraq. In the RLS system, each tower has one UTAMS microphone array at the top of each tower, as shown in Fig. 3. Each array consists of four microphones and processing equipment. Analyzing the time delays between an acoustic wavefront's interaction with each microphone in the array UTAMS provides an azimuth of origin. The azimuth from each tower is reported to the UTAMS processor at the control station, and a POO is triangulated and displayed. The UTAMS subsystem can also detect and locate the point-of-impact (POI). Because of sound speed limitations,

FIGURE 1
View of IR sensors, FLIR, and tower head arrangement.

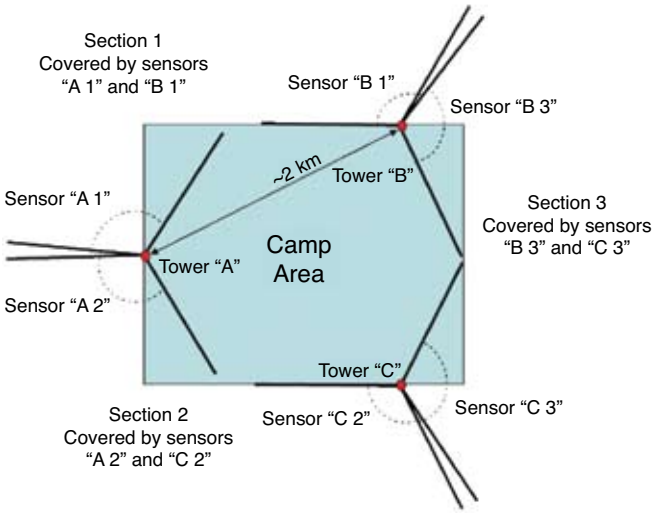

FIGURE 2
Typical tower arrangement around protected area.

FIGURE 3
UTAMS array attached to tower head.

the time to detect and report the POO can be up to 30 s for a 13-km launch. For rocket artillery, UTAMS often detects the POI prior to the POO, providing very little if any warning time.

The towers used in the RLS system are commercially obtainable heavy-duty all-terrain portable tower systems. Each tower can be raised to a height of 32 m and is capable of lifting a payload of 250 kg. Figure 4 shows the tower in its raised and lowered positions. The towers can be operated in winds up to 100 kts, is C-130 aircraft transportable, and can be erected in less than 30 min once in position. Each tower is powered with a 7.5 kW generator that can run continuously for 4 days between refueling. Once raised, the tower head can be rotated remotely to adjust the sensor coverage and overlap between towers.

System Performance: Testing of the RLS system is currently in progress. Preliminary tests were conducted at NRL in October 2005. A stimulator was used to simulate rocket launches. The infrared subsystem performed as expected, detecting and geo-locating the simulated rocket launches within expected errors. However, the physical constraints of the laboratory prevent the towers from being placed at their optimum separation. The system was also tested at Yuma Proving Ground (Arizona) in November 2005. Last-minute changes to the testing schedule prevented the system from being tested against the design rocket threats. However, the UTAMS performed well against mortar firings, and the RLS infrared system again geo-located simulated targets within expected position errors. The Yuma tests also provided extensive false-alarm testing.

(a) Raised position (b) Lowered position

FIGURE 4
Portable tower position.

The false-alarm rate of the system was determined to be extremely low. Additional testing is currently under way at NRL.

Conclusions: The RLS system provides an expeditionary, unattended, and rapid rocket detection capability for the protection of FOB's. The system can provide long warning times and accurate POO information for rocket threats and moderate warning times for mortar threats. Current plans include further testing against design threats in early 2006, and possible integration of the system with the Critical Area Protection System currently in use in Iraq by the Marines. Longer range plans include the use of higher-speed processors to allow the infrared subsystem to also detect and geo-locate mortars, rocket-propelled grenades, and machine-gun fire.

[Sponsored by ONR]

Tactical Situational Awareness of Enemy Gunfire

M. Pauli, J. Price, and W. Seisler
Tactical Electronic Warfare Division

Introduction: NRL has been conducting research into locating hostile gunfire based on detecting the infrared (IR) muzzle flash. As Fig. 5 shows, the IR flash is very pronounced and significantly larger than the visible flash. Recently, four integrated HMMWV-based gunfire detection and location (GDL) systems were developed under Office of Naval Research (ONR) sponsorship. GDL augmented the IR detection capability with a slewable electro-optic payload for day/night imaging, situational awareness, rangefinding, and day/night designation of hostile fire. When a gun flash is detected by GDL, the electro-optic payload sensors are automatically slewed and centered on the location of the detected gun flash. The GDL operator monitors the day/night sensor images and determines a course of action. By firing the electro-optic payload's integral laser, the operator can immediately alert others to the gun flash location. Parallel research efforts are developing improvements to the optics, the detection algorithms, networking to dismounted warfighters, IR/directional-acoustic integration, and rapid all-azimuthal capability. These efforts combine to provide for both operational experimentation and science and technology insertion to meet U.S. Marine Corps needs.

Technical Challenges of Gunfire Detection: Significant challenges involved in developing real-time automated detection, location, and identification of hostile gunfire include:

- Detecting a short-duration event,
- Rejecting natural and man-made false alarms, and
- Wide-area real-time coverage.

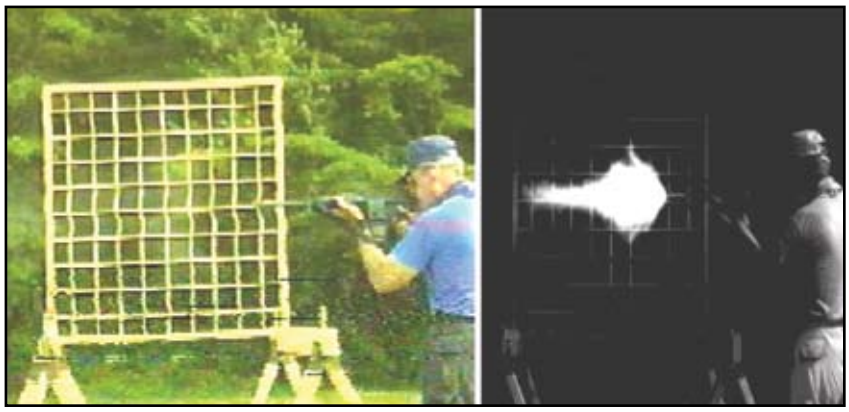

FIGURE 5
Imagery of gunflash in visible and infrared bands.

A key characteristic of gunflash events is their short persistence, only a few milliseconds. Consequently, detection cameras must operate with 100% stare efficiency (duty factor). Other considerations for camera selection include adaptability for spectral and temporal filtering to reduce false targets. For GDL, a commercial midwave IR (3-5 μm) band camera with a 320 × 240 detector array was selected. For production cost reasons, larger array sizes and multispectral cameras were rejected. To improve the signal-to-noise ratio and false-alert rejection, a narrow subband filter tailored to the spectral characteristics of typical gunfire was installed in the camera.

A major challenge lay in developing automated image-processing algorithms that reliably recognize gunfire while rejecting natural and man-made clutter, such as passing cars and solar glints. Algorithm improvements extended the detection range of the earlier generation software while reducing false alarms. Field testing of the systems was used to create and expand a database (library) of various gunfire events and false-alarm sources. Algorithm improvements were tested using the database and then validated in real-time operations in subsequent testing. Compared with acoustic detection, the IR detection approach provides much greater location precision and can unambiguously handle multiple shots. However, an IR detection system integrated with an acoustic detection has provided GDL a robust way of rejecting spurious IR glint event declarations for operations in a high clutter environment. Additionally, for single-shot events, the GDL IR-acoustics combination provides passive ranging using time difference between the flash and the sound.

Another challenge has been to develop a system capable of detecting gunfire from any direction of attack. An anamorphic lens has extended the GDL instantaneous azimuth coverage to 130 deg, in contrast to the earlier generation system's 30-deg coverage. The resulting distorted image adds complexity in locating a gunshot from a particular pixel location in the camera. To overcome this distortion, a calibration process was implemented that maps the camera's detected pixel position to gimbal coordinates. This enables the electro-optical payload to be directed to the detection location.

Gunfire Detection and Location (GDL) System: Figure 6 shows a GDL system installed on a HMMWV. The upper stage of the GDL equipment includes a slewable electro-optic payload that allows for event confirmation, precision location, and response. This payload contains a thermal camera, night-reflectance camera, visible camera, laser rangefinder, night vision laser designator, and daytime laser designator. The daytime designation problem is especially challenging because the laser required is not eyesafe. NRL developed techniques to maximize the effectiveness of the designators and reduce the laser hazard zone. Special narrowband contrast enhancement goggles and modulation techniques improve the visibility of the laser designation. Marines can locate hostile fire by looking

FIGURE 6
GDL system installed on a HMMWV.

at the laser designations or by viewing the hostile fire imagery (from the gimballed day/night cameras) in a remote hand-held or helmet-mounted monocular device, developed at NRL. The slewable GDL electro-optic payload can also be operated in a perimeter defense mode for Marine situational awareness when not engaging hostile fire. The current GDL systems were designed for U.S. Marine Corps wargaming experiments to evaluate the available technology and to establish developmental requirements.

[Sponsored by ONR]

Engineered Band Structure in Micromachined Quantum Wells

T.H. Stievater,[1] W.S. Rabinovich,[1] P.G. Goetz,[1] D. Park,[2] J.B. Boos,[2] D.S. Katzer,[2] M.L. Biermann,[3] S. Kanakaraju,[4] and L.C. Calhoun[4]
[1]*Optical Sciences Division*
[2]*Electronics Science and Technology Division*
[3]*Eastern Kentucky University*
[4]*University of Maryland*

Introduction: The ability to engineer the optical and electronic properties of epitaxially grown compound semiconductor heterostructures in the *growth* (vertical) direction has enabled the explosive growth and success of semiconductor lasers, photodetectors, and modulators. However, high-quality *laterally* patterned band structure in these materials has proven much more elusive. Materials with precise lateral band structure control are of particular importance for applications in integrated photonics and artificial quantum confined systems. In addition, the ability to engineer birefringence in the plane of the semiconductor heterostructure has important implications for electro-optic polarization modulators and for birefringent phase-matching in nonlinear frequency conversion.

We describe how micromachining semiconductor heterostructures into suspended structures partially detached from the substrate can be used not only to laterally pattern band structure but also to provide a better understanding of the interaction between strain, band structure, and optical absorption in these materials. Suspended quantum wells grown with strain provide a direct comparison of two sets of strain components in the same sample. Thus, by carefully comparing the optical properties of an as-grown area with a suspended area, important photonic, electronic, and mechanical properties of these microstructures can be discerned. Knowledge of these properties can then be used to design future-generation micromachined and nanomachined semiconductor heterostructures. Our work also shows that compound semiconductor-based microelectromechanical systems (MEMS) are potential replacements for some silicon-based MEMS due to their greater material flexibility and control over strain.[1-3]

Micromachining Quantum Wells: The epitaxially grown semiconductor heterostructures studied in this work are $In_{.53}Ga_{.47}As$ (lattice-matched) multiple quantum wells (MQW's) with either InAlAs or InGaAlAs strained barriers. The MQW is grown on a 1.5-μm thick InAlAs or InP sacrificial layer, which itself is grown on an InGaAs etch stop layer on the InP substrate. Standard photolithography and a nonselective wet etch are used to pattern the MQW into mesas. A timed $HCl:H_3PO_4$ (1:1) selective etch is then used to etch the sacrificial layer both where it had been exposed as well as partially underneath the MQW, thereby releasing the MQW from the substrate. These suspended MQW's can be fabricated into various shapes, including microbridges, microcantilevers, or micropedestals.

Band Structure Deformation: MQW's with strained barriers that are released from the substrate produce strain in the QW layers as the strain in the barriers partially relaxes. Thus, the strain tensor in a suspended quantum well is markedly different than the strain tensor in the unreleased (as-grown) areas of the quantum well (Fig. 7). This postgrowth strain engineering leads to in-plane band structure engineering: strain in semiconductors couples to band structure through the deformation potentials. The coupling is a function of the components of the strain tensor and the crystal symmetry of the semiconductor and can be measured using polarization-specific optical absorption spectroscopy. Simply put, net compressive strain in the quantum well leads to a blue shift of the band gap and net tensile strain leads to a red shift. In addition, an anisotropy of the in-plane strain components in the quantum well leads to an optical absorption anisotropy between the two orthogonal linear polarizations.

Figure 8 shows an example of laterally engineering band structure in a MQW with tensile barriers. The MQW forms the top of a micropedestal such that the central portion (the dark rectangle in the inset of Fig. 8(a)) is still attached to the sacrificial layer, while the outer portion is freely suspended above the substrate. Partial strain relaxation in the barriers of the suspended areas leads to a net compressive strain in the quantum well layers. Thus, the band gap in the quantum well is expected to be bluer in the suspended area than in the central area that is still attached. Figure 8(b) shows the optically mapped heavy-hole

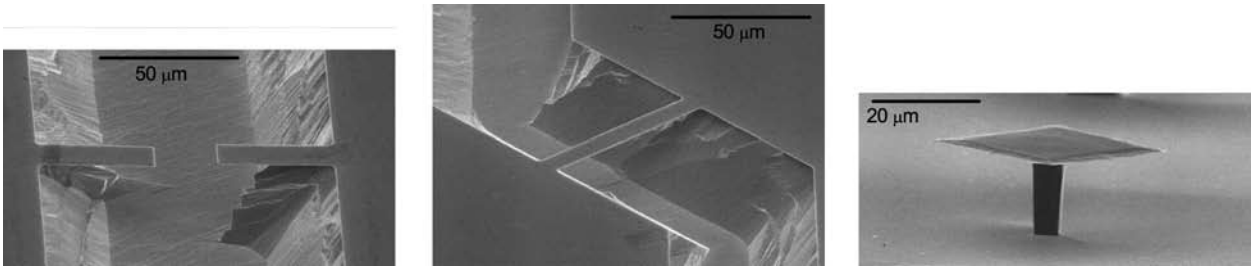

(a) (b) (c)

FIGURE 7
Micromachined quantum wells patterned as (a) microcantilevers, (b) microbridges, and (c) micropedestals. In each case, the suspended membrane is a multiple InGaAs quantum well that is about 400-nm thick with tensile barriers.

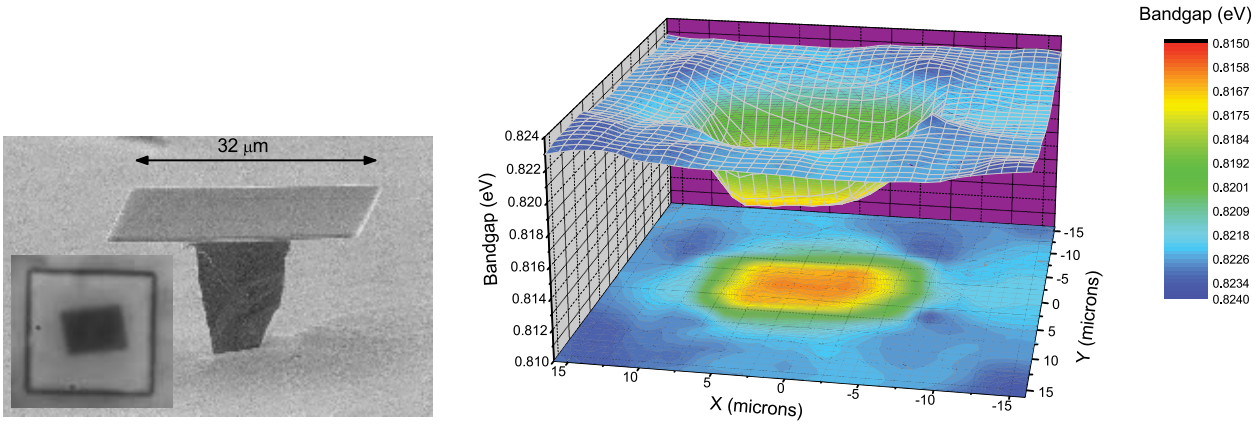

(a) (b)

FIGURE 8
Band structure deformation in a quantum well micropedestal. Strain relaxation in the suspended area of the quantum well results in a blue-shift of the band gap energy.

band gap across the surface of the micropedestal, confirming this expectation. A 9 meV band gap shift results from a sample grown with an initial barrier strain of 0.69% and is in excellent agreement with our band structure models.

Figure 9 shows band structure deformation along a microbridge in two different samples. A microbridge differs from a micropedestal or a microcantilever in that the barrier strain component in the direction parallel to the bridge length cannot relax, but the components perpendicular to the bridge length are free to relax. Thus, the in-plane strain components in the quantum well are anisotropic, leading to anisotropic optical absorption and therefore birefringence. The differential transmission spectra in Fig. 9 are a measure of the optical absorption at a given wavelength. In Fig. 9(a), an initial tensile barrier strain induces anisotropic compressive strain in the quantum well. This leads to a blue-shift and decreased (increased) absorption at the heavy (light) hole for light polarized parallel to the microbridge. In Fig. 9(b), an initial compressive barrier strain induces anisotropic tensile strain in the quantum well. This leads to a red-shift and increased (decreased) absorption at the heavy (light) hole for light polarized parallel to the microbridge. Thus, micromachined microbridges lead not only to a shifted band gap but also to a modification of the band structure symmetry, from one that is isotropic in the growth plane to one that is highly anisotropic. The measured optical absorption spectra in Fig. 9 are also in excellent agreement with our band structure models.

Summary: This demonstration of controlled three-dimensional band-structure patterning represents the beginning of a wide range of new research avenues based on the combination of micromachining, MEMS, and optically active III-V semiconductors. Potential applications include arrays of surface-normal modulators, optically active piezoelectric materials, quasi-phase matching in waveguides, and directly patterned quantum-dot arrays.

[Sponsored by ONR]

References

[1] T.H. Stievater, W.S. Rabinovich, D. Park, P.G. Goetz, J.B. Boos, D.S. Katzer, M.L. Biermann, S. Kanakaraju, and L.C. Calhoun, "Strain Relaxation, Band Structure Deformation, and Optical Absorption in Free-Hanging Quantum-Well Microstructures," *J. Appl. Phys.* **97**, 114326-1 - 114326-11 (2005).

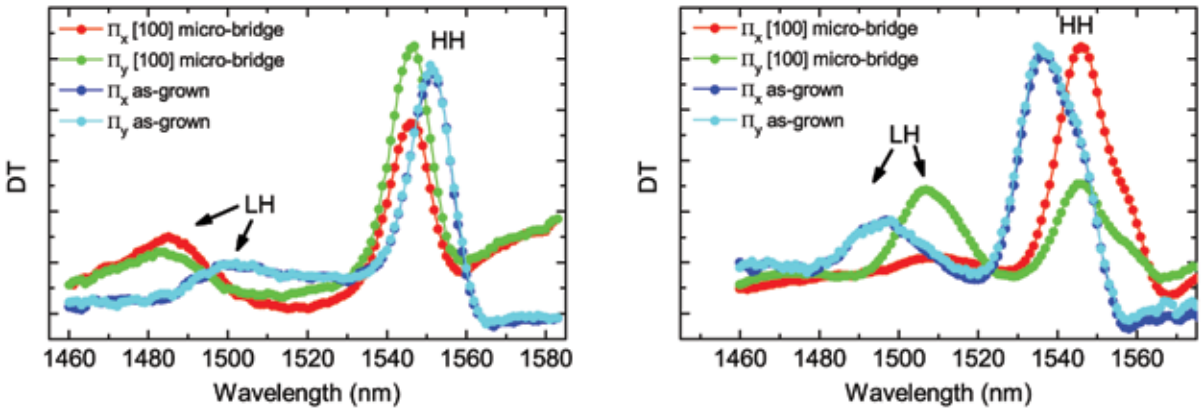

FIGURE 9
Band structure deformation and induced birefringence along a quantum well microbridge similar to that of Fig. 7(b). HH: heavy hole. LH: light hole. DT: differential transmission. Π_x: polarization parallel to the microbridge. Π_y: polarization orthogonal to the microbridge.

[2] T.H. Stievater, W.S. Rabinovich, D. Park, P.G. Goetz, J.B. Boos, D.S. Katzer, and M.L. Biermann, "Using Local Band Structure to Image Strain in Semiconductor Microstructures," *Appl. Phys. Letters* **86**, 111915-1 - 111915-3 (2005).
[3] T.H. Stievater, W.S. Rabinovich, J.B. Boos, D.S. Katzer, and M.L. Biermann, "Laterally Patterned Bandstructure in Micromachined Semiconductors," *Appl. Phys. Letters* **83**, 4933-4935 (2003). ★

Composite Propeller Performance Monitoring with Embedded FBGs

M. Seaver, S.T. Trickey, and J.M. Nichols
Optical Sciences Division

Introduction: Composite propeller blades are of Navy and commercial interest because they offer significant advantages in reduced weight, reduced maintenance, and increased performance. Potential benefits include design flexibility not achievable with metal that can increase mechanical efficiency, cavitation reduction, propeller weight reduction, and underwater blade replacement, to name a few.

One of the major benefits claimed for fiber Bragg grating (FBG) sensors is their ability to be embedded in composite materials with minimal effects on the performance of the material. In spite of embedded FBGs being routinely touted during discussions of smart materials, most reports dealing with embedded FBGs have been limited to simple structures such as composite plates or beams and tested under laboratory conditions. NRL was asked to contribute embedded FBG sensors as part of a composite propeller manufacturing and testing program being put together in the Propulsion and Fluid Systems Division of the Naval Systems Warfare Centers Carderock Division. This was an opportunity to both advance the state of the art in FBG sensing and provide propeller designers with the high-quality strain data that can lead to improved fluid dynamics models and better propeller designs.

Optical Design: Embedding FBG sensors in composite materials poses two major challenges. Bend-induced losses must be minimized, and the fiber optic leads must exit the material with sufficient fiber to allow external connections. These challenges mean that manufacturers must learn how to handle optical fiber and may need to modify their manufacturing processes to accommodate the sensors and preserve the fiber leads. Problems in these areas were encountered and overcome during this effort.

The sensor wavelengths and locations were chosen based on strains predicted by a finite-element model (FEM) of the propeller. Figure 10 shows sensor locations for both the pressure and suction side arrays. For reference purposes, we number the sensors starting from nearest the hub. The sensor spacings (in mm) are measured along the mid-chord of the blade, relative to the base of the propeller blade. The sensor wavelengths were chosen to ensure that wavelengths would not cross under worst-case loading conditions. All sensors were manufactured in polyimide-jacketed fiber, and the FBGs were rejacketed to maximize physical strength and strain transfer. Optical signals are transferred between the stationary demodulation system and the rotating propeller. This is done by using a commercial fiber optic rotary joint designed for bidirectional signal transfer and capable of rotation rates up to 2000 rpm and underwater operation. Figure 11 shows the downstream end of the propeller mounted in the water tunnel, with the stationary fiber extending out of the rotary joint.

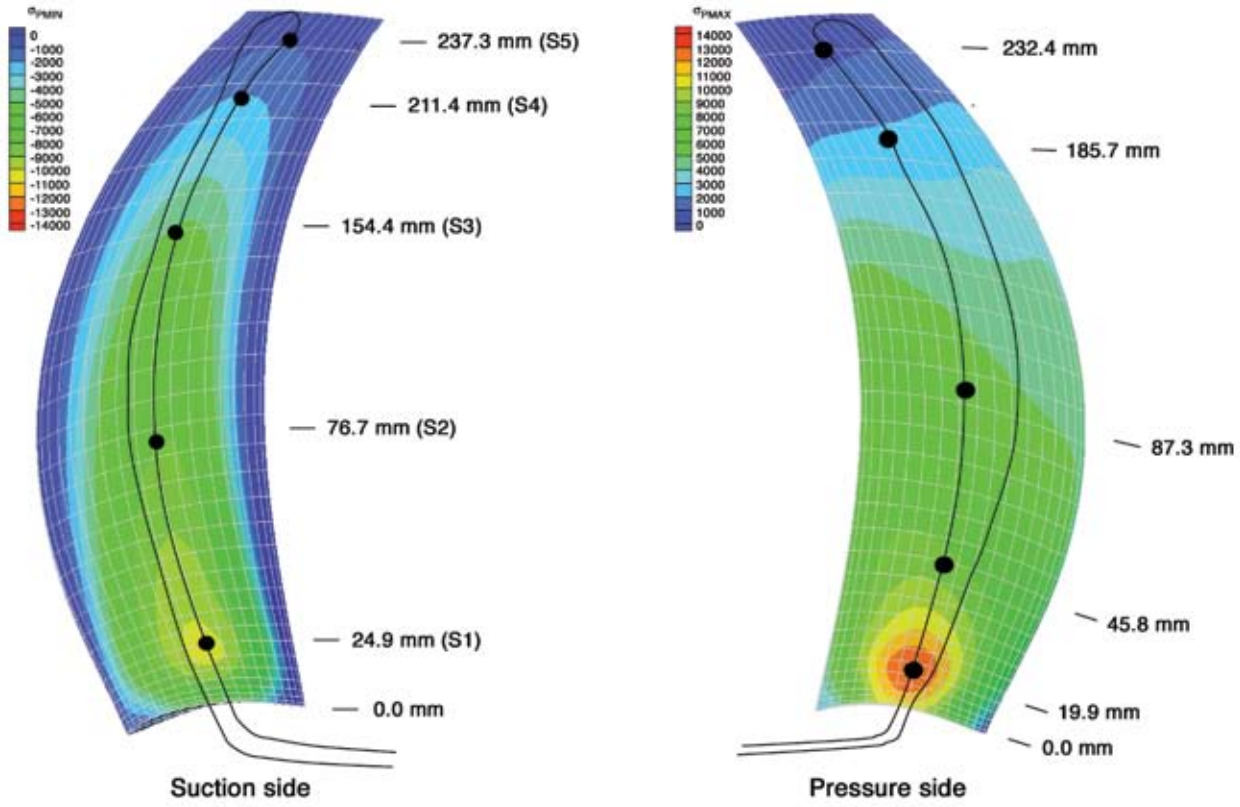

FIGURE 10
Predicted strain values for design thrust and sensor locations (in mm) for both sides of the propeller. The designations S1 – S5 identify the suction side sensors.

FIGURE 11
The downstream end of the propeller, showing the stationary side of the fiber optic rotary joint and the optical fiber carrying signals to the data acquisition system.

Results: Measurements were made using the suction side array under thrust loads that varied from 80% to 120% of design thrust with the propeller downstream of a four-quadrant wake screen. The wake screen is divided into eight equal angle segments that alternate between low- and high-velocity flow regions. Thirty seconds of strain data were recorded at each thrust setting. Figure 12 shows a short segment from one measurement at 100% of design thrust. This figure shows the strains from all five suction side sensors and the unsteady dynamics produced by the wake screen. Sensors 1 and 2, those nearest the blade root, look moderately sinusoidal; sensors 3 and 4, which are roughly mid-blade, show additional frequency content; sensor 5 shows only modest fluctuations. It's also interesting to note that sensor 3 shows the largest peak-to-peak fluctuations. Detailed interpretation of these results and how they relate to the flow fields awaits the results of a coupled unsteady flow/propeller mechanics model being developed by Y.L. Young at Princeton University.

Conclusions: We have successfully embedded fiber Bragg grating strain gauges in composite propeller blades and measured dynamic strains while the propeller was being tested in a water tunnel. Preliminary data analysis shows that the mean strains scale with load, while the strain fluctuations due to the presence of a wake screen increase as load decreases. Quantitative analysis awaits comparisons between the measured strains and the results of unsteady flow hydrodynamics modeling.

Acknowledgments: The authors acknowledge Ben Chen and Rich Szwerc of the Naval Surface Warfare Center Carderock Division (NSWCCD) for including fiber sensors in their composite propeller program funded jointly by the Navy FCT (Foreign Comparative Testing) program and the ONR NICOP program (managed by Dr. Ki-Han Kim), and Scott Gowing (also from NSWCCD) for designing the rotary joint housing and for his efforts and explanations during the water tunnel tests. The people of AIR Fertigung-Technologie GmbH demonstrated remarkable abilities at learning to handle optical fiber as they included embedded sensors in their manufacturing processes.

[Sponsored by ONR]

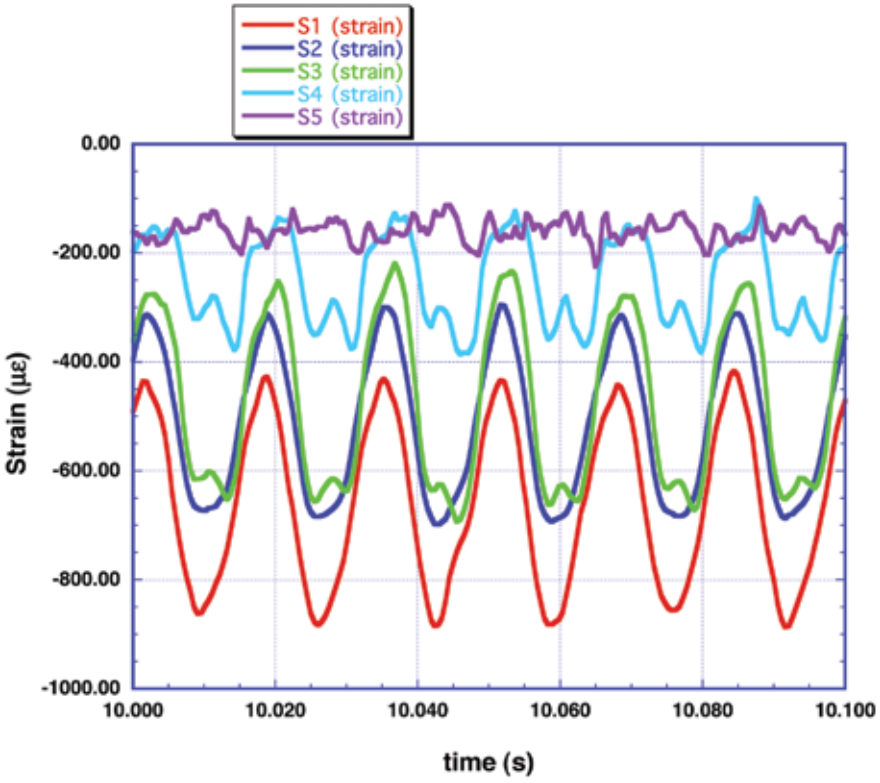

FIGURE 12
A short segment of data, showing the dynamic strains on all five suction side sensors for the propeller operating at design thrust behind the wake screen.

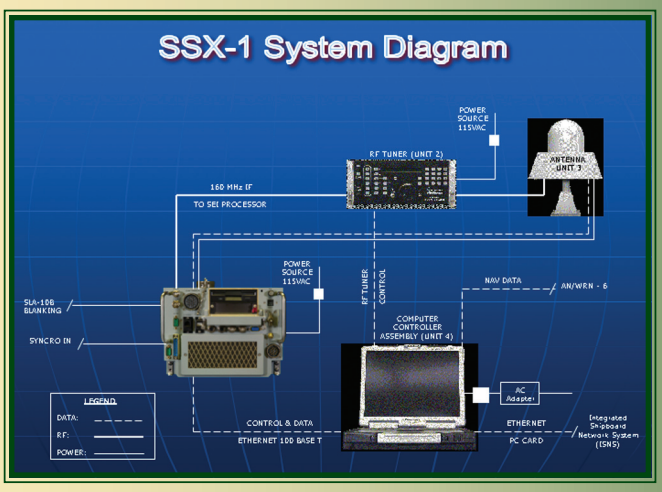

Specific Emitter Identification

Achievement: Specific emitter identification (SEI) provides electronics intelligence (ELINT) signal collection platforms with the capability to identify uniquely a radar transmitter with such accuracy as to make it possible to assign a "fingerprint" to that particular signal. In using SEI techniques, systems with a radar transmitter can be cataloged and tracked, and the data interchangeability between SEI systems allows a signal to be collected by one system and then "handed off" to another system for tracking. For example, SEI can be used to covertly track a contraband transport whose signal of interest can be collected by an aircraft and then transmitted electronically to a ship for subsequent tracking.

On April 14, 1982, R. Goodwin was the recipient of the Navy Superior Civilian Service Award. He was cited for:

> "performing and directing the research and development efforts that led to the achievement of an important, new Navy capability in real-time pulsed-emitter characterization."

In June 1993, the National Security Agency (NSA) recognized the superior capability of NRL's SEI concept and equipment after a competition among numerous participants from industry and other service laboratories. The NSA test served as an impartial means for selecting an SEI methodology for use as a national standard. As a result of the test, NSA issued a message (DTG 011440Z, June 1995) that stated in part, "Accordingly, NSA has selected the Naval Research Laboratory processor (L-MISPE) to be the standard for conducting SEI/UMOP collection operations...."

Since that decision, SEI platforms have been very successful at cataloging and tracking platforms of interest. In one application, a library of over 300,000 specific radar signals has been compiled. This library is shared among the sites to aid in performing tactical intelligence and surveillance tasks.

Impact: SEI identifies any radar by its unique characteristics with such accuracy as to "fingerprint" it. In fact, it can distinguish between identical models produced off the same assembly line. With SEI systems deployed on ships, aircraft, submarines, and ground sites, NRL's technology has had significant warfighting impact. It saw combat action in Kosovo and in Operation Iraqi Freedom. Furthermore, Coast Guard vessels, Naval warships, and aircraft have used it to support drug interdiction, enforce treaties, and monitor the movement of materials used in weapons of mass destruction.

High-Altitude Aerogravity Survey for Improved Geoid Determination

V.A. Childers and S.A. Martinka
Marine Geosciences Division

Introduction: Shallow water (littoral) regions present unique challenges for Naval operations. Warfighter support in the littoral region is hampered by our inability to relate tide and ocean circulation models directly to nautical charts via an absolute vertical datum. Various water measurements of critical importance to the Navy (such as tide gauges, ocean bottom pressure/inverted echo sounders, satellite altimetry, and heights now easily measured by GPS) are made with respect to different vertical reference frames (tidal datums and ellipsoidal frames), and there is no mechanism for conversion from one frame to another.

An accurate geoid can provide the vertical reference required to relate the various vertical reference frames. The geoid is the surface of equal gravitational potential that most closely approximates mean sea level (in a motionless ocean) located with respect to the ellipsoidal (GPS) reference frame. Historically, the gravity field had not been sufficiently determined to produce a geoid accurate enough to relate the reference frames. Since 2003, however, the Gravity Recovery and Climate Experiment (GRACE) satellite has revolutionized our ability to construct geoids by accurately resolving the long-wavelength component of the global gravity field to wavelengths as short as 350-400 km. NRL has been combining GRACE data with short-wavelength terrestrial, marine, and airborne gravity to create a geoid for the Gulf of Mexico accurate to 5 cm (as compared with tide gauge data located by GPS surveys).

NRL's interest in accurate geoid determination dovetails closely with the mission of NOAA's National Geodetic Survey (NGS): to maintain and evolve a National Spatial Reference System based on the most accurate geoid possible for North America. NRL has recently partnered with NGS to conduct high-altitude airborne surveys at critical locations along the Gulf Coast. These surveys are designed to improve the geoid determination by filling in regions with little or no gravity data coverage, by identifying errors in existing land and marine data, and by resolving systematic errors in the 1988 North American Vertical Datum (NAVD88) orthometric reference frame.

High-Altitude Survey: In May 2005, NGS and NRL performed the first-ever high-altitude airborne gravity survey aboard the NOAA Cessna Citation jet (Fig. 1). The survey was conducted over southwestern peninsular Florida and the ocean just north of Cuba (Fig. 2) at an average altitude of 28,000 ft (~8,535 m) and speed of 260 kts (~480 km/h). The NRL Lacoste and Romberg gravimeter was installed on the aircraft along with Trimble GPS receivers. NASA-Goddard Space Flight Center also operated a LIDAR on the aircraft for imaging instantaneous ocean heights. The survey encroached on the beginning of the 2005 hurricane season in the Gulf of Mexico. Constant storm buildup dramatically limited the data recovery (red lines vs blue (planned) lines, Fig. 2(a)). The gridded gravity anomaly data from the survey are displayed in Fig. 2(b).

The NRL airborne gravimetry methodology has been optimized for low-altitude surveys (1,000-3,000 ft) aboard the Navy P-3 Orion aircraft. The P-3 is a large, 4-engine turbo-prop aircraft designed for submarine surveillance and is significantly larger than the Cessna Citation jet. The differences in aircraft dynamics and survey altitudes have posed significant challenges to successfully processing the aerogravity data. Corrections calculated as part of the gravity processing were adapted to accommodate the increased altitude. Most notably, the height correction (which corrects the predicted gravity value to the aircraft altitude) was modified from the simplification appropriate at low altitudes to the full expression that appropriately accounts for the mass of the atmosphere. As the measurement height goes up, the shorter wavelengths of the gravity field are increasingly attenuated, thus reducing the signal-to-noise ratio in these wavelengths. To compensate for this effect, we had to perform longer period low-pass filtering than expected.

Aircraft motion, as detected by inertial measurement units, differs noticeably between the two aircraft. The aircraft motion is a combination of the aircraft dynamics (a function of aircraft size and shape) and the differing atmospheric characteristics at the two altitudes. We compared the pitch, roll, and yaw of the Citation during two flights with P-3 measurements during a Gulf of Mexico survey in 2004. There is a pronounced difference in the roll characteristics of the two aircraft (Fig. 3). The horizontal accelerations of the aircraft contribute to driving the gravimeter's stabilized platform off-level. The off-level corrections we perform improve the result, but imperfectly. We expect that the peak in the roll power for the Citation could play a significant role in the increased error that seemed to remain in the filtered gravity anomaly.

Summary: The preliminary results suggest that there is a bias difference of 3-4 mGals between the terrestrial Florida gravity measurements and the offshore marine gravity data, although the data recovery was sparse. NRL and NGS will follow this survey with the second field season in January 2006 along the Gulf Coast.

[Sponsored by ONR]

FIGURE 1
The NOAA Cessna Citation aircraft used for the Florida survey.

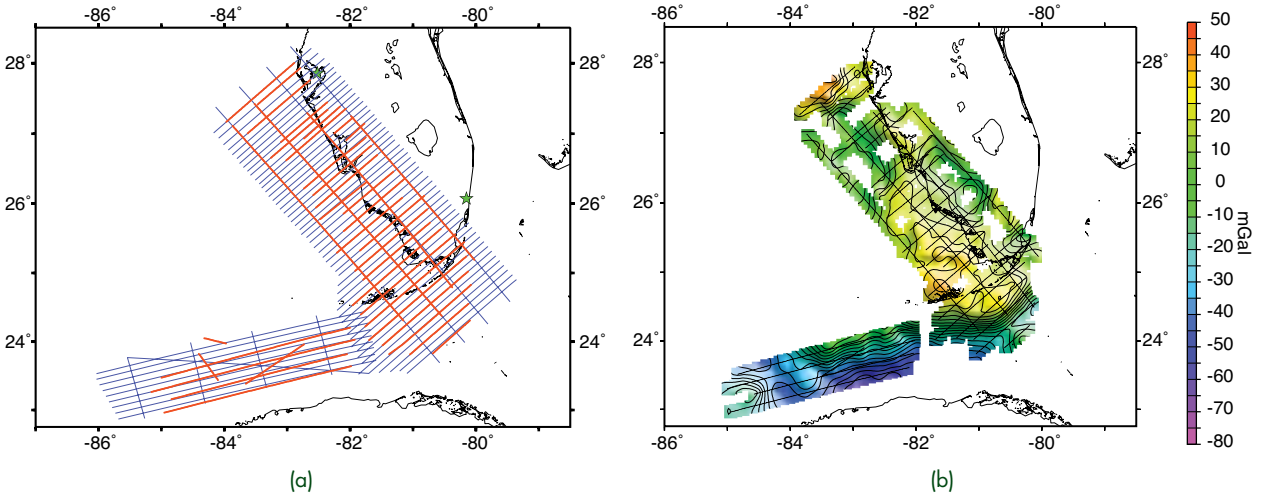

FIGURE 2
(a) The actual lines flown (in red) are shown with the planned survey lines (blue). The low data recovery was caused by the poor weather. (b) The gridded free-air gravity anomaly, with the tracks identified by black lines. The contour interval is 5 mGal.

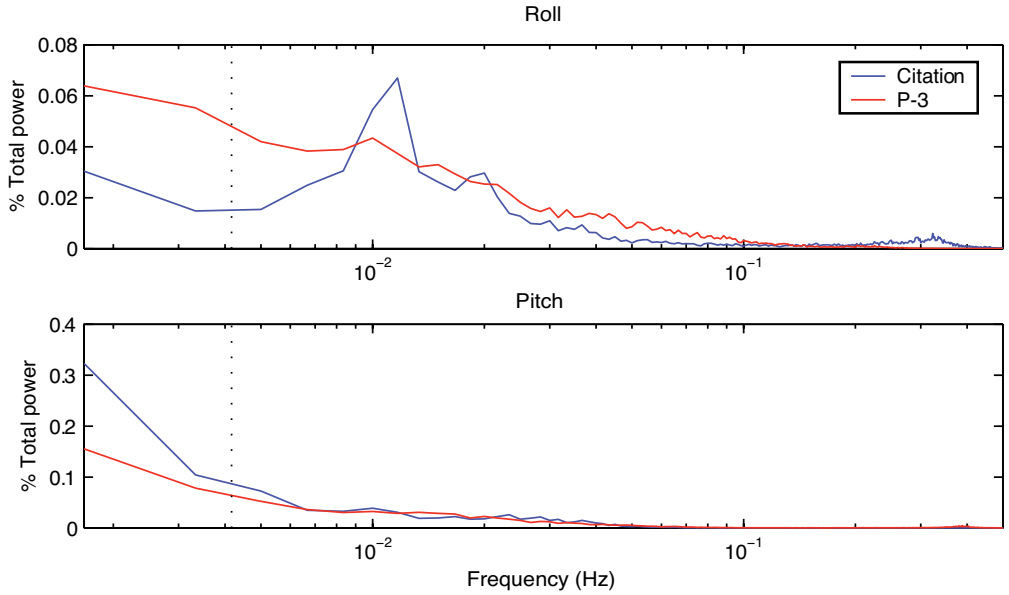

FIGURE 3
Comparison of Citation and P-3 aircraft motion. Normalized power spectra from inertial attitude data from data tracks from two flights for the Citation (blue) and the P-3 (red) were ensemble averaged using 10-min windows. Note the peak in the roll power in the Citation motion at a 1.42-min period.

Azimuthal Variation of the Microwave Emissivity of Foam

L.A. Rose,[1] D.J. Dowgiallo,[2] M.D. Anguelova,[3] J.P. Bobak,[1] W.E. Asher,[4] S.C. Reising,[5] and S. Padmanabhan[5]
[1]*Remote Sensing Division*
[2]*Interferometrics, Inc.*
[3]*NRC Research Associate*
[4]*University of Washington, Seattle*
[5]*Colorado State University*

Introduction: Successful naval operations require excellent knowledge of the ocean wind speed and direction. In addition, the global ocean wind vector is a key element for weather forecasting and for climate and oceanography studies. WindSat, a satellite-borne multifrequency polarimetric microwave radiometer developed by the Naval Research Laboratory, has demonstrated the ability to remotely sense the global ocean wind vector from space.[1] The wind direction signal measured by WindSat is about two orders of magnitude smaller than the background scene, and only a little larger than the radiometer noise floor. Therefore, any small uncertainties in the geophysical model used to retrieve the wind direction will introduce errors in the retrieved wind vector. One such uncertainty is the contribution of sea foam on the wind direction signal.

Down-looking radiometers, such as WindSat, receive energy emitted from the ocean surface and the atmosphere. The energy from the ocean surface, quantified as the brightness temperature, is related to surface physical temperature by

$$T_B = e_S \cdot T_W,$$

where T_B is the brightness temperature, T_W is the physical temperature of ocean water surface, and e_S is surface emissivity, which depends on the measurement frequency, polarization, incidence angle, and the azimuth angle between wind direction and the direction from which observations are made. The emissivity of the sea surface also depends on physical properties of the water surface such as temperature, salinity, and surface roughness, which is primarily wind-driven.

The presence of foam and roughness created by wind and breaking waves greatly increases the surface emission at microwave frequencies. The surface emissivity is sometimes written as

$$e_S = f \cdot e_F + (1 - f) \cdot e_R,$$

where f is the fraction of the surface covered with foam, e_F is the emissivity of foam, and e_R is the emissivity of the foam-free, rough water surface.

Past studies of e_F have focused on incidence angle, frequency, and polarization dependencies.[2] To better understand the azimuthal dependence of e_F, we conducted the Polarimetric Observations of the Emissivity of Whitecaps EXperiment (POEWEX) in 2002 and 2004. POEWEX involved simultaneous radiometric and video measurements of breaking waves at microwave frequencies of 6.8, 10.8, 18.7, and 36.5 GHz, which match those used by WindSat.

Outdoor Wave Tank Experiment: Since breaking waves and foam on the open ocean are intermittent and highly variable, POEWEX was conducted under controlled conditions in the Oil and Hazardous Materials Simulated Environmental Test Tank (OHMSETT) in Leonardo, New Jersey.[3] The outdoor saltwater wave tank uses a mechanical wave generator to produce waves with a period of about 2 s. An artificial shoal in the center of the tank causes reproducible breaking waves at the same location. In situ physical measurements with an underwater video camera and conductivity probe agreed well with similar measurements of breaking waves in the ocean. Thus, the radiometric emission observed in the wave tank is representative of that from breaking waves in the open ocean.

Figure 4 shows the experimental setup, with the radiometers suspended beneath the cradle of a boom-lift crane observing a breaking wave. The drawing in Fig. 4 shows the five azimuth angles from which observations were made. A video camera bore-sighted with the radiometers provided video images from which the fractional coverage of foam in the radiometer field of view (FOV) was determined.

Results: Figure 5 presents results at 53 deg incidence angle and 90 deg azimuth. The upper part of the figure shows video images of the breaking waves. The artificial shoal creating the breaking point is seen as a black rectangle, and overlaid circles define the radiometer FOVs. The lower part of Fig. 5 plots time series of the antenna temperatures at 10.8, 18.7, and 36.5 GHz for the vertical (red) and horizontal (blue) polarizations and for the foam fraction (yellow). Maximum and minimum values of antenna temperature and foam fraction can be seen at approximately 2.5 and 4 s, respectively. By observing the radiometer antenna temperatures for the two cases when the foam fraction is maximum and minimum, the foam emissivity can be expressed as[3]

$$e_F = \frac{(1 - f_2)(Ta_1 - T_{sky}) - (1 - f_1)(Ta_2 - T_{sky})}{(f_1 - f_2)(T_w - T_{sky})}.$$

Here Ta_1 and Ta_2 are, respectively, the maximum and minimum values of antenna temperature when the

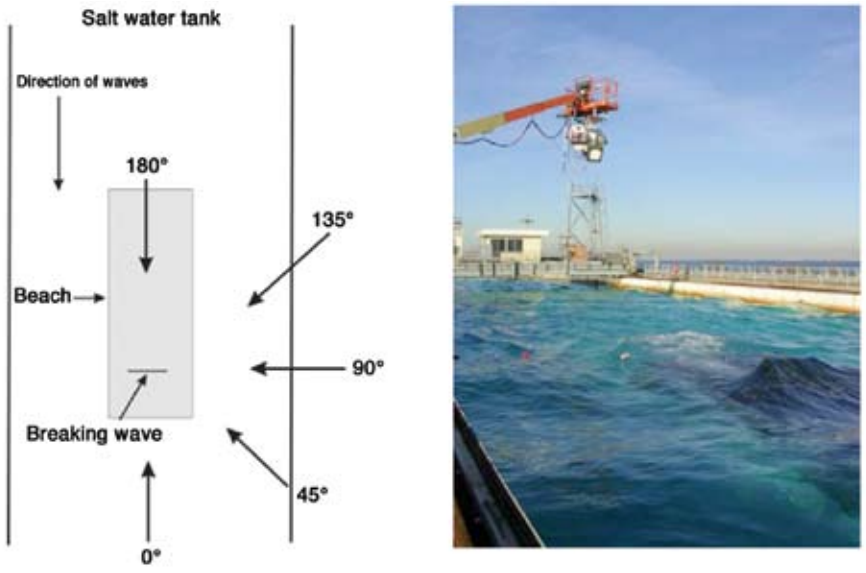

FIGURE 4
On the right: radiometers observing waves at OHMSETT. On the left: drawing showing azimuth angles from which observations were made.

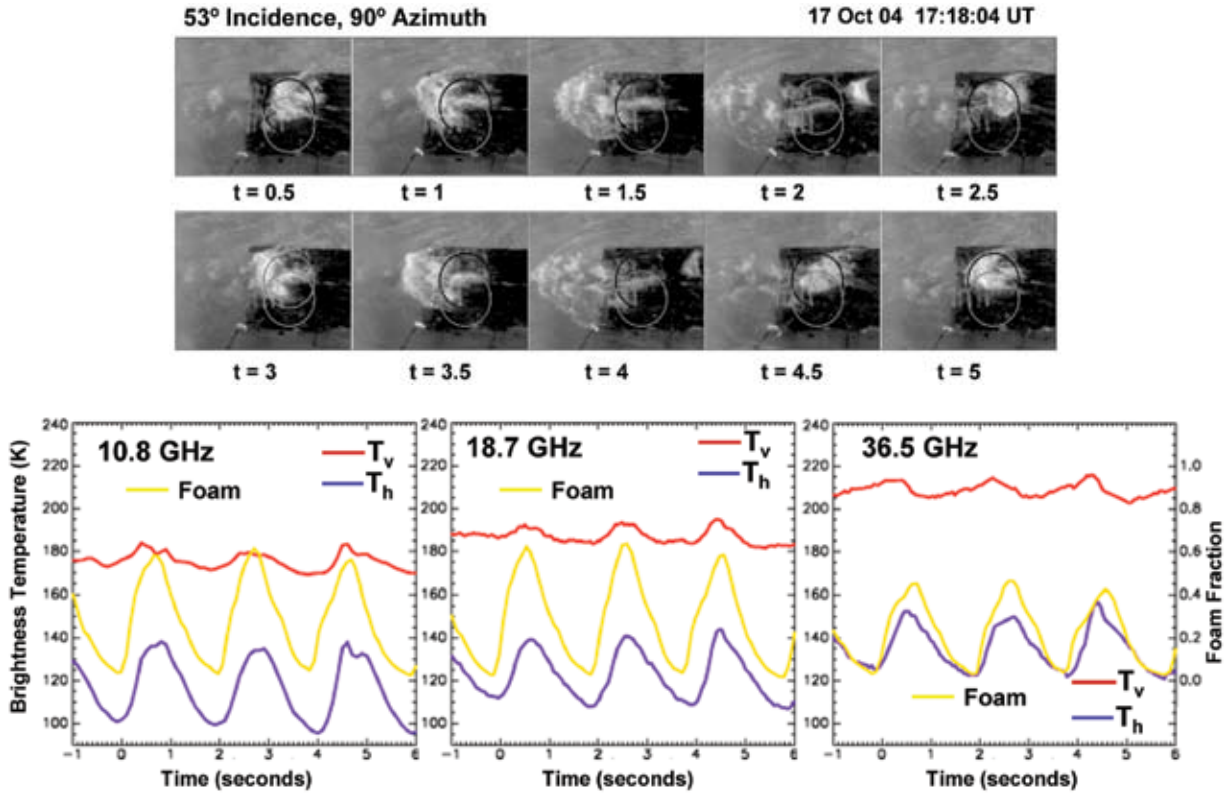

FIGURE 5
Video images of breaking waves on the shoal in the outdoor test tank and plots of antenna temperature and foam fraction vs time.

breaking wave is in the FOV on the shoal, f_1 and f_2 are the foam fractions corresponding to the maximum and minimum values of antenna temperature, and T_{sky} is the brightness temperature of downwelling sky radiation.

Figures 6 and 7 show the emissivity of foam at an incidence angle of 53 deg as a function of azimuth angle for all four frequencies in the vertical and horizontal polarization. At all frequencies, both plots show variation of emissivity with azimuth angle, but the

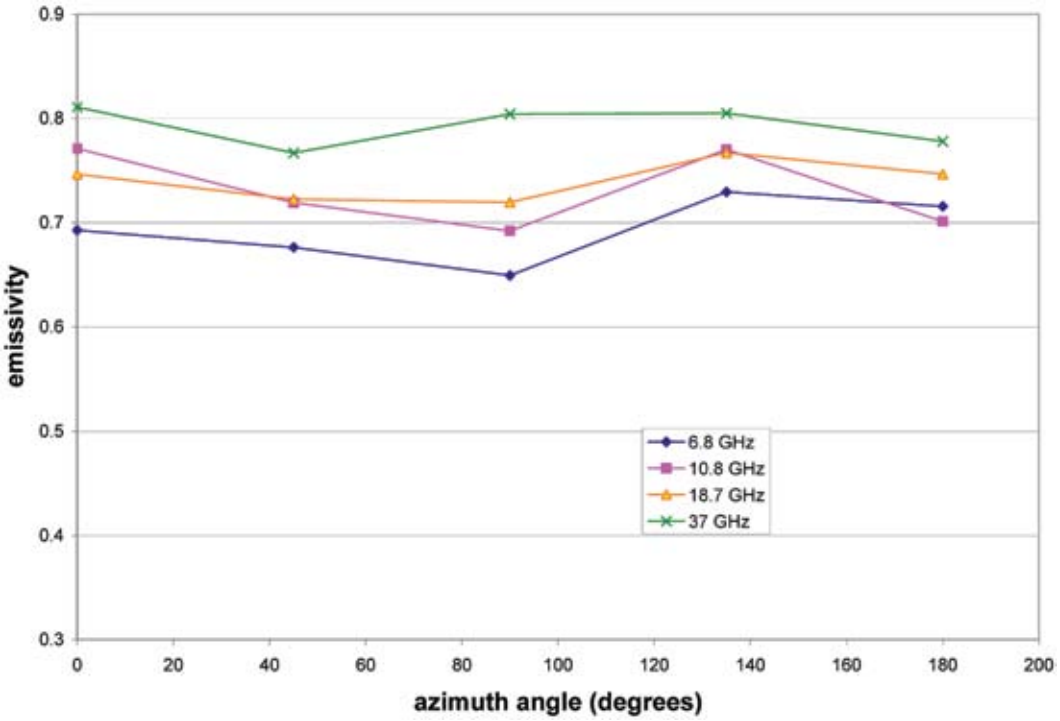

FIGURE 6
Foam emissivity vs azimuth angle, vertical polarization.

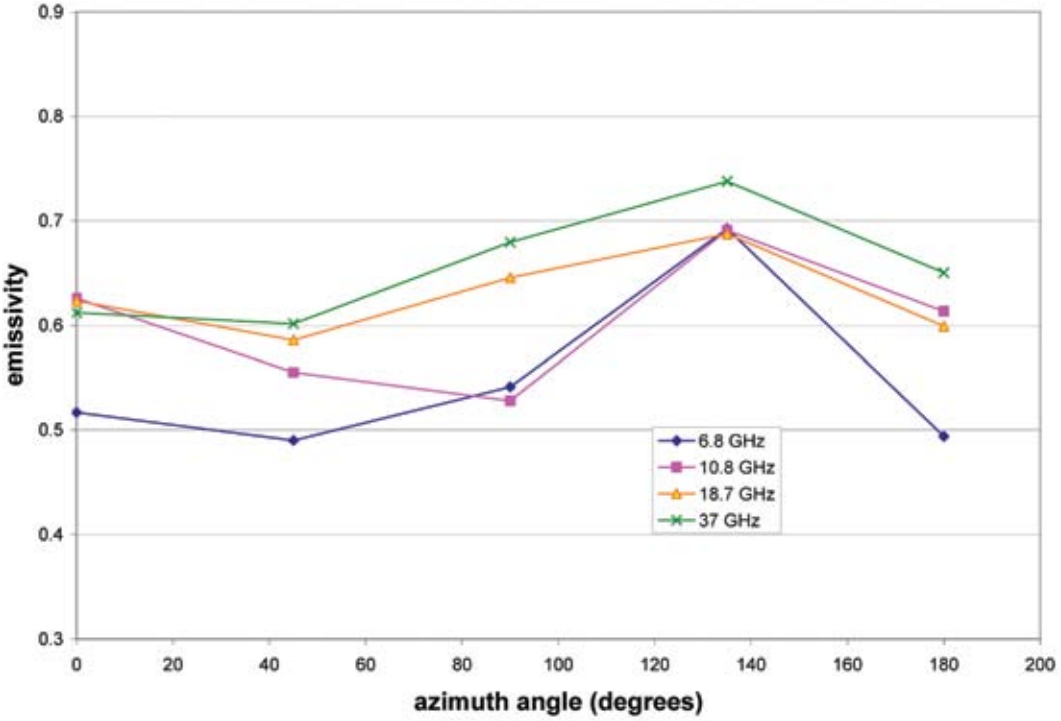

FIGURE 7
Foam emissivity vs azimuth angle, horizontal polarization.

variation is more pronounced for the horizontal polarization. This is the first experimental evidence of an azimuthal variation in foam emissivity.

Azimuthal variations in foam emissivity are most probably explained by the asymmetric distribution of foam on the wave slopes. Newly formed foam on the forward face of the wave covers much less area than the decaying foam in the wave's trough. Although perhaps not as dominant, some contribution to the azimuthal asymmetry of foam emissivity may also come from the different thickness of new and old foam. We continue to investigate these effects. Characterizing the azimuthal dependence of the microwave foam emissivity has the potential to improve the accuracy of wind vector retrievals from physically based algorithms.

[Sponsored by IPO]

References

[1] P.W. Gaiser, et al., "The WindSat Spaceborne Polarimetric Microwave Radiometer: Sensor Description and Early Orbit Performance," *IEEE Trans. Geosci. Rem. Sens.* **42**, 2347-2361 (2004).

[2] L.A. Rose, et al., "Radiometric Measurements of the Microwave Emissivity of Foam," *IEEE Trans. Geosci. Remote Sens.* **40**(12), 2619-2625 (2002).

[3] S. Padmanabhan, et al., "Effects of Foam on Ocean Surface Microwave Emission Inferred from Radiometric Observations of Reproducible Breaking Waves," *IEEE Trans. Geosci. Rem. Sens.*, WindSat Special Issue (Feb. 2006).

WindSat Polarimetric View of Greenland

L. Li and P. Gaiser
Remote Sensing Division

Introduction: WindSat is the first spaceborne microwave polarimetric radiometer that measures all four elements of the Stokes vector, the brightness temperatures at vertical and horizontal polarizations (T_V and T_H), and the real and imaginary parts of the cross-correlation of the vertical and horizontal polarization known as the third and fourth Stokes parameters (T_U and T_F).[1] WindSat was developed by NRL and had been in operation since January 2003. The polarimetric signatures of the third and fourth Stokes measurements are mostly related to the asymmetric structures of the ocean-wind-driven surface roughness. Prior to the launch of WindSat, it was a common belief that land polarimetric signatures at satellite footprint scales would be below the instrument noise level and would not carry any useful geophysical information. However, postlaunch data processing reveals significant land signals in the T_U and T_F, particularly over Greenland and the Antarctic ice sheets, which are the most environmentally sensitive Earth media, playing a significant role in global sea level and climate changes. Understanding this polarimetric signature, uniquely afforded by WindSat, and its relation with the snow properties and microstructures will have a profound impact on climate study.

Methodology: By observing the changes in the microwave signature, one can infer temporal and spatial variations in the physical properties of the ice sheet. A simple and effective way to represent the microwave signature is to construct an empirical observation model that can describe and separate different effects in the measurements using a small number of model parameters.[2] Over Greenland, it is well-known that T_V and T_H respond mostly to the dielectric properties of the snow,[2] ice and firn. WindSat data now show that T_U and T_F respond most strongly to the asymmetric structure of the snowpack and can be strong functions of the observation geometry, including the azimuth look angle. Therefore we examine the azimuthal modulations of T_U and T_F to separate observation geometry effects from environmental variations. The temporal and spatial variations of these azimuthal modulation coefficients can provide insight about the microwave scattering mechanism and its related geophysical processes.

Results: Figure 8 depicts T_U (left panel) and T_F (right panel) Stokes measurements at 10.7 GHz over the North Hemisphere for the period 1-10 February 2004. T_U shows coherent large-scale signals varying between ±2.5 K over the ocean and about 0.5 to 1 K signals over ice-free land. The variation for T_F over ocean and land is much smaller, less than ±1 K. However, over Greenland, both parameters show variations up to eight times larger than the ocean signature, where T_U varies between ±10 K and T_F from −10 to +20 K. Such large polarimetric signatures can be attributed mostly to the volume scattering by the porous Greenland snow media. Figure 9 illustrates the azimuthal dependence of polarimetric data extracted from the WindSat data at a location on the Summit of the Greenland ice sheet for April 2003. The two clusters of points are from ascending (near 210°) and descending (near 340°) revs. T_U and T_F are plotted for 10.7, 18.7, and 37 GHz, and all clearly show very well-defined azimuthal dependences. The solid lines represent the empirical model expressed as second-order harmonic functions, suggesting an excellent model fit to the data.

Figure 10 shows the time-series of first- and second-order harmonic coefficients of empirical observation model for T_U and T_F at 10.7, 18.7, and 37 GHz channels at the Greenland Summit. The first harmonic coefficients describe the scattering signatures that are related to the asymmetric structure of the snowpack, possibly induced by the surface slope or skewness of the snow dune. The second harmonic coefficients

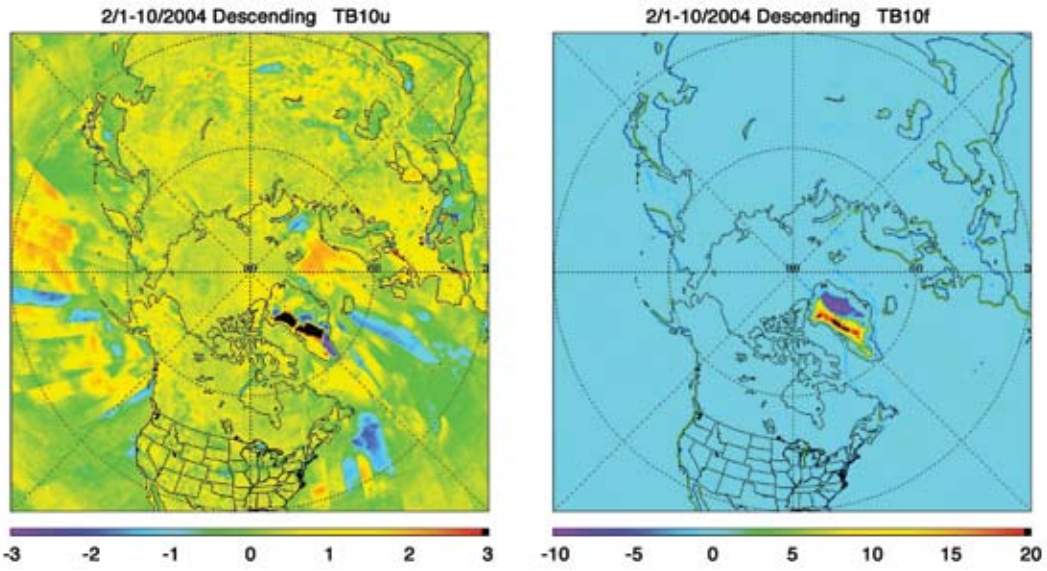

(a) Third Stokes parameters (b) Fourth Stokes parameters

FIGURE 8
Composite WindSat polarimetric measurements at 10.7 GHz. The descending pass data were collected by WindSat during 1–10 February 2004.

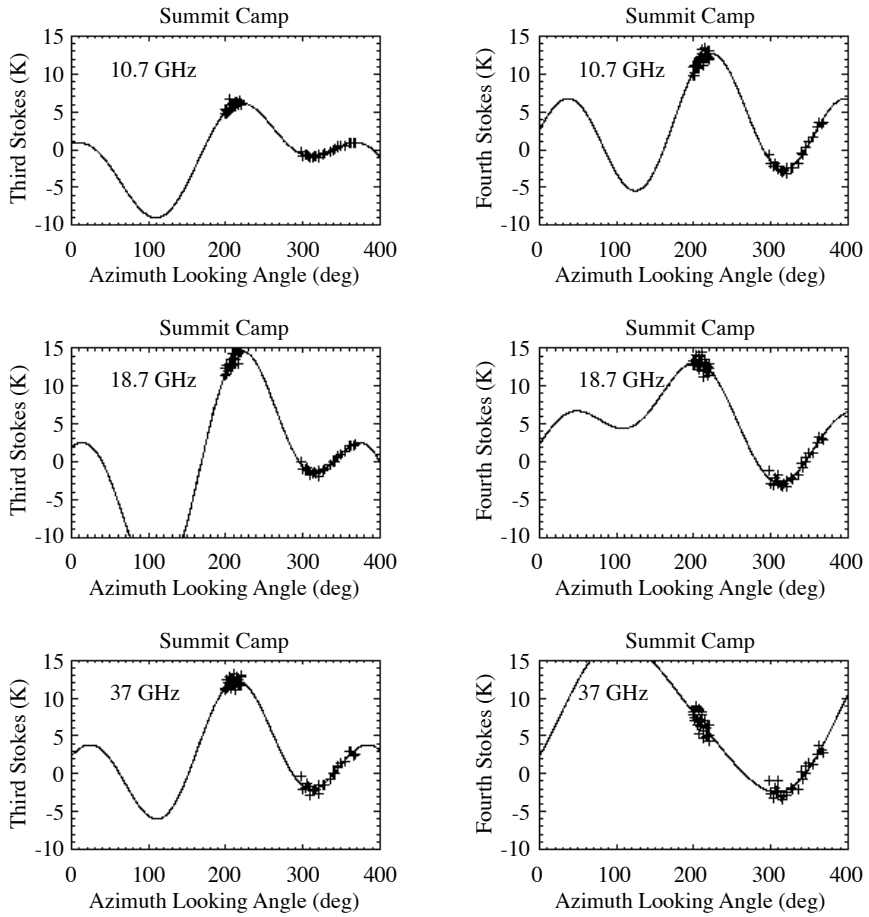

FIGURE 9
Third and fourth Stokes parameters observed by WindSat over the Summit study site in Greenland during April 2003. The solid line is the fitted second-order harmonic model. The left column shows the third Stokes parameter while the right column shows the fourth Stokes parameter. The top row is 10.7 GHz, the center row is 18.7 GHz, and the bottom row is 37 GHz.

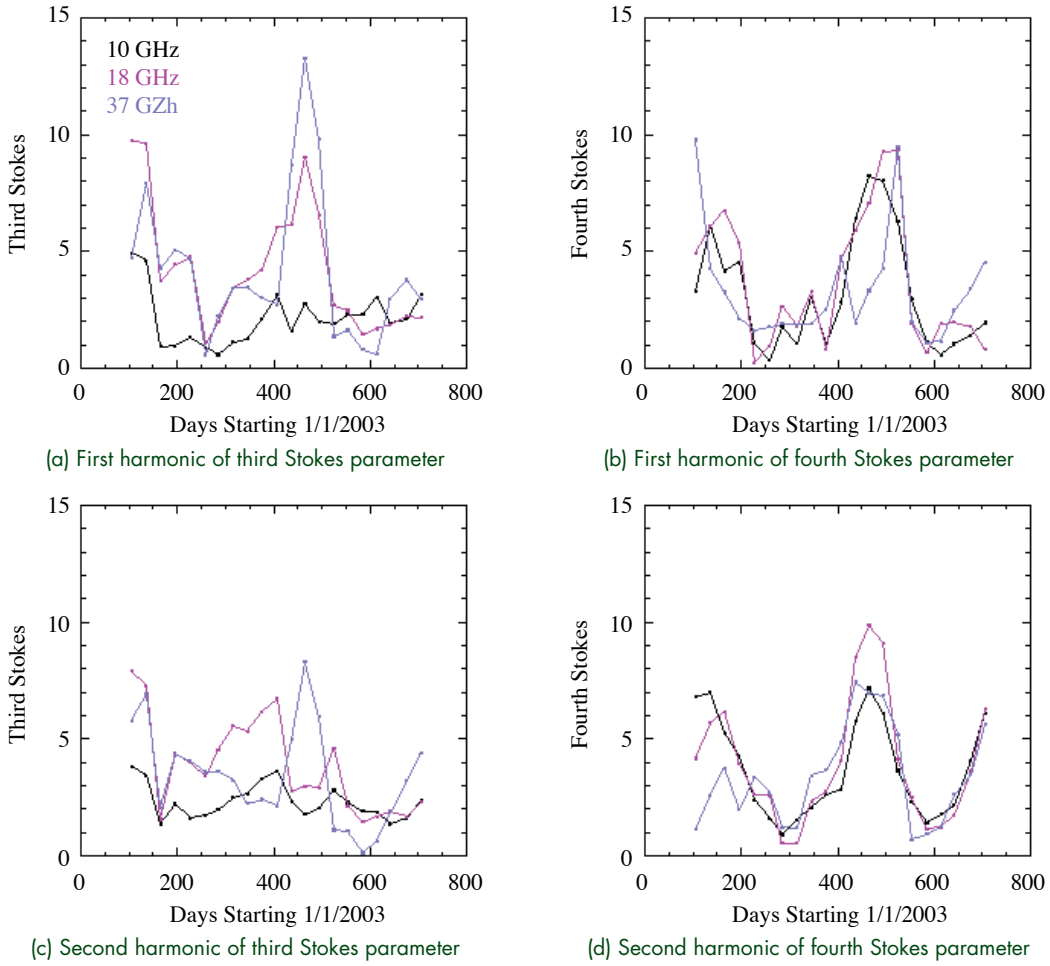

(a) First harmonic of third Stokes parameter

(b) First harmonic of fourth Stokes parameter

(c) Second harmonic of third Stokes parameter

(d) Second harmonic of fourth Stokes parameter

FIGURE 10
Time series of WindSat observations over the Greenland Summit study site from 1 April 2003 to 30 December 2004. The 10.7, 18.7, and 37.0 GHz data are color-coded with black, purple, and blue, respectively.

describe asymmetric features of the snowpack in directions parallel and orthogonal to the dune direction. The T_F signals are stronger than those from T_U over Greenland. This is a striking contrast to relatively weak polarimetric signatures generated by ocean surface scattering and indicates significant volume scattering contributions to the polarimetric signals. All harmonic coefficients peak in late winter to early spring when the snow metamorphism is most intense, and are weak in the middle summer when the penetration depth is dramatically reduced. This again highlights the importance of volume scattering in the polarimetric signals.

Summary: WindSat polarimetric data exhibit distinct geophysical and observation geometry signatures over Greenland that are correlated with geophysical variations, including snow microstructure, melting, and metamorphism. Therefore, WindSat provides an unprecedented and unique dataset for environmental and climate studies in the polar region. Furthermore, these results demonstrate how future polarimetric microwave radiometer missions can be exploited for climate studies.

[Sponsored by ONR]

References

[1] P.W. Gaiser, et al., "The WindSat Spaceborne Polarimetric Microwave Radiometer: Sensor Description and Early Orbit Performance," *IEEE Trans. Geosci. Rem. Sens.* **42**, 2347-2361, (2004).

[2] I.S. Ashcraft and D. Long, "Observation and Characterization of Radar Backscatter over Greenland," *IEEE Trans. Geosci. Rem. Sens.* **43**, pp. 225-237 (2005). ★

Deep Space Program Science Experiment (*Clementine*)

Achievement: The Deep Space Program Science Experiment (*Clementine*) program was a highly successful lunar mapping mission that tested new spacecraft hardware. During the 1980s, the Ballistic Missile Defense Organization (BMDO) developed advanced sensor and component technologies for missile defense systems. In 1991, a joint NASA/DoD study concluded that a collaborative deep space mission could test these developments and provide a significant science return. The DoD's goals were to test lightweight miniature sensors and components by exposing them to a long-duration space environment while obtaining imagery of the Moon and the near-Earth asteroid, Geographos. The BMDO tasked NRL with responsibility for mission design, spacecraft engineering, spacecraft manufacture and test, launch vehicle integration, terrestrial support, and flight operations.

In 1994, NRL put a satellite, equipped with a sensor payload, into orbit around the Moon. The spacecraft successfully used much newly developed hardware, including imaging sensors provided by the Lawrence Livermore National Laboratory. A high-quality mapping mission of the lunar surface was completed with outstanding success — a complete imaging of the lunar surface (1.8 million images) in eleven discrete wavebands with coarse altimetry over most of the lunar surface.

This imaging of the Moon's surface was a great success in its scientific returns: relative positions of widely separated lunar features could be accurately determined for the first time, including those on the Moon's far side; some regions in the lunar south pole were imaged with good resolution for the first time, with some data indicating the presence of ice; and complete multispectral imaging provided information on local mineral composition over the entire lunar surface. These images helped resolve issues such as the character and evolution of the primitive lunar crust, thermal evolution of the Moon and lunar volcanism, and the impact record and redistribution of crustal and mantle materials. *Clementine's* images are available for students everywhere to explore in a 3-D interactive environment on the Internet.

Impact: With *Clementine's* success, the U.S. returned to the Moon for the first time since the end of the Apollo lunar missions. NRL's satellite demonstrated that the goal of "faster, better, cheaper" was attainable: it was built in only 22 months (less than half the usual time) for 1/5 the usual cost for similar space probes. The probe was so simple to operate that its mission control center comprised eight engineers working in a warehouse in Alexandria, Virginia.

Anthropogenic Noise and the Marine Environment

R. Hillson and H.-J. Shyu
Information Technology Division

Introduction: The impact of anthropogenic noise on the marine environment is a subject of increasing concern to the United States Navy. Sources of noise include ambient noise from ship traffic, acoustic sources such as air guns used in petroleum exploration, and active sonar operations conducted for military operations. The Navy has acknowledged that the use of active sonar was a contributing factor to the cetacean strandings in the Bahamas in March 2000 (see Ref. 1 for a joint report by the Navy and the National Marine Fisheries Service). The Office of Naval Research (ONR) subsequently initiated the Effects of Sound on the Marine Environment (ESME) program to address these issues, and to explore comprehensive approaches for reducing the adverse effects of anthropogenic noise on the marine environment. NRL was designated as the ESME systems integrator, and during the process developed the ESME Software Workbench.[2]

The ESME workbench, written in MATLAB™, integrates data sets and computer models contributed by the ESME team of experts in the areas of oceanography, underwater acoustic propagation, and marine mammal physiology and behavior. Complex simulations can be rapidly constructed from an underlying set of conceptual models. Models are incorporated for simulating active acoustic sources and for simulating marine mammal movements. (A simulated marine mammal will be referred to as an "animat.") Additional models are provided for estimating the received time series along an animat's track, and for predicting the animat's cumulative acoustic exposure.

Background: The ESME workbench models the complete sound path: from the sound source(s) (active sonar or other acoustic sources), through the water column and the sea floor, to the simulated receivers (animats). Table 1 lists the key contributors and institutions. Mr. Shyu was the lead developer for the ESME workbench and was responsible for integrating the software modules and models into the workbench.

The ESME workbench includes a number of predefined data sets and/or parameter options for acoustic sources, bathymetry, sound velocity profiles, ocean surface conditions, species-specific animal movement, and sediment properties. The user can provide additional or alternative data sets, such as animal distribution and habitat preferences, or diving and group behavior. Acoustic sources can be specified as repetitive waveforms with known frequency characteristics (e.g., a constant frequency source, or as a frequency-modulated ramp or "chirp"), and as either an omnidirectional source or a beamformed (i.e., directional) source with some predefined radiation pattern. Source movements can be simulated to

Table 1 — ESME Workbench Contributors

Contributor	Organization	Module	Programming Language
H.-J. Shyu D. Armoza R. Hillson	Naval Research Laboratory	ESME MATLAB workbench development and system integration	MATLAB and Visual C++
M. Porter M. Siderius	Heat, Light, and Sound Research Inc.	Acoustic propagation loss (Bellhop, Kraken), and received time series generator	FORTRAN and MATLAB
D. Mountain A. Hubbard	Boston University	Mammalian auditory system model. Requires received time series as input	MATLAB
D. Ketten	WHOI/Harvard Medical School	Parameters for the Boston University auditory model	Text
J. Miller G. Potty	University of Rhode Island	Geoacoustic and sediment models	MATLAB
J. Finneran	SPAWAR	Temporary Threshold Shift (TTS) estimation functions. Requires received time series as input	MATLAB
D. Houser	Biomimetics, Inc.	Marine mammal movement models	Visual C++
G. Gawarkiewicz C. Linder	Woods Hole Oceanographic Institution (WHOI)	Sound speed profile data	Text format

create scenarios in which ships using active sonar move along predefined paths. Several different measures of acoustic exposure are included, including two models for estimating the likelihood of the animats incurring temporary threshold shifts (TTS's), a temporary decrease in auditory sensitivity. These sound exposure values may then be used to estimate the environmental risk of a given sound usage scenario by using either user-defined thresholds of risk or metrics set by legal and regulatory agencies.

The workbench also includes a sophisticated framework for simulating the movement behavior of marine mammals. Since all marine mammals must surface to breathe, the framework includes movement models of representative diving patterns for several species of marine mammals. Diving models, for example, are minimally specified for a species by entering a set of parameters—the average depth and duration of a typical dive, for example. The movement models also allow the user to select different hypothetical response patterns to an acoustic source, including avoidance behavior.

The workbench is menu-driven, with a graphical user interface. Figure 1 shows the main menu for the workbench, including schematic representations of sonar beamforming patterns. Figure 2 shows a simulated sound field. As required by certain models (Table 1), the workbench can compute the received acoustic waveform (i.e., time series) along the animat's track. For complex simulations involving moving platforms, and long simulated periods of time (e.g., hours rather than seconds), the instantaneous or cumulative acoustic energy (dB re 1 μPa^2-s) is typically computed for reasons of computational efficiency, rather than the received time series. Figure 3 provides a graphical representation of the instantaneous and cumulative acoustic exposure for a single animat.

Conclusions: By integrating models and data sets provided by different subject matter experts, the ESME workbench provides the analyst with the ability to quickly construct and run scenarios for modeling acoustic exposure. Complex but realistic scenarios with moving platforms, beamformed acoustic sources, and multiple moving receivers (animats) can be rapidly generated. In addition, the ESME workbench provides a means for exploring the implications of alternative hypotheses—for example, by simulating different *hypothetical* behavioral response patterns to anthropogenic noise, and estimating the parametric variation in the estimated acoustic exposure. In general, we feel the workbench provides a useful approach to the problem

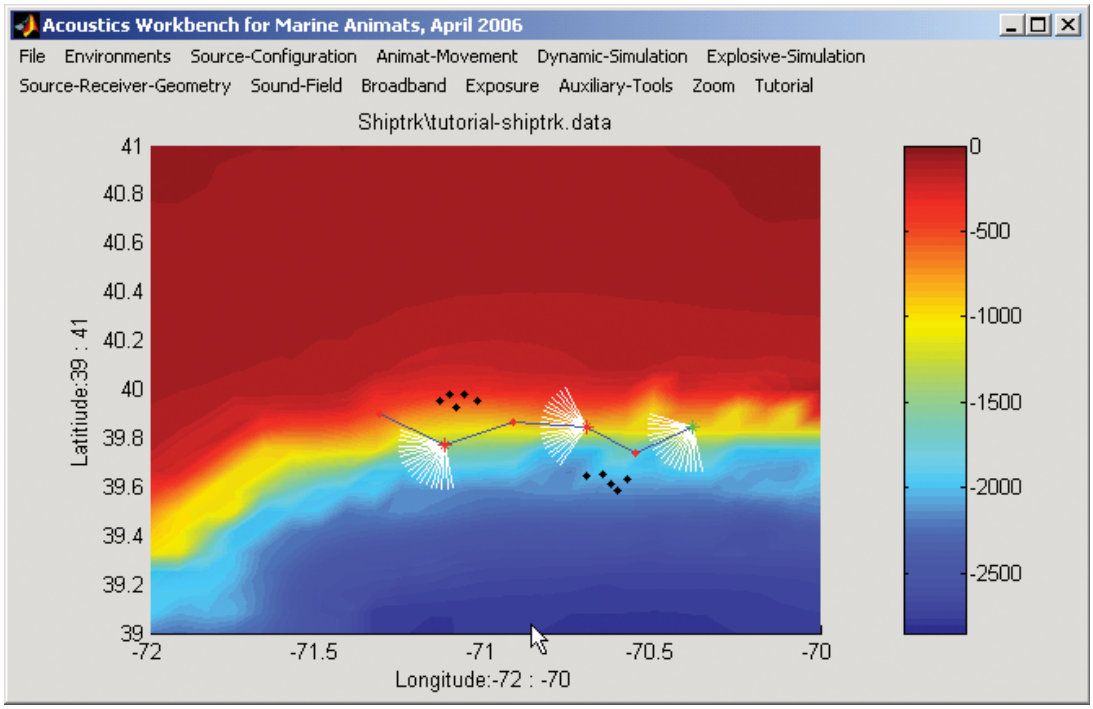

FIGURE 1
The ESME workbench main menu. The bathymetry is from the Mid-Atlantic Bight area. A simulated ship track (the blue line segments) with simulated sonar beam patterns (the white spotlights), and two pods of marine mammal animats (the 10 black dots) are shown. Resolution for the bathymetric database is 5 arc-minutes, and depth is in meters.

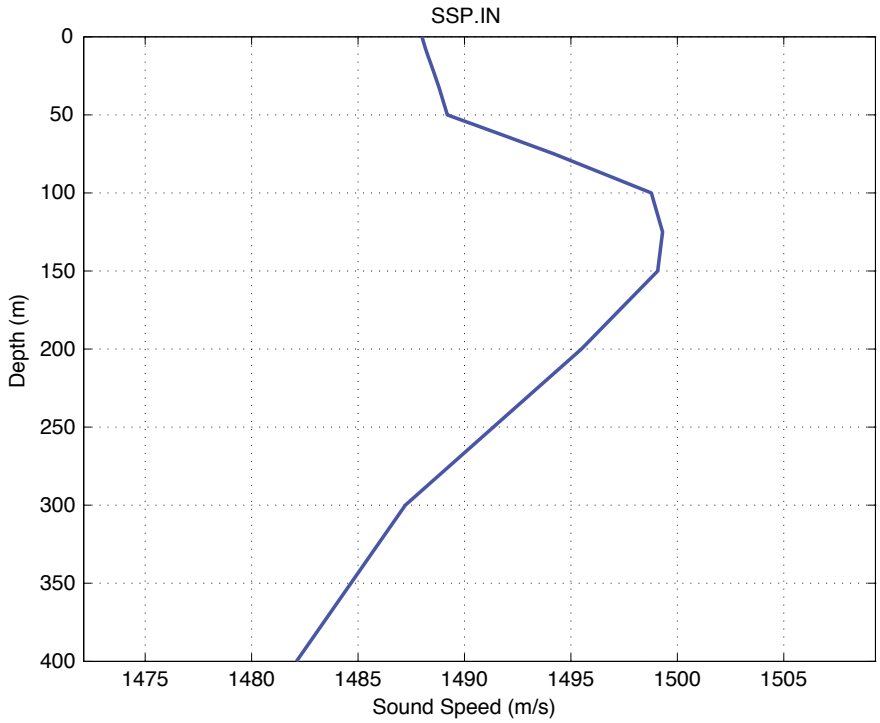

FIGURE 2(a)
Winter sound speed profile for the Mid-Atlantic Bight test site.

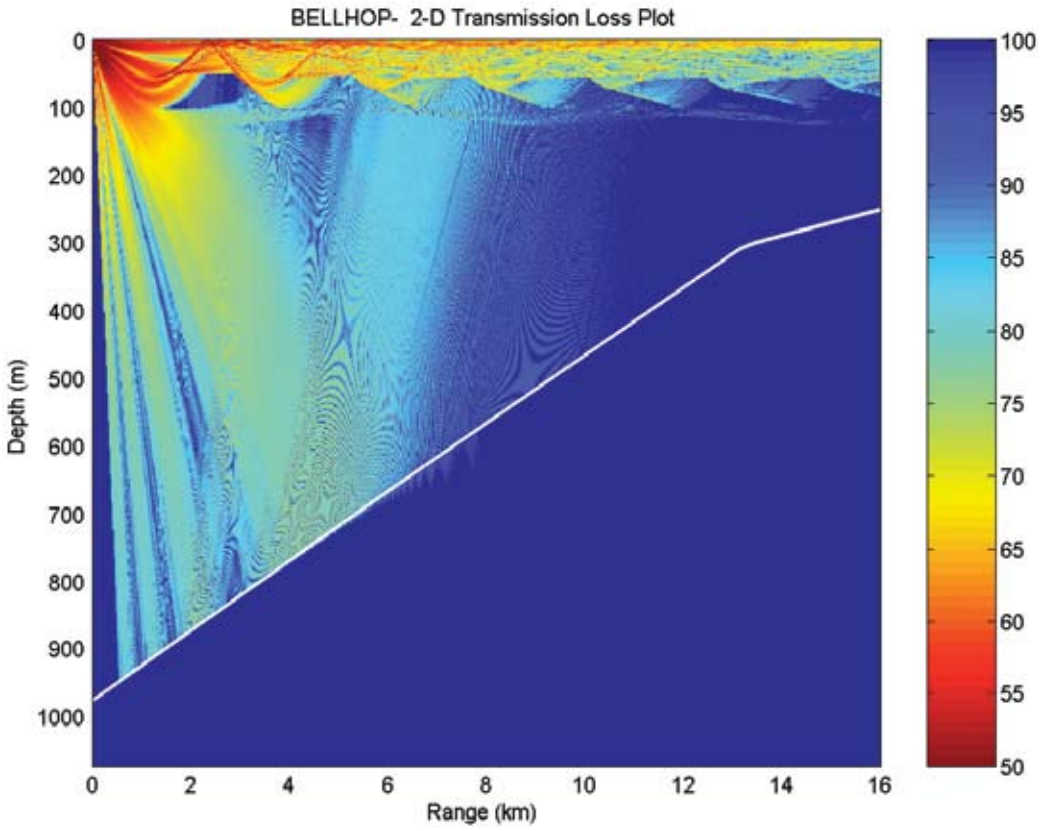

FIGURE 2(b)
A 2-d transmission loss plot generated using the sound speed profile shown in Fig. 2(a), illustrating simulated beamforming. A prominent surface duct is visible, a feature that reflects the structure of the winter sound speed profile. The scale shows the transmission loss in decibels (dB re 1 μPa^2-s). The greater the transmission loss, the lower the received sound level at a given location.

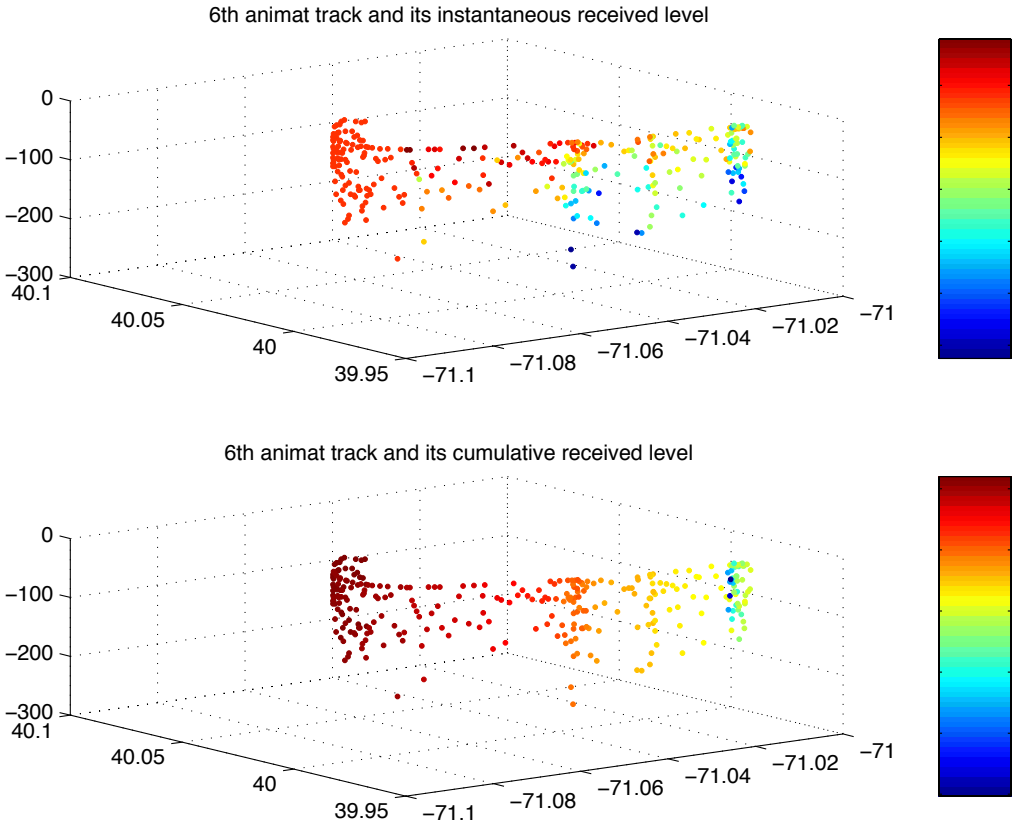

FIGURE 3
A track for a simulated marine mammal ("animat"). Latitude ranges from 26.1 to 26.35 degrees, and longitude from –77 to –78.1 degrees. The vertical axis corresponds to depth in meters. The colored dots represent the position of the animat during a sequence of dives. The ascending color scale, from blue to red, corresponds to the instantaneous received level (top) and cumulative acoustic energy exposure (bottom) in dB (re 1 μPa^2-s).

of estimating the effects of anthropogenic noise on the marine environment, given the ease and flexibility of the simulation framework and the increasing sophistication of the underlying data and models.

Simulation continues to provide a viable alternative to conducting experiments that are ethically, technically, or financially unfeasible. Continuing research in the areas of oceanography, underwater acoustic propagation, and cetacean behavior, physiology, and auditory processing will inevitably lead to improved models that enhance our ability to accurately predict the effects of sound on the marine environment.

Acknowledgments: The authors acknowledge the contributions of their ESME collaborators (cited in Table 1), and their sponsors at the Office of Naval Research, particularly Drs. Robert Gisiner and Scott Harper.

[Sponsored by ONR]

References

[1] *Joint Interim Report Bahamas Marine Mammal Stranding Event of 15-16 March 2000* at www.nmfs.noaa.gov/prot_res/overview/Interim_Bahamas_Report.pdf.

[2] H.-J. Shyu and R. Hillson, "A Software Workbench for Estimating the Effects of Sound Exposure in Marine Mammals," accepted for publication in the *IEEE J. Ocean. Eng.* (special issue on the ESME program). ★

Active Control of Nuclear-Enhanced Radiation Belts

G.I. Ganguli, M. Lampe, W.E. Amatucci, and A.V. Streltsov
Plasma Physics Division

Introduction: A high-altitude nuclear detonation by a hostile power could flood the Earth's radiation belts with MeV "killer" electrons, which would remain trapped by the geomagnetic field for years. This orders-of-magnitude enhancement of the normal radiation belts would disable low-Earth-orbit satellites within weeks,[1] thereby degrading military capabilities and severely impacting the economy. This threat has been called a potential "Pearl Harbor in space." Development of an effective countermeasure is a national priority.

NRL recognized the importance of this threat early on and initiated a comprehensive 6.1 program in FY04 that includes theory, computer simulation, and laboratory experiment. We are developing quantitative physics models that are needed as a precursor to space-based tests. The ultimate objective is to avoid catastrophic radiation damage to space assets by restoring the radiation belt to its natural state within a week.

Background: It has been known since the 1960s that the natural particle population in the radiation belt is controlled by a feedback process: electromagnetic waves are amplified by the "loss-cone" electron distribution naturally present in the radiation belt, and the waves in turn scatter and precipitate particles. There is every reason to believe that the killer nuclear-generated electrons could be similarly precipitated, if it were possible to introduce a sufficiently energetic spectrum of waves with the right wavelength and frequency. Mainline remediation efforts emphasize the use of whistler waves transmitted from a space-based antenna and amplified by the free energy available within the radiation belt. A technical panel in 2001 assessed the available technology and concluded that remediation could be achieved within a week, with only a modest investment of energy from a few satellite-based antennas emitting at 6 kW, if 20 dB amplification of the appropriate waves could be assured. However, while there is clear experimental evidence for sporadic whistler amplification and secondary emission,[2] the circumstances necessary to trigger the process are not well understood or predictable. Nonlinear processes appear to be at work that depend sensitively on the wave frequency, require triggering waves above a threshold strength, and also require the presence of natural magnetospheric inhomogeneities known as ducts. The parametric dependences and scaling laws are unknown. Nor is there any predictive capability for the operation of a high-intensity space-based antenna system within the nonlinear magnetospheric plasma medium. We are currently addressing these issues.

Current Research: To understand whistler dynamics in nuclear-enhanced radiation belts, we needed to develop wholly new types of fast numerical simulation models using techniques such as elimination of the displacement current and enforcement of quasi-neutrality. These models have yielded valuable insights. For example, Fig. 4 shows a test that illustrates saturation of whistler amplification by magnetic trapping. The study is now being extended to include inhomogeneities and wave packets of finite size, which lead to de-trapping and, hence, extended amplification and triggered emission. Figure 5 illustrates a full-wave simulation of whistler propagation in ducts with diameter comparable to the whistler wavelength. Earlier ray tracing models are inappropriate for these narrow ducts, which could be self-generated by a large-amplitude whistler, thereby enabling amplification and unattenuated propagation over large distances, even in the absence of natural ducts.

These theoretical investigations of nonlinear whistler optics are complemented by experiments in the NRL Space Chamber. We have investigated the resonance-cone propagation of low-power whistlers and the self-ducting of large-amplitude whistlers to develop the technique for lossless long-distance propagation. Figure 6(a) shows propagation of small-amplitude whistlers in the Space Chamber plasma, illustrating the low-frequency cutoff at the lower-hybrid resonant frequency and the confinement of wave power within the lower-hybrid resonance cone. Figure 6(b) demonstrates the self-ducting of high-power whistler waves. The data show collimation of the whistler radiation pattern two meters downstream, with the transmitting antenna located on the chamber axis (solid line) and 10 cm off axis (dashed line).

A New Remediation Concept: We are also developing a radically different approach for rapid remediation based on massive injection of energy over a short duration. If a large quantity of neutral vapor such as lithium is released from a satellite moving in the equatorial plane, the vapor is photo-ionized over a period of about an hour. The resulting ions, moving at ~7 km/s normal to the geomagnetic field, spin up into a highly unstable "ring" distribution, which emits large amplitude electromagnetic waves in the desired

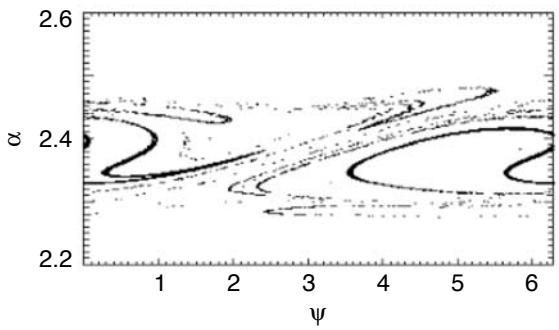

FIGURE 4
Computer simulation showing electron density in a 2-D section of phase space (pitch angle α vs electron gyration phase Ψ) that illustrates the phenomenon of phase trapping.

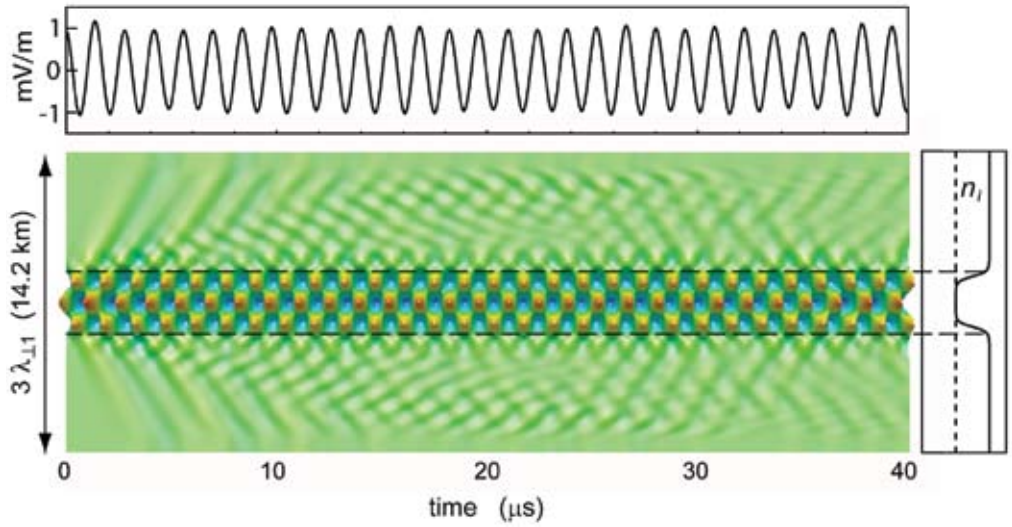

FIGURE 5
Computer simulation showing wave ducting within a tube of reduced electron density. The upper curve shows the wave amplitude essentially constant. In the absence of a duct, the wave would expand and thus fall off in amplitude.

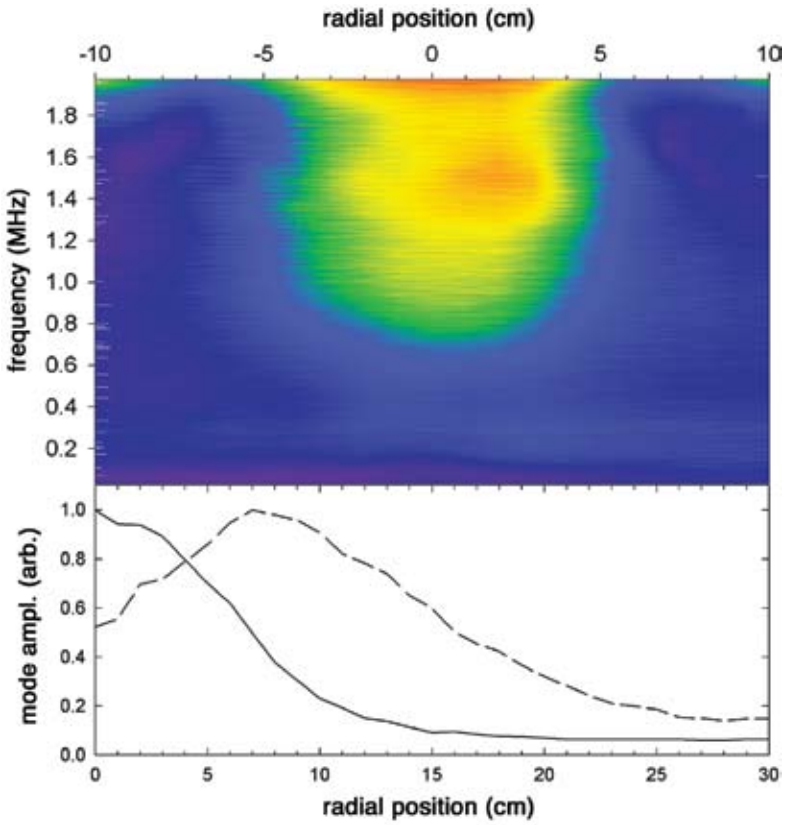

FIGURE 6
(a) Experimental measurements of whistler wave resonance cone width as a function of wave frequency. (b) Demonstration of whistler wave self-ducting with transmitting antenna located at $r = 0$ (solid) and $r = 10$ cm (dashed).

frequency and wavelength range. These waves can precipitate the killer electrons within hours, as opposed to a week. The process in effect taps the orbital kinetic energy to create a giant ion magnetron in the radiation belt. A ton of neutral lithium would carry 10 GJ of energy, vastly more than could ever be introduced through electromagnetic antennas.

[Sponsored by ONR]

References

[1] D.G. Dupont, "Nuclear Explosions in Orbit," *Sci Am.* **290**(6), 100, 2004.

[2] R.A. Helliwell, "VLF Wave Stimulation Experiments in the Magnetosphere from Siple Station, Antarctica," *Rev. Geophys.* **26**, 551, 1988. ★

A Real-Time Experiment Using PCTides 2.0

P.G. Posey, G.M. Dawson, and R.A. Allard
Oceanography Division

Introduction: A real-time test of the Naval Research Laboratory's (NRL) globally relocatable tidal prediction system (PCTides 2.0) was performed during the naval exercise Autonomous Underwater Vehicle Fest 2005 (AUVFest 2005) that occurred June 6-16, 2005 in the Puget Sound, Washington, area. AUVFest 2005 was sponsored by the Office of Naval Research (ONR) and involved two weeks of intensive AUV experimentation and demonstration. PCTides 2.0[1] consists of a barotropic ocean model designed to forecast tidal currents and sea-level water elevations on or near continental shelves (Fig. 7). The system is set up to run on a PC or UNIX platform with a global database of bathymetry, boundary conditions, and tidal station data for assimilation purposes. During AUVFest 2005, PCTides 2.0 predicted water elevations and tidal currents using a series of grids with increasing resolution (Fig. 8). Tidal forecasts from the 1.5-km nest are presented here. The grids were run daily, producing a 5-day forecast of tidal height and currents with graphical results posted to the Naval Oceanographic Office (NAVOCEANO) website. During the exercise, the PCTides 2.0 tidal phase forecasts provided the optimum dive window for an AUV recovery exercise and a successful recovery of a bottom "crawler" stuck in the mud. Feedback from the divers was that the modeled tidal phase forecasts were "dead on."

Model Assessment: Two Acoustic Doppler Current Profilers (ADCPs) were deployed during AUVFest 2005 in the Hood Canal and Keyport areas. As of October 2005, the Keyport ADCP has not been recovered. Prior to AUVFest 2005, two ADCPs were deployed in the same area, and a preliminary study was performed using PCTides 2.0. These results showed good agreement and provided confidence in the system's forecasting ability for this region.

PCTides 2.0 forecasts of water-level elevations and tidal currents were compared to the ADCP at the Hood Canal location, demonstrating the ability of PCTides 2.0 to produce an accurate forecast. As the model resolution increased from 12 to 1.5 km, the predicted elevations improved. The root mean square error (rmse) decreased from 22 to 16 cm as the model resolution

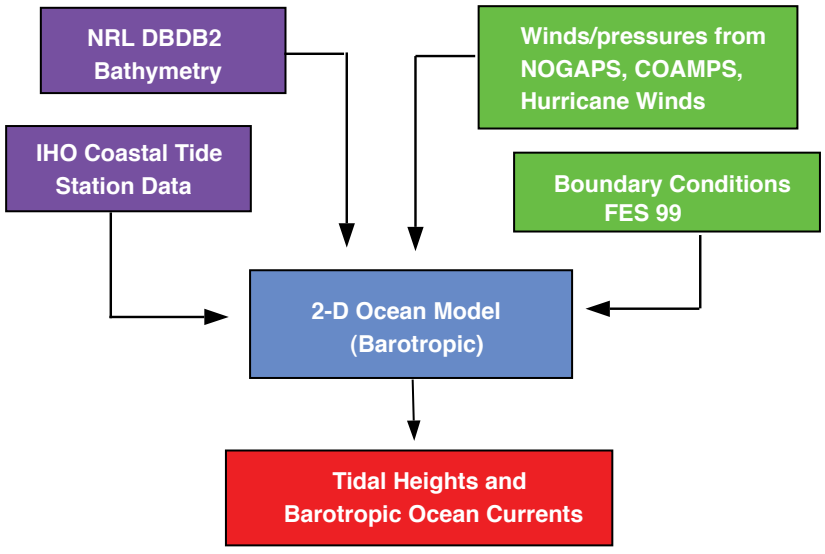

FIGURE 7
Components of the PCTides 2.0 system.

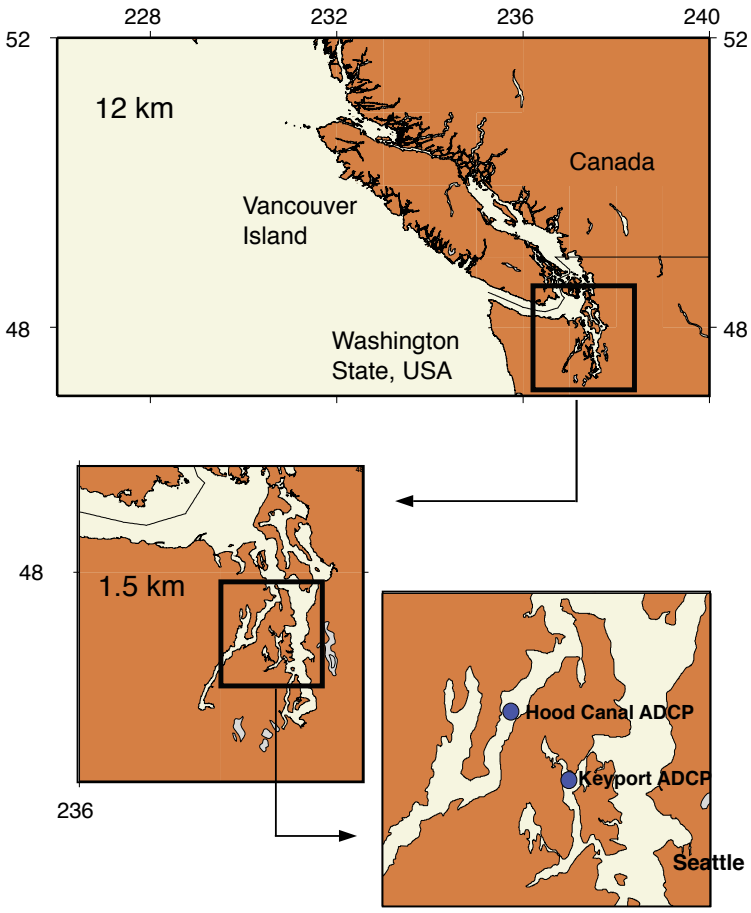

FIGURE 8
PCTides 2.0 grids (12 and 1.5 km) used in the AUVFest 2005. ADCP locations (circles) at Hood Canal and Keyport are shown in zoomed-in area.

increased. The rmse for the phase for all grids was less than 25 min. As shown in Fig. 9(a), comparisons of the PCTides 2.0 water-level elevations forecasts were in excellent agreement to the observations.

The PCTides 2.0 depth-averaged current magnitudes agreed well with the Hood Canal observations. As the grid resolution increased to 1.5 km (Fig. 9(b)), the current magnitudes continued to improve, with rmse decreasing to 5 cm/s. The predicted tidal direction followed the same pattern as the tidal magnitudes. Both the 12- and 1.5-km grids had a mean error in current direction of 20 deg.

Summary: During the past five years, PCTides 2.0 has been rigorously tested in many areas and has produced realistic results within a short time frame (days). In the past two years, PCTides 2.0 has also been used to forecast tidal conditions due to storm surge. The model's forecasted storm surge have compared well against hurricane data from Isabel (2003) and Katrina (2005). In August 2005, PCTides 2.0 was accepted into the Oceanographic and Atmospheric Master Library (OAML) and can be distributed to all Department of Defense agencies. PCTides 2.0 currently has two patent applications pending. Overall, the PCTides 2.0 system has been shown to produce accurate and timely predictions of tidal conditions with favorable feedback from the Navy users.

Acknowledgments: We acknowledge the help from NAVOCEANO with the collection of the ADCP data (Dr. Frank Bub and Mr. Bryan Mensi).

[Sponsored by CNMOC]

Reference

[1] R.H. Preller, P.G. Posey, and G.M Dawson, "Hurricane Isabel: A Numerical Model Study of Storm Surge Along the East Coast of the United States," 85th American Meteorological Society Annual Meeting, San Diego, CA. P2.9 (2005). ★

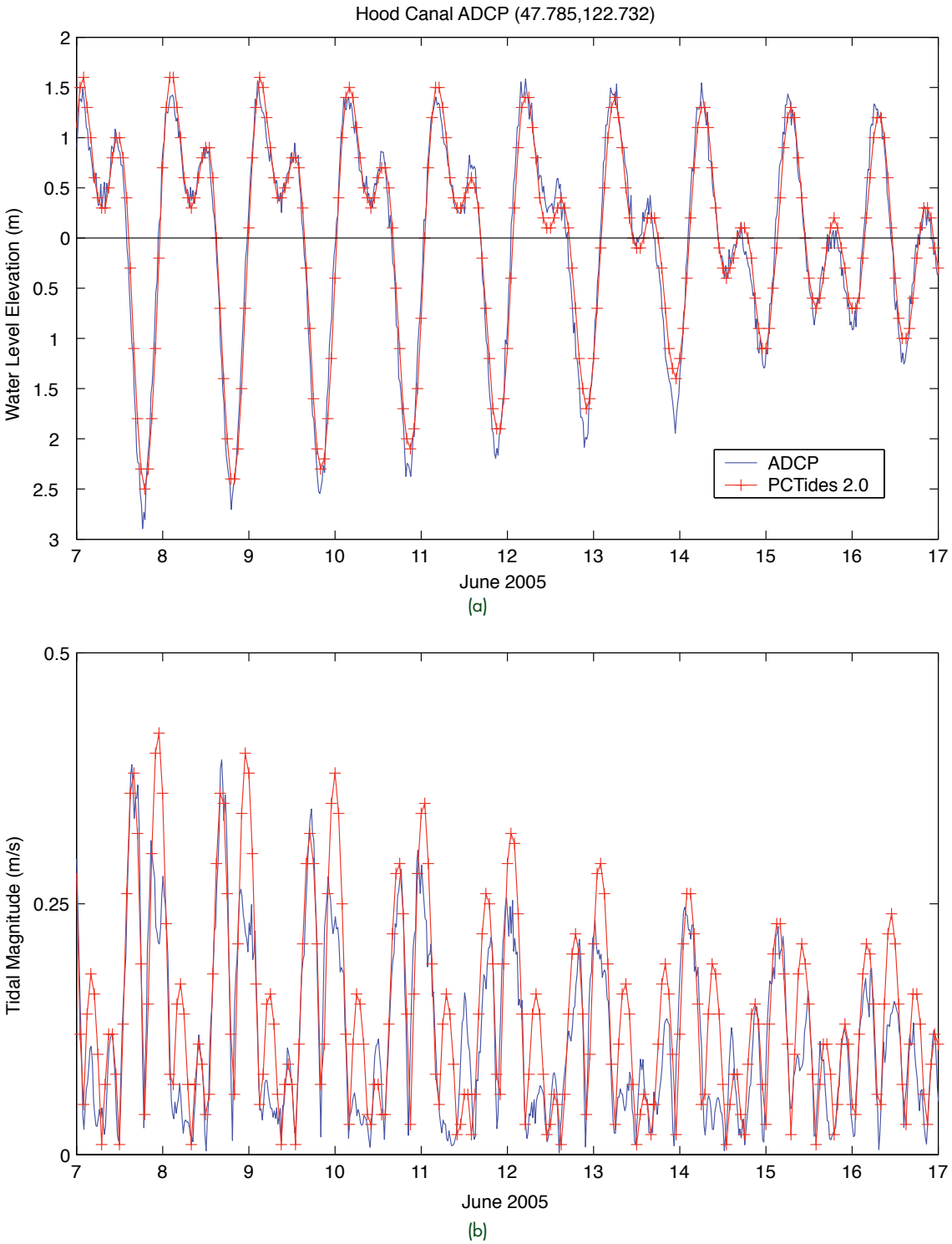

FIGURE 9
Hood Canal ADCP (blue) compared to PCTides 2.0 1.5 km forecasts for (a) water level elevation in meters and (b) tidal current magnitude in meters/seconds.

Erosion During Hurricane Isabel

C.D. Rowley, T.R. Keen, and J.D. Dykes
Oceanography Division

Introduction: A better understanding of the complex interplay between ocean waves, water levels, and currents, and the movement of sediment in the dune-beach system will improve predictions of coastal environmental hazards, water-column optics, bar movement, and mine burial—all of which have tactical implications. Historically, this interaction of different processes has been modeled by using simple parameterizations. In this study, we explicitly simulate the above processes through a suite of numerical models. We use a depiction of the landfall of Hurricane Isabel (2003) on the barrier islands of Cape Hatteras, North Carolina, to examine potential erosion that contributes to barrier island breaching and washover. This prototype for a rapidly relocatable nearshore sediment transport modeling system will take advantage of recent advances in Navy technology for global deep-ocean and coastal environmental modeling.

Modeling Coastal Erosion: We coupled a suite of individual models representing different physical ocean processes. The ocean environment is simulated using a parametric model of tropical cyclone winds; a numerical model for the surface gravity wave field in coastal areas (Simulating WAves Nearshore[1]); and the Navy Coastal Ocean Model[2] for the coastal ocean tides and currents. Sedimentation and erosion processes are simulated using the Littoral Sedimentation and Optics Model,[3] which couples a bottom boundary layer model representing the interaction of the waves and currents near the seabed with a sedimentation model. The sedimentation model calculates potential erosion, which is the volume of sediment per unit coastline length removed from the adjacent land point.

We show that when the modeled potential erosion exceeds the material available for erosion in the dune-beach system, dune removal and washover may occur. If there is a substantial difference in water levels on the offshore and onshore sides of the barrier island, a pressure gradient can drive a cross-island flow, and a breach channel may develop. Using simple geometric arguments based on the average height of the dune-beach system before the storm, the tide and storm surge water levels depicted by the circulation model, and the conservation of the volume of sediment eroded from the dune-beach system, we derive a critical dune system mean height, $H_c = E/L + n$, where E is the model potential erosion due to the storm, L is the width of the dune-beach system, and n is the model offshore water level due to storm surge and tides. When H_c exceeds the actual mean height of the dune-beach system, there is the potential for washover, and if the difference of water levels across the island is significant, for breaching.

Hurricane Isabel at Ocracoke and Hatteras Islands: The modeled oceanographic factors all reach their maximum intensities along Hatteras Island during the 12-h period around Isabel's landfall at 1100 UTC on 18 September 2003 (Fig. 10). Modeled waves near Hatteras Island exceed 7 m. Modeled currents

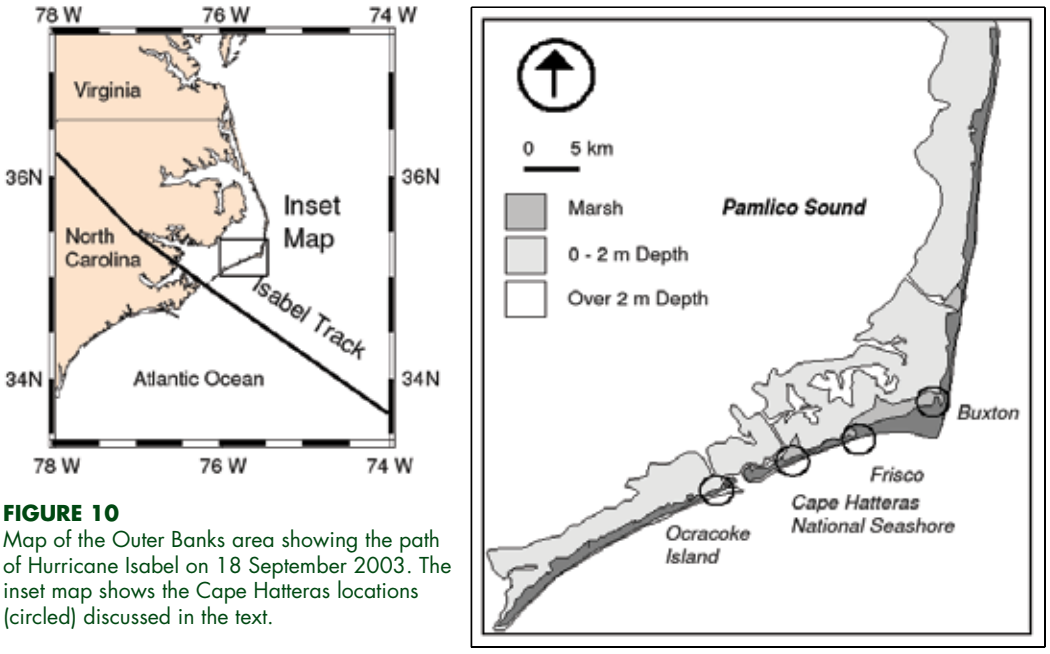

FIGURE 10
Map of the Outer Banks area showing the path of Hurricane Isabel on 18 September 2003. The inset map shows the Cape Hatteras locations (circled) discussed in the text.

along south Hatteras Island are westward during the storm build-up and peak at more than 1 ms^{-1} prior to landfall, then reverse direction with the shift in the wind direction as the eye moves inland. The tidal signal dominates the regional pattern of predicted water level, and adds to the storm surge setup that extends from Ocracoke Island eastward and northward along Hatteras Island (Fig. 11). Substantial set-down on the inshore side of the barrier islands establishes a large (0.5 to 1 m) cross-island water level difference.

The National Oceanic and Atmospheric Administration (NOAA) flew several reconnaissance flights over the Outer Banks after Hurricane Isabel to assess the damage. The erosion observed in the aerial photography is consistent with the alongshore variation in the model potential erosion (Table 2). For example, at the eastern end of Ocracoke Island (50 km from landfall), washover terraces and perched fans were deposited 650 m inland (Fig. 12(a)). In contrast, in the Cape Hatteras National Seashore along the western end of Hatteras Island (60 km east of the storm track), newly incised channels in addition to dune erosion and washover deposition are evident (Fig. 12(b)). The lower dunes and smaller volume of sand there imply a smaller mean height and a greater vulnerability to the higher critical height value. The observed damage to the barrier island suggests that indeed the critical height exceeded the actual dune-beach system mean height. Overall, the comparison between the model results and the observed erosion indicates that where the reservoir of sand in the dune-beach system was insufficient, the dunes were removed and breaching occurred.

Future Developments: The coupled modeling approach depicts the complexity of interacting ocean and sedimentation processes, and shows promise for further study of beach erosion and breaching during such notable storms as Hurricanes Ivan and Katrina. Ongoing development at NRL of accurate, relocatable, coastal models for the littoral environment and sedimentation processes to include additional processes such as wave-driven flow and inundation will better support a wide range of Navy applications.

Acknowledgments: Aerial photographs of the Outer Banks were acquired from the North Carolina Geodetic Survey.

[Sponsored by ONR]

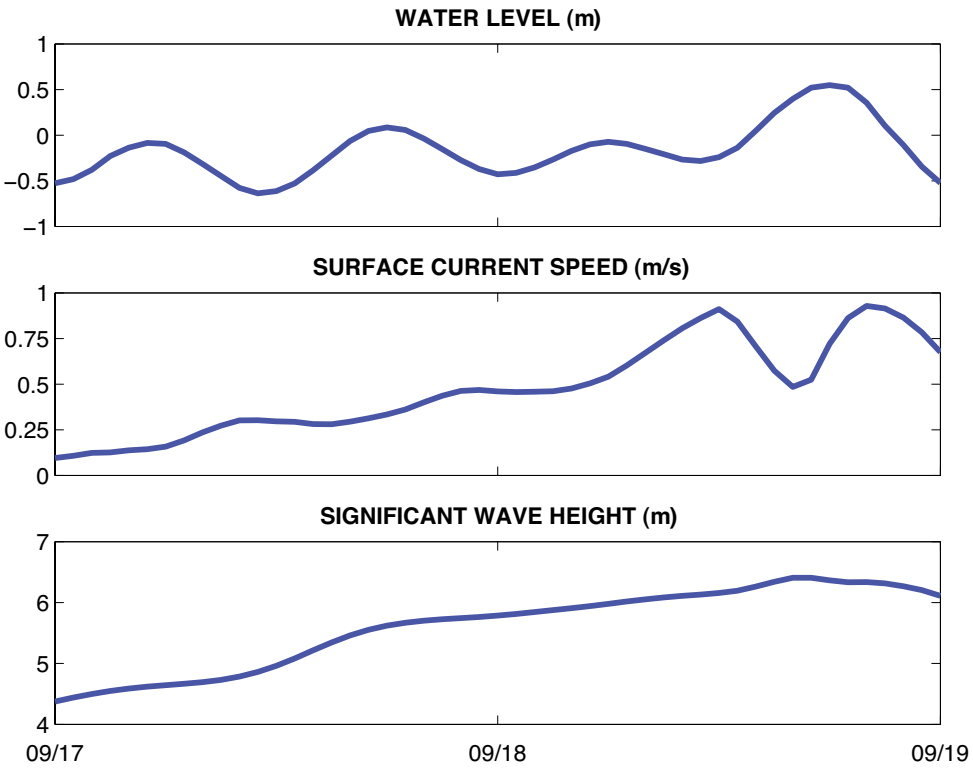

FIGURE 11
Oceanographic conditions at Ocracoke Island before and during landfall of Hurricane Isabel: the offshore water level showing the combined effect of tides and storm surge (top), the surface current speed (middle), and the significant wave height (bottom). The bottom axis shows the 0000 UTC times for 17-19 September 2003. The storm made landfall approximately 50 km west of this location at 1100 UTC 18 September.

Table 2 — Estimates from the aerial photography of the dune-beach width L, predicted values of the erosion potential E, the water level n, and the critical height H_c, at three locations along the North Carolina Outer Banks during the landfall of Hurricane Isabel in September 2003.

Location	L	E	n	H_c
Ocracoke Island	250	38	0.55	0.70
Cape Hatteras National Seashore	100	65	0.58	1.20
Frisco	200	7	0.54	0.58

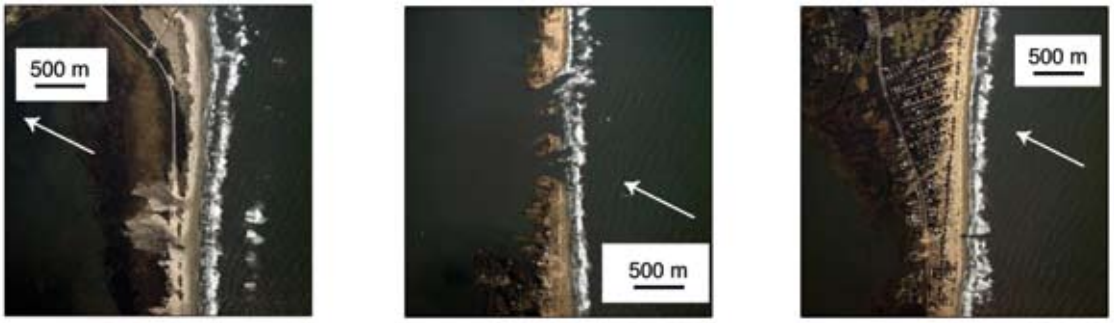

(a) Ocracoke Island (b) Cape Hatteras National Seashore (c) Frisco

FIGURE 12
Aerial photographs taken after Hurricane Isabel on the Outer Banks. The photographs are oriented with Pamlico Sound to the left.

References

[1] N. Booij, R.C. Ris, and L.H. Holthuijsen, "A Third-Generation Wave Model for Coastal Region: 1. Model Description and Validation," *J. Geophys. Res.* **104**, 7649-7666 (1999).

[2] C.N. Barron, A.B. Kara, P.J. Martin, R.C. Rhodes, and L.F. Smedstad, "Formulation, Implementation, and Examination of Vertical Coordinate Choices in the Global Navy Coastal Ocean Model (NCOM)," *Ocean Model.* **11,** 347-375 (2006).

[3] T.R. Keen and S.M. Glenn, "A Coupled Hydrodynamic-Bottom Boundary Layer Model of Ekman Flow on Stratified Continental Shelves," *J. Phys. Oceanogr.* **24**, 1732-1749 (1994). ★

Frequency Agile Target Array Controller

R.L. Lloyd
Tactical Electronic Warfare Division

Background: NRL has developed and operates a large number of unique test facilities to conduct its research. One such facility, the Central Target Simulator (CTS), was designed to conduct real-time hardware-in-the-loop (HIL) simulations over the 8-18 GHz frequency range to evaluate and improve U.S. Navy electronic warfare (EW) systems, technologies, and techniques for countering the antiship missile (ASM) threat. The CTS uses actual radio frequency (RF) system hardware (e.g., missile seekers, EW equipment) and mathematically derived computer models to perform a realistic electromagnetic and physically dynamic simulation of the various elements of naval tactical engagements.

Many of the more advanced missiles that now threaten U.S. Navy ships use radar seekers with frequency agile capabilities to acquire and track their targets. In addition to rapidly reducing (decorrelating) the effects of sea clutter, frequency agile radars are also better able to resist the effects of noise and interference. For instance, noise jamming (the intentional emission of RF energy at same transmit frequency) is a common method for interfering with radar operation. However, if the missile radar is frequency agile, effective jamming becomes more difficult to achieve because of the need to either spread RF energy over the full agility bandwidth or make an intelligent prediction of the next incoming transmitted frequency (which can be very difficult in a tactical scenario). Accordingly, NRL is actively pursuing the development of effective countermeasure technologies for such threat systems, and

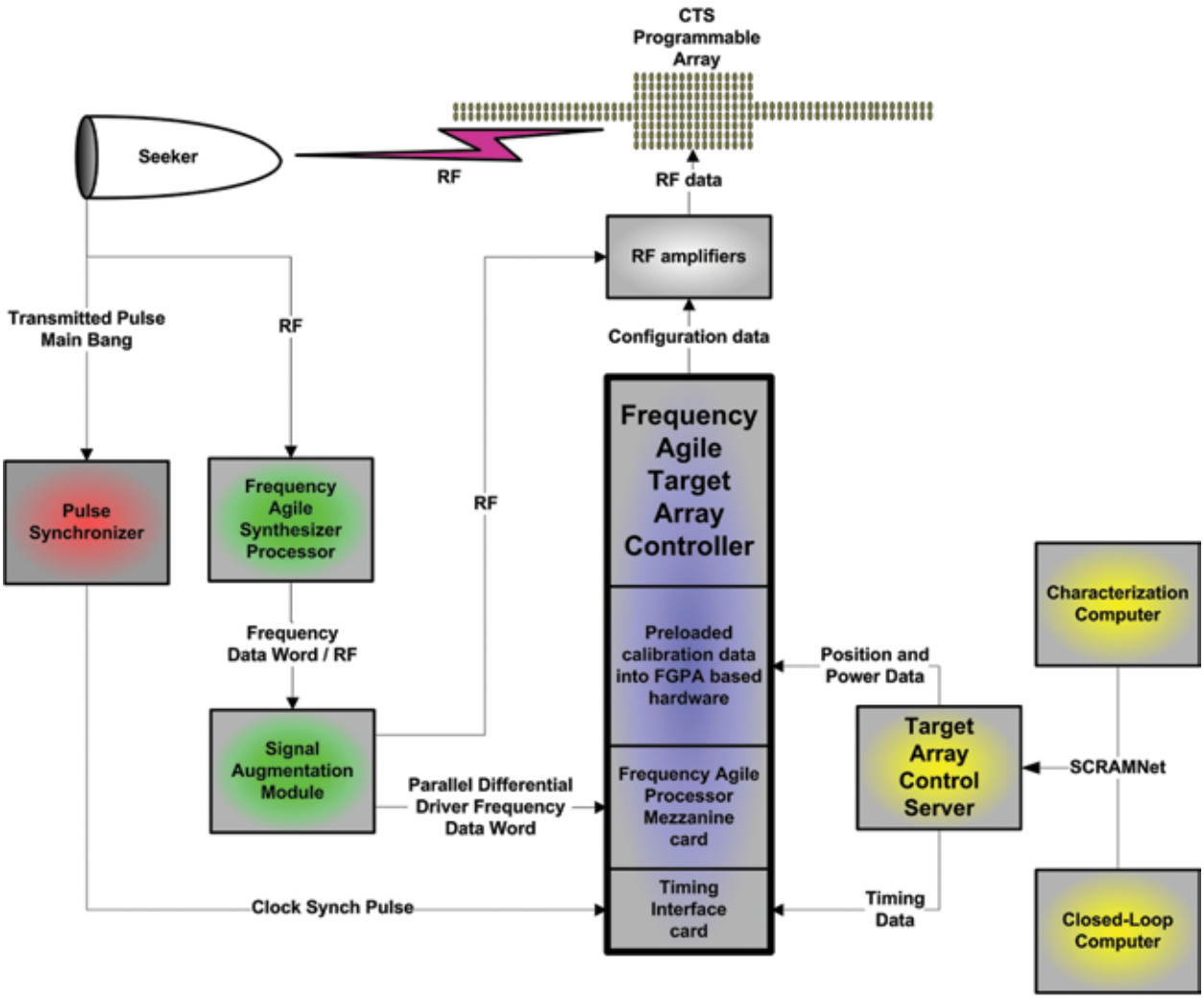

FIGURE 13
Data flow block diagram for a frequency agile simulation.

the CTS facility was recently upgraded to generate RF target returns that accurately follow the pulse-to-pulse frequency agile transmissions for such seekers.

Frequency Agile Upgrade: This CTS upgrade has three major components. The first is the Frequency Agile Signal Processor (FASP), which is an instantaneous frequency measurement (IFM) system. On a pulse-by-pulse basis, the FASP rapidly measures the seeker's transmit frequency and tunes a fast synthesizer to this value so that the simulated returns are correctly radiated. The second component of the upgrade is a new calibration system. The calibration system measures the amplitude and phase of the RF paths and the associated components (attenuators, phase shifters, and solid state and tube amplifiers) over a 1.0 GHz bandwidth and stores the resulting data in the form of calibration tables. The third component is the Frequency Agile Target-Array Controller (FATAC), which has two main functions. First, it generates the timing signals for simulating up to 16 targets on each of the two programmable position array feeds and a single target on each of the two fixed position array feeds. Secondly, it generates signals to control amplifier selection, attenuator, and phase shifter values and switch settings to route the RF to the desired antenna on the CTS array. In generating these control signals, FATAC uses the calibration data to compensate for component variations that are a function of frequency. The FATAC has an interface to the FASP by which it obtains the correct frequency information.

Frequency Agile Target-Array Controller: FATAC is the focal point of the digital and timing data required to set up and control the CTS programmable array (PA) in real time (Fig. 13). Achieving this task requires that FATAC hardware process the calibration data to develop the necessary PA steering com-

mands, attenuation settings, and return delay values, along with the timing signals needed to generate the simulated radar target echoes. However, this is a complicated task. The commands and settings to the PA depend on the simulated target's current angle, range, amplitude, and on the transmitted frequency of the pulse during its associated pulse repetition interval (PRI). Since the frequency is not known until the instance of pulse transmission, all possible frequency/table variations must be accessible and able to be processed within a 2 μs timeframe based on the minimum target simulated range. This is accomplished only by preloading all of the frequency associated calibration tables into FATAC processor's integrated memory. This memory, along with the associated algorithms and combinational logic, is resident on commercial off-the-shelf field programmable gate array (FPGA)-based circuit boards. The timing and synchronization signals are also generated by an FPGA-based circuit board that was custom designed and built by NRL. FPGA technology allows rapid redesign, customization, and scalability.

Summary: The Frequency Agile Target-Array Controller is a significant upgrade to NRL's laboratory simulation capability. It directly enables the development and evaluation of effective electronic countermeasure technologies for use against frequency agile missile threats to the U.S. Navy and provides a significant capability for continuing future research.

[Sponsored by ONR]

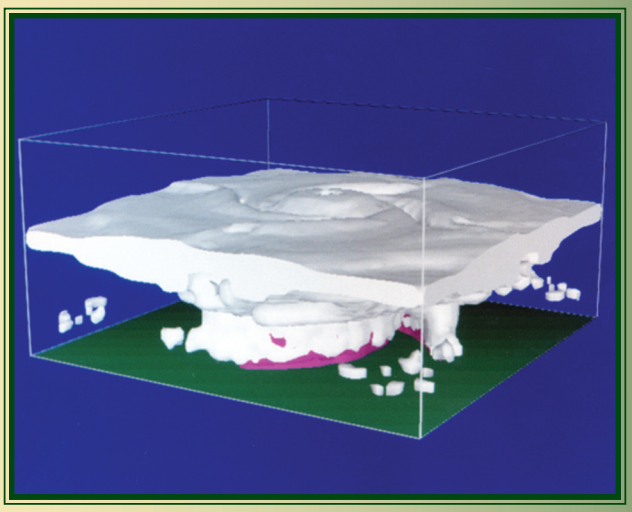

Mesoscale Prediction Systems

Achievement: Two mesoscale prediction systems have been developed and transitioned to operations by NRL: the Navy Operational Regional Atmospheric Prediction System (NORAPS) and the Coupled Ocean/Atmosphere Mesoscale Prediction System (COAMPS). NORAPS, implemented in 1982, became the first globally relocatable limited-area model of its kind, and in 1985, it became the first regional model in the world to use data assimilation. NORAPS supported naval operations in Operation Desert Shield, Operation Desert Storm, Operation Tandem Thrust, Bosnia, Somalia, and Haiti.

COAMPS replaced NORAPS as the Navy operational mesoscale model in 1998. COAMPS allows for more accurate forecasts over areas that exhibit steep topographic features and strong convection, predicts tropical cyclone track and structure, predicts the distribution of aerosols, and explicitly predicts water and ice clouds, as well as rain and snow. It has been used to supply forensic re-analyses of the atmospheric conditions (wind, temperature, moisture, and pressure) during Operation Desert Storm in support of the Presidential Advisory Committee's investigation into Gulf War Illness. For example, it produced estimates of where chemicals, accidentally released from the demolition of a large ammunition storage site near Khamisiyah, Iraq, may have been transported. Independent expert panels praised NRL's efforts for providing the most accurate assessment of the mesoscale meteorology during that time.

COAMPS is supporting operations in Afghanistan and Iraq by providing high-resolution wind simulation data to help evaluate the effects of wind variability on munitions targeting and the probable atmospheric effects upon aircraft detection and ranging systems. Measurements from instruments aboard earth-observing satellites, combined with dust modeling research, were used to provide real-time assessments of atmospheric dust conditions and dust storm prediction. In fact, a database of dust source regions in Southwest and East Asian deserts was developed based on field studies, satellite remote sensing, and topography. It allows high-resolution dust storm forecasts for Iraq, Iran, and Afghanistan. COAMPS was also used to produce local forecasts aboard an aircraft carrier, a world-first accomplishment.

Impact: NRL's NORAPS and COAMPS are mesoscale data assimilation systems used for generating high-resolution numerical analyses and short-term (0 to 48 hour) predictions of the atmosphere for limited areas of the Earth. Weather maps produced from these systems are distributed to operational DoD commands around the world to support mission planning, ship and aircraft operations, and hazardous weather avoidance. COAMPS has also been requested and is routinely used by other organizations. For example, DoE's Lawrence Livermore National Laboratory uses the model to assist in providing transport and dispersion forecasts of hazardous material releases. The Weather Channel also uses COAMPS data.

NRL's Forward Technology Solar Cell Experiment Flies as Part of MISSE-5 Aboard Space Shuttle *Discovery* Mission

R.J. Walters[1] and J.C. Garner[2]
[1]*Electronics Science and Technology Division*
[2]*Spacecraft Engineering Department*

Introduction: The Naval Research Laboratory led the scientific team that designed, built, and launched the 5th Materials on the International Space Station Experiment (MISSE-5). The team consisted of NRL, NASA Glenn Research Center, Ohio Aerospace Institute, NASA Langley Research Center, U.S. Naval Academy, and the Air Force Space Test Program. MISSE-5 is a completely self-contained experiment system with its own power generation, storage, and communications systems. The primary MISSE-5 payload is the Forward Technology Solar Cell Experiment (FTSCE), which is currently functioning on-orbit. MISSE-5 was launched aboard the Shuttle return to flight mission (STS-114) on July 26, 2005. Astronaut Soichi Noguchi deployed MISSE-5 on the exterior of the International Space Station (ISS) during the spacewalk on August 3, 2005, just before Astronaut Steve Robinson performed the tile repair on the Shuttle *Discovery*. Figure 1 is a photograph of MISSE-5 deployed on the ISS. The experiment will remain in orbit for about one year, after which it will be returned to Earth for postflight testing and analysis.

Forward Technology Solar Cell Experiment: FTSCE was initially conceived in response to various on-orbit and ground test anomalies associated with space power systems. The Department of Defense (DoD) required a method of rapidly obtaining on-orbit validation data for new space solar cell technologies, and NRL was tasked to devise an experiment to meet this requirement. Rapid access to space was provided by the NASA Langley Research Center MISSE Program, which provides access to space for new materials and devices being considered for use in space (http://misse1.larc.nasa.gov/). Experiments are placed into a Passive Experiment Container (PEC) which is a metal box approximately 2×2 ft^2 $\times$ 4 in. thick. The experiments are mounted on custom-designed trays that mount within the PEC. When closed, the PEC provides the container for the experiments for launch on the Shuttle and transfer to the ISS. For deployment, the PEC is clamped to a handrail on the exterior of the ISS by an astronaut who then opens the PEC to expose the experiments. After a period of time, an astronaut closes the PEC, and it is returned to Earth for postflight analysis of the experiments.

While on-orbit, FTSCE is measuring a 39-point current vs voltage (IV) curve on each of 36 experimental solar cells, and the data are continuously telemetered to Earth. The experiment also measures solar cell temperature and orientation of the solar cells to the Sun. A range of solar cell technologies are included in the experiment, including state-of-the-art triple junction InGaP/GaAs/Ge solar cells from several vendors, thin film amorphous Si and CuIn(Ga)Se_2 cells, and next-generation technologies like single-junction GaAs cells grown on Si wafers and metamorphic InGaP/InGaAs/Ge triple-junction cells. Figure 2 shows an example of data from a triple junction solar cell measured on-orbit. Also shown are data from the same cell measured in the NRL solar cell laboratory that have been corrected to the measurement angle and temperature. The data change with time as the ISS solar angle changes. The on-orbit and laboratory data agree very well, and the data show no signs of solar cell degradation.

FIGURE 1
MISSE-5 passive experiment container attached to the exterior of the International Space Station (ISS). Visible within the container is the Forward Technology Solar Cell Experiment. This photograph was taken by the Shuttle *Discovery* crew after undocking from the ISS.

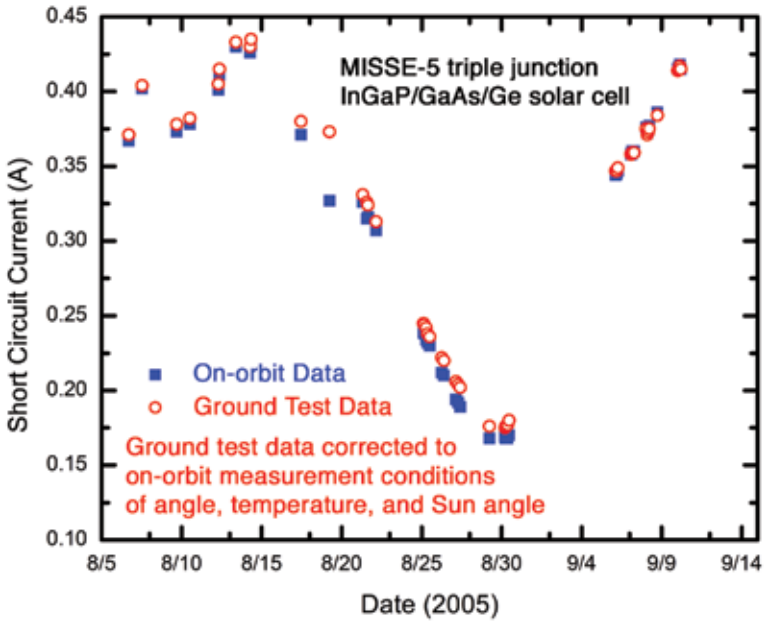

FIGURE 2
Solar cell current measured in a triple junction solar cell onboard the Forward Technology Solar Cell Experiment. The on-orbit data change with time as the ISS solar angle changes. Also plotted are data from this solar cell that were measured in the NRL solar cell laboratory prior to launch. The ground-measured data have been corrected to match the on-orbit measurement conditions, and excellent agreement can be seen.

Thin-Film Materials Experiment: In addition to FTSCE, MISSE-5 also contains a Thin-Film Materials experiment. A team led by NASA Langley Research Center has transformed the outer layer of a MISSE-5 thermal blanket into a 3 1/2-oz experiment to evaluate the in-space survivability of 200 advanced materials that are being developed to enable future U.S. space missions. The materials experiment can be seen in the photograph of MISSE-5 taken by Soichi Noguchi's helmet camera during deployment (Fig. 3). Some of the materials include DC 93-500 silicone; POSS-coated polyethylene; multiwall carbon nanotubes in polyimide; white paint on black Kapton; double aluminized Kapton, which is ISS Solar Array Blanket box material; germanium on black Kapton; silicone paint on Kapton; AZ93 White Coating; cellulose acetate; perfluoroalkoxy (Teflon PFA), high-temperature polyimide resin; and amorphous fluoropolymer (Teflon AF). The survivability of these materials will be established by comparing pre- and postflight characterization test data.

Communications System: The communications system (referred to as PCSat2), was built by the U.S. Naval Academy and transmits and receives in the Amateur Radio band, providing a node on the Amateur Radio Satellite Service (http://www.ew.usna.edu/~bruninga/pec/pc2ops.html). The PCSat2 subsystem operates in the ITU Amateur Satellite Service in cooperation with ARISS (Amateur Radio on the International Space Station) and provides a PSK-31 multiuser transponder, an FM voice repeater for possible use with ISS crew communications, and an AX.25 packet system for use as a packet digipeater and a terminal node controller. PCSat2 uses the same dual redundant AX.25 command and control system as used on PCsat (NO-44) offering eight on/off commands,

FIGURE 3
Thin-Film Materials Experiment on MISSE-5. The photograph was taken by Astronaut Soichi Noguchi's helmet camera while he was deploying MISSE-5.

five telemetry channels, and a serial port for the FTSCE telemetry. It also supports the Digital Comms Relay support of the PCsat2/APRS mission. The packet uplink is on 145.825 MHz, and the default downlinks are in the 435 MHz band to avoid any possible interference with existing ARISS missions. PCSat2 has quad redundant transmit inhibits for extravehicular activity safety issues, thus it is easy to deactivate to avoid any issues with other UHF ARISS experiments that may be activated in the future.

Acknowledgments: The authors acknowledge the active participation of the following individuals in MISSE-5: S.N. LaCava, J.A. Vasquez, W.R. Braun, R.E. Ruth, and J.H. Warner (Naval Research Laboratory); J.R. Lorentzen and S.R. Messenger (SFA, Inc.); CDR R. Bruninga (Ret.) (U.S. Naval Academy); P.P. Jenkins (Ohio Aerospace Institute); J.M. Flatico (QSS Group, Inc.); and D.M. Wilt, M.F. Piszczor, L.C. Greer, and M.J. Krasowski (NASA Glenn Research Center).

[Sponsored by ONR]

Laboratory Demonstration of a Prototype Geosynchronous Servicing Spacecraft

N.G. Creamer, S.P. Arnold, S.T. Butcher, C.G. Henshaw, B.E. Kelm, P. Oppenheimer, F. Pipitone, and F.A. Tasker
Spacecraft Engineering Department

Introduction: The benefits of autonomous spacecraft rendezvous and capture for future military, civil, and commercial space missions are far-reaching and intriguing. These include satellite reposition, service life extension, debris removal, repair, replenishment, technology refresh, on-orbit assembly, and salvage. Because of the large number of high-value assets in the geosynchronous (GEO) belt, autonomous servicing of these spacecraft could provide the greatest utility. Furthermore, requiring modification of the target spacecraft bus to accompany aided docking sensors and mechanisms is impossible for existing GEO assets and impractical for most future assets that rely on existing standardized bus designs. Hence, development of a general-purpose space "tug" to service an unaided geosynchronous target is highly desirable. This tug will require the utilization and integration of many challenging technologies, such as long-range sensors for acquisition and tracking, machine vision for target imaging, algorithms for feature recognition and pose estimation, manipulators for end effector positioning, and intelligent robot arm control algorithms.

To evaluate and test these critical issues, the Defense Advanced Research Projects Agency (DARPA) is sponsoring the Spacecraft for the Universal Modification of Orbits (SUMO) project, a technology risk-reduction program executed by the Naval Center for Space Technology at the Naval Research Laboratory. The purpose of the program is to demonstrate the integration of machine vision, robotics, mechanisms, and autonomous control algorithms to accomplish approach and grapple of common hardpoint interfaces traceable to existing and future spacecraft hardware. To date, the SUMO program has consisted of three phases: an exploratory study phase in 2002, a concept design phase in 2003,[1] and a laboratory demonstration phase in 2004-2005. As described here, the laboratory demonstration phase provided realistic test and evaluation of the critical technologies associated with unaided target approach and capture.

SUMO Testbed Description: NRL's Proximity Operations Testbed was the primary test facility for the SUMO laboratory demonstrations. This facility represents a dual-platform spacecraft motion simulator that provides a realistic test environment for verification of sensor and control technologies. The facility consists of two independent 6 degree-of-freedom platforms, a local-area network architecture for real-time ground-to-platform and platform-to-ground communications, and software to emulate spacecraft mass properties, thruster and reaction wheel actuators, and on-orbit environmental disturbances. Figure 4 shows the testbed with the SUMO pursuer hardware and the target mock-up. The SUMO hardware consists of a 7 degree-of-freedom robot arm with an end effector and a force/torque sensor, visual stereo cameras on the platform and end effector for 3-D target mapping, active target illumination using a pulsed xenon flashlamp, and an electronics bank for arm control and hardware synchronization. The target platform emulates a realistic launch vehicle interface to a user-selected Boeing 702 GEO communications bus or a Lockheed Martin A2100 GEO communications bus.

Test Scenario and Results: A typical real-time test scenario consists of an approach of the SUMO platform toward the target along a desired flightpath, stationkeeping within arm's reach of the target, and capture of a target hardpoint using the arm and its end effector. During approach and stationkeeping, the relative pose (position and attitude) of the target is determined using range images and Tripod Operator[2] software. Figure 5 shows a set of target intensity images and the corresponding 3-D point cloud obtained during a typical approach. Capture of the target structural hardpoint is achieved by maneuvering the robot arm to within the end effector camera field-of-view, using real-time path planning logic to avoid potential obstacle collisions. Once inside the camera

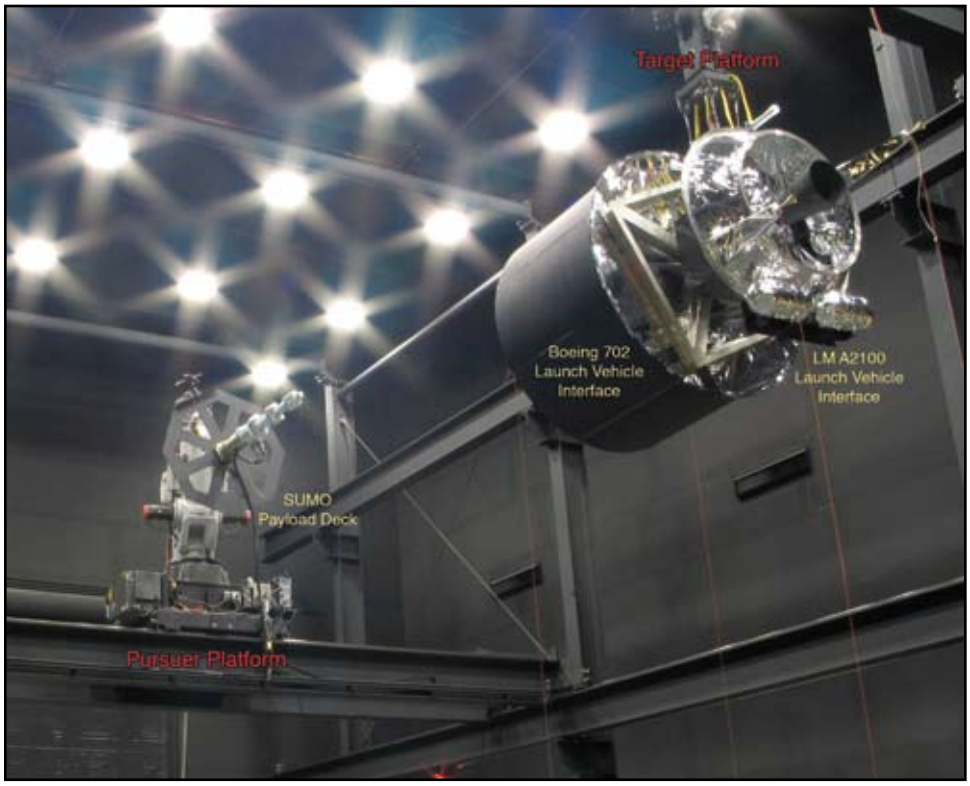

FIGURE 4
NRL's Proximity Operations Testbed with SUMO payload and common communication bus targets.

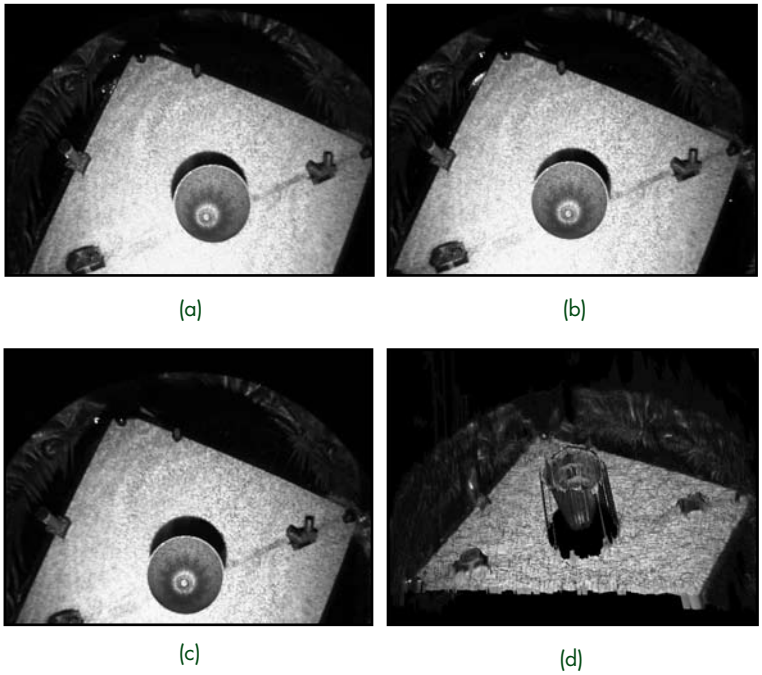

FIGURE 5
Typical target images. (a) Left camera intensity image; (b) Right camera intensity image: (c) Top camera intensity image; (d) 3-D point cloud image.

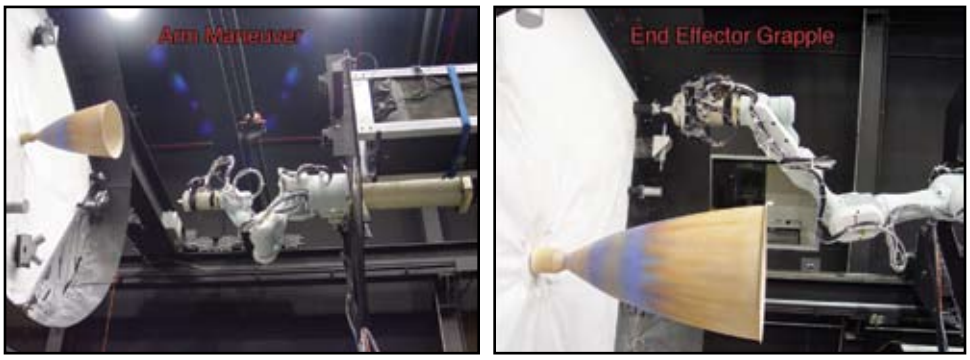

FIGURE 6
Arm maneuver and grapple of a target hardpoint.

field-of-view, the target hardpoint is recognized and triangulated to determine its relative position. Hardpoint capture is then achieved by commanding the end effector tool to reach out and grapple the identified feature, using active compliance control from the force/torque sensor to provide soft spring-like contact. Figure 6 shows a typical arm maneuver and end effector grapple. For this particular target, the hardpoint feature is represented by the protruding launch vehicle bolt hole interface.

Summary: The critical technologies of machine vision, robotics, mechanisms, and autonomy associated with the capture of GEO spacecraft are being evaluated, integrated, and tested at NRL. Successful fusion of these technologies promises to enable future autonomous servicing missions, offering a potentially revolutionary advancement in spacecraft operations.

[Sponsored by DARPA]

References

[1] A.B. Bosse, et al., "SUMO: Spacecraft for the Universal Modification of Orbits," *Proc. SPIE* **5419**, 36-46 (2004).

[2] F. Pipitone, "Technique for Estimating the Pose of Surface Shapes Using Tripod Operators," U.S. Patent # 6,393,143, May 21, 2002. ★

Secure Voice Technology

Achievement: In the 1990s, the Department of Defense introduced a new narrowband voice-processing algorithm, called the Mixed-Excitation Linear Predictor (MELP), for supporting tactical communications. NRL scientists in the 1970s had specified and developed the predecessor LPC voice-processing algorithm for use with the DoD's Advanced Narrowband Digital Voice Terminal (ANDVT), DoD's most widely used operational tactical terminal. Because of this work, the DoD's Voice Processor Consortium asked the Laboratory to investigate means of converting MELP voice data into the ANDVT voice data (and vice versa) so that these two DoD tactical secure phones can interoperate directly. Without the use of conversion software, 40,000 ANDVTs that are supporting tactical voice communication for users in DoD and special government agencies would have been made redundant and there would have been a potentially long transition period.

In response to the DoD request, NRL scientists took only six weeks to develop a voice communications processing algorithm for the translation process. The NRL solution resolved the conversion problem, and the resulting algorithm has been widely disseminated both within the DoD and within NATO forces.

NRL has also developed an enhanced version of the LPC algorithm, which was incorporated into the 2400 b/s version of the third generation Secure Terminal Unit (STU-III) telephone. NRL's Line Spectrum Pair (LSP) technology was incorporated into the 4800 b/s version of the STU-III. The Navy has deployed over 60,000 STU-IIIs incorporating the 2400 b/s algorithm, with 35,000 of these also having the 4800 b/s algorithm.

Impact: A range of NRL's voice communications processing algorithms and technologies have been widely disseminated and used within the DoD and the armed forces of allied countries. Almost all low-data-rate DoD or COTS vocoders now use the NRL-developed LSP technology. The NRL narrowband voice translation system provides direct interoperability between old and new speech parameters, allowing the new and the legacy ANDVT phones to work together. The result of this development was that 40,000 legacy phones did not have to be retired prematurely, and there was no long transition period between the new and old systems. The continued use of these legacy units resulted in a one-time cost savings of nearly $460 million for the DoD.

PROGRAMS FOR NRL EMPLOYEES

The Human Resources Office continues to support and provide traditional and alternative methods of training for employees. NRL employees are encouraged to develop their skills by attending training to enhance their job performance in order to continue to meet the future needs of NRL as well as their own goals for growth.

One common study procedure is for employees to work full time at the Laboratory while taking job-related scientific courses at universities and schools in the Washington area. The training ranges from a single course to full graduate and postgraduate programs. Tuition for training is paid by NRL. The formal programs offered by NRL are described here.

GRADUATE PROGRAMS

• The **Advanced Graduate Research Program** (formerly the Sabbatical Study Program, which began in 1964) enables selected professional employees to devote full time to research or pursue work in their own or a related field for one year at an institution or research facility of their choice without the loss of regular salary, leave, or fringe benefits. NRL pays all travel and moving expenses for the employee. Criteria for eligibility include professional stature consistent with the applicant's opportunities and experience, a satisfactory program of study, and acceptance by the facility selected by the applicant. The program is open to employees in Career Track NP Levels III and IV; NO Levels III, IV, and V; and NR Level IV who have completed 6 years of Federal Service, 4 of which have been at NRL.

• The **Edison Memorial Graduate Training Program** enables employees to pursue advanced studies in their fields at local universities. Participants in this program work 24 hours each workweek and pursue their studies during the other 16 hours. The criteria for eligibility include a minimum of one year of service at NRL, a bachelor's or master's degree in an appropriate field, and professional standing in keeping with the candidate's opportunities and experience.

• To be eligible for the **Select Graduate Training Program**, employees must have a college degree in an appropriate field and must have demonstrated ability and aptitude for advanced training. Students accepted into this program devote three academic semesters to graduate study. While attending school, they receive one-half of their salary, and NRL pays for tuition and laboratory expenses.

• The **Naval Postgraduate School (NPS)**, located in Monterey, California, provides graduate programs to enhance the technical preparation of Naval officers and civilian employees who serve the Navy in the fields of science, engineering, operations analysis, and management. It awards a master of arts degree in national security affairs and a master of science degree in many technical disciplines.

NRL employees desiring to pursue graduate studies at NPS may apply for a maximum of six quarters away from NRL, with thesis work accomplished at NRL. Specific programs are described in the NPS catalog. Participants will continue to receive full pay and benefits during the period of study.

• In addition to NRL and university offerings, application may be made to a number of noteworthy programs and fellowships. Examples of such opportunities are the **Capitol Hill Workshops**, the **Legislative Fellowship (LEGIS) program**, the **Federal Executive Institute (FEI)**, the **Fellowship in Congressional Operations**, and the **Executive Leadership Program for Mid-Level Employees**. These and other programs are announced from time to time, as schedules are published.

• Research conducted at NRL may be used as **thesis material for an advanced degree**. This original research is supervised by a qualified employee of NRL who is approved by the graduate school. The candidate should have completed the required course work and should have satisfied the language, residence, and other requirements of the graduate school from which the degree is sought. NRL provides space, research facilities, and supervision but leaves decisions on academic policy to the cooperating schools.

CONTINUING EDUCATION

• **Undergraduate and graduate courses** offered at local colleges and universities are subsidized by NRL

for employees interested in improving their skills and keeping abreast of current developments in their fields. These courses are also available at a number of government installations in the Washington, DC, area.

• NRL offers **short courses** to all employees in a number of fields of interest including technical subjects, computer operation, and supervisory and management techniques. Laboratory employees may attend these courses at nongovernment facilities as well. Interagency courses in management, personnel, finance, supervisory development, and clerical skills are also available.

For further information on any of the above programs, contact the Employee Relations and Development Branch (Code 1850) at (202) 767-2365.

• The **Scientist-to-Sea Program (STSP)** provides increased opportunities for Navy R&D laboratory/center personnel to go to sea to gain first-hand insight into operational factors affecting system design, performance, and operations on a variety of ships. NRL is a participant of this Office of Naval Research (ONR) program. For further information contact Mike McCord (Code 7120) at (202) 767-2945.

PROFESSIONAL DEVELOPMENT

NRL has several programs, professional society chapters, and informal clubs that enhance the professional growth of employees. Some of these are listed below.

• The **Counseling Referral Service (C/RS)** helps employees to achieve optimal job performance through counseling and to resolve problems such as family and work-related stress and relationship difficulties, behavioral, emotional, and substance use problems that may adversely impact job performance.

C/RS provides confidential assessments and short-term counseling, training workshops, and referrals to additional resources in the community. (Contact Lois Burleigh, MSW, LGSW at (202) 767-6857.)

• The NRL **Women in Science and Engineering (WISE) Network** was formed in 1997 through the merger of the NRL chapter of WISE and the Women in Science and Technology Network. Luncheon meetings and seminars are held to discuss scientific research areas, career opportunities, and career-building strategies. The group also sponsors projects to promote the professional success of the NRL S&T community and improve the NRL working environment. Membership is open to all S&T professionals. (Contact Dr. Kathy Wahl at (202) 767-5419 or Ms. Jennifer Stepnowski at (202) 767-8533).

• **Sigma Xi**, the scientific research society, encourages and acknowledges original investigation in pure and applied science. As an honor society for research scientists, individuals who have demonstrated the ability to perform original research are elected to membership in local chapters. The NRL Edison Chapter, comprising approximately 400 members, recognizes original research by presenting awards annually in pure and applied science to outstanding NRL staff members. The chapter also sponsors lectures at NRL on a wide range of scientific topics for the entire NRL community. These lectures are delivered by scientists from all over the nation and the world. The highlight of the Sigma Xi lecture series is the Edison Memorial Lecture, traditionally featuring a distinguished scientist. (Contact Dr. Paul Sheehan at (202) 404-3386.)

• The **NRL Mentor Program** was established to provide an innovative approach to professional and career training and an environment for personal and professional growth. It is open to permanent NRL employees in all job series and at all sites. Mentorees are matched with successful, experienced colleagues having more technical and/or managerial experience who can provide them with the knowledge and skills needed to maximize their contribution to the success of their immediate organization, to NRL, to the Navy, and to their chosen career fields. The ultimate goal of the program is to increase job productivity, creativity, and satisfaction through better communication, understanding, and training. NRL Instruction 12400.1A provides policy and procedures for the program. (Contact Ms. Dawn Brown at (202) 767-2957.)

• Employees interested in developing effective self-expression, listening, thinking, and leadership potential are invited to join either of two NRL chapters of **Toastmasters International**. Members of these clubs, who possess diverse career backgrounds and talents, meet two to four times a month in an effort to learn to communicate not by rules but by practice in an atmosphere of understanding and helpful fellowship. NRL's Commanding Officer and Director of Research endorse Toastmasters as an official training medium at NRL. (Contact Kathleen Parrish at (202) 404-4963 for more information.)

EQUAL EMPLOYMENT OPPORTUNITY (EEO) PROGRAMS

Equal employment opportunity is a fundamental NRL policy for all employees regardless of race, color, national origin, sex, religion, age, or disability. The NRL EEO Office is a service organization whose major functions include counseling employees in an effort to resolve employee/management conflicts, process-

ing formal discrimination complaints, providing EEO training, and managing NRL's affirmative employment recruitment program. The NRL EEO Office is also responsible for sponsoring special-emphasis programs to promote awareness and increase sensitivity and appreciation of the issues or the history relating to females, individuals with disabilities, and minorities. (Contact the NRL Deputy EEO Officer at (202) 767-5264 for additional information on any of their programs or services.)

OTHER ACTIVITIES

• The **Community Outreach Program** traditionally has used its extensive resources to foster programs that provide benefits to students and other community citizens. Volunteer employees assist with and judge science fairs, give lectures, tutor, mentor, coach, and serve as classroom resource teachers. The program also sponsors African American History Month art and essay contests for local schools, student tours of NRL, an annual holiday party for neighborhood children, and other programs that support the local community. Also through this program, NRL has active partnerships with four District of Columbia public schools. (Contact Mr. Dom Panciarelli at (202) 767-2541.)

• Other programs that enhance the development of NRL employees include four computer user groups (**IBM PC**, **Mac**, **NeXT**, and **Sun**) and the **Amateur Radio Club**. The **NRL Recreation Club** encourages wide interest in sports for employees with its many facilities and programs, such as a heated indoor pool, hot tub, table tennis, basketball courts, recreation room, free weight room, new selectorized weight equipment, and volleyball courts. Sportswear and NRL and seasonal paraphernalia are available at the Recreation Club. The **Showboaters** theater group has been "in the dark" for a number of years. Visit our website at www.nrl.navy.mil/showboaters/Past_Productions.html.)

PROGRAMS FOR NON-NRL EMPLOYEES

Several programs have been established for non-NRL professionals. These programs encourage and support the participation of visiting scientists and engineers in research of interest to the Laboratory. Some of the programs may serve as stepping-stones to federal careers in science and technology. Their objective is to enhance the quality of the Laboratory's research activities through working associations and interchanges with highly capable scientists and engineers and to provide opportunities for outside scientists and engineers to work in the Navy laboratory environment. Along with enhancing the Laboratory's research, these programs acquaint participants with Navy capabilities and concerns and provide a path to full-time employment.

RECENT PH.D., FACULTY MEMBER, AND COLLEGE GRADUATE PROGRAMS

• The **National Research Council (NRC) Cooperative Research Associateship Program** selects associates who conduct research at NRL in their chosen fields in collaboration with NRL scientists and engineers. The tenure period is two years (renewable for a possible third year).

• The **NRL/ASEE Postdoctoral Fellowship Program**, administered by the American Society for Engineering Education (ASEE), aims to increase the involvement of highly trained scientists and engineers in disciplines necessary to meet the evolving needs of naval technology. Appointments are for one year (renewable for a second and possible third year).

• The **Naval Research Enterprise Intern Program (NREIP)** is a ten-week program involving 69 NROTC colleges/universities and their affiliates. The Office of Naval Research (ONR) is offering summer appointments at Navy laboratories to current sophomores, juniors, seniors, and graduate students from participating schools. Academia Research Management (ARM) is handling the administration of the application process through a website. Electronic applications are sent for evaluation to the point of contact at the Navy laboratory identified by the applicant. ONR will provide directly to the student a stipend of $5,500 to undergraduates and $6,500 to graduate students.

• The American Society for Engineering Education also administers the **Navy/ASEE Summer Faculty Research and Sabbatical Leave Program** for university faculty members to work for 10 weeks (or longer, for those eligible for sabbatical leave) with professional peers in participating Navy laboratories on research of mutual interest.

• The **NRL/United States Naval Academy (USNA) Cooperative Program for Scientific Inter-**

change allows faculty members of the U.S. Naval Academy to participate in NRL research. This collaboration benefits the Academy by providing the opportunity for USNA faculty members to work on research of a more practical or applied nature. In turn, NRL's research program is strengthened by the available scientific and engineering expertise of the USNA faculty.

• The **National Defense Science and Engineering Graduate Fellowship Program** helps U.S. citizens obtain advanced training in disciplines of science and engineering critical to the U.S. Navy. The three-year program awards fellowships to recent outstanding graduates to support their study and research leading to doctoral degrees in specified disciplines such as electrical engineering, computer sciences, material sciences, applied physics, and ocean engineering. Award recipients are encouraged to continue their study and research in a Navy laboratory during the summer.

For further information about the above six programs, contact Ms. Lesley Renfro at (202) 404-7450.

PROFESSIONAL APPOINTMENTS

• **Faculty Member Appointments** use the special skills and abilities of faculty members for short periods to fill positions of a scientific, engineering, professional, or analytical nature.

• **Consultants and experts** are employed because they are outstanding in their fields of specialization or because they possess ability of a rare nature and could not normally be employed as regular civil servants.

• **Intergovernmental Personnel Act Appointments** temporarily assign personnel from state or local governments or educational institutions to the Federal Government (or vice versa) to improve public services rendered by all levels of government.

COLLEGE STUDENT PROGRAMS

The student programs are tailored to undergraduate and graduate students to provide employment opportunities and work experience in naval research. These programs are designed to attract applicants for student and full professional employment in fields such as engineering, physics, mathematics, and computer sciences. The student employment programs are designed to help students and educational institutions gain a better understanding of NRL's research, its challenges, and its opportunities. Employment programs for college students include the following:

• The **Student Career Experience Program** (formerly known as the Cooperative Education Program) employs students in study-related occupations. The program is conducted in accordance with a planned schedule and a working agreement among NRL, the educational institution, and the student. Primary focus is on the pursuit of bachelors degrees in engineering, computer science, or the physical sciences.

• The **Student Temporary Employment Program (STEP)** enables students to earn a salary while continuing their studies and offers them valuable work experience.

• The **Summer Employment Program** employs students for the summer in paraprofessional and technician positions in engineering, physical sciences, computer sciences, and mathematics.

• The **Student Volunteer Program** helps students gain valuable experience by allowing them to voluntarily perform educationally related work at NRL.

For additional information on these undergraduate and graduate college student programs, contact Code 1810 at (202) 767-8313.

HIGH SCHOOL STUDENT PROGRAMS

• The **DoD Science & Engineering Apprentice Program (SEAP)** offers high school students, grades 9 to 12, the opportunity to serve for eight weeks as junior research associates. Under the direction of a mentor, students gain a better understanding of research, its challenges, and its opportunities through participation in scientific programs. Criteria for eligibility are based on science and mathematics courses completed and grades achieved; scientific motivation, curiosity, and capacity for sustained hard work; a desire for a technical career; teacher recommendations; and achievement test scores. The NRL Program is the lead program and the largest in DoD.

For additional information, contact Dawn Brown (Code 1850) at (202) 767-2957.

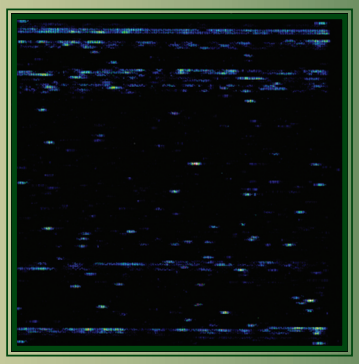

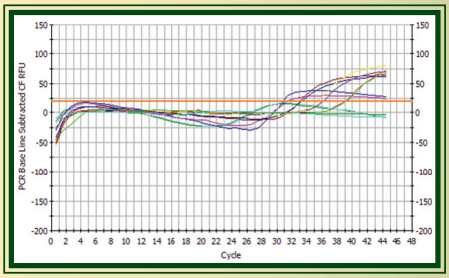

Project Silent Guardian

Achievement: Concerned about military and civilian health during upcoming special events in the National Capital Region (NCR), the Office of the Secretary of Defense (OSD) requested that the Air Force Surgeon General's (AF/SG) office implement biosurveillance technology developed by NRL scientists for the U.S. Air Force's Epidemic Outbreak Surveillance (EOS) project.

The EOS biosurveillance technology, Re-sequencing Pathogen Microarrays, is a system that can identify large numbers (20-100 depending on the chip) of pathogens simultaneously, including bio-threat agents and emerging diseases such as avian flu. The approach was previously demonstrated successfully for adenovirus and influenza detection in a limited patient population. The challenge OSD presented to the NRL was to take the complex technology from the laboratory to production scale and implement the approach as a demonstration project from 1 December 2004 to 31 March 2005.

NRL, along with critical help from the AF/SG office, the Joint Program Executive Office for Chemical and Biological Defense, and private industry, moved from routine laboratory research to Full Operational Capability in less than six weeks. The NRL EOS Team trained incoming Air Force personnel, developed solutions for problems that arose in analyzing large numbers of samples, and set up two complete production lines of equipment and reagents.

Laboratory practices consistent with those prescribed by the College of American Pathologists were established and the project was coordinated with the U.S. Food and Drug Administration through an informal Investigational Device Exemption submission.

Impact: NRL successfully responded to high-level concerns for military and civilian health during special events held in the Washington D.C. area during the 2005 Presidential Inauguration. The combined Silent Guardian team, composed of NRL scientists, Navy reservists, and U.S. Air Force staff, successfully made the first demonstration of a capability for rapidly (i.e., less than 24 hours) obtaining data for a broad range of pathogens in clinical specimens collected from the general population. In addition, the team demonstrated accurate detection of samples spiked with inactivated bio-threat agents in blind trials, identified numerous cases of influenza in patient samples collected from military treatment facilities within the NCR, and clearly demonstrated the utility of the Epidemic Outbreak Surveillance protocol for medical diagnostics as well as surveillance.

TECHNICAL OUTPUT

The Navy continues to be a pioneer in initiating new developments and a leader in applying these advancements to military requirements. The primary method of informing the scientific and engineering community of the advances made at NRL is through the Laboratory's technical output—reports, articles in scientific journals, contributions to books, papers presented to scientific societies and topical conferences, patents, and inventions.

The figures for calendar year 2005 presented below represent the output of NRL facilities in Washington, D.C.; Bay St. Louis, Mississippi; and Monterey, California.

In addition to the output listed, NRL scientists made more than 894 oral presentations during 2005.

Type of Contribution	Unclassified	Classified	Total
Articles in periodicals, chapters in books, and papers in published proceedings	1247	0	1247*
NRL Formal Reports	11	4	15
NRL Memorandum Reports	61	7	68
Books	3	0	3
Patents granted			91
Statutory Invention Registrations (SIRs)			0

*This is a provisional total based on information available to the Ruth H. Hooker Research Library on March 1, 2006. Additional publications carrying a 2005 publication date are anticipated.

KEY PERSONNEL

Area Code (202) unless otherwise listed
Personnel Locator - 767-3200
DSN-297 or 754

Code	Office		Phone Number
	EXECUTIVE DIRECTORATE		
1000	Commanding Officer	CAPT D.R. Gahagan, USN	767-3403
1000.1	Inspector General	CAPT W.B. Jackson, USN	767-3621
1001	Director of Research	Dr. J.A. Montgomery	767-3301
1001.1	Executive Assistant	Mr. D. DeYoung	767-2445
1002	Chief Staff Officer	CAPT W.B. Jackson, USN	767-3621
1004	Head, Technology Transfer	Dr. J.A. Montgomery (Acting)	767-3301
1006	Head, Office of Program Administration and Policy Development	Mrs. L. McDonald	767-3091
1008	Office of Counsel	Mr. J. McCutcheon	767-2244
1030	Public Affairs Officer	Mr. R. Thompson	767-2541
1100	Director, Institute for Nanoscience	Dr. R.J. Colton*	767-4194
1200	Head, Command Support Division	CAPT W.B. Jackson, USN	767-3621
1220	Head, Security	Ms. M.S. Overton	767-0793
1400	Head, Military Support Division	LCDR G. Morris, USN (Acting)	767-2273
1600	Commanding Officer, Scientific Development Squadron One	CDR P. Herring	301-342-3751
1800	Director, Human Resources Office	Ms. J. Deschak (Acting)	767-8314
1830	Deputy EEO Officer	Ms. D. Erwin	767-5264
3005	Deputy for Small Business	Ms. M. Thompson	767-6263
3540	Head, Safety Branch	Mr. K.J. Pawlovich	767-2232
	BUSINESS OPERATIONS DIRECTORATE		
3000	Comptroller/Associate Director of Research	Mr. D. Therning	767-2371
3200	Head, Contracting Division	Mr. J.C. Ely	767-5227
3300	Head, Financial Management Division	Mr. D. Therning (Acting)	767-3405
3400	Supply Officer	Ms. C. Hartman	767-3446
3500	Director, Research and Development Services Division	Mr. S. Harrison	767-3697
	SYSTEMS DIRECTORATE		
5000	Associate Director of Research	Dr. H. Gursky (Acting)	767-6343
5300	Superintendent, Radar Division	Dr. E.L. Mokole	404-2700
5500	Superintendent, Information Technology Division/ NRL Chief Information Officer*	Dr. J.D. McLean	767-2903
5600	Superintendent, Optical Sciences Division	Dr. T.G. Giallorenzi	767-3171
5700	Superintendent, Tactical Electronic Warfare Division	Dr. F. Klemm	767-6278
	MATERIALS SCIENCE AND COMPONENT TECHNOLOGY DIRECTORATE		
6000	Associate Director of Research	Dr. B.B. Rath	767-3566
6030	Head, Laboratory for Structure of Matter	Dr. J. Karle	767-2665
6100	Superintendent, Chemistry Division	Dr. J.S. Murday	767-3026
6300	Superintendent, Materials Science and Technology Division	Dr. D.U. Gubser	767-2926
6400	Director, Lab. for Computational Physics and Fluid Dynamics	Dr. J.P. Boris	767-3055
6700	Superintendent, Plasma Physics Division	Dr. S. Ossakow	767-2723
6800	Superintendent, Electronics Science and Technology Division	Dr. G.M. Borsuk	767-3525
6900	Director, Center for Bio/Molecular Science and Engineering	Dr. J.M. Schnur	404-6000
	OCEAN AND ATMOSPHERIC SCIENCE AND TECHNOLOGY DIRECTORATE		
7000	Associate Director of Research	Dr. E.O. Hartwig	404-8690
7100	Superintendent, Acoustics Division	Dr. E.R. Franchi	767-3482
7200	Superintendent, Remote Sensing Division	Dr. R.M. Bevilacqua (Acting)	767-3391
7300	Superintendent, Oceanography Division	Dr. R. Preller	228-688-4670
7400	Superintendent, Marine Geosciences Division	Dr. H.C. Eppert, Jr.	228-688-4650
7500	Superintendent, Marine Meteorology Division	Dr. S.W. Chang	831-656-4721
7600	Superintendent, Space Science Division	Dr. H. Gursky	767-6343
	NAVAL CENTER FOR SPACE TECHNOLOGY		
8000	Director	Mr. P.G. Wilhelm	767-6547
8100	Superintendent, Space Systems Development Department	Mr. R.E. Eisenhauer	767-0410
8200	Superintendent, Spacecraft Engineering Department	Mr. J.P. Schaub (Acting)	404-3727

*Additional Duty

CONTRIBUTIONS BY DIVISIONS, LABORATORIES, AND DEPARTMENTS

SUBJECT INDEX

AUTHOR INDEX

EMPLOYMENT NRL OPPORTUNITIES

NRL offers a wide variety of challenging positions that involve the full range of work, from basic and applied research to equipment development. The nature of the research and development conducted at NRL requires professionals with experience. Typically there is a continuing need for electronics, mechanical, aerospace, materials engineers, metallurgists, computer scientists, and oceanographers with bachelor's and/or advanced degrees and physical and computer scientists with Ph.D. degrees.

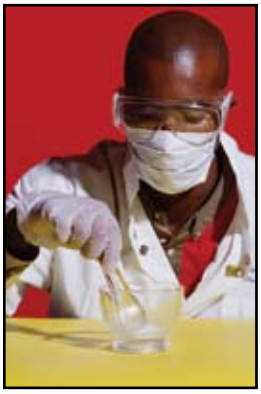

Chemists. Chemists are recruited to work in the areas of combustion, polymer science, bioengineering and molecular engineering, surface science, materials, synthesis, nanostructures, corrosion, fiber optics, electro-optics, microelectronics, electron-device technology, and laser physics.

Physicists. Physics graduates may concentrate on such fields as materials, solid-state physics, fiber optics, electro-optics, microelectronics, vacuum science, plasma physics, fluid mechanics, signal processing, ocean acoustics, information processing, artificial intelligence, electron-device technology, radio-wave propagation, laser physics, ultraviolet/X-ray/gamma-ray technology, electronic warfare, electromagnetic interaction, communications systems, radio frequency/microwave/millimeter wave/infrared technology, computational physics, radio and high energy astronomy, solar physics, and space physics.

Biologists. Biologists conduct research in areas that include biosensor development, tissue engineering, molecular biology, genetic engineering, proteomics, and environmental monitoring.

Oceanographers, Meteorologists, and Marine Geophysicists. These employees work in the areas of ocean and atmospheric dynamics, air-sea interaction, upper-ocean dynamics, oceanographic bio-optical modeling, oceanic and atmospheric numerical modeling and prediction, data assimilation and data fusion, retrieval and application of remote sensing data, benthic processes, aerogeophysics, marine sedimentary processes, advanced mapping techniques, atmospheric physics, and remote sensing. Oceanographers and marine geophysicists are located in Washington, D.C., and the Stennis Space Center, Bay St. Louis, Mississippi. Meteorologists are located in Washington, D.C., and Monterey, California.

for Highly Innovative, Motivated, *and* Creative Personnel

Electronics Engineers and Computer Scientists. These employees may work in the areas of communications systems, electromagnetic scattering, electronics instrumentation, electronic warfare systems, radio frequency/microwave/millimeter wave/infrared technology, radar systems, laser physics technology, radio-wave propagation, electron device technology, spacecraft design, artificial intelligence, information processing, signal processing, plasma physics, vacuum science, microelectronics, electro-optics, fiber optics, solid state, software engineering, computer design/architecture, ocean acoustics, stress analysis, and expert systems.

Mechanical and Aerospace Engineers. These employees may work in areas of spacecraft design, remote sensing, propulsion, experimental and computational fluid mechanics, experimental structural mechanics, solid mechanics, elastic/plastic fracture mechanics, materials, finite-element methods, nondestructive evaluation, characterization of fracture resistance of structural alloys, combustion, CAD/CAM, and multi-functional material response.

Materials Scientists/Engineers. These employees are recruited to work on materials, microstructure characterization, electronic ceramics, solid-state physics, fiber optics, electro-optics, microelectronics, fracture mechanics, vacuum science, laser physics and joining technology, and radio frequency/microwave/millimeter wave/infrared technology.

For more information on current vacancy listings,
visit http://hroffice.nrl.navy.mil/

NAVAL RESEARCH LABORATORY

4555 Overlook Ave., SW • Washington, DC 20375-5320

LOCATION OF NRL IN THE CAPITAL AREA

Quick Reference Telephone Numbers

	NRL Washington	NRL-SSC	NRL-Monterey	NRL CBD	NRL VXS-1 Patuxent River
Hotline	(202) 767-6543	(202) 767-6543	(202) 767-6543	(202) 767-6543	(202) 767-6543
Personnel Locator	(202) 767-3200	(228) 688-3390	(831) 656-4763	(410) 257-4000	(301) 342-3751
DSN	297- or 754-	828	878	—	342
Direct-in-Dialing	767- or 404-	688	656	257	342
Public Affairs	(202) 767-2541	(228) 688-5328	(202) 767-2541	—	(202) 767-2541

Additional telephone numbers are listed on page 246.

President announces

ROGER EASTON

recipient of

National Medal of Technology

President George W. Bush announced that Roger L. Easton is the recipient of the National Medal of Technology for his extensive pioneering achievements in spacecraft tracking, navigation and timing technology that led to the development of the NAVSTAR-Global Positioning System (GPS).

The National Medal of Technology is the highest honor awarded by the President of the United States to America's leading innovators. Established by an act of Congress in 1980, the Medal of Technology was first awarded in 1985. The Medal is given annually to individuals, teams, and/or companies/divisions for their outstanding contributions to the Nation's economic, environmental and social well-being through the development and commercialization of technology products, processes and concepts; technological innovation; and development of the Nation's technological manpower. The purpose of the National Medal of Technology is to recognize those who have made lasting contributions to America's competitiveness, standard of living, and quality of life through technological innovation, and to recognize those who have made substantial contributions to strengthening the Nation's technological workforce. By highlighting the national importance of technological innovation, the Medal also seeks to inspire future generations of Americans to prepare for and pursue technical careers to keep America at the forefront of global technology and economic leadership.

Roger Easton was awarded the National Medal of Technology for "his invention of the Minitrack satellite tracking system used to track Vanguard satellites and determine orbits; his development of the Naval Space Surveillance System still in use today cataloging all known man-made space objects orbiting Earth; his invention of a "Navigation System Using Satellites and Passive Ranging Techniques" and his subsequent development of Time Navigation and Navigation Technology Satellites that formed the technological basis for modern GPS."

Easton conceived, patented, and led the development of critical enabling technologies for the United States Global Positioning System (GPS). GPS today is a constellation of Earth-orbiting satellites providing precise navigation and timing data to military and civilian users. Easton, as a scientist and engineer at NRL, developed his concept for a time-based navigational system with passive ranging, circular orbits, and space-borne high precision clocks synchronized to a master clock. The U.S Patent Office received his invention, "Navigation System Using Satellites and Passive Ranging Techniques," on October 8, 1970. His earlier work exploiting space-based systems for geodesy, navigation, and timing laid the foundations for his visionary leap to the concept he dubbed TIMATION, for time navigation. He tested his concepts at NRL through development and launch of four experimental satellites: TIMATION I and II (in 1967 and 1969) and Navigation Technology Satellites (NTS) 1 and 2 (in 1974 and 1977). NTS-2, the first satellite to fly in the GPS 12 hour orbit and transmit GPS signals, flew the first cesium atomic frequency standard in space. Using time measurements from NTS-2, he experimentally verified Einstein's theory of relativity. A relativistic offset correction that he applied is still in use by every satellite in the GPS constellation.

WWW.NRL.NAVY.MIL